

RESPONSES OF THE PLANKTONIC FORAMINIFERA TO  
ENVIRONMENTAL CONDITIONS ACROSS THE  
CRETACEOUS/PALEOGENE BOUNDARY IN THE GÖYNÜK BASIN,  
NORTHWEST ANATOLIA, TURKEY

A THESIS SUBMITTED TO  
THE GRADUATE SCHOOL OF NATURAL AND APPLIED SCIENCES  
OF  
MIDDLE EAST TECHNICAL UNIVERSITY

BY

RENGİN ÖZDER

IN PARTIAL FULFILLMENT OF THE REQUIREMENTS  
FOR  
THE DEGREE OF MASTER OF SCIENCE  
IN  
GEOLOGICAL ENGINEERING

SEPTEMBER 2019



Approval of the thesis:

**RESPONSES OF THE PLANKTONIC FORAMINIFERA TO  
ENVIRONMENTAL CONDITIONS ACROSS THE  
CRETACEOUS/PALEOGENE BOUNDARY IN THE GÖYNÜK BASIN,  
NORTHWEST ANATOLIA, TURKEY**

submitted by **RENGİN ÖZDER** in partial fulfillment of the requirements for the degree of **Master of Science in Geological Engineering Department, Middle East Technical University** by,

Prof. Dr. Halil Kalıpçılar  
Dean, Graduate School of **Natural and Applied Sciences**

\_\_\_\_\_

Prof. Dr. Erdin Bozkurt  
Head of Department, **Geological Engineering**

\_\_\_\_\_

Prof. Dr. Sevinç Özkan Altıner  
Supervisor, **Geological Engineering, METU**

\_\_\_\_\_

Assist. Prof. Dr. Fatma Toksoy Köksal  
Co-Supervisor, **Geological Engineering Dept., METU**

\_\_\_\_\_

**Examining Committee Members:**

Prof. Dr. Muhittin Görmüş  
Geological Engineering Dept., Ankara University

\_\_\_\_\_

Prof. Dr. Sevinç Özkan Altıner  
Geological Engineering, METU

\_\_\_\_\_

Prof. Dr. Veysel Işık  
Geological Engineering Dept., Ankara University

\_\_\_\_\_

Assoc. Prof. Dr. H. Evren Çubukçu  
Geological Engineering Dept., Hacettepe University

\_\_\_\_\_

Assist. Prof. Dr. Ayşe Özdemir  
Geophysical Engineering Dept., Van Yüzüncü Yıl University

\_\_\_\_\_

Date: 06.09.2019

**I hereby declare that all information in this document has been obtained and presented in accordance with academic rules and ethical conduct. I also declare that, as required by these rules and conduct, I have fully cited and referenced all material and results that are not original to this work.**

Name, Surname: Rengin Özder

Signature:

## ABSTRACT

### **RESPONSES OF THE PLANKTONIC FORAMINIFERA TO ENVIRONMENTAL CONDITIONS ACROSS THE CRETACEOUS/PALEOGENE BOUNDARY IN THE GÖYNÜK BASIN, NORTHWEST ANATOLIA, TURKEY**

Özder, Rengin

Master of Science, Geological Engineering

Supervisor: Prof. Dr. Sevinç Özkan Altın

Co-Supervisor: Assist. Prof. Dr. Fatma Toksoy Köksal

September 2019, 254 pages

The aim of this study is to reveal the evolutionary response of the planktonic foraminifera after the Cretaceous/Paleogene (K/Pg) boundary interval in the Göynük Basin, Northwest Anatolia, Turkey. To achieve this purpose, a multidisciplinary study including biostratigraphy and mineralogy was carried out. In the Göynük area, an 8.55 m-thick section was measured, and a total of 47 samples were collected from the Seben Formation and the Hisarözü member of this formation composed of marls and clayey limestones.

In the Göynük section, five biozones were identified in the ascending order; *Pseudoguembelina hariaensis* Zone, P0, P1a, P1b, and P1c zones. The K/Pg boundary was delineated between the *P. hariaensis* and P0 zones. In order to study the evolutionary recovery of the planktonic foraminifera, a quantitative analysis was carried out from the samples of the P1b and P1c zones. Results indicate that the r/K-strategists and r-strategists occurred together in the P1b zone, whereas in the P1c zone, K-strategists were totally dominant.

Microtektites have been recorded from uppermost Maastrichtian of the Göynük section; microspherules are highly abundant in the P0 zone where the r-strategists are dominant.

Mineralogical studies, on the other hand, indicate that clay minerals in carbonate dominated marl samples are kaolinite, Ca-montmorillonite and illite. In the boundary, rutile, ilmenite, zircon, apatite, hematite, micas, hornblende inferring magmatic origin are present. Hg exists in the groundmass.

All these microfacies, mineralogical, and geochemical findings, coinciding with the magnetic susceptibility results carried out in this study, might be the evidence of different phases of global Deccan volcanism, the possible cause of the delayed recovery of the planktonic foraminifera following the K/Pg mass-extinction in the Göynük Basin. Furthermore, the presence of the microtektites and microspherules probably indicate the effects of the Chicxulub impact.

Keywords: Planktonic Foraminifera, Delayed Recovery, Mineralogy and Mineral Chemistry, Cretaceous/Paleogene Boundary, Göynük Basin

## ÖZ

### **GÖYNÜK HAVZASINDA (KUZEYBATI ANADOLU, TÜRKİYE) PLANKTONİK FORAMİNİFERLERİN KRETASE/PALEOJEN SINIRI VE SONRASINDAKİ ORTAMSAL KOŞULLARA TEPKİLERİ**

Özder, Rengin  
Yüksek Lisans, Jeoloji Mühendisliği  
Tez Danışmanı: Prof. Dr. Sevinç Özkan Altıner  
Ortak Tez Danışmanı: Dr. Öğr. Üyesi Fatma Toksoy Köksal

Eylül 2019, 254 sayfa

Çalışmanın amacı, planktonik foraminiferlerin Kretase-Paleojen (K/Pg) sınırı ve sonrasındaki ortamsal koşullardaki değişimlere gösterdikleri evrimsel tepkileri ortaya koymaktır. Bu amaçla, Göynük Havzasında (Kuzeybatı Anadolu, Türkiye) çökelen marnlardan oluşan Seben Formasyonu ve bu formasyonun marn ve killi kireçtaşlarından oluşan Hisarözü üyesini kapsayan istif boyunca 8,55 m kalınlığında bir stratigrafik kesit ölçülmüş ve 47 örnek toplanmıştır.

Kesit boyunca 5 biyozone tanımlanmıştır; *Pseudoguembelina hariaensis* zonu, P0, P1a, P1b, ve P1c. K/Pg sınırı *Pseudoguembelina hariaensis* zonu ile P0 zonu arasında tanımlanmıştır. Çalışma sırasında evrimsel gelişimleri takip edebilmek amacıyla P1b ve P1c zonlarına karşılık gelen örneklerden sayısal analiz yapılmıştır. Sonuç olarak, P1b zonunda r/K-strategist ve r-strategistler gözlemlenirken, P1c zonunda ağırlıklı olarak K-strategistler gözlemlenmiştir.

Evrimsel gelişimi tanımlama sırasında mikrotektit'ler üst Maastrichtiyen'de tayin edilmiş olup, mikroküreler P0 zonundunda r-strategistlerle bulunmaktadır.

Ek olarak, mineralojik çalıřmalar ile karbonat dominant marnlarda kil minerallerinden kaolinit, Ca-montmorillonit, ve illit'in varlıęı saptanmıřtır. Sınırda ve P1b zonunda görölen rutile, ilmenit, zircon, apatit, hematit, mika ve hornblend'in varlıęı magmatic kökeni iřaret etmektedir. Civa ise genel hamurda saptanmıřtır.

Bu çalıřma ile elde edilen mikrofasiyes, mineralojik, ve jeokimyasal sonuçlar, manyetik duyarlılık analizi ile birlikte Deccan volkanizmasının farklı fazlarının, planktonik foraminiferlerde gözlemlenen evrimsel gecikmeye sebep olduęu söylenebilir. Aynı zamanda, mikrotektit ve mikrokürelerin varlıęı Chicxulub çarpımasının etkisini göstermektedir.

Anahtar Kelimeler: Planktonik Foraminifer, Ertelenmiř Evrimsel Geliřim, Mineraloji ve Mineral Kimyası, Kretase/Paleosen Sınırı, Göynük Havzası

to my beloved grandparents Pakize Erbilgin and Hulusi Erbilgin always in my  
memories...

## ACKNOWLEDGEMENTS

First of all, I would like to express my special thanks of gratitude to my supervisor Prof. Dr. Sevinç ÖZKAN ALTINER for the continuous support of my M. Sc. study and related research, for her patience, motivation, and immense knowledge. Her guidance helped me in all the time of research and writing of this thesis. She also gave me the golden opportunity in my personal life by her valuable advices and endless help. Her motivation, endurance, and understanding approach felt stronger and doughtier. It is a great honor to work with her.

I would like to express my appreciation to my co-supervisor Assist. Prof. Dr. Fatma TOKSOY KÖKSAL for monitoring the steps of this thesis with her great attitudes, motivation and supports. She helped me every part of this thesis with her clear guidance and vision. Her considerations and valuable advices about the mineralogical and mineral chemistry analyses were very useful for me.

I would like to express my gratitude to Prof. Dr. Demir ALTINER who supports me not only graduate, also undergraduate studies. His scientific view always impressed me to become self-confident geologist. It is a great honor to meet him.

I would like to thank Dr. Ulaş Avşar for magnetic susceptibility analysis, Dr. Aynur HAKYEMEZ for field excursion, and Mrs. Aynur KÜÇÜK for allowing me to use the equipments of EPMA analysis in the Central Laboratory in METU.

I would like to thank Mrs. Gonca ALPTEKİN for XRD analysis, Mr. Orhan KARAMAN for preparing the thin sections.

I would like to thank to my friends Akın Çil, Damla ALTINTAŞ, Gamze TANIK, S. Görkem ATASOY, A. Uygur KARABEYOĞLU, Begüm AKGÜMÜŞ, and Ezgi VARDAR for their help, friendship as lab partners.

I would like to give special thanks to my family, my friends and every person who touch my soul during this thesis. However, the one special thanks to my mother Belgin

ERBİLGİN ÖZDER, who is my best friend, sister, confidante, for her motivation, wisdom, encouragements and endless support since losing my father Ahmet Yalçın ÖZDER. She has always been a role model for me with her strong stance, patient, affectionate, and enthusiasm on science.

The last and very special thanks to my grandparents Pakize ERBİLGİN and Hulusi ERBİLGİN. I would like to thank to them for grooving me as a human with loveliness, politeness, morals, and respectfulness. I feel their prays, and support in every part of my soul.

## TABLE OF CONTENTS

ABSTRACT .....	v
ÖZ .....	vii
ACKNOWLEDGEMENTS.....	x
TABLE OF CONTENTS .....	xii
LIST OF TABLES.....	xv
LIST OF FIGURES .....	xvi
CHAPTERS	
1. INTRODUCTION.....	1
1.1. Purpose and Scope .....	1
1.1. Geographical Setting.....	3
1.2. Methods of Study.....	4
1.2.1. Sample Preparation for Biostratigraphy .....	5
1.2.2. Sample Preparation for Mineralogical and Mineral Geochemistry Analysis.....	10
1.3. Previous Works .....	11
1.3.1. Previous Works on K/Pg Boundary.....	11
1.3.2. Previous Works on the Göynük Basin.....	14
1.4. Regional Geological Settings.....	17
2. STRATIGRAPHY .....	25
2.1. LITHOSTRATIGRAPHY .....	25
2.1.1. Microfacies Analysis .....	32
2.2. BIOSTRATIGRAPHY .....	40
2.2.1. <i>Pseudoguembelina hariaensis</i> Interval Zone .....	45

2.1.2. <i>Guembelitra cretacea</i> (P0) Partial Range Zone .....	46
2.1.3. <i>Parvularugoglobigerina eugubina</i> (P1a) Total Range Zone.....	47
2.1.4. P1b Interval Zone .....	49
2.1.5. P1c Interval Zone.....	51
3. PLANKTONIC FORAMINIFERAL SPECIES TURNOVER ACROSS THE K/PG BOUNDARY INTERVAL.....	55
3.1. Life-history Strategists .....	56
3.2. Responses of Planktonic Foraminifera to the Environmental Conditions across the K/Pg Boundary Interval.....	59
3.3. Quantitative Analysis .....	62
3.4. Marker Events Across the K/Pg Boundary Beds: Microspherules and Microtektites.....	67
4. MINERALOGICAL AND GEOCHEMICAL FEATURES .....	71
4.1. Mineralogy and Mineral Chemistry Analysis .....	72
4.1.1. X-Ray Diffractometry Analyses .....	72
4.1.2. Electron Microprobe Analysis.....	81
4.2. Magnetic Susceptibility .....	102
5. SYSTEMATIC TAXONOMY .....	107
5.1. Early Danian Planktonic Foraminifera.....	108
5.2. Late Maastrichtian Planktonic Foraminifera.....	140
6. DISCUSSION & CONCLUSION.....	177
6.1. Discussion .....	177
6.1.1. Planktonic Foraminiferal Turnover and Mass extinction and Recovery Pattern at Göynük Section .....	178
6.1.2. Mineralogical and Mineral Chemistry Results.....	180

6.1.3. The Reasons Behind the Delayed Recovery: Chicxulub or Deccan .....	184
6.2. Conclusion .....	190
REFERENCES .....	193
A. PLATES .....	219

## LIST OF TABLES

### TABLES

<b>Table 1.1:</b> Applied washing techniques to the each type of lithologies.....	8
<b>Table 1.2:</b> Best methods obtained from different techniques in each sample.....	9
<b>Table 2.1:</b> Microfacies Types of the studied samples in the Göynük Basin in both Classifications .....	37
<b>Table 2.2:</b> Correlation Maastrichtian and Danian Biozones and our biozonation in the Göynük Basin.....	53
<b>Table 3.1:</b> Relative abundances of planktonic foraminifera in the early Danian, P1b and P1c zones > 63 m size fraction at Göynük, Bolu, Turkey.....	64
<b>Table 4.1:</b> The percentage data of clay minerals.....	79
<b>Table 4.2:</b> The quantitative data from Electron Microprobe Analysis (EPMA) of each recorded mineral .....	96
<b>Table 4.3:</b> Semi-quantitative EDS values for the hematite spherules.....	100
<b>Table 4.4:</b> The all values from Magnetic Susceptibility Analysis .....	104

## LIST OF FIGURES

### FIGURES

<b>Figure 1.1:</b> Geographic setting of the study area and the location of the measured section.....	3
<b>Figure 1.2:</b> A) Geological map of the NW Anatolia and the location of the Göynük basin B) Main structural features of Turkey with the main tectonic units (Oçakoğlu et al., 2018).....	18
<b>Figure 1.3:</b> a. Location of the study area (generalized geology simplified from Altner et al., 1991), b. Geological map of the study area (simplified from Gedik and Aksay, 2002).....	19
<b>Figure 1.4.</b> Generalized stratigraphic columns spanning late Jurassic to Eocene from different parts of the Central Sakarya Basin. (1) Saner (1977) and Duru et al. (2002), (2) Besbelli (1991) and Gedik and Aksay (2002), (3) Timur and Aksay (2002), Tansel (1980) and Altner et al. (1991), and (4) Yıldız et al. (2015) and Kasapoğlu et al. (2016).....	20
<b>Figure 1.5:</b> Correlation table of the lithostratigraphic units (Modified from Açıkalın, 2015) (not to scale).....	23
<b>Figure 1.6:</b> Generalized tectonostratigraphic and sequence stratigraphic columnar section of the Göynük Basin (Modified from Açıkalın, 2015)(not to scale).....	24
<b>Figure 2.1:</b> Field photo of the studies Gk-section. Red dots indicate the position of the samples along the section. Red line showing the position of the K/Pg boundary. ....	26
<b>Figure 2.2:</b> Lithostratigraphy and biostratigraphy of the measured sections. Please note that marl- clayey limestone alternations after the K/Pg boundary.....	28
<b>Figure 2.3:</b> Closer look to the measured section. Red line: Position of the clayey limestone bed. ....	29

<b>Figure 2.4:</b> Thin section microphotographs of several samples. PF: planktonic foraminifera, BF: benthic foraminifera, UF: Undefined fossil fragment.....	30
<b>Figure 2.5:</b> Microphotographs taken from the marl samples A: iron-bubbles from sample Gk-9, B: Mica mineral from sample Gk-9, C: Glaucophanes from sample Gk-26, D: Alteration of Biotite from sample Gk-27 .....	31
<b>Figure 2.6:</b> Thin section view of K/Pg boundary with microspherules. ....	32
<b>Figure 2.7:</b> Folk's Classification of Carbonate Rocks(1959) and its expanded version by Kendall (2005). The one that was recognized in this study have been marked by a red square. ....	34
<b>Figure 2.8:</b> Dunham's Classification of Carbonate Rocks (1962) and its expanded version by Kendall (2005). The one that was recognized in this study have been marked by a red square. ....	34
<b>Figure 2.9:</b> Mount Classification of Mixed Siliciclastic-Carbonate Rocks (1985). The one that was recognized in this study have been marked by a red square. ....	35
<b>Figure 2.10:</b> Mount Classification of Mixed Siliciclastic-Carbonate Rocks (1985) (From Flügel, 2004) .....	36
<b>Figure 2.11:</b> Wackestone and mudstone in thin section view, respectively. ....	36
<b>Figure 2.12:</b> Distribution of Standard Microfacies (SMF) types in the Facies Zones (FZ) of Wilson (1975) on a rimmed carbonate platform model (Flügel, 2004). The one that was recognized in this study have been marked by a red square. ....	38
<b>Figure 2.13:</b> Generalized distribution of microfacies types (RMF) in different parts of a homoclinal carbonate ramp (Flügel, 2004). The one that was recognized in this study have been marked by a red square. ....	39
<b>Figure 2.14:</b> Stratigraphical distribution of recorded taxa in the studied section .....	43
<b>Figure 3.1:</b> The relationship between density and diversity (Simplified from Benton and Harper, 1997) .....	57
<b>Figure 3.2:</b> Life-history strategies of planktonic foraminifera with early Danian genera of the Göynük section (Samples are from Göynük samples) .....	59

<b>Figure 3.3:</b> Early Danian evolution illustrating the high-stress environment, small species, and low diversity (r-strategists), complex morphological, high abundance species (K-strategists), and in between intermediate-strategists. ....	62
<b>Figure 3.4:</b> Relative abundance patterns of life-history strategists. The boundary between P1b and P1c is located in between sample 36 and 38. In P1b zone, the sample 26 to 36, K-strategists are relatively low, intermediate- and r- strategists are relatively high in abundance. After the P1b zone, in P1c zone, K-strategists dominate the environment and depletion occurs in r-strategists. ....	66
<b>Figure 3.5:</b> Relative abundance patterns of <i>Guembelitria</i> cretacea. The boundary of the P1b and P1c zones is located in between the samples 36 and 38. The drastically decline on the abundance of opportunistic species can be easily observed.....	66
<b>Figure 3.6:</b> Microspherule blooms in thin sections A) sample Gk-10, just above the boundary, P0 zone B) sample Gk-26, P1b zone, rich in biserial and triserial planktonic foraminifera Sph: Microspherules, PF: planktonic foraminifera.....	68
<b>Figure 3.7:</b> A) Scanning Electron Microscope (SEM) Image of microspherule individuals embedded in a clast. Sample from Gk-10, P0 zone, B) Close-up view of microspherule specimen in A .....	68
<b>Figure 3.8:</b> Microtektites replaced with calcite in both thin-section views and Scanning Electron Microscopy (SEM) view A) sample from Gk-01, inside of the late Maastrichtian, B) sample from Gk-9, 8 cm below the K/Pg boundary, C) sample from Gk-21, in P1a zone .....	70
<b>Figure 4.1:</b> X-ray diffractograms of the sample Gk-1 A) Random sample pattern, B) Oriented samples (Air-dried (AD), Ethylene Glycol (EG), heated at 350°C (350), and 500°C (500)).....	73
<b>Figure 4.2:</b> Representative random XRD patterns of the samples (Red arrows shows the variations from each sample).....	75
<b>Figure 4.3:</b> Random XRD patterns from the Göynük section for the samples A) Gk-1 B) Gk-10 (included K/Pg boundary and P0 zone) showing the decline of both clay and quartz contents at the boundary .....	76

<b>Figure 4.4:</b> XRD pattern of the random sample Gk-16 from the Göynük section that show ilmenorutile.....	77
<b>Figure 4.5:</b> XRD patterns of random samples from the Göynük section A)Gk-26 B) Gk-27 (The samples started P1b zone and fluctuations can be easily observed).....	78
<b>Figure 4.6:</b> The graph showing the total clay percentages of the Göynük samples. The lowest value is from end of the P1b zone. ....	80
<b>Figure 4.7:</b> EPMA BSE images and EDS patterns for rounded to subrounded quartz grains except C, C) the angular quartz grain.....	82
<b>Figure 4.8:</b> EPMA BSE images and EDS patterns for angular quartz grains .....	83
<b>Figure 4.9:</b> EPMA BSE images and EDS patterns for plagioclase.....	84
<b>Figure 4.10:</b> EPMA BSE images and EDS patterns of orthoclase.....	84
<b>Figure 4.11:</b> EPMA BSE images and EDS patterns for plagioclase.....	85
<b>Figure 4.12:</b> EPMA BSE images and EDS patterns of oxidized biotite.....	87
<b>Figure 4.13:</b> Back scattered electron (BSE) image with element maps of the oxidized biotite by EPMA .....	88
<b>Figure 4.14:</b> EPMA BSE images and EDS pattern of zircon.....	89
<b>Figure 4.15:</b> EPMA BSE images and EDS patterns of sphene.....	90
<b>Figure 4.16:</b> EPMA BSE images and EDS patterns of apatite .....	92
<b>Figure 4.17:</b> EPMA BSE images and EDS patterns of rutile.....	93
<b>Figure 4.18:</b> EPMA BSE images and EDS patterns of ilmenite.....	93
<b>Figure 4.19:</b> EPMA BSE images and EDS patterns of Hematite .....	94
<b>Figure 4.20:</b> EPMA back scattered electron (BSE) image showing isolated and aggregated hematite spherules .....	94
<b>Figure 4.21:</b> A) secondary electron (SE) image B) back scattered electron (BSE) image C) element maps of the hematite spherules by EPMA.....	95
<b>Figure 4.22:</b> EPMA back scattered electron images and EDS patterns for A) hematite spherules aggregates B) isolated hematite spherules .....	100
<b>Figure 4.23:</b> The map of the microtektite from the sample Gk-12 .....	101
<b>Figure 4.24:</b> Magnetic Susceptibility Graph of Rock Samples.....	105
<b>Figure 4.25:</b> Magnetic Susceptibility Graph of Thin Sections.....	105

**Figure 5.1:** Proposed phylogenetic relationships of the main earliest Danian planktonic foraminiferal genera based on evidence reported here and previous phylogenetic studies (Modified from Arenillas et al., 2015)..... 109

**Figure 6.1:** Conceptual model of the sedimentary marine record of continental magnetite dissolution caused by volcanic acid rains (Font et al., 2014). ..... 183

**Figure 6.2:** Correlation of a) the age (U–Pb dating on zircon; Schoeneetal.,2015) of the Deccan lavas flow in India with the KPg marine sedimentary records marked by b) the low MS interval at Gubbio (Italy) (Ellwoodetal.,2003); c) the low MS interval containing akaganéite (Fontetal.,2011) ,d) the depletion in detrital and biogenic magnetite (Font et al., 2014), and e) mercury anomalies at Bidart (France) (Font et al., 2016); and f) the magnetite-depleted interval containing akaganéite at Zumaia (Font et al., 2018) ..... 184

**Figure 6.3:** Summary of major results in the Göynük section. Note also the good correlation between the biozones and the results ..... 187

**Figure 6.4:** Paleogeographic Distribution map with Deccan Trap and Chicxulub impact (Modified from Punekar et al., 2014) ..... 189

## CHAPTER 1

### INTRODUCTION

#### 1.1. Purpose and Scope

The K/Pg boundary (66.0 Ma) is one of the five severe mass extinctions in the Earth history. It has the most significant global environmental and climatic catastrophes causing the extinction of numerous taxa including dinosaurs. Investigations reveal that there are two hypotheses on the principle causes of the mass extinction. One is the bolide impact, called as Chicxulub, on the Yucatan Peninsula (Mexico), and other is the volcanic eruptions, called as Deccan Trap, on the Krishna Godovari Basin (India). Alvarez and his colleagues (1980) claimed that the bolide impact cause for the K/Pg mass extinction based upon anomalous enrichment in Ir and other impact-derived materials, such as microtektites and Ni-rich spinels (Alvarez et al., 1980). On the other hand, other scientists revealed that the Deccan volcanic eruptions had three phases and the second phase is the major cause of the extinction (Perch-Nielsen et al., 1982; Keller, 1988a, b; Keller et al., 1993).

The effects of this mass-extinction were also recorded in the planktonic foraminifera. Although the 96% of the planktonic foraminifera species, especially keeled, large and well-ornamented ones, were extincted, only the limited of them were able to survive (Keller, 1988a, 2002; Silva and Sliter, 1999; Esmeray, 2008; Gallala et. al., 2009; Karabeyoğlu, 2017; Punekar et al., 2014). Pardo and Keller (2008) called them as an opportunistic species, which are interpreted as having thrived in eutrophic surface waters where the complex and generalist species cannot be survived because they adapted to oligotrophic and mesotrophic, environmental conditions, respectively.

After the K/Pg boundary, when the environmental conditions became stable, the complex and generalist planktonic foraminifera started to evolve, and their diversity gradually increased. On the other hand, deep-water benthic foraminifers also affected from destructive event. However, they were not totally extinct, like planktonic foraminifera, their diversity, abundance, and ornamentations decreased (Alegret et al., 2003, 2004, 2013; Culver, 2003; Coccioni et al., 2007; Punekar et al., 2014; Rostami et al., 2018; Vardar, 2018).

The main purpose of this thesis is to reveal the relationship between the evolutionary recovery of planktonic foraminifera and the normalization of environmental conditions after the K/Pg boundary. To achieve the main objective,

- the stratigraphic section has been measured in the Göynük basin, NW Turkey,
- the planktonic foraminifera of the studied sequence have been identified,
- the K/Pg boundary has been delineated,
- the relative diversity and abundance of Danian planktonic foraminifera were determined by quantitative analysis,
- the evolutionary recovery of Danian planktonic foraminiferal assemblages have been recorded,
- in order to determine environmental variations some mineralogical, mineral chemical, and magnetic susceptibility analyses have been carried out on the collected samples,

Finally, in the light of the findings, an assumption has been made about the cause of mass extinction in the Göynük Basin.

## 1.1. Geographical Setting

The study area is located approximately northwest of the Göynük town, which is located 292 km northwest of Ankara (Figure 1.1). It is situated on the topographic map of Adapazarı-H25 of 1/100000 scale. The coordinates of the measured section are  $40^{\circ}22'982\text{N}$  and  $30^{\circ}58'404\text{E}$  and its elevation is 1163 m.



**Figure 1.1:** Geographic setting of the study area and the location of the measured section

## **1.2. Methods of Study**

Throughout the study, detailed literature survey, field and laboratory works were done respectively. During the laboratory works paleontological, mineralogical and magnetic susceptibility were carried out.

During the field analyses, a total of 8.55 m thick stratigraphic section was measured, sampling was done with high resolution, with 3-70 cm intervals, and a total of 47 samples were collected. The first 9 sample, Gk-1 to Gk-9, are belonging to Upper Cretaceous, Gk-10 to Gk-42, samples are belonging to Early Paleocene. There are 5 more samples, Gk-04 to Gk-00, belonging to Upper Cretaceous, are found below the Gk-1 with minor fault plane. In total, 47 samples were collected.

For micropaleontological and microfacies analysis, laboratory works were carried on. Each sample was washed out by different washing methods in order to extract foraminiferal individuals from the rock samples and Scanning Electron Microscope (SEM) photos were taken from each species. Furthermore, quantitative analysis was applied on the Danian forms, greater than 63  $\mu\text{m}$  size fractions. In addition, thin sections from all samples were also analyzed under microscope to determine the microfacies types.

Detecting mineralogical differences between samples clay mineralogy were carried out by using XRD. Furthermore, EPMA mapping method has been applied to identify undetectable minerals in XRD because of their amounts are less than 5%, mercury and any other heavy elements in the dough. Moreover, all mineralogical findings were compared with the results from magnetic susceptibility analyses, which were performed in Middle East Technical University (METU).

### **1.2.1. Sample Preparation for Biostratigraphy**

A total of 47 samples have been collected in the Göynük Basin, consisting of marls and clayey limestones. The sampling interval ranges from 3 to 70 cm, and each sample have been collected very carefully, narrowing around the possible K/Pg boundary. During the field study any lithological changes of the succession have been observed and photographed.

In order to establish the biostratigraphic framework to determine the evolutionary patterns of the planktonic foraminifera. For this reason, the extraction of planktonic foraminifera from the rock samples became crucial. There are several washing techniques that have been applied based on composition of the samples. However, comparing the methods that used in previous studies, extraction of planktonic foraminifera from the rocks always being a problem (e.g. Pardo et. al., 1999; Arenillas et. al., 2000; Abramovich et. al., 2003).

In the first stage, the collected samples were crushed into small fragments, less than 1 cm<sup>3</sup> in order to dissolve better (Lirer, 2000). In the second stage, different chemical solvents were used for dissolution of the samples. Started with standard washing technique, Knitter Method (Knitter, 1979), extract the planktonic foraminifera by using hydrogen peroxide. This method has been tried with different percentage of diluted and different time intervals for becoming successful. However, this method become successful in only marl deposits. Best fitting method is 50% hydrogen peroxide in 2 hours for marl deposits.

For extracting planktonic foraminifera in clayey limestone sediments, stronger treatment needed. For this purpose, acetic acid (CH<sub>3</sub>COOH) were used with different ratios (Knitter, 1979; Lirer, 2000). In the Knitter method, the sample is covered with acetic acid and added chloroform in 1:1 ratio. Because the acetic acid is a strong chemical and dissolve the wall of planktonic foraminifera, chloroform is added to get lighter solution. On the other hand, Lirer method proposed that usage of 80% acetic

acid and 20% H<sub>2</sub>O together for extraction without disturbing the wall of the foraminifers. This is not preferable method since water can only decrease the molality of the acetic acid. During the choosing best method, acetic acid concentration also differentiated. On the other hand, Esmeray (2008) claimed that mixed the acetic acid and hydrogen peroxide with different percentages can be increased the power of chemicals. During her study, samples were crushed into small fragments and soaked into the mixture of 50% diluted H<sub>2</sub>O<sub>2</sub> and 50% diluted acetic acid with the ratio 1:10, i.e. for 25 gr. sample 250 ml mixture, with different time intervals. However, in our samples, it did not work. In order to obtain best method, different concentration of acetic acid and H<sub>2</sub>O<sub>2</sub> were tried but none of them can be removed the clay in expected amount. Moreover, this method damaged the wall of planktonic foraminifera. Each method that have been tried were listed in Table 1.1.

In the third stage, after disaggregation of sediment particles, residues have washed under the distilled water with gently rubbing and using the sieves of 425, 250, 63, 38 microns for obtaining clear foraminiferal sample residues. In addition to washing, hand-rubbing under the water is useful for helping to remove clay content and to clean specimens. The cleaning under the water is important because some acid ions stand on the residues and dissolution may continue, distilled water helps to remove clay and acid upon drying. After the rubbing stage, the samples dried in an oven over a night with 50°C.

Some researchers maintain that using magnetic splitter and/or boiling with NaHCO<sub>3</sub> and ultrasonic treatment are useful for removing clay particles. However, these methods are only useful for foraminifera having a little residue. It may useful for some other samples but in the Göynük section, there is no needed to apply it.

Thin section analysis has been carried out to determine the microfacies types. On the contrary, the best usage of thin sections is to compare washing method, it shows the general fossil content of the sample (Table 1.2).

To obtain statistical representation of the species population, 15 samples were analyzed with splitting on the splitter 4 times to obtain approximately 300 specimens from the >63  $\mu\text{m}$  size fraction. Planktonic foraminifers were picked from each split and identified in detail. Identification of species is based on standard taxonomic concepts (Robaszynski, 1984; Nederbragt, 1998; Olsson et al., 1999; Keller, 2002; Esmeray, 2008; Karabeyođlu, 2017).

**Table 1.1:** Applied washing techniques to the each type of lithologies

Solvent Type	Time duration
50% diluted H <sub>2</sub> O	2 hours
50% diluted H <sub>2</sub> O	4 hours
50% diluted H <sub>2</sub> O	24 hours
50% diluted H <sub>2</sub> O	2 days
50% diluted H <sub>2</sub> O	4 days
50% diluted H <sub>2</sub> O	7 days
30% diluted CH <sub>3</sub> COOH+Chloroform	2 hours
30% diluted CH <sub>3</sub> COOH+Chloroform	4 hours
30% diluted CH <sub>3</sub> COOH+Chloroform	6 hours
30% diluted CH <sub>3</sub> COOH+Chloroform	24 hours
50% diluted CH <sub>3</sub> COOH+Chloroform	2 hours
50% diluted CH <sub>3</sub> COOH+Chloroform	4 hours
50% diluted CH <sub>3</sub> COOH+Chloroform	6 hours
50% diluted CH <sub>3</sub> COOH+Chloroform	24 hours
65% diluted CH <sub>3</sub> COOH+Chloroform	2 hours
65% diluted CH <sub>3</sub> COOH+Chloroform	4 hours
65% diluted CH <sub>3</sub> COOH+Chloroform	6 hours
65% diluted CH <sub>3</sub> COOH+Chloroform	24 hours
30% H <sub>2</sub> O(50% diluted)+ 70% CH <sub>3</sub> COOH (50% diluted)	30 minutes
30% H <sub>2</sub> O(50% diluted)+ 70% CH <sub>3</sub> COOH (50% diluted)	1 hour
30% H <sub>2</sub> O(50% diluted)+ 70% CH <sub>3</sub> COOH (50% diluted)	2 hours
30% H <sub>2</sub> O(50% diluted)+ 70% CH <sub>3</sub> COOH (50% diluted)	4 hours
30% H <sub>2</sub> O(50% diluted)+ 70% CH <sub>3</sub> COOH (50% diluted)	6 hours
40% H <sub>2</sub> O(50% diluted)+ 60% CH <sub>3</sub> COOH (50% diluted)	30 minutes
40% H <sub>2</sub> O(50% diluted)+ 60% CH <sub>3</sub> COOH (50% diluted)	1 hour
40% H <sub>2</sub> O(50% diluted)+ 60% CH <sub>3</sub> COOH (50% diluted)	2 hours
40% H <sub>2</sub> O(50% diluted)+ 60% CH <sub>3</sub> COOH (50% diluted)	4 hours
40% H <sub>2</sub> O(50% diluted)+ 60% CH <sub>3</sub> COOH (50% diluted)	6 hours
50% H <sub>2</sub> O(50% diluted)+ 50% CH <sub>3</sub> COOH (50% diluted)	30 minutes
50% H <sub>2</sub> O(50% diluted)+ 50% CH <sub>3</sub> COOH (50% diluted)	1 hour
50% H <sub>2</sub> O(50% diluted)+ 50% CH <sub>3</sub> COOH (50% diluted)	2 hours
50% H <sub>2</sub> O(50% diluted)+ 50% CH <sub>3</sub> COOH (50% diluted)	4 hours
50% H <sub>2</sub> O(50% diluted)+ 50% CH <sub>3</sub> COOH (50% diluted)	6 hours
60% H <sub>2</sub> O(50% diluted)+ 40% CH <sub>3</sub> COOH (50% diluted)	30 minutes
60% H <sub>2</sub> O(50% diluted)+ 40% CH <sub>3</sub> COOH (50% diluted)	1 hour
60% H <sub>2</sub> O(50% diluted)+ 40% CH <sub>3</sub> COOH (50% diluted)	2 hours
60% H <sub>2</sub> O(50% diluted)+ 40% CH <sub>3</sub> COOH (50% diluted)	4 hours
60% H <sub>2</sub> O(50% diluted)+ 40% CH <sub>3</sub> COOH (50% diluted)	6 hours
70% H <sub>2</sub> O(50% diluted)+ 30% CH <sub>3</sub> COOH (50% diluted)	30 minutes
70% H <sub>2</sub> O(50% diluted)+ 30% CH <sub>3</sub> COOH (50% diluted)	1 hour
70% H <sub>2</sub> O(50% diluted)+ 30% CH <sub>3</sub> COOH (50% diluted)	2 hours
70% H <sub>2</sub> O(50% diluted)+ 30% CH <sub>3</sub> COOH (50% diluted)	4 hours
70% H <sub>2</sub> O(50% diluted)+ 30% CH <sub>3</sub> COOH (50% diluted)	6 hours

**Table 1.2:** Best methods obtained from different techniques in each sample

Sample No	Lithology	Applied Method
GK-42	Calcerous Mudstone	50% diluted CH <sub>3</sub> COOH+Chloroform (2 hours)
GK-41	Marl	50% diluted H <sub>2</sub> O <sub>2</sub> (1 hour)
GK-40	Calcerous Mudstone	50% diluted CH <sub>3</sub> COOH+Chloroform (2 hours)
GK-39	Marl	50% diluted H <sub>2</sub> O <sub>2</sub> (2 hours)
GK-38	Calcerous Mudstone	50% diluted CH <sub>3</sub> COOH+Chloroform (2 hours)
GK-37	Marl	50% diluted H <sub>2</sub> O <sub>2</sub> (1 hour)
GK-36	Calcerous Mudstone	50% diluted CH <sub>3</sub> COOH+Chloroform (2 hours)
GK-35	Marl	50% diluted H <sub>2</sub> O <sub>2</sub> (2 hours)
GK-34	Calcerous Mudstone	50% diluted CH <sub>3</sub> COOH+Chloroform (2 hours)
GK-33	Marl	50% diluted H <sub>2</sub> O <sub>2</sub> (2 hours)
GK-32	Calcerous Mudstone	50% diluted CH <sub>3</sub> COOH+Chloroform (2 hours)
GK-31	Marl	50% diluted H <sub>2</sub> O <sub>2</sub> (2 hours)
GK-30	Calcerous Mudstone	50% diluted CH <sub>3</sub> COOH+Chloroform (2 hours)
GK-29	Calcerous Marl	50% diluted H <sub>2</sub> O <sub>2</sub> (2 hours)
GK-28	Calcerous Marl	50% diluted H <sub>2</sub> O <sub>2</sub> (2,5 hours)
GK-27	Calcerous Marl	50% diluted H <sub>2</sub> O <sub>2</sub> (4 hours)
GK-26	Calcerous Mudstone	50% diluted CH <sub>3</sub> COOH+Chloroform (2 hours)
GK-25	Calcerous Mudstone	50% diluted CH <sub>3</sub> COOH+Chloroform (1,5 hours)
GK-24	Calcerous Marl	50% diluted CH <sub>3</sub> COOH+Chloroform (2 hours)
GK-23	Calcerous Marl	50% diluted CH <sub>3</sub> COOH+Chloroform (2 hours)
GK-22	Calcerous Marl	50% diluted CH <sub>3</sub> COOH+Chloroform (2 hours)
GK-21	Calcerous Marl	50% diluted CH <sub>3</sub> COOH+Chloroform (2 hours)
GK-20	Calcerous Marl	50% diluted CH <sub>3</sub> COOH+Chloroform (2 hours)
GK-19	Marl	50% diluted H <sub>2</sub> O <sub>2</sub> (2 hours)
GK-18	Marl	50% diluted H <sub>2</sub> O <sub>2</sub> (2 hours)
GK-17	Marl	50% diluted H <sub>2</sub> O <sub>2</sub> (2 hours)
GK-16	Marl	50% diluted H <sub>2</sub> O <sub>2</sub> (2 hours)
GK-15	Marl	50% diluted H <sub>2</sub> O <sub>2</sub> (2 hours)
GK-14	Marl	50% diluted H <sub>2</sub> O <sub>2</sub> (2 hours)
GK-13	Marl	50% diluted H <sub>2</sub> O <sub>2</sub> (2 hours)
GK-12	Marl	50% diluted H <sub>2</sub> O <sub>2</sub> (2 hours)
GK-11	Marl	50% diluted H <sub>2</sub> O <sub>2</sub> (2 hours)
GK-10	Marl	50% diluted H <sub>2</sub> O <sub>2</sub> (2 hours)
GK-9	Marl	50% diluted H <sub>2</sub> O <sub>2</sub> (2 hours)
GK-8	Marl	50% diluted H <sub>2</sub> O <sub>2</sub> (2 hours)
GK-7	Marl	50% diluted H <sub>2</sub> O <sub>2</sub> (2 hours)
GK-6	Marl	50% diluted H <sub>2</sub> O <sub>2</sub> (2 hours)
GK-5	Marl	50% diluted H <sub>2</sub> O <sub>2</sub> (2 hours)
GK-4	Marl	50% diluted H <sub>2</sub> O <sub>2</sub> (2 hours)
GK-3	Marl	50% diluted H <sub>2</sub> O <sub>2</sub> (2 hours)
GK-2	Marl	50% diluted H <sub>2</sub> O <sub>2</sub> (2 hours)
GK-1	Marl	50% diluted H <sub>2</sub> O <sub>2</sub> (2 hours)
GK-00	Marl	50% diluted H <sub>2</sub> O <sub>2</sub> (1/2 hours)
GK-01	Marl	50% diluted H <sub>2</sub> O <sub>2</sub> (1/2 hours)
GK-02	Marl	50% diluted H <sub>2</sub> O <sub>2</sub> (1/2 hours)
GK-03	Marl	50% diluted H <sub>2</sub> O <sub>2</sub> (1/2 hours)
GK-04	Marl	50% diluted H <sub>2</sub> O <sub>2</sub> (1/2 hours)

### **1.2.2. Sample Preparation for Mineralogical and Mineral Geochemistry Analysis**

During this study, to define mineralogical content and changes, geochemical and mineralogical analyses were carried out by XRD and EPMA for the samples from the Göynük Basin, and to compare the results with other researches.

During the sample preparation for XRD, the material, as pure as possible, was ground to fine powder less than 100  $\mu\text{m}$  in size. Powder samples sieved below 63  $\mu\text{m}$  were used for non-clay mineral identification while oriented slides (air dried, ethylene glycolated, heated at 350°C and 500°C) were used for clay mineral identification. Rigaku Miniflex II was used for the analyses. The samples were prepared and analyzed at the Department of Geological Engineering in Middle East Technical University (METU).

The second important technique is EPMA to chemically analyze small selected areas of the solid samples to about 1 mm size by using X-ray spectrum. However, these analyses are different from XRD due to contain lines characteristic of the element present, hence a qualitative and semi-quantitative analysis can be obtained in EPMA. Spatial distributions of specific elements along a line and/or in two-dimensional ‘maps’.

Sample preparation for EPMA is critical to get good analytical results. For example, if the sample sizing is too aggressive, the method can cause deep damage on both morphology and chemistry. For this purpose, polished thin section of the samples were prepared carefully at the Department of Geological Engineering, METU and were covered with gold plandium at EPMA laboratory of Central Laboratory, METU. The JXA-8230 Electron Probe Microanalyzer was used for measuring the both qualitative and quantitative data by sending electron beam to the sample.

The third analysis is magnetic susceptibility (MS). All analyzed samples were crushed and rubbed into boxes with perfect surface for subsequent magnetic measurements. In

this study, thin sections were also analyzed (see Chapter 4) even though analyses on thin section was not applied in literature. Magnetic properties of the samples were performed at the Department of Geological Engineering, METU using a MS2/MS3 Magnetic Susceptibility Equipment of Bartington Instruments, and its Bartsoft software. The measured values are reported as mass-normalized values ( $\text{m}^3/\text{kg}$ ).

### **1.3. Previous Works**

#### **1.3.1. Previous Works on K/Pg Boundary**

Cretaceous/Paleogene boundary marks not only the boundary defined as mass extinction, but also the boundary between Mesozoic and Cenozoic eras, which corresponds to 66 Ma (Smit, 1982; Arenillas et al., 2002, 2016; Keller, 1998, 2002, 2004, 2006; Molina et al., 2006; Rostami et al., 2018). It is the major extinction events of the Phanerozoic, and one of the five great mass extinctions (Raup and Sepkoski, 1982). The most authors mentioned that the earth's ecosystem turnover extremely. 80% of the earth's biota extinct during that time, such as ammonites, brachiopods and any other organisms.

The meteorite impact, claimed by Alvarez and his colleagues (1980), is found as the reason of the mass extinction. According to them, Ir anomalies, microtektites and microspherules, and Ni-rich spinels are the evidences for Chicxulub meteorite. Furthermore, abundance of microspherules with shocked quartz grains are found in the previous studies (Bohor et al., 1984; Bohor and Izett, 1986; Keller, 1989). Based on these studies, the earth's crust and the atmosphere was affected from rapid global climate change because of bolide impact. In addition, scientists examined that earth's crust was contagion from global darkness and intense dust clouds, huge fires, tsunamis, acid rains and storms. Moreover, continental movements and seismic activities in both locally, and globally were occurred on this time (Alvarez et al., 1980;

Hildebrach et al., 1991; Schulte et al., 2010). During this phase photosynthesis was done very limited because of amount of dust and limited light absorption, so many plant species also depleted (Twitchett, 2006). When the atmospheric conditions change, the heat of atmosphere was decreased. As a result of decreasing temperature, globally ice-age phase started and continued for years.

Although many researchers mentioned bolide impact in their studies, another group of authors claimed that main cause of the mass extinction is volcanism, Deccan Trap. The idea of volcanic events as a cause of mass extinction has been suggested for over three decades (Kennett and Watkins, 1970; Vogt, 1972; Courtillot et al., 1986; Chenet et al., 2007; Schoene et al., 2015). Deccan volcanism has the largest lava flow in earth history, 1.5 million km<sup>3</sup> lava flooding, and it consists of three phases. The initial and smallest phase occurred in Maastrichtian (Chenet et al., 2008; Keller et al., 2012; Schöbel et al., 2014; Punekar et al., 2014; Mateo et al., 2018). The onset of the main phase, the second one coincides with the boundary, the studies show that this phase is related for the mass extinction (Keller et al., 2012; Font et al., 2017; Punekar et al., 2014; Mateo et al., 2018). The final and important phase is third phase, occurred in Early Danian (Chenet et al., 2008; Punekar et al., 2014).

The effect of each phases of Deccan volcanism was seen on the global climate and biota. Because of the volume of lava, SO<sub>2</sub>, CO<sub>2</sub>, Cl<sub>2</sub>, and many other gases released into atmosphere, and they have potential contact with limestone, and other type of sediments that are not included in estimates (Keller et al., 2012; Punekar et al., 2014). Moreover, sea-level fluctuations and climatic changes also recorded in beds (Esmeray, 2008; Kominz et al., 2008; Schulte et al., 2009; Hart et al., 2016).

Global Stratotype Section and Point (GSSP) of the K/Pg boundary found in El Kef, NW Tunisia which is defined by International Commission on Stratigraphy (ICS) (Cowie et al., 1989). The El Kef section is GSSP point because the presence and abundance of microfossils, without any hiatuses or unconformities and completeness of sedimentation. Furthermore, 2-3 mm red-layer has been found completely, and

called boundary layer (Keller et al., 2002). The boundary clay was observed in Göynük and Haymana basins in Turkey (Esmeray, 2008; Karabeyoğlu, 2017; Vardar, 2018).

K/Pg event has great attitude for many scientists and the most popular boundary until today. Scientists have been observing the lithological, geochemical, mineralogical, structural and paleontological changes across this boundary (Font et al., 2016, 2017, 2018). In order to construct the paleogeographic distribution of K/Pg boundary event, many studies with high-resolution sampling on the continuous K/Pg sections have been carried out in Tethyan, Atlantic, and Pacific provinces. The most significant sections are located in Tunisia; El Kef, Elles, Ain Settera, and El Mellah (Smit, 1982; Keller, 1988a,b, 2011; Keller et al., 1996; Arenillas et al., 2000a, b; Zaghib-Turki et al., 2000; Dupuis et al., 2001; Karoui-Yaakoub et al., 2002), in Spain; Caravaca, Agost, Zumaya (Molina et al., 2006; Arenillas et al., 1998, 2006; Arz et al., 2000; Font et al., 2016, 2017), in France; Bidart (Bonte, 1984; Gallala et al., 2009), in Mexico; Bochil, El Mulato, Yucatan Peninsula (Hildebrand et al., 1991; Ward et al., 1995; Molina et al., 2006; Schulte et al., 2005), in Bulgaria; Bjala (Preisinger et al., 2002), in Egypt; Dakhla (Zaid et al., 2015), in Italy, Gubbio, Erto (Luterbacher and Premoli-Silva, 1964; Luciani, 2002), in Iran; Alborz (Rostami et al., 2018), and in Turkey; Göynük, Haymana, Isparta, Ordu (Yıldız and Gürel, 2005; Sagular and Görmüş, 2006; Esmeray, 2008; Açıkalın et al., 2015; Karabeyoğlu, 2017; Vardar, 2018)

The paleontological studies reveal that the abundance of *Guembelitra cretacea* observing in the P0 zone, which is the main survivor after the mass extinction. In addition, *Hedbergella holmdelensis*, and *Hedbergella mountmonensis* are the other survivors. The previous studies also reveal that the bloom of *Guembelitra cretacea* is indicator for P0 zone (Keller, 1988, 1989a, b, 1996; Keller et al., 1993, 2002; Punekar, 2017).

In addition, recent results done in Turkey, revealed that drastically increase in abundance of echinoderm pellets at the boundary, and dinoflagellates abundances are

also clueing for impact theory (Esmeray-Senlet, 2015; Karabeyoğlu, 2017). This statement was started by Alvarez et al. (1980), to suggest the bolide impact based upon the discovery of an Ir anomaly, and microtektites. However, Keller (2012) claimed that the impact occurred inside of the Cretaceous, these anomalies and abundances can be observed as a result of reworking. She also mentioned that because of tectonism and turbidites, which were abundant during the boundary, the reworking process can be seen.

On a global basis, the K/Pg mass extinction has been directly linked to a period of large igneous provinces (LIPs), Deccan Traps in India (Wignall, 2001; Courtillot and Renne, 2003). This rapid and massive volcanism released aerosols and toxic gases that contributes to dramatic climate change, increased acid rains, and ocean acidification (Courtillot et al., 1986; D'Hondt et al., 1994; Wignall, 2001; Self et al., 2008; Ward, 2009; Gertsch et al., 2011; Keller et al., 2012; Font et al., 2014; Abrajevitch et al., 2015). However, the most important results from LIPs is foundation of key proxy elements such as mercury (Hg), which have been identified as possible markers for LIPs (Grasby et al., 2015; Font et al., 2016, 2017, 2018).

Based on Font and his colleagues (2011, 2014, 2016, 2017), Hg composition and dissolution of detrital magnetite and disappearance of biogenic magnetite, from magnetic susceptibility analysis, induced the Deccan volcanism (Zaid, 2015; Font et al., 2017, 2018; Rostami et al., 2018).

### **1.3.2. Previous Works on the Göynük Basin**

The Göynük Basin has been studied by various researches since 1930s for different purposes because of the study area's potential and importance for geology of Turkey, which is in between Pontides in the north and Anatolide-Tauride Platform in the south and has continuous successions from Jurassic to Miocene (Foley, 1938; Şengör and Yılmaz, 1981; Göncüoğlu et al., 2000; Yılmaz et al., 2010; Ocakoğlu et al., 2018).

The researchers have studied around the region to determine both tectonism and stratigraphy of it. Moreover, some studies have been included sequence stratigraphy with paleontological and geochemical analysis.

The first studies were carried by Foley (1938) and Stchepinsky (1940 a, b) to research mineral deposits, and the detailed stratigraphy was carried on. After Foley and Stchepinsky, Rondot (1956), Abdülselemoğlu (1956), and Ürgün (1956) tried to investigate detailed geological map of the region.

In the 1960s, several studies have been carried on related to petroleum potential of the basin. Türkünal (1963), Kalafatçioğlu and Uysallı (1964), and Beseme (1968) carried out the important studies in terms of both stratigraphical and general geology of the basin. These studies became very important framework not only petroleum geologists, but also for geologists who used this stratigraphical frame as a base of their works.

Detailed sedimentological studies were done by Altınlı (1973a, 1973b, 1976, 1977). He reported the sedimentation started in Jurassic in Sakarya continent. He also interpreted the depositional environment and facies change of the region by sections.

Saner (1977, 1980) studied in the Mudurnu- Göynük basin and construct the paleogeographic maps of the region. Many formations and members in the basin were defined during this study in the first time. Moreover, he claimed Mudurnu- Göynük basin as a forearc basin, which is the very important in terms of geological evolution of the basin.

After these stratigraphical studies, detailed lithological and sequence stratigraphical analysis were carried out. In 1979, Kazancı defined conglomeritic rocks in Haramiköy, around Nallıhan region, on the other hand Varol defined turbiditic limestones of the Seben formations in terms of petrography and microsedimentary studies. In 1984, they worked together on sandy sedimentary units in the Seben formation and constructed the Upper Cretaceous lithostratigraphy of the Sakarya region. In addition, Önal et al. (1988) defined depositional environments of Soğukçam limestones in the north of Çayırhan, Nardın formation, and Group of Kızılçay. This

study also included the age of rock units, the relation with each other, and the disintegration of the facies.

The first biostratigraphical works were carried out by Meriç (1974), Toker (1976), Dizer and Meriç (1981), Meriç and Şengüler (1986). Especially, foraminiferal biozones for Late Cretaceous- Paleogene constructed with using planktonic foraminifera and nannoplankton during this study. Moreover, there have been several studies carried on Central Sakarya region related to petroleum potential. For this reason, 3 detailed geological maps were prepared around Göynük basin (Besbelli, 1991). A lot of stratigraphic section was measured and detailed biostratigraphical studies done in Mudurnu and Seben basin (Şeker and Kesgin, 1991).

Altiner et al. (1991) made stratigraphical analysis of Jurassic- Cretaceous boundary in Mudurnu, Nallıhan and Bilecik. Consequently, detailed ammonite, nannoplankton, and planktonic foraminifera analysis were carried out in these stratigraphical analysis. In addition to this study, Koçyiğit et. al. (1991) performed tectonic evolution on that region.

Ophiolitic and metamorphic rocks on the southern part of Mudurnu- Göynük Basin were discovered by Göncüoğlu et. al. (2000), and they claimed that the basin was a fore-arc basin during Campanian-Maastrichtian, and carbonatous limestone deposited during Early Paleogene. Another metamorphic study was carried on by Okay et. al. (2002). They claimed that İzmir-Ankara suture zone was long term plate boundary from Late Paleozoic to Early Tertiary as evidence of blue schist facies lateral continuity.

Most recent studies related to depositional environment, paleontology, mineralogy, geochemistry, and isotope analysis of the Mudurnu-Göynük basin were carried out by Ocakoğlu et al. (2007, 2018), Açıkalin et al. (2016).

For the lightening of all these previous studies, the aim of this study is to delineate the evolutionary recovery of the planktonic foraminifera after the K/Pg mass extinction by using high-resolution of quantitative data, mineralogical content and mineral

chemistry, and magnetic susceptibility. Furthermore, this study has been carried out to calibrate results of the previous studies on late Cretaceous/early Paleogene of the Göynük basin.

#### **1.4. Regional Geological Settings**

The Göynük basin is located about 96 km SW of Bolu in the Central Sakarya Region, Turkey. It is limited by Pontides to the north, and Anatolide-Tauride Platform to the south (Okay and Tüysüz, 1999). At the beginning, it has been formed by rifting on the Sakarya continent- the continent which was surrounded by the Intra-Pontid Ocean to the north and the northern branch of the Neo-Tethys, i.e. İzmir-Ankara-Erzincan Suture zone, to the south (Şengör and Yılmaz, 1981; Saner, 1980). In other words, the Göynük Basin consists of both Paleo- and Neo- Tethys outcrops from Jurassic to Miocene (Figure 1.2).

The basement of the succession starts with the existence of pre-Jurassic metamorphic and granitic deposits (Şengör and Yılmaz, 1981; Altın et al., 1991; Yılmaz, 2008; Yılmaz et al., 2010; Açıklım et al., 2015). These deposits are separated as three types; Variscan basement (Okay, 2008), Paleozoic granitoids (Okay et al., 2006; Topuz et al., 2007), and Karakaya complex (Bingöl et al., 1975; Şengör et al., 1984; Altın et al., 1991; Göncüoğlu et al., 1997; Okay and Göncüoğlu, 2004) (Figure 1.3, 1.4).

Saner (1980) stated that above the crystalline basement, overlying an unconformity, Early Jurassic Bakırköy and Mudurnu Formations start. In the central part of the succession, the upper Jurassic to lower Cretaceous, Soğukçam Limestone, which is the ammonite bearing pelagic limestone, deposited in Callovian to Aptian/Albian above the Mudurnu Formation (Altın et al., 1991). In the western portion of the succession, shallow marine reefal carbonates deposited as Bilecik Formation interfinger with the deeper pelagic carbonates (Soğukçam Limestone) (Duru et al., 2002; Ocakoğlu et al., 2018). On the other hand, in the eastern portion of the Central

Sakarya region, Soğukçam limestone overlies the Yosunlukbayırı Formation which is composed of radiolarian, and ammonite-bearing yellowish to green colored clayey limestone, detrital limestone and shale at the base and monotonous detrital limestone at the top (Altıner et al., 1991).

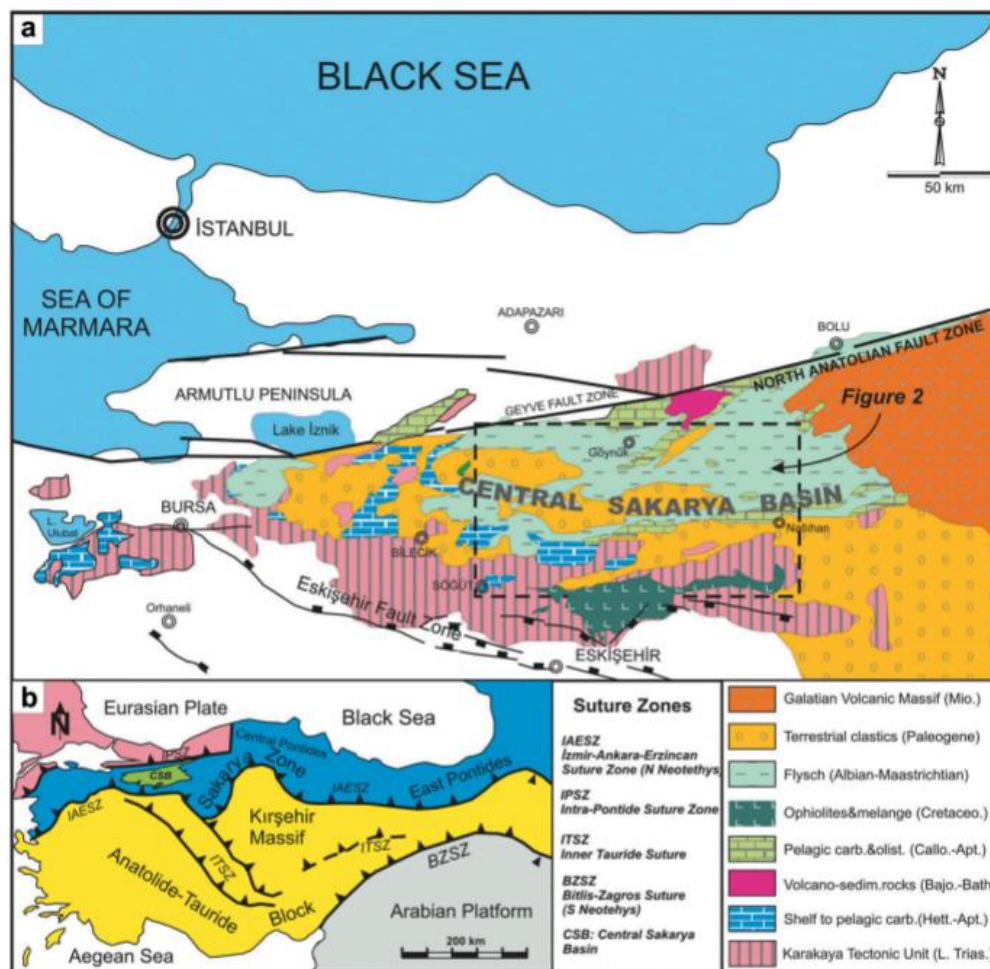


**Figure 1.2:** A) Geological map of the NW Anatolia and the location of the Göynük basin B) Main structural features of Turkey with the main tectonic units (Ocakoğlu et al., 2018).

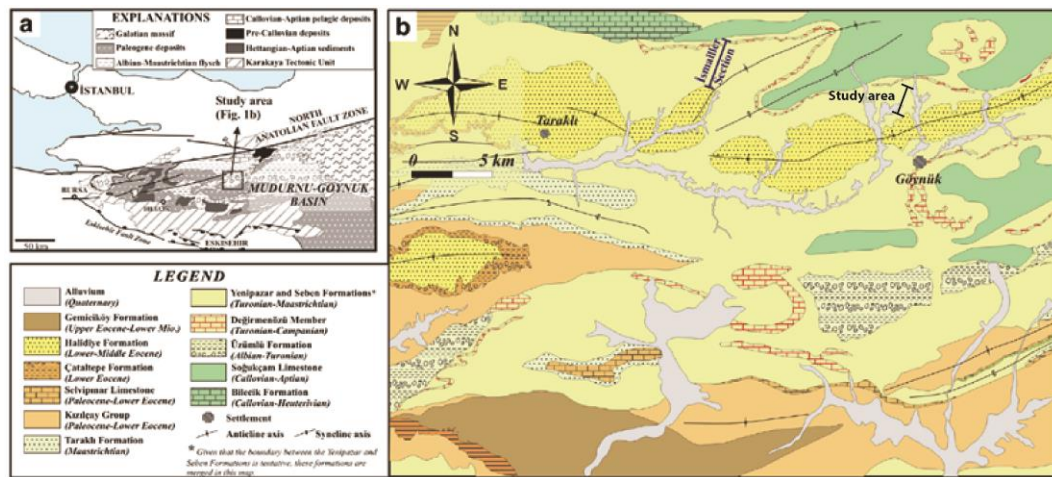


**Figure 1.3:** a. Location of the study area (generalized geology simplified from Altner et al., 1991), b. Geological map of the study area (simplified from Gedik and Aksay, 2002).

The Vezirhan Formation, on the other hand, is composed of pelagic carbonates and Barremian-Albian in age. In the western portion of the Central Sakarya Region, Vezirhan Formation overlies the Bilecik Formation with conformably and it consists of white-red colored clayey limestones (Saner, 1977, 1980).

The Albian- Campanian age was characterized to the Yenipazar Formation, which is consist of pelagic carbonates and continue with turbiditic-volcano-turbiditic successions (Saner, 1980; Altner et al., 1991; Yılmaz et al., 2010). Laterally, Yenipazar formation included Üzümlü Member, volcanoclastics and preserved lava, Değirmenözü Member, pelagic carbonates, and Eymür Member, submarine canyon-fill deposits (Ocakoğlu, 2018). The Üzümlü member record as long-lived submarine volcanism with alternation of rhyolitic lava, tuff, agglomerate, and siliciclastic deposits (Demirkol, 1977; Saner, 1977; Göcüoğlu et al., 1996). The Değirmenözü member, on the other hand, is composed of thin-bedded, pink to beige fossiliferous pelagic limestones with tuff intervals, and it is deposited in the Santonian to early Campanian on the central and eastern parts of the Central Sakarya Region (Saner, 1980; Gedik and Aksay, 2002; Ocakoğlu et al., 2007, 2018). The Eymür member is

composed of terrestrial to shallow marine conglomeratic wedge. It is directly linked with the relative sea-level drop during the mid-Campanian which is only recorded in the eastern part of the Central Sakarya Region (Ocakoglu et al., 2009, 2013, 2018).

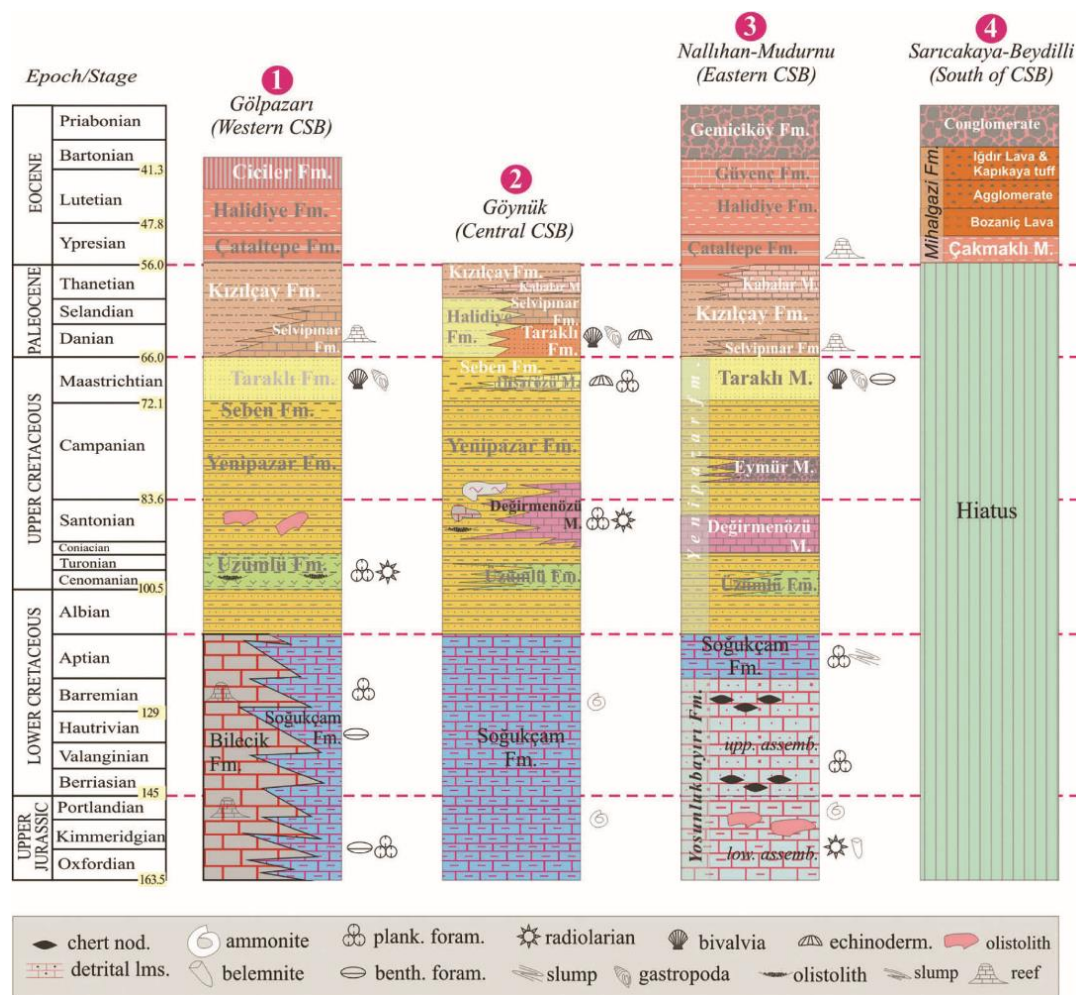


**Figure 1.4:** Generalized stratigraphic columns spanning late Jurassic to Eocene from different parts of the Central Sakarya Basin. (1) Saner (1977) and Duru et al. (2002), (2) Besbelli (1991) and Gedik and Aksay (2002), (3) Timur and Aksay (2002), Tansel (1980) and Altiner et al. (1991), and (4) Yıldız et al. (2015) and Kasapoğlu et al. (2016).

Yenipazar Formation has been placed in various localities with different time intervals in various studies. For example, Saner (1980) claimed that this formation deposited in mid-Campanian in Geyve and Taraklı basin while Altner et al. (1991) stated at the end of the Santonian with paleontological evidences from Mudurnu basin, on the contrary, Şeker and Keskin (1991) and Besbelli (1991) stated to the top of Cenomanian in the Seben and Göynük basins, respectively.

The Yenipazar Formation underlies the Seben Formation, is siliciclastic turbidites and pelagic mudstones. In some localities in the Central Sakarya Region, these two formations laterally change. The Seben Formation is consisted of grey, blue, and green colored marl deposits with some sandstone intercalations. According to Besbelli (1991), these sandstone intercalations are the results of low flow regime turbiditic currents. He also stated that the Hisarözü member in the Seben Formation with composed of limestone and marl alternations. On the other hand, Ocakoğlu et al. (2009) and Açıkalın et al. (2015) revealed that this formation was deposited in front of the large deltaic system.

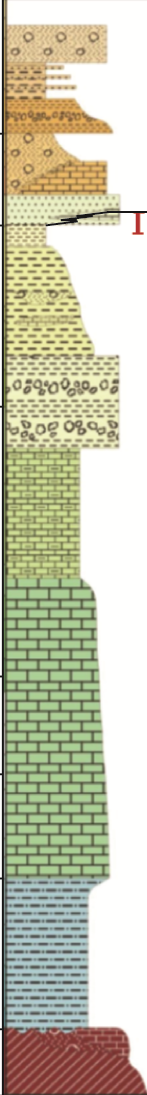
The Taraklı Formation overlies the Seben and Yenipazar Formations, is formed from thick mudstone and sandstone alternations in Paleocene (Ocakoğlu et al., 2018). Mudstone include both micro-fossils and macro-fossils which indicates Early Paleocene. Sandstone beds, on the other hand, include some cross-bedded gravel lenses with abundant macrofossils (Ocakoğlu et al., 2018). The Halidiye Formation, on the other hand, laterally continue with the Taraklı Formation, which is consisted of sandstone and marl alternations (Besbelli, 1991; Ocakoğlu et al., 2018).

The Taraklı Formation is conformably overlain by the Selvipınar Formation, dominantly fossiliferous, partly detrital carbonate. The Kızılçay Formation, Late Paleocene, conformably overlies the Selvipınar formation (Ocakoğlu et al., 2018). The Selvipınar Formation is composed of reefal carbonates whereas the Kızılçay Formation is composed of terrestrial red clastics. These red clastics are dominated by conglomerates and mudstones (Ocakoğlu et al., 2012).

In the Eocene, the Çaltepe Formation, which is the deposition of a shallow marine coarse clastics with abundant molluscs and corals, is deposited in both eastern and western part of the Central Sakarya Region (Ocakoglu et. al., 2018) (Figure 1.5, 1.6).

As the regional geological settings, our studied section is started with the Seben Formation and continue with the Hisarözü Member of Seben Formation which shows the transition of Cretaceous/Paleogene.



Period		Epoch	Lithology	Description
Paleogene	Eocene			CİCİLER FM: shallow marine sandstone-mudstone alternation
				HALİDİYE FM: deep marine mudstone-sandstone alternation
				ÇALTEPE FM: mudstone-sandstone alternation
	Paleocene			Kızıldağ Group: terrestrial deposits Selvîpınar Lmst: bioclastic limestone
				TARAKLI FM: deltaic sandstone
				SEBEN FM: marl deposits
Cretaceous	Upper		YENİPAZAR FM: flysch deposits with mudstone-sandstone-pebble alternation Değirmenözü Member: pelagic limestone	
			ÜZÜMLÜ FM: sandstone-mudstone alternation	
	Lower		VEZİRHAN FM: pelagic limestone	
			2. BİLECİK LMST: shallow marine limestone 1. SOĞUKÇAM LMST: deep marine foraminiferal limestone	
Jurassic	Upper		2. BAKIRKÖY FM: shallow marine detrital deposits 1. MUDURNU FM: tuff, volcanic sandstone and shale alternation	
	Middle			
	Lower			
Before Jurassic				OPHIOLITIC MELANGE with limestone blocks of Permian period

**Figure 1.6:** Generalized tectonostratigraphic and sequence stratigraphic columnar section of the Göynük Basin (Modified from Açıkalın, 2015)(not to scale)

## CHAPTER 2

### STRATIGRAPHY

#### 2.1. LITHOSTRATIGRAPHY

The studied Göynük section (Gk) is in the Central Sakarya Region, comprises Jurassic to Eocene sedimentary sequence (Saner, 1980; Altınar et al., 1991; Besbelli, 1991; Göncüoğlu et al., 2000; Gedik and Aksay, 2002; Açıkalın, 2015; Ocakoğlu et al., 2018). The section is ingrained of Upper Cretaceous Seben Formation, characterized by marl and Lower Paleogene Hisarözü Member of Seben Formation, characterized by alternating clayey limestone and marl deposits. K-Pg boundary is located between these two formations (Figure 2.1).

Seben Formation has been stated by Saner (1977), giving exposure on both Göynük, Mudurnu, Gölpazarı and Nallıhan villages, in the Central Sakarya region. The type section is located in the Ahmetbeyler village (Meriç, 1974). Although the calcareous mudstone intercalations observed in the Hisarözü member of the formation, the main lithological unit of the Seben Formation is marl. It consists of pelagic fossils with nanoplanktons. Its age has been determined as upper Maastrichtian based on the planktonic foraminiferal taxa (*Abathomphalus mayaroensis*, *Rasita contusa*, *R. fornicata*, *Gansserina gansseri*, *Globotruncanita stuartiformis*, *Globotruncana arca*, *Ammodiscus* sp., *Bulimina* sp., *Bolivina* sp., *Heterohelix* sp., *Pseudotextularia* sp., *Ptanoglobulina* sp., *Racemiguembelina* sp., *Pleurostomella* sp., *Stensioeina* sp.).

Seben Formation overlies the Yenipazar Formation with conformable and shows lateral continuity in various localities, its period has been determined as Cretaceous (Saner, 1980; Duru et al., 2002; Ocakoğlu et al., 2018). The lithology of this formation

is grey, blue, and green colored marl deposits. It has a wide range of exposures around the Central Sakarya Region (Saner, 1980; Duru et al., 2002; Ocakoğlu et al., 2018).



**Figure 2.1:** Field photo of the studies Gk-section. Red dots indicate the position of the samples along the section. Red line showing the position of the K/Pg boundary.

Seben Formation is underlying conformably the Halidiye Formation. Halidiye Formation shows laterally changes Taraklı Formations. The lithology of the Halidiye Formation is started with thin sandstone intercalations and continued with the sandstone mudstone alternations (Meriç, 1974).

The Hisarözü member of the Seben Formation, on the other hand, has been stated by Besbelli (1991). According to Gedik and Aksay, the unit shows vertical transition with the Yenipazar Formation, which contained pelagic fossils. It shows marl and clayey limestone alterations in the Göynük section (Figure 2.2).

The total thickness of measured section is 8.55 m, which corresponds 5.63 m of the Maastrichtian, the K-Pg boundary, and 2.92 m of the Danian and 47 samples was collected. The sampling was actually started with the sample Gk-1 from the marl unit and was continued up to the sample Gk-42 from the clayey limestones. After the completing of this measurement, the sampling was restarted approximately 2 meters below the sample Gk-1 and 5 more samples (Gk-04-00) were collected. Although the minor fault was detected between the samples Gk-00 and Gk-1 during the field work, the sampling was continued after the adjustment in the route of the section.



A total of 14 samples within the interval between the samples Gk-04 to Gk-9 corresponds the Maastrichtian part of the Seben Formation. A total of 33 samples within the interval between Gk-10 to Gk- 42 was collected from the Danian part including K/Pg boundary. The sampling interval ranges from 3 to 70 cm. However, around the K/Pg boundary, this sampling interval varies from 3 to 10 cm.

The interval between the samples Gk-11 to Gk-26 is composed of the monotonous marl deposits. The alternation of marl and clayey limestone deposits was sampled within the interval from the samples Gk-27 to Gk-42 (Figure 2.3). These samples are also rich in planktonic and also benthic foraminifera with minor amounts of minerals such as biotite, zircon, iron-rich fragments, etc. (Figure 2.4).



**Figure 2.3:** Closer look to the measured section. Red line: Position of the clayey limestone bed.

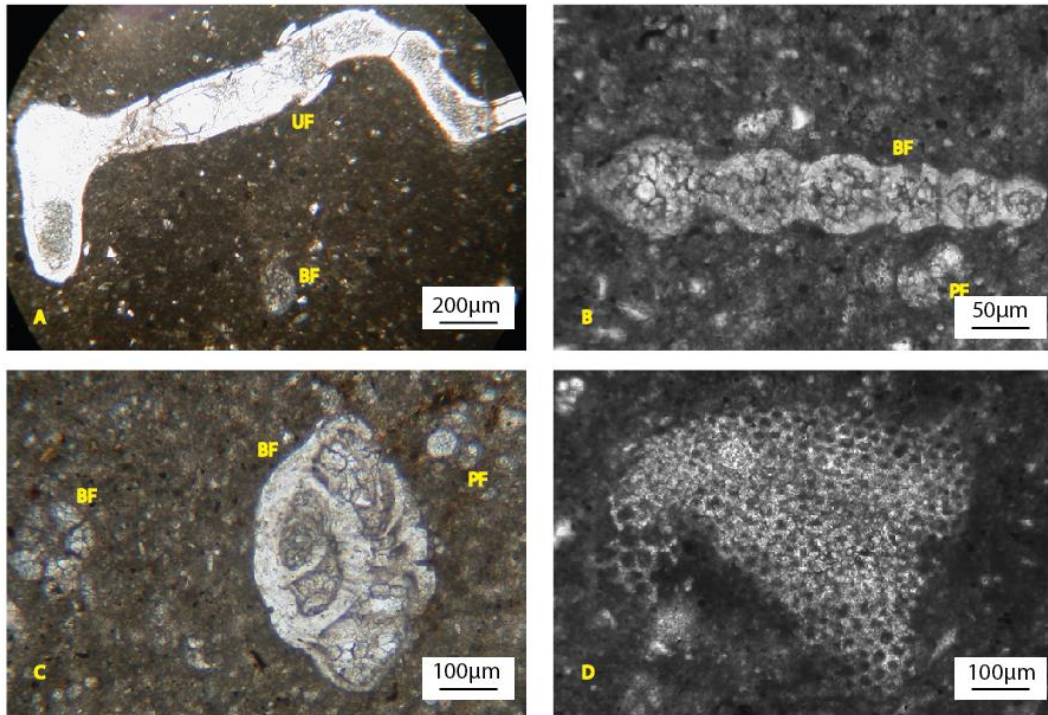


**Figure 2.4:** Thin section microphotographs of several samples. PF: planktonic foraminifera, BF: benthic foraminifera, UF: Undefined fossil fragment.

A brownish horizon having plant root was also recognized between the samples Gk-9 and Gk-10 in this study. This horizon was interpreted as a probable K/Pg boundary during the field work. The red line in the figure 2.1 marks the dark brownish layer having plant root. However, the lateral continuity of the reddish-brownish layer having the plant root was not observed at the outcrop. In some of the previous studies, the K/Pg boundary was also defined by 2-3 mm thick reddish oxidized horizon (e.g. Keller, 2002; Esmeray, 2008; Gallala et al., 2009; Açıkalın et al., 2015; Karabeyoğlu et al., 2019). According to Açıkalın et al. (2015), Karabeyoğlu (2017), and Oçakoğlu et. al. (2018) a few mm-thick reddish to brownish horizon was recognized in both of the Mudurnu-Göynük and Haymana basins. Similar to this study, the lateral continuity of the reddish layer can also not be observed in the Haymana Basin.

In addition, thin-section analysis of the studied samples gave some significant findings such as microspherules, microtektites, and glaucophane grains. The orange to brownish colored iron-rich bubble-shaped forms and green colored glaucophane grains were recognized in some samples (Gk-9, 11, 12, 26, 27, 28) (Fig.2.5). The marl of the sample Gk-10 contains microspherules which can only be observed under the microscope. Another interesting aspect of this finding is that no planktonic foraminifera or any other fossils were observed in these samples. These microspherules are made up of calcite and their abundances are gradually decreased through up the section. The same microspherules were recognized by Karabeyoğlu (2017) at the boundary, in the Haymana Basin, and he interpreted them as *Thoracospharea* (Figure 2.6).

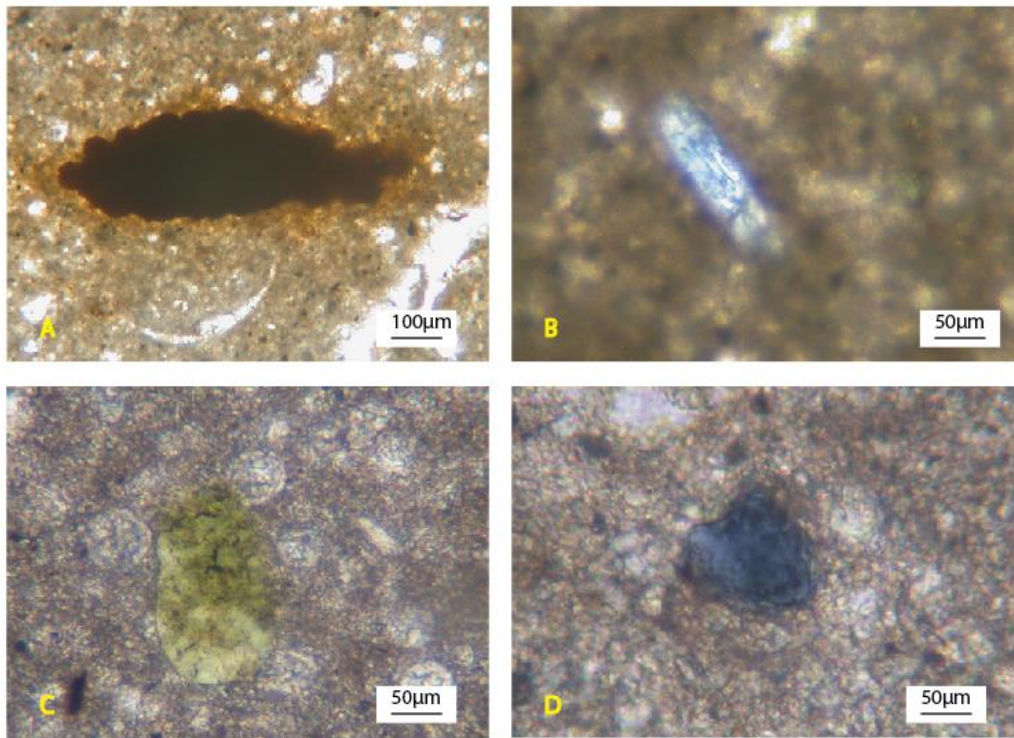


**Figure 2.5:** Microphotographs taken from the marl samples A: iron-bubbles from sample Gk-9, B: Mica mineral from sample Gk-9, C: Glaucophane from sample Gk-26, D: Alteration of Biotite from sample Gk-27

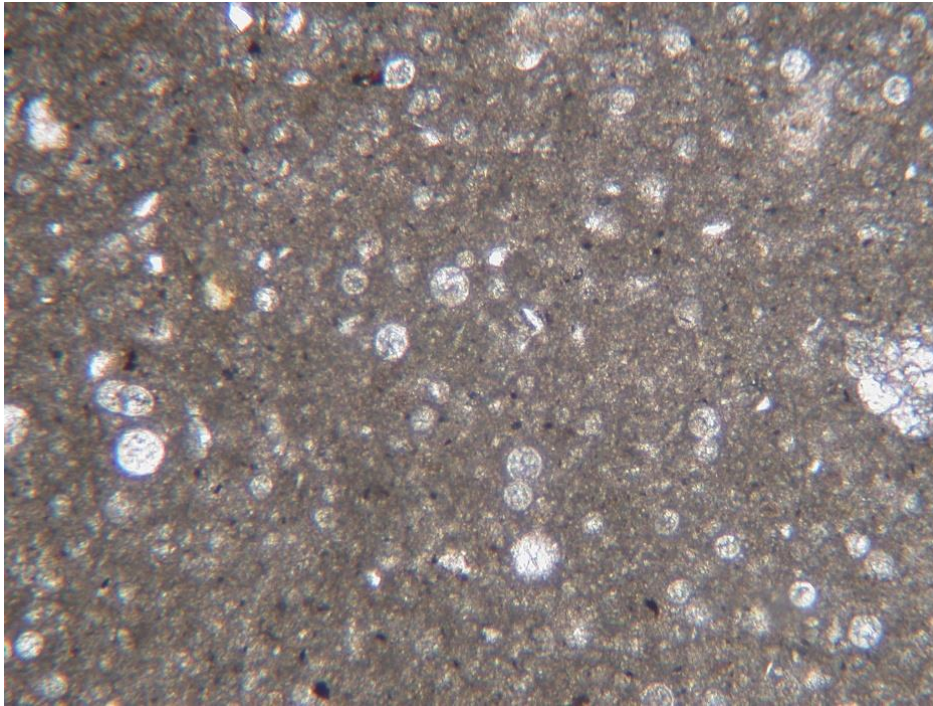


**Figure 2.6:** Thin section view of K/Pg boundary with microspherules.

### **2.1.1. Microfacies Analysis**

The thin-sections of the samples were examined under the microscope in order to define the depositional environment of the studied sequence. According to Flügel (2004), the aim of the microfacies analysis is to recognize the overall patterns reflecting the history of carbonate rocks by using to examine sedimentological and paleontological characteristics. It is the fundamental association to the development of models for carbonate sedimentation. The microfacies analysis can be done by not only thin sections, also peels, polished slabs and rock samples. However, for the Göynük section, only thin sections used for defining the microfacies. Moreover, grain types and frequency, matrix types, depositional fabrics, fossil groups and depositional texture can be used as clues to determine the types of the microfacies (Flügel, 2004).

All of the 47 samples were examined under the microscope. For the classification of the rocks, three main classifications were used such as Folk's classification (1959), Dunham's classification (1962), and Mount's classification (1985). In the Folk's classification, carbonate rocks are accepted as similar to siliciclastic rocks in their mode of deposition. During this classification three main condition that requires to look out; (a) separation of carbonates with micritic or spary matrix, (b) differentiation of fundamental grain types, (c) frequency and proportion of the grain types (Figure 2.7, 2.11). According to the Folk's classification, the studied samples are defined as biomicrite because of their micritic matrix, lack of allochems (less than 10%), and fossil rich content.

The Dunham's classification (1962), widely used for microfacies analysis, includes five textural classes; (a) carbonates whose were originally bound together during deposition (boundstones), (b) carbonates whose originally not bound together, which is divided by mud-support (mudstone and wackestone) or grain-support (packstone and grainstone). The subdivision is based on more or less than 10% of grain bulk boundary (Figure 2.8). The main difference between the Folk's classification and the Dunham's classification is the Dunham's classification can be applied in the field and laboratory studies in other words under the microscope, however, the Folk's classification can be used in only laboratory studies. Based on the Dunham's classification, the studied samples are described as mudstone to wackestone because of mud-supported sedimentation. The mudstone microfacies type is characterized by very low (less than 10%) content of the grains such as planktonic foraminifera. However, wackestone microfacies comprises relatively rich grains (more than 10%) including both planktonic foraminifera and benthic foraminifera.

In the Mount's classification (1985), four components used; (a) siliciclastic sand, (b) non-carbonate mud, (c) carbonate grains or allochems, (d) carbonate mud. The name of the rocks reflects both the dominant grain type and the most abundant antithetic component (Figure-2.9, 2.10) (Flügel, 2004). Based on the Mount's classification, the carbonate contents of the studied samples are higher than siliciclastic content.

# Folk Classification

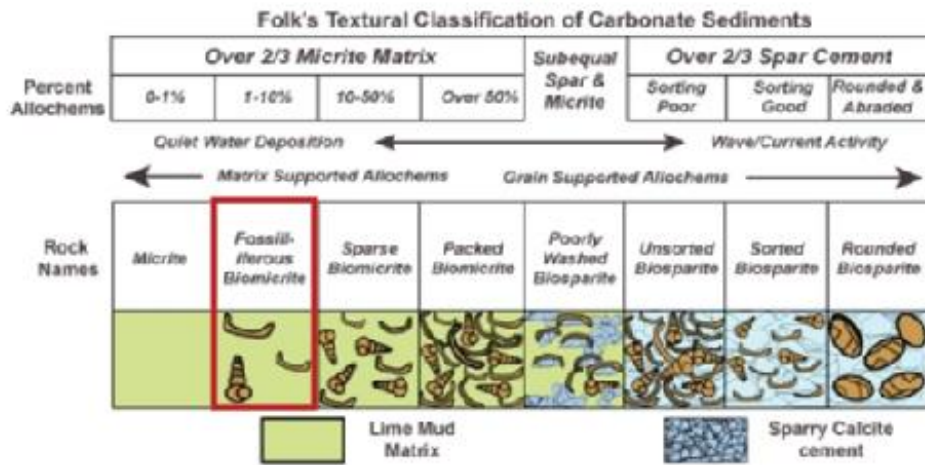


**Figure 2.7:** Folk's Classification of Carbonate Rocks (1959) and its expanded version by Kendall (2005). The one that was recognized in this study have been marked by a red square.

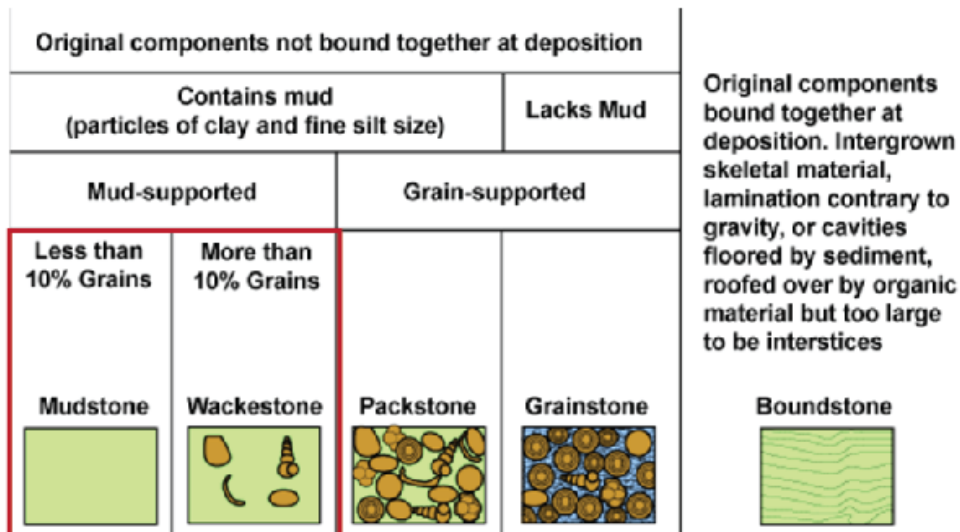


**Figure 2.8:** Dunham's Classification of Carbonate Rocks (1962) and its expanded version by Kendall (2005). The one that was recognized in this study have been marked by a red square.

In the Mount's classification (1985), four components used; (a) siliciclastic sand, (b) non-carbonate mud, (c) carbonate grains or allochems, (d) carbonate mud. The name of the sediment type reflects both the dominant grain type and the most abundant antithetic component (Figure-2.9, 2.10) (Flügel, 2004).

Depositional facies are identified by the concept of the Standard Microfacies Types (SMF) and Ramp Microfacies Types (RMF). By looking all classifications, the facies alternate toe-of-slope and deep sea for SMF and alternate outer ramp to basin for RMF, which is the same identification with the early studies (Table 2.1, Figure 2.12, 2.13) (Açıklalın, 2016).

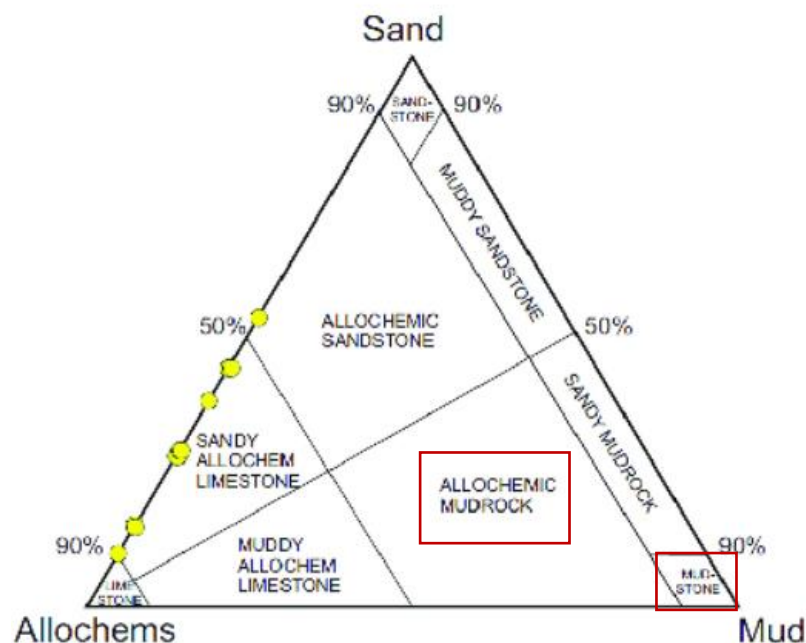


**Figure 2.9:** Mount Classification of Mixed Siliciclastic-Carbonate Rocks (1985). The one that was recognized in this study have been marked by a red square.

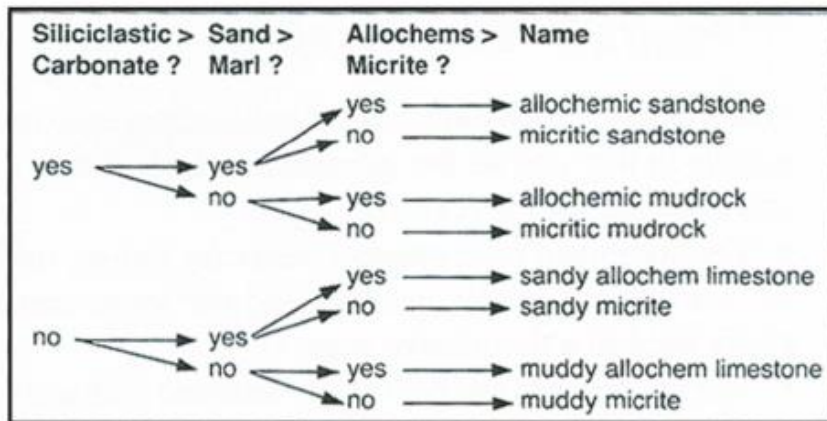


**Figure 2.10:** Mount Classification of Mixed Siliciclastic-Carbonate Rocks (1985)  
(From Flügel, 2004)

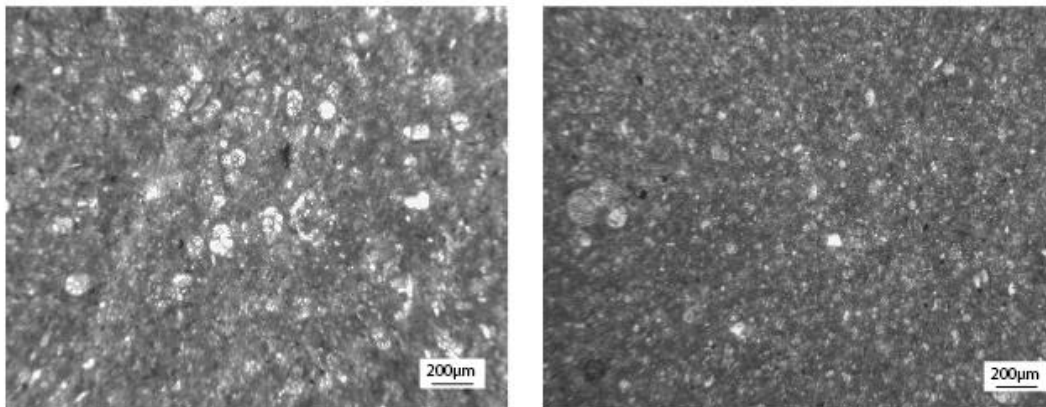


**Figure 2.11:** Wackestone and mudstone in thin section view, respectively.

**Table 2.1:** Microfacies Types of the studied samples in the Göynük Basin in both Classifications

	Folk's Classification	Dunham's Classification	Mount's Classification	Facies
Gk-42	Biomicrite	Wackestone	Allochemic Mudrock	Slope to basin/outer ramp
Gk-41	Biomicrite	Mudstone	Allochemic Mudrock	
Gk-40	Biomicrite	Mudstone to Wackestone	Allochemic Mudrock	Slope to basin/outer ramp
Gk-39	Biomicrite	Mudstone to Wackestone	Micritic Mudrock	Deeper Lagoon/slope
Gk-38	Biomicrite	Wackestone	Micritic Mudrock	Deeper Lagoon/slope
Gk-37	Biomicrite	Mudstone	Allochemic Mudrock	Slope to basin/outer ramp
Gk-36	Biomicrite	Wackestone	Micritic Mudrock	Deeper Lagoon/slope
Gk-35	Biomicrite	Mudstone	Allochemic Mudrock	Slope to basin/outer ramp
Gk-34	Biomicrite	Wackestone	Micritic Mudrock	Deeper Lagoon/slope
Gk-33	Biomicrite	Mudstone	Allochemic Mudrock	Slope to basin/outer ramp
Gk-32	Biomicrite	Wackestone	Allochemic Mudrock	Slope to basin/outer ramp
Gk-31	Biomicrite	Mudstone	Allochemic Mudrock	Slope to basin/outer ramp
Gk-30	Biomicrite	Mudstone to Wackestone	Micritic Mudrock	Deeper Lagoon/slope
Gk-29	Biomicrite	Mudstone	Allochemic Mudrock	Slope to basin/outer ramp
Gk-28	Biomicrite	Mudstone	Allochemic Mudrock	Slope to basin/outer ramp
Gk-27	Biomicrite	Mudstone to Wackestone	Micritic Mudrock	Slope to basin
Gk-26	Biomicrite	Mudstone to Wackestone	Micritic Mudrock	Slope to basin
Gk-25	Biomicrite	Mudstone	Micritic Mudrock	Basin
Gk-24	Biomicrite	Mudstone	Micritic Mudrock	Basin
Gk-23	Biomicrite	Mudstone to Wackestone	Micritic Mudrock	Slope to basin
Gk-22	Biomicrite	Mudstone	Micritic Mudrock	Basin
Gk-21	Biomicrite	Mudstone	Micritic Mudrock	Basin
Gk-20	Biomicrite	Mudstone	Micritic Mudrock	Basin
Gk-19	Biomicrite	Mudstone	Micritic Mudrock	Basin
Gk-18	Biomicrite	Mudstone	Micritic Mudrock	Basin
Gk-17	Biomicrite	Mudstone	Micritic Mudrock	Basin
Gk-16	Biomicrite	Mudstone	Micritic Mudrock	Basin
Gk-15	Biomicrite	Mudstone	Micritic Mudrock	Basin
Gk-14	Biomicrite	Mudstone	Micritic Mudrock	Basin
Gk-13	Biomicrite	Mudstone	Micritic Mudrock	Basin
Gk-12	Biomicrite	Mudstone	Micritic Mudrock	Basin
Gk-11	Biomicrite	Mudstone	Micritic Mudrock	Basin
Gk-10	Biomicrite	Mudstone	Micritic Mudrock	Basin
Gk-9	Biomicrite	Mudstone	Micritic Mudrock	Basin
Gk-8	Biomicrite	Mudstone	Micritic Mudrock	Basin
Gk-7	Biomicrite	Mudstone	Micritic Mudrock	Basin
Gk-6	Biomicrite	Mudstone	Micritic Mudrock	Basin
Gk-5	Biomicrite	Mudstone	Micritic Mudrock	Basin
Gk-4	Biomicrite	Mudstone	Micritic Mudrock	Basin
Gk-3	Biomicrite	Mudstone	Micritic Mudrock	Basin
Gk-2	Biomicrite	Mudstone to Wackestone	Micritic Mudrock	Slope to basin
Gk-1	Biomicrite	Mudstone to Wackestone	Allochemic Mudrock	Slope to basin/outer ramp
Gk-00	Biomicrite	Wackestone	Allochemic Mudrock	Slope to basin/outer ramp
Gk-01	Biomicrite	Wackestone	Allochemic Mudrock	Slope to basin/outer ramp
Gk-02	Biomicrite	Wackestone	Allochemic Mudrock	Slope to basin/outer ramp
Gk-03	Biomicrite	Wackestone	Allochemic Mudrock	Slope to basin/outer ramp
Gk-04	Biomicrite	Wackestone	Allochemic Mudrock	Slope to basin/outer ramp

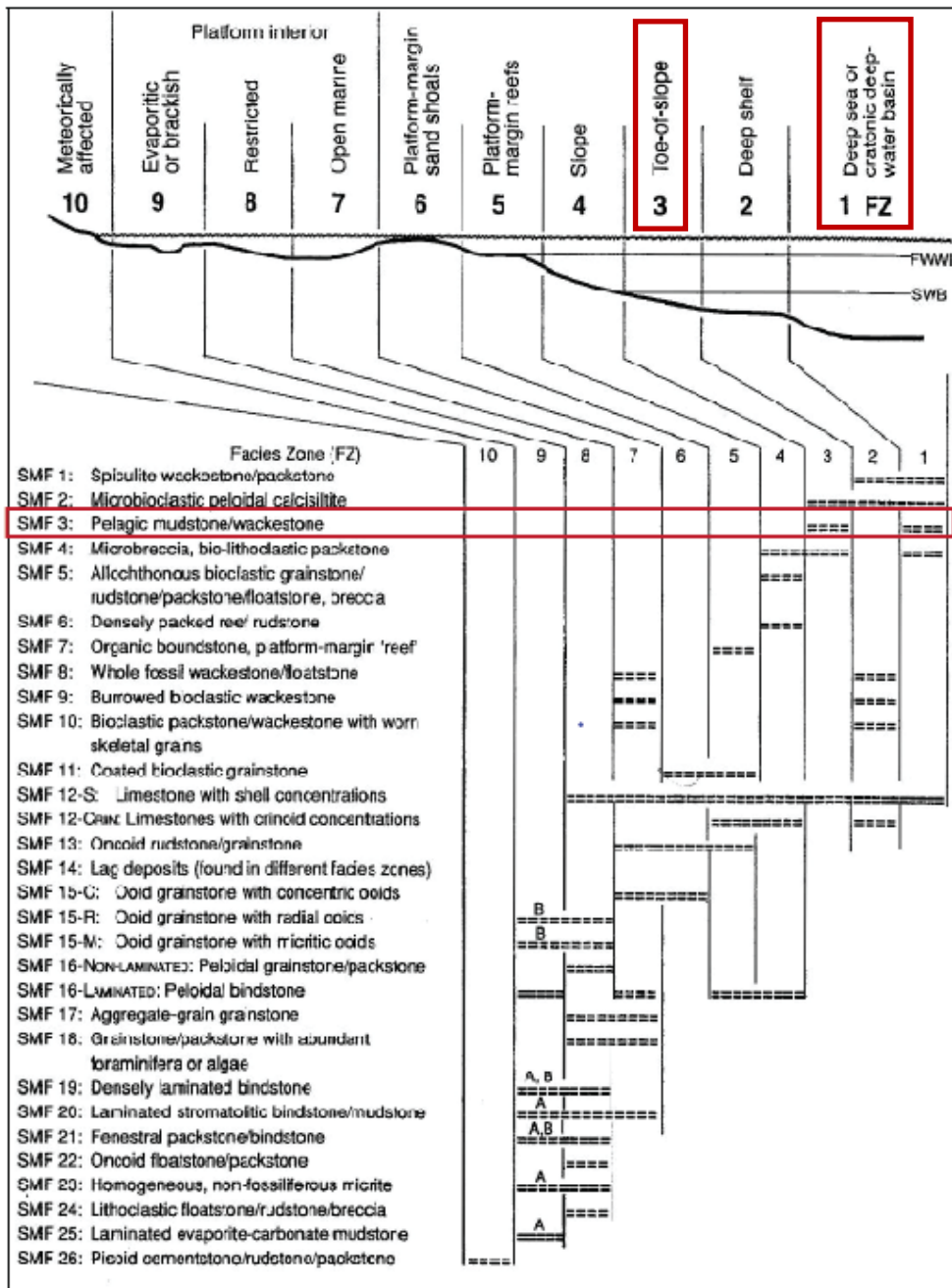


**Figure 2.12:** Distribution of Standard Microfacies (SMF) types in the Facies Zones (FZ) of Wilson (1975) on a rimmed carbonate platform model (Flügel, 2004). The one that was recognized in this study have been marked by a red square.

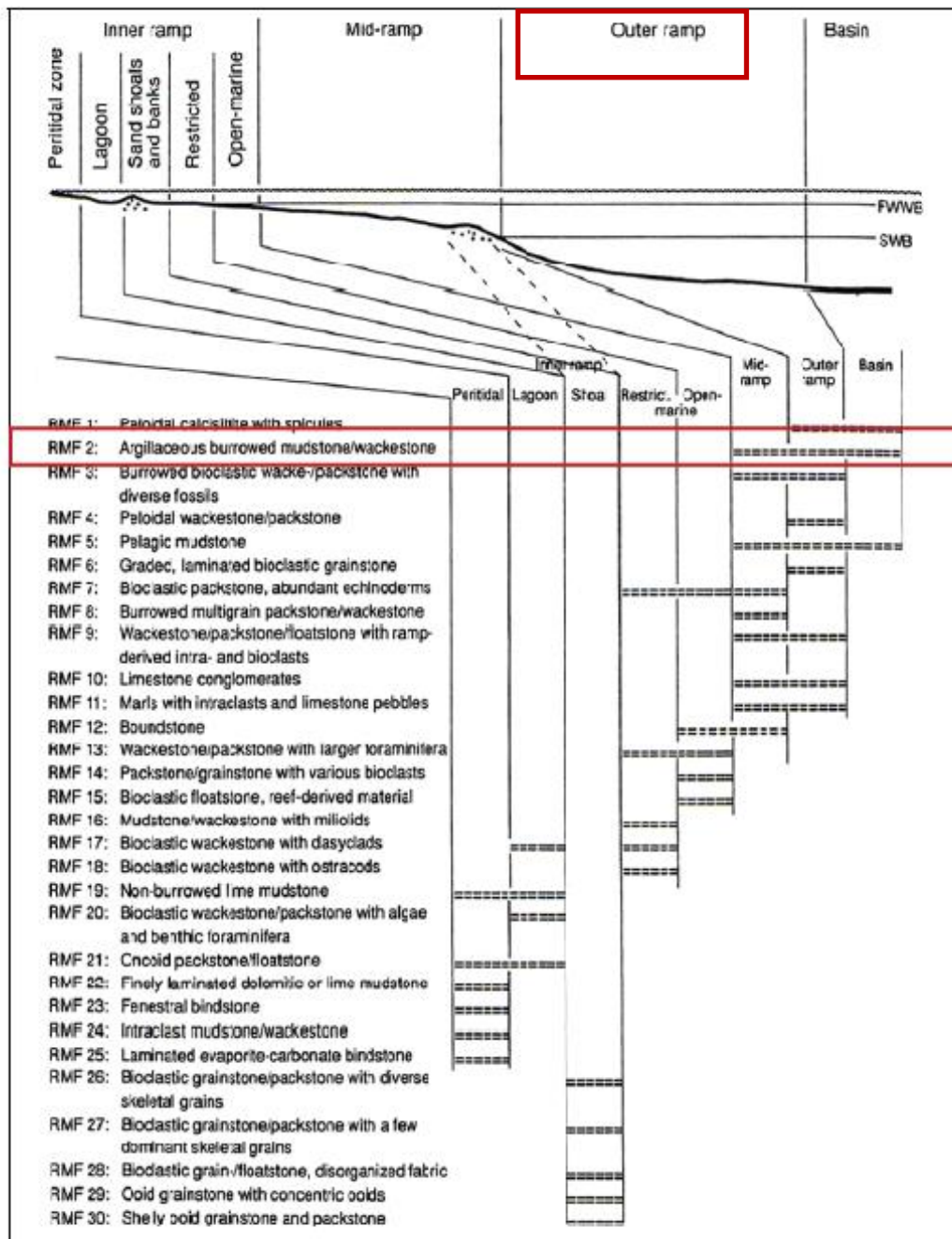


**Figure 2.13:** Generalized distribution of microfacies types (RMF) in different parts of a homoclinal carbonate ramp (Flügel, 2004). The one that was recognized in this study have been marked by a red square.

## 2.2. BIOSTRATIGRAPHY

Biostratigraphy is the most important part of this study because the chronostratigraphic time lines are determined by some marker bioevents. Planktonic foraminiferal biostratigraphy has been established by using bioevents such as first occurrence datum (FOD) and last occurrence datum (LOD) of some marker species. In addition to planktonic foraminifera, some benthic foraminifera are also recognized. However, they were not used in the biozonation. Although there are numerous studies on the planktonic foraminifera of Maastrichtian and K/Pg boundary in different locations parts around the world, there is a limited number of the study carried out on planktonic foraminifera of Danian.

According to previous studies, the Maastrichtian was represented by biozone; *Abathomphalus mayaroensis* total range zone as youngest zone (Smit, 1982; Keller, 1993; Berggren et al., 1995; Premoli-Silva, 2004, Gallala et al., 2009). However, it has been found that *Abathomphalus mayaroensis* zone is a problematic because of its long stratigraphical range of the nominal taxon (□ 1.2 m.y.). In default of *Abathomphalus mayaroensis* total range zone, *Plummerita hantkeninoides* total range zone has been identified for uppermost Maastrichtian (Keller, 1995; Pardo et al., 1996; Li and Keller, 1998; Arenillas et al., 2000; Obaidalla, 2005; Punekar, 2016; Karabeyoğlu, 2017). In our samples, *Plummerita hantkeninoides* has not been encountered, even if the section exhibits no hiatus. In some of the previous researches carried on the higher latitudes of the Atlantic and Antarctic oceans (DSDP sites 738C, 752B, and 690C, Keller 1993), the Haymana Basin (Esmeray, 2008), and the Bidart section in France (Gallala et al., 2009) the *Plummerita hantkeninoides* was not also recorded because they were restricted to the deeper water of tropical and subtropical realms. Therefore, the most reliable index species of the uppermost Maastrichtian, *Pseudoguembelina hariaensis*, was recorded in the studied section.

On the other hand, the Danian stage is subdivided into five biozones; *Guembelitra cretacea* (P0), *Parvularugoglobigerina eugubina* (P $\alpha$ ), P1a, P1b, and P1c from older to younger (Smit, 1982; Berggren et. al., 1995; Arenillas et. al., 2000; Obaidalla, 2005; Gallala et al., 2009). On the contrary, *Parvularugoglobigerina eugubina* zone is a problematic zone. This zone associated with P1a total range zone by different authors (Smit, 1982; Keller et. al., 1995; Keller, 1993; Pardo et. al., 1999; Esmeray, 2008; Punekar, 2016; Karabeyođlu, 2017).

In this study 5 biozones have been established from Maastrichtian to Danian in the ascending order; *Pseudoguembelina hariaensis* zone, *Guembelitra cretacea* (P0) zone, P1a zone, P1b zone, and P1c zone (Figure 2.13). The boundary between P1b and P1c zones has been delineated for the first time in this study.



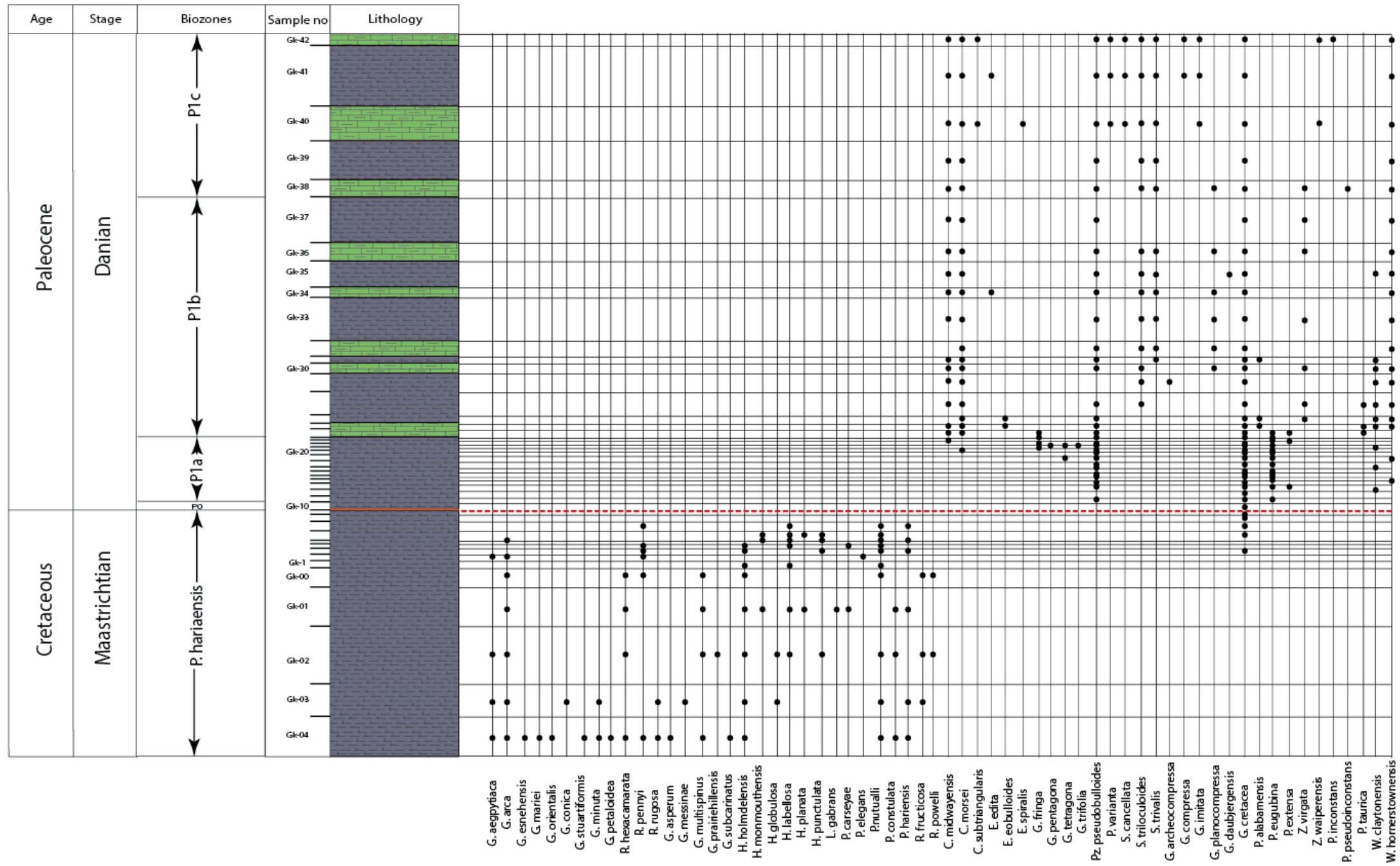


Figure 2.14: Stratigraphical distribution of recorded taxa in the studied section



### 2.1.1. *Pseudoguembelina hariaensis* Interval Zone

**Author:** Li and Keller, 1998

**Definition:** This interval zone represents from the First Occurrence Datum (FOD) of the *Pseudoguembelina hariaensis* to extinction of all high ornamented, large, complex Cretaceous form including the nominated taxon.

**Remarks:** This zone is the uppermost biozone in the Late Maastrichtian, and lowest biozone in the studied sequence. Moreover, its top marks of the K/Pg boundary. The upper limit of this zone coincides with the mass extinction of large, highly ornamented, complex taxa.

In the studied section, First Occurrence Datum (FOD) of the *Pseudoguembelina hariaensis* was recorded in the first Sample (Gk-04), so all Cretaceous samples correspond to this zone (Gk-04 to Gk-9). This zone is represented by 5.43 m-thick succession in the Gk-section. The recorded characteristic planktonic foraminiferal assemblage of this zone shows a gradual decrease in both numbers of species and individual numbers from bottom to top.

Based on faunal changes and comparison with zone *Pseudoguembelina hariaensis* assemblages elsewhere in the Tethys region, including Turkey, is nearly the same except some planktonic foraminifera species.

Species of planktonic foraminifera that are identified in this zone: *Globotruncana aegyptiaca*, *Globotruncana arca*, *Globotruncana esnehensis*, *Globotruncana mariei*, *Globotruncana orientalis*, *Globotruncanita conica*, *Globotruncanita stuartiformis*, *Globotruncanella minuta*, *Globotruncanella petaloidea*, *Rugoglobigerina hexacamerata*, *Rugoglobigerina pennyi*, *Rugoglobigerina rugosa*, *Globigerinelloides asperum*, *Globigerinelloides messinae*, *Globigerinelloides multispinus*, *Globigerinelloides prairiehillensis*, *Globigerinelloides subcarinatus*, *Hedbergella holmdelensis*, *Hedbergella monmouthensis*, *Heterohelix globulosa*, *Heterohelix*

*labellosa*, *Heterohelix planata*, *Heterohelix punctulata*, *Laeviheterohelix glabrans*, *Planoglobulina carseyae*, *Pseudotextularia elegans*, *Pseudotextularia nuttalli*, *Pseudoguembelina costulata*, *Pseudoguembelina hariaensis*, *Racemiguembelina fructicosa*, *Racemiguembelina powelli*.

**Estimated Age:** Late Maastrichtian with the time span between 66.83 Ma and 65.45 Ma.

**Stratigraphic Distribution:** From sample Gk-04 to the sample Gk-9.

### 2.1.2. *Guembelitra cretacea* (P0) Partial Range Zone

**Author:** Keller, 1988, emendation of Smit, 1982

**Definition:** This zone represents interval from the Last Occurrence Datum (LOD) of the *Pseudoguembelina hariaensis* and extinction of complex Cretaceous species to the First Occurrence Datum (FOD) of the *Parvularugoglobigerina eugubina*.

**Remarks:** This zone is the lowermost biozone in the Early Danian, and marks of the K/Pg boundary. The upper limit of this zone coincides with the FOD of *Parvularugoglobigerina eugubina* by Luterbacher and Premoli-Silva (1964). Lithologically, this zone is marked by a dark, red clay layer at the base (Keller, 1998; Arenillas et al., 2000; Obaidalla, 2005; Karabeyoğlu, 2017). In the Göynük section, this the presence of red clay layer partially preserved.

This zone was initially defined by Smit (1982) as an interval between LOD of Cretaceous taxa and FOD of *Globigerina minutula*. The taxonomic concept is the same with Keller (1993), Keller et al. (1995), and Esmeray (2008). Obaidalla (2005) define this zone as *G. conusa* and placed this zone just above the K/Pg boundary. Nevertheless, other authors followed the definition of the Keller (1988), emended of Smit (1982) as the biostratigraphically interval between LOD of *Abathomphalus*

*mayaroensis* and /or *Plummerita hantkeninoides* taxon range zones with the FOD of *Parvularugoglobigerina eugubina* zone (Berggren et al., 1995; Pardo et al., 1999; Gallala et al., 2009; Punekar et al., 2016).

In addition, this zone is characterized by the blooms of *Guembelitra cretacea*, survived species from the K/Pg boundary. Because of the abundance of this species some researchers preferred to use the *G. cretacea* zone instead of the P0 zone (Berggren et al., 1995; Pardo et al., 1999; Arenillas et al., 2000; Esmeray, 2008; Gallala et al., 2009; Karabeyoğlu, 2017).

In the studied section, FOD of the *Parvularugoglobigerina eugubina* was recorded to the Gk-11, so P0 zone is characterized by high abundance of opportunistic *Guembelitra cretacea* taxa, similar with previous studies (Smit, 1982; Keller et al., 1995; Li and Keller, 1998; Berggren et al., 1995; Pardo et al., 1999; Arenillas et al., 2000; Esmeray, 2008; Gallala et al., 2009; Punekar, 2016; Karabeyoğlu, 2017) (Table 2.2). This biozone corresponds to 8 cm thick part of the Gk-section. The only species of planktonic foraminifera that identified in this zone is *Guembelitra cretacea*.

**Estimated Age:** Early Danian with the time span between 65.45 Ma to 64.97 Ma.

**Stratigraphic Distribution:** The single sample Gk-10.

### **2.1.3. *Parvularugoglobigerina eugubina* (P1a) Total Range Zone**

**Author:** Liu (1993) emendation of Pa Zone of Blow (1979) and *Globigerina eugubina* Zone of Luterbacher and Premoli Silva (1964).

**Definition:** This zone represents the interval from the FOD of the *Parvularugoglobigerina eugubina* to LOD of the *Parvularugoglobigerina eugubina*.

**Remarks:** This zone is the taxon range zone of *Parvularugoglobigerina eugubina*. In the studied section, the FOD and LOD of the *Parvularugoglobigerina eugubina* were

recognized in the sample Gk-11, and Gk-25, respectively. This zone corresponds to 78 cm thick portion of the Gk-section.

This biozone was described in two ways by some of the authors. The first is *Parvularugoglobigerina eugubina* (Pa) zone because of the taxon range zone of this species (Arenillas et al., 2000; Obaidalla, 2005; Gallala et al., 2009). The second is the P1a zone, similar with this study, because of the new evolved planktonic foraminifera assemblages after the P0 zone in addition to *Parvularugoglobigerina eugubina* (Smit, 1982; Pardo et al., 1999; Esmeray, 2008; Karabeyoğlu, 2017). However, in addition to these terminologies, some of the studies revealed that P1a biozone can be subdivided in to two parts; P1a(1), and P1a(2), based on the FOD of *Parasubbotina pseudobulloides* and/or *Subbotina triloculinoides* (Keller et al., 1995; Li and Keller, 1998; Keller, 1993; Punekar, 2016). In addition to this definition, Keller (2012) claimed that this subdivision helps to easily recognize biozones because the sections, acrossing the K/Pg boundary, are located in tectonically active regions with dominated by turbidites. This means that the undulating erosional surfaces are mainly observed in the studied sections. Erosion of the earliest Danian, included P0 and P1a zones, is commonly observed throughout Egypt, Sinai, Negev (Keller and Benjamini, 1991; Keller, 2002; Keller et al., 2002; Tantawy, 2003; Adatte et al., 2005), Madagascar (Abramovich et al., 2002), and North Atlantic (Keller et al., 1993, 2013). According to Keller (2012), this subdivision helps to easily recognize P1a zone around the world.

The characteristic planktonic foraminiferal assemblage of this zone shows a gradual recovery of the planktonic foraminifera species, some complex and general species starts to evolve in this zone (*Chiloguembelina midwayensis*, *Chiloguembelina morsei*, *Eoglobigerina eobulloides*, *Globigerina fringa*, *Parasubbotina pseudobulloides*, *Parvularugoglobigerina eugubina*, *Parvularugoglobigerina extensa*, *Zeuvingerina virgata*, *Woodringina claytonensis*, *Woodringina hornerstownensis*). This is not whole/complete recovery. However, the opportunistic species *Guembelitra cretacea* was seen in this biozone, not as much as P0.

Species of planktonic foraminifera identified in this zone: *Guembelitra cretacea*, *Chiloguembelina midwayensis*, *Chiloguembelina morsei*, *Eoglobigerina eobulloides*, *Globigerina fringa*, *Parasubbotina pseudobulloides*, *Parvularugoglobigerina eugubina*, *Parvularugoglobigerina extensa*, *Zeauvigerina virgata*, *Woodringina claytonensis*, *Woodringina hornerstownensis*.

**Estimated Age:** Early Danian with the time span between 64.97 Ma to 64.5 Ma.

**Stratigraphic Distribution:** From sample Gk-11 to the sample Gk-25.

#### 2.1.4. P1b Interval Zone

**Author:** Berggren et al., 1995; emendation of Berggren and Miller, 1988.

**Definition:** This zone represents interval from the LOD of the *Parvularugoglobigerina eugubina* to the FOD of the *Parasubbotina varianta*.

**Remarks:** This zone is the interval biozone in the Early Danian. In the studied section, LOD of the *Parvularugoglobigerina eugubina* was recorded in the sample (Gk-26), FOD of the *Parasubbotina varianta* was recognized in the sample (Gk-38). This zone corresponds to 2,67 m-thick succession of the Gk-section. According to Berggren and Miller (1988), P1b zone was defined as subzone. However, Berggren et al. (1995) defined this zone as a biozone.

This biozone was described differently by some authors. Smit (1982), Arenillas et al. (2000), and Gallala et al. (2009) described it as *P. pseudobulloides* zone which includes nearly P1b and P1c zones. They defined this interval as between the FOD of *Subbotina triloculinoides* and FOD of *Globanomalina compressa*. In addition, the *P. pseudobulloides* zone was defined by Obaidalla et al. (2005) by using the LOD of *P. eugubina* and FOD of *S. triloculinoides*. The P1b zone is defined as including P1a and P1b zones and P1b and P1c zones from Berggren et al. (1995) and Pardo et al. (1999),

respectively. On the other hand, Keller et al. (1995), Li and Keller (1998), Keller (1993), Punekar (2016), defined the P1b zone as an interval between LOD of the *Parvularugoglobigerina eugubina* and FOD of the *Parasubbotina varianta*.

In terms of planktonic foraminiferal assemblages, this biozone is dominated by *Guembelitra cretacea*, with biserial species (*Woodringina hornerstownensis*, *W. claytonensis*, *Chiloguembelina morsei*, *C. midwayensis*, and *Zeauvigerina virgata*). Moreover, the complex forms (*Eoglobigerina edita*, *Eoglobigerina eobulloides*, *Globigerina fringa*, *Globigerina pentagona*, *Globigerina tetragona*, *Globigerina trifolia*, *Parasubbotina pseudobulloides*, *Parasubbotina varianta*, *Subbotina triloculinoides*, *Subbotina trivialis*, *Globanomalina archeocompressa*, *Globanomalina planocompressa*, *Parvularugoglobigerina alabamensis*, *Praemurica pseudoinconstans*, *Praemurica taurica*) were recorded in the studied Göynük section. Furthermore, *Globoconusa daubjergensis* was observed in the P1b zone similar with the Wadi Hamama and the Wadi Nukhul sections (Punekar, 2016).

Species of planktonic foraminifera that were identified in this zone: *Chiloguembelina midwayensis*, *Chiloguembelina morsei*, *Eoglobigerina edita*, *Eoglobigerina eobulloides*, *Globigerina fringa*, *Globigerina pentagona*, *Globigerina tetragona*, *Globigerina trifolia*, *Parasubbotina pseudobulloides*, *Parasubbotina varianta*, *Subbotina triloculinoides*, *Subbotina trivialis*, *Globanomalina archeocompressa*, *Globanomalina planocompressa*, *Globoconusa daubjergensis*, *Guembelitra cretacea*, *Parvularugoglobigerina alabamensis*, *Zeauvigerina virgata*, *Praemurica pseudoinconstans*, *Praemurica taurica*, *Woodringina claytonensis*, *Woodringina hornerstownensis*.

**Estimated Age:** Early Danian with the time span between 64.5 Ma to 63 Ma.

**Stratigraphic Distribution:** From sample Gk-26 to the sample Gk-37.

### 2.1.5. P1c Interval Zone

**Author:** Berggren et al., 1995; emendation of Berggren and Miller, 1988.

**Definition:** This zone represents interval from the FOD of the *Parasubbotina varianta* to the FAD of the *Praemurica trinidadensis*.

**Remarks:** This zone is the interval biozone and the uppermost biozone of this study. In the studied section, the FOD of the *Parasubbotina varianta* was recognized in the sample (Gk-38). However, the FOD of the *Praemurica trinidadensis* was not recorded because of the sampling limit of the studied section. This zone corresponds to 1,89 m thick portion of the Gk-section.

In literature, this biozone was recognized in very limited studies by using similar assemblage of planktonic foraminiferal taxa. In these studies, the zone spanned the interval between FOD of the *Parasubbotina varianta* and the FOD of the *Praemurica trinidadensis* (Keller et al., 1995; Li and Keller, 1998; Keller, 1993; Punekar, 2016). As mentioned above, some researchers defined this biozone inside of the P1b, and *P. pseudobulloides* zone (Smit, 1982; Gallala et al., 2009).

The planktonic foraminiferal assemblages of this zone shows a rapid recovery of the equilibrium species, many complex and general species begin to evolve in this zone. Morphologically complex planktonic foraminiferal assemblages which were adapted ecologically normal environmental conditions were evolved in this biozone (*Chiloguembelina subtriangularis*, *Eoglobigerina spiralis*, *Parasubbotina varianta*, *Subbotina cancellata*, *Globanomalina compressa*, *Globanomalina imitata*, *Praemurica inconstans*, *Praemurica pseudoinconstans*). On the other hand, the opportunistic species like *Guembelitra cretacea* drastically decline in abundance within this biozone. In the uppermost part of P1c zone, only 3% of the whole individuals was identified as the *Guembelitra cretacea*. This indicates that the

recovery process was completed. This zone has been recorded for the first time in Turkey.

Species of planktonic foraminifera that identified in this zone: *Eoglobigerina edita*, *Eoglobigerina spiralis*, *Parasubbotina pseudobulloides*, *Parasubbotina varianta*, *Subbotina cancellata*, *Subbotina triloculinoides*, *Subbotina trivialis*, *Parvularugoglobigerina extensa*, *Globanomalina compressa*, *Globanomalina imitata*, *Globanomalina planocompressa*, *Praemurica inconstans*, *Praemurica pseudoinconstans*, *Chiloguembelina midwayensis*, *Chiloguembelina morsei*, *Chiloguembelina subtriangularis*, *Woodringina hornerstownensis*, *Zeauvigerina virgata*, *Zeauvigerina waiparaensis*, *Guembelitra cretacea*.

**Estimated Age:** Early Danian with the time span between 63 Ma to 62.3 Ma.

**Stratigraphic Distribution:** From sample Gk-38 to the sample Gk-42.

**Table 2.2:** Correlation Maastrichtian and Danian Biozones and our biozonation in the Göynük Basin.

Age	Datum events in this study	This Study	Smit, 1982	Keller <i>et al.</i> , 1995 Li & Keller, 1998	Keller, 1993	Berggren <i>et al.</i> , 1995	Pardo <i>et al.</i> , 1999	Arenillas <i>et al.</i> , 2000	Obaidalla, 2005	Esmeray, 2008	Gallala, 2009	Punekar, 2016	Karabeyoğlu, 2017	
		Turkey, Göynük Basin		Tunisia, El Kef & Elles	ODP Site 738C	Standard Zonation	Kazakhstan Koshan		Egypt, Wadi Nukbul	Turkey, Haymana Basin	France, Bidart	Wadi Hamama Wadi Nukhul	Turkey, Haymana Basin	
Danian	<i>P. varianta</i> ↑ <i>P. eugubina</i> ↓ <i>P. eugubina</i> ↑	P1c	P1b	P1c	P1c	P1	P1c	Unzoned	<i>P. pseudobulloides</i>	<i>S. triloculinooides</i>	Unzoned	<i>P. pseudobulloides</i>	P1c	Unzoned
		P1b		P1b	P1b		P1b	P1c		<i>P. pseudobulloides</i>		P1b		
		P1a		P1a	P1a		P1a (2)	P1a		P1a (2)		<i>P. eugubina</i> P1a	<i>P. eugubina</i>	
	P1a (1)		P1a (1)			<i>P. eugubina</i> P1a	P1a (1)							
	P0	<i>G. cretacea</i> P0	P0	P0	<i>G. cretacea</i> P0	<i>G. cretacea</i> P0	<i>G. cretacea</i> P0	<i>G. cretacea</i> P0	<i>G. comusa</i>	<i>G. cretacea</i> P0	<i>G. cretacea</i> P0	P0	<i>G. cretacea</i> P0	
Maastrichtian	Ext. Cretaceous ↓	<i>P. hantkeninoides</i>	<i>A. mayaroensis</i>	<i>P. hantkeninoides</i>	Unzoned	<i>A. mayaroensis</i>	Unzoned	<i>P. hantkeninoides</i>	<i>A. mayaroensis</i>	<i>P. hantkeninoides</i>	<i>P. hantkeninoides</i>	<i>A. mayaroensis</i>	<i>P. hantkeninoides</i>	<i>P. hantkeninoides</i>
				<i>P. palpebra</i>	Unzoned									
		<i>P. hantkeninoides</i>												
		<i>R. fructicosa</i>												
		<i>P. intermedia</i>		Unzoned										



## CHAPTER 3

### PLANKTONIC FORAMINIFERAL SPECIES TURNOVER ACROSS THE K/PG BOUNDARY INTERVAL

Due to the major extinction, one of the largest and most significant species turnovers in the evolutionary history of planktonic foraminifera occurs across the K/Pg boundary (e.g. Alvarez et al., 1980; Smit, 1982; Hildebrand et al., 1991; Gallala et al., 2009; Arenillas et al., 2000; Keller, 2002; Schulte et al., 2010; Punekar et al., 2014, 2016; Asgharian-Rostami et al., 2018). The usage of the planktonic foraminifera is preferable because of their abundance, diversity, easily recognizability, and collectability. Moreover, their preservation is better than other organisms, important for in many cases that usage of fossils such as understanding the evolutionary recovery patterns (Eicher, 1976).

This great turnover is characterized by a change from latest Maastrichtian (latest Cretaceous) assemblages dominated by large-sized, robust, and coarsely ornamented species to early Danian assemblages comprised only of minute, nondescript, thin-walled forms that lack ornamentation (e.g. Keller et al., 2002; Pardo and Keller, 2008; Punekar, 2017). Only three of the species (*Hedbergella monmouthensis*, *Hedbergella holmdelensis*, and *Guembelitra cretacea*) can survive from the K/Pg boundary that is morphologically small, ecologically stressed planktonic foraminifera. Moreover, these high-stressed, three species continued to dominate in the early Danian (earliest Paleogene) (Keller, 1988a, 1989a, 1989b; MacLeod and Keller, 1994; Keller and Pardo, 2004; Pardo and Keller, 2008; Esmeray, 2008; Keller and Abramovich, 2009; Açıkalın et al., 2015; Karabeyoğlu, 2019). The aftermath of the P0 zone, in the Danian planktonic foraminiferal assemblages, the numerous new species of trochospirally coiled and biserial forms originated (Luterbacher and Premoli Silva, 1964; Smit, 1982; Liu and Olsson, 1992; Molina et al., 1996; Keller, 1998; Punekar, 2017). This

evolutionary recovery on the planktonic foraminifera assemblages happened in two phases; the first one includes to the appearance of genera, *Parvularugoglobigerina*, *Woodringina*, and *Chiloguembelina*, and the second one includes to the appearance of *Eoglobigerina*, *Globigerina*, *Parasubbotina*, *Globanomalina*, *Praemurica*, and *Subbotina*. According to Punekar (2016) *Zeauvigerina* observed in both Cretaceous and Paleogene planktonic foraminifera assemblages, but at the boundary, they could not be observed.

A limited number of studies have been conducted on the recovery of organisms following the K/Pg boundary on microfossils compared to extensive research on extinction of K/Pg mass-extinction. In this chapter, the evolutionary recovery of the planktonic foraminifera and their responses on the environmental conditions are discussed.

### **3.1. Life-history Strategists**

The biotic responses of organisms to any environmental conditions can be expressed by historical strategies (MacArthur and Wilson, 1967; Hallock, 1985). Under the optimum ecological, in other words equilibrium, conditions such as enough food supply, normal salinity, etc., the species become more stable and diverse with less need to reproduce rapidly and in great numbers. These equilibrium species are high diverse, well-ornamented, complex taxa which are called K-strategists. They adapt themselves to live in high stable, oligotrophic environments. On the other hand, r-strategists are small ecological opportunists which have low diversity but high abundance in the eutrophic environment. The dramatical changes in the ecosystem such as volcanism or large impact cause the decline in normal environmental conditions, K-strategists could not be able to adapt themselves to these hostile conditions, starting to decline, and sudden increase on opportunistic species, r-strategists. In other words, there is inverse relationship between K-strategists and r-

strategists (Figure 3.1). There are also intermediate strategists to live in mesotrophic environments with the tendency towards both K- and r-strategists. They are observed in both low-oxygen environments and optimum assemblages (Premoli-Silva and Sliter, 1995). The mesotrophic ecological conditions are ranging from eutrophic environments during seasonal blooms to oligotrophic environments when upwelling or runoff decline seasonally (Premoli-Silva and Sliter, 1995).

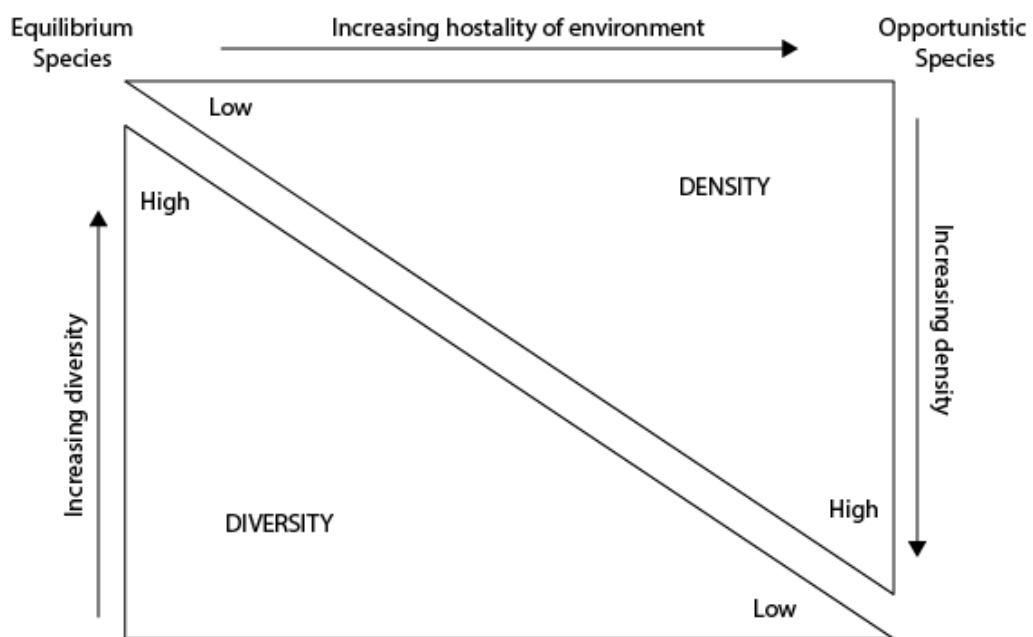


**Figure 3.1:** The relationship between density and diversity (Simplified from Benton and Harper, 1997)

In planktonic foraminifers, the size and ornamentations are often directly linked with the life-history strategies (Hallock, 1985). K-strategist, equilibrium planktonic foraminifera species are typically larger, morphologically complex, highly ornamented, specialized forms in low abundance. In contrast, r-strategist,

opportunistic planktonic foraminifera species are typically small, nondescript, morphologically less complex, weakly calcified forms that lack of ornamentation in high abundance. (Premoli-Silva and Sliter, 1995). The r/K-strategist, generalist planktonic foraminiferal diversity is not high as K-strategists because of mesotrophic environmental conditions. The generalist genera, mainly biserial in form (Premoli-Silva and Sliter, 1995).

In this study, a total of 62 species of planktonic foraminifera distributed in 21 genera were recorded. The degree of preservation are varied from excellent to poor and presented variable abundance. The distributions of the K-, r- and r/K-strategist planktonic foraminifera in the studied sequence and the wide applicability of these taxa for paleogeographic inferences can contribute to the better understanding of the geological evolution of the Göynük basin. After the detailed taxonomic study, three strategist groups were determined by considering the size and morphological characteristics of planktonic foraminiferal taxa. In this study, the K-strategist taxa are defined as *Globotruncana*, *Globotruncanita*, *Globotruncanella*, *Rugoglobigerina*, *Globigerinelloides*, *Heterohelix*, *Laeviheterohelix*, *Planoglobulina*, *Pseudotextularia*, *Pseudoguembelina*, *Racemiguembelina* in the late Maastrichtian, Cretaceous and *Parvularugoglobigerina*, *Eoglobigerina*, *Globigerina*, *Parasubbotina*, *Globanomalina*, *Praemurica*, and *Subbotina* in the early Danian, Paleocene. The r-strategist assemblage is dominated by only *Guembelitra cretacea* in this study. The assemblages of intermediate strategists are characterized by *Chiloguembelina*, *Woodringina*, and *Zeauvigerina* in this study (Figure 3.2).

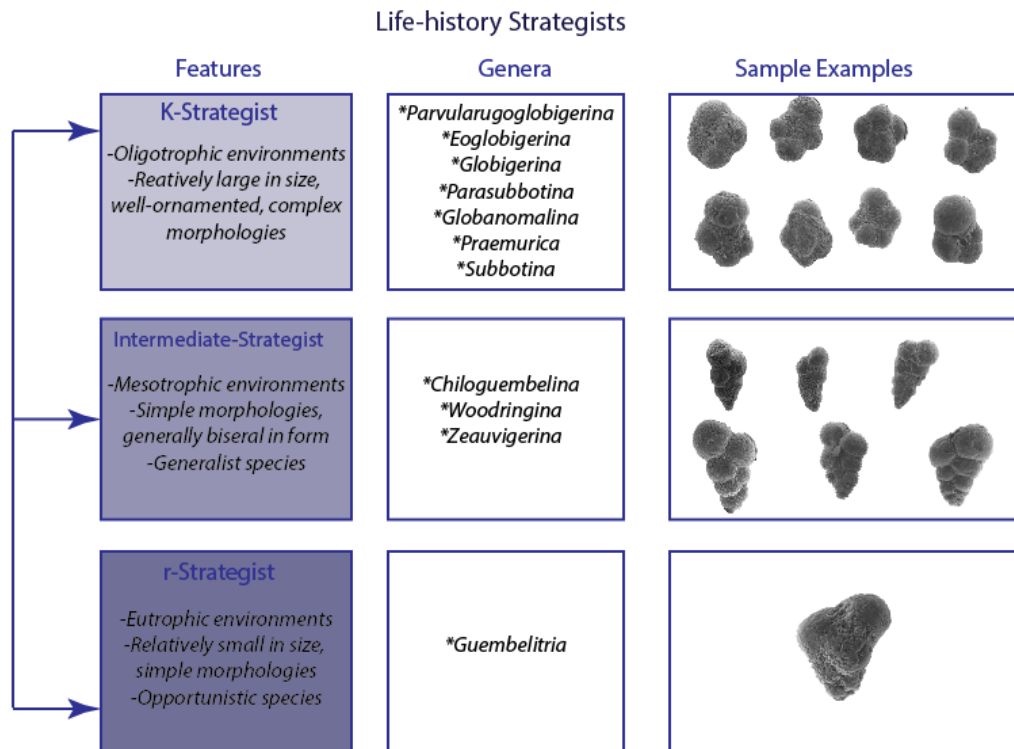


**Figure 3.2:** Life-history strategies of planktonic foraminifera with early Danian genera of the Göynük section (Samples are from Göynük samples).

### 3.2. Responses of Planktonic Foraminifera to the Environmental Conditions across the K/Pg Boundary Interval

In the basal part of the studied section, in the interval between Gk-04 to Gk-00 and Gk-1 to Gk-9, the planktonic foraminiferal assemblages are represented by genera *Globotruncana*, *Globotruncanita*, *Globotruncanella*, *Rugoglobigerina*, *Globigerinelloides*, *Hedbergella*, *Heterohelix*, *Laeviheterohelix*, *Planoglobulina*, *Pseudotextularia*, *Pseudoguembelina*, *Racemiguembelina*. These are K-strategists taxa comprised by the highly ornamented, large forms with high diversity. Consequently, it can be concluded that the environmental conditions were

oligotrophic during the late Maastrichtian (MacLeod et al., 2000; Pardo and Keller, 2008; Punekar, 2016).

In the K/Pg boundary beds of the studied section, in the sample Gk-10 the planktonic foraminiferal assemblage is represented by only *Guembelitra cretacea*. This species is unique in great blooms during times of high-stressed environments and disappear when the conditions return to the optimum. In other words, they have had a wider range of tolerance enabling to survive in high environmental stress rather than the other species (Abramovich and Keller, 2003, 2009; Keller, 2005; Punekar, 2017). The *Guembelitra* blooms mark that the environmental equilibrium was destroyed as a result of the K/Pg boundary events. This species thrived in high-stress environments of the immediate aftermath of the K/Pg mass extinction; in zone P0 and the lower part of P1a zone.

*Parvularugoglobigerina*, K-strategists, start to evolve and dominate the P1a zone. The opportunistic species get away from the optimum resemble conditions, and new genera start to evolve from *Guembelitra*, which are *Eoglobigerina*, *Globigerina*, *Parasubbotina*. In addition, generalist genera *Chiloguembelina*, *Woodringina* and *Zeauvigerina* are also indicated. These genera suggest the high-stressed environmental conditions are not totally finished after the K/Pg mass extinction because they adapted to mesotrophic ecological conditions. The both oligotrophic and mesotrophic environmental strategists indicates the environmental condition turns to normal, density/diversity relationship is getting in balance and evolutionary recovery is started. However, in the most upper part of the P1a zone and the lowest part of the P1b zone, the renewed high-stress conditions follow a period of recovery, as indicated by reappearing of *Guembelitra cretacea*. During the P1b zone, the reappearance of *Guembelitra cretacea*, r-strategist, reveals the eutrophic environments and interrupts the marine evolutionary recovery of planktonic foraminifera (Figure 3.3). Although the continuity of the genera *Eoglobigerina*, *Globigerina*, *Parasubbotina*, *Parvularugoglobigerina*, the species richness remains low, and they are dwarfed through zone P1b. Low oxygen tolerant small biserial species, on the other hand, are

the group of ecological generalists, in other words intermediate strategists, dominate the P1b zone. Therefore, the abundance of both r-strategists and intermediate strategists indicate that the mesotrophic to eutrophic ecological conditions. The *Globoconusa daubjergensis* is the another species coinciding with high-stress environments in open marine settings (Punekar, 2016). Similarly, this species is identified in P1b samples. Interestingly, the onset of the renewed high-stress environments is marked by the extinction of *P. eugubina*, as well as documented in previous studies (Keller, 1988a, 1989a, 1989b; Keller and Benjamini, 1991; Canudo et al., 1991; Keller et al., 2013; Punekar et al., 2014; Punekar, 2016; Mateo et al., 2018). According to Punekar (2016), P1a and P1b zones are called as long-delayed marine recovery because of variations on the planktonic foraminiferal assemblages.

Long after the K/Pg mass extinction and the environmental shifting on P1b zone, the complex, high diversity, K-strategists; *Eoglobigerina*, *Parasubbotina*, *Subbotina*, *Parvularugoglobigerina*, *Globanomalina*, *Praemurica* are dominated with reduced abundance of stress-tolerant species. The first larger (> 150 µm) trochospiral species morphologies and higher diversity are recorded in P1c zone after the K/Pg boundary. In addition, the intermediate forms are also depleted in abundance. All these results show that the high-stress conditions are totally extinct and evolutionary and delayed recovery turns to onset of recovery (Figure 3.4).

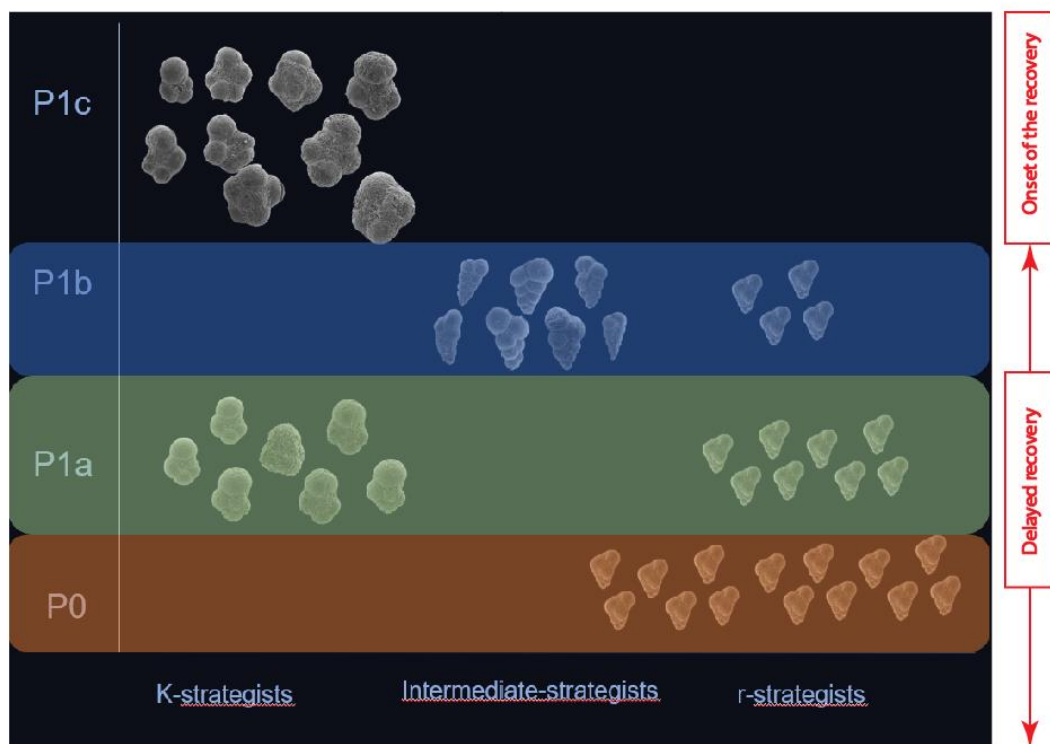


**Figure 3.3:** Early Danian evolution illustrating the high-stress environment, small species, and low diversity (r-strategists), complex morphological, high abundance species (K-strategists), and in between intermediate-strategists.

### 3.3. Quantitative Analysis

Quantitative analysis is an integral part of the biozonation that helps the desired ecological variations, making easier to explore relationships, and to reveal these relationships against the unpredicted occurrences (Parker and Arnold, 1999).

In this study, quantitative analysis carried on in order to determine relative abundances and variations in between evolutionary delayed and onset recovery of the planktonic foraminifera after the K/Pg boundary, P1b and P1c zones. Although the high-resolution faunal assemblages identified with quantitative data in both late Cretaceous, P0 and P1a zones, P1b and P1c are still lacking. This study reveal that the relative

abundances of planktonic foraminiferal assemblages in P1b and P1c zones by using quantitative data.

The detailed quantitative analysis was carried out in two sizes 63-150  $\mu\text{m}$ , and  $> 150 \mu\text{m}$  in the earlier studies on before K/Pg boundary (e.g. Keller, 1998a, 1998b; Karabeyoğlu, 2017). However, the studies on after the K/Pg boundary only  $>63 \mu\text{m}$  size sieve used because of the domination of small size forms. For this purpose, only  $>63 \mu\text{m}$  sieve size were used, and average 300 individuals of planktonic foraminifera picked up (Table 3.1).

According to results, in the P1b zone, the faunal assemblages is dominated by *Guembelitra cretacea* (average 35%). The simple biserial forms; *Chiloguembelina* (average 30%) and *Woodringina* (average 20%) is the other dominated genera in the samples. Species of other genera such as *Parasubbotina*, *Subbotina*, *Zeuwigera*, *Eoglobigerina*, *Parvularuglobigerina*, *Globanomalina*, *Praemurica* are represented, but their abundances are very low (less than 15%). The contribution of their abundances of each genus does not reach to 5% of the total abundance of the samples. The most interesting planktonic foraminifera species is *Globoconusa daubjergensis*. *Globoconusa daubjergensis* is frequently accompanied with the blooms of *Guembelitra* genus. The earlier studies documented that this species observing during the hostile environmental conditions (Keller, 1988a, 1988b, 2002, 2004, 2006). Based on Punekar et al. (2014), the abundance of *Globoconusa daubjergensis* is observed in the P1b zone in Egypt and Israel, coincide with the blooms of *Guembelitra cretacea*. In the Göynük section, this species indicated in P1b zone, but less as documented.

**Table 3.1:** Relative abundances of planktonic foraminifera in the early Danian, P1b and P1c zones > 63 µm size fraction at Göynük, Bolu, Turkey

Biozone	P1b										P1c				
	Gk-26	Gk-27	Gk-28	Gk-29	Gk-30	Gk-31	Gk-32	Gk-33	Gk-34	Gk-35	Gk-36	Gk-38	Gk-40	Gk-41	Gk-42
Sample No	8-split	8-split	8-split	8-split	8-split	8-split	8-split	8-split	8-split	8-split	8-split	8-split	8-split	8-split	8-split
Split No	2										1				
<i>Eoglobigerina edita</i>	1	2													
<i>Eoglobigerina eobulloides</i>															
<i>Eoglobigerina spiralis</i>	28	28	24		51	38	33	42	46	32	36	31	1	27	31
<i>Parasubbotina pseudobulloides</i>														36	51
<i>Parasubbotina varianta</i>														1	1
<i>Subbotina cancellata</i>														1	3
<i>Subbotina triloculinoides</i>			8	11	16		11	12	16	18	21	19	23	21	26
<i>Subbotina trivialis</i>						3	6	4	6	15	9	35	29	18	31
<i>Parvularugoglobigerina alabamensis</i>	7	3	7			1									
<i>Parvularugoglobigerina extensa</i>	11	5		1	2		1				3	2	2		5
<i>Globanomalina archeocompressa</i>															
<i>Globanomalina compressa</i>															
<i>Globanomalina imitata</i>															
<i>Globanomalina planocompressa</i>					3		1	1	3	5		3	15	12	32
<i>Praemurica inconstans</i>															
<i>Praemurica pseudoinconstans</i>												1			1
<i>Praemurica taurica</i>	3		2												
<i>Globoconusa daubjergensis</i>															
<i>Chiloguembelina midwayensis</i>	21	17	20	18	39	41	56	48	42	33	39	32	43	37	33
<i>Chiloguembelina morsei</i>	82	105	73	81	75	51	33	38	27	59	51	43	37	38	34
<i>Chiloguembelina subtriangularis</i>														2	4
<i>Woodringina claytonensis</i>	16		25	28	19	10				9					
<i>Woodringina hornerstownensis</i>	30	47	51	77	7		3	22	14	22	48	51	41	39	32
<i>Zeavivigerina virgata</i>		2	3		3			1			2	2	1		2
<i>Zeavivigerina waiparaensis</i>															
<i>Guembelirritia cretacea</i>	101	95	108	78	83	91	88	92	85	70	64	45	28	11	9
Total Count	300	304	321	294	298	235	232	260	241	261	278	264	285	244	308

In the P1c zone, the domination of the faunal assemblages of the *Guembelitra cretacea* abruptly declined, below the 5% in total abundance. On the contrary, the *Subbotina cancellata*, *S. trivialis*, *S. triloculinoides*, *Eoglobigerina spiralis*, *E. edita*, *Globanomalina imitata*, *G. archeocompressa*, *G. compressa*, *G. planocompressa*, *Parasubbotina varianta*, *P. pseudobulloides*, *Praemurica inconstans*, *P. pseudoinconstans* are well-preserved species for P1c zone. However, *Parasubbotina varianta* is the most important form for this zone because it is the marker for biozone. In addition to these K-strategists, the intermediate-strategists, *Chiloguembelina*, *Woodringina*, and *Zeauvigerina* was counted in P1c zone. These biserial forms are small and less in amount rather than P1b zone (Figure 3.4).

The results from quantitative analysis revealed that the distribution of planktonic foraminiferal assemblages, hostile environmental conditions reappear during P1b zone due to increasing in abundance of r-strategist species, opportunistic species, such as *Guembelitra cretacea* (Figure 3.5). There is also observed simple biserial forms, called as generalist forms, such as the genera *Chiloguembelina*, *Woodringina*, and *Zeauvigerina*, in the P1b zone. However, their abundances are not as much as opportunistic forms. On the contrary, the complex forms, K-strategist species, are indicated really less in amount in the P1b zone. On the other hand, in the P1c zone, complex forms, K-strategists, dominate the faunal assemblage. The opportunist and generalist species can be also existed but not like P1b zone.

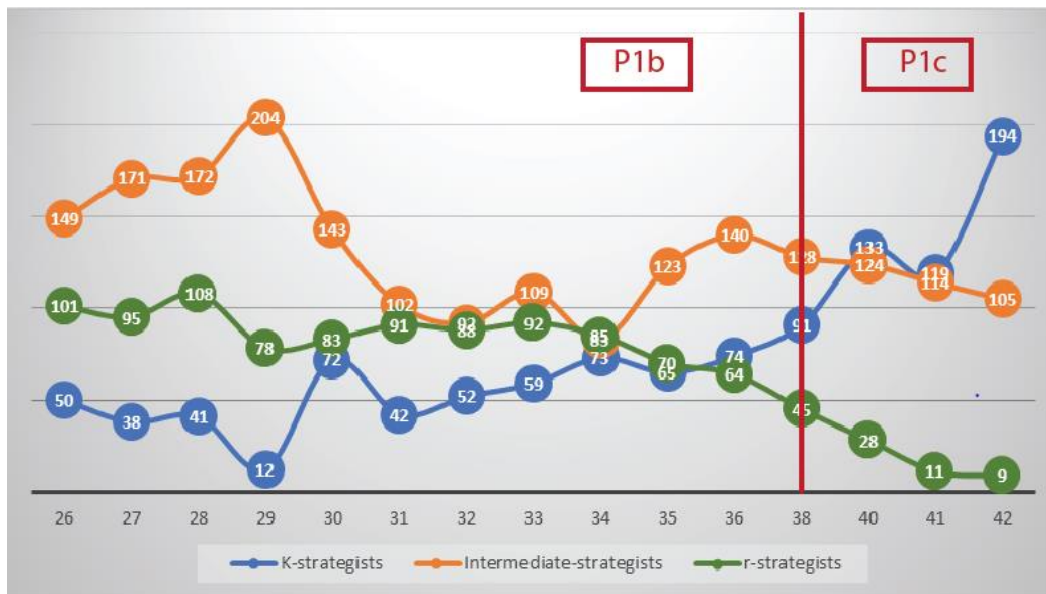


**Figure 3.4:** Relative abundance patterns of life-history strategists. The boundary between P1b and P1c is located in between sample 36 and 38. In P1b zone, the sample 26 to 36, K-strategists are relatively low, intermediate- and r- strategists are relatively high in abundance. After the P1b zone, in P1c zone, K-strategists dominate the environment and depletion occurs in r-strategists.

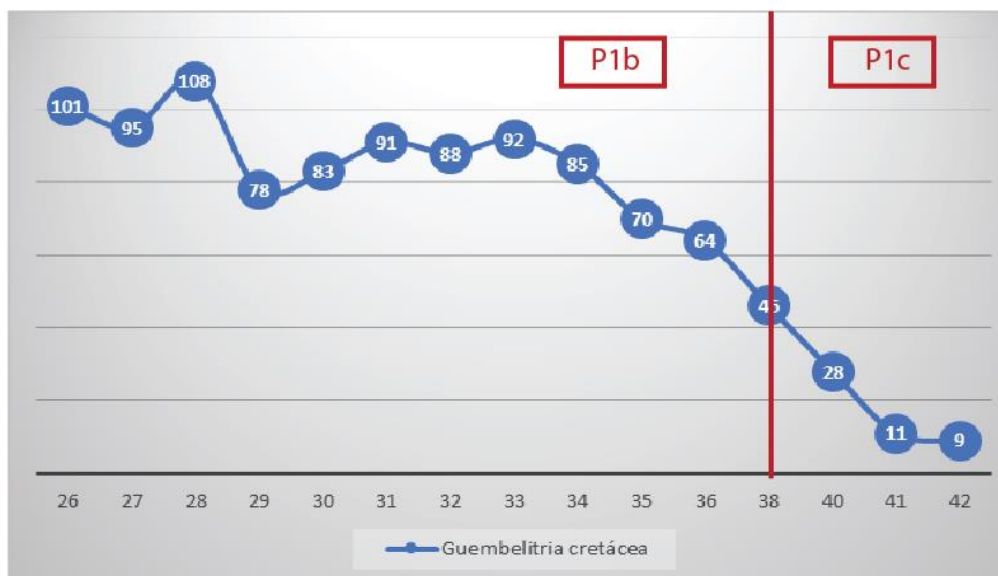


**Figure 3.5:** Relative abundance patterns of *Guembelitra cretacea*. The boundary of the P1b and P1c zones is located in between the samples 36 and 38. The drastically decline on the abundance of opportunistic species can be easily observed.

### **3.4. Marker Events Across the K/Pg Boundary Beds: Microspherules and Microtektites**

The studies carried on the Caribbean, Central and North America, Haiti, and NE Mexico have provided the stratigraphic position of impact spherules relative to K/Pg boundary (Maurrasse and Sen, 1991; Smit et al. 1992; Stinnesbeck et al. 1993; Smit, 1999; Keller et al. 2003a, b, 2007, 2009, 2011). The spherules firstly described in detailed by Schulte et al. (2009) based on geochemical and mineralogical analyses. Based on the results, the spherules have locally enhanced Si, Al, and K contents due to the presence of siliciclastic detritus, and has Ca- and Mg-enrichment, indicating the occurrence of calcite and dolomite clasts.

In the Göynük section, some microspherules were observed right after the K/Pg boundary. In the P0 zone, the sample Gk-10 is full of these microspherules. In addition to the P0 zone, in both thin sections and washing samples, the samples Gk-11 to Gk-28, P1a and P1b zone, presence of microspherules in the background was observed.

In the previous studies, *Thoracosphaera*, individuals from calcareous dinoflagellate, is the spherical forms that are detected as bloom of them just after the K/Pg boundary. Açıkalın et al. (2015) and Karabeyoğlu (2017) recognized these blooms of *Thoracosphaera* immediately above the K/Pg boundary Göynük and Haymana basin, respectively, in Turkey. However, the analysis reveal that *Thoracosphaera* is full of calcite. In the studied section, the bloom of *Thoracosphaera* is observed P0 zone and their abundances relatively declined in the other zones (Figure 3.6, 3.7).

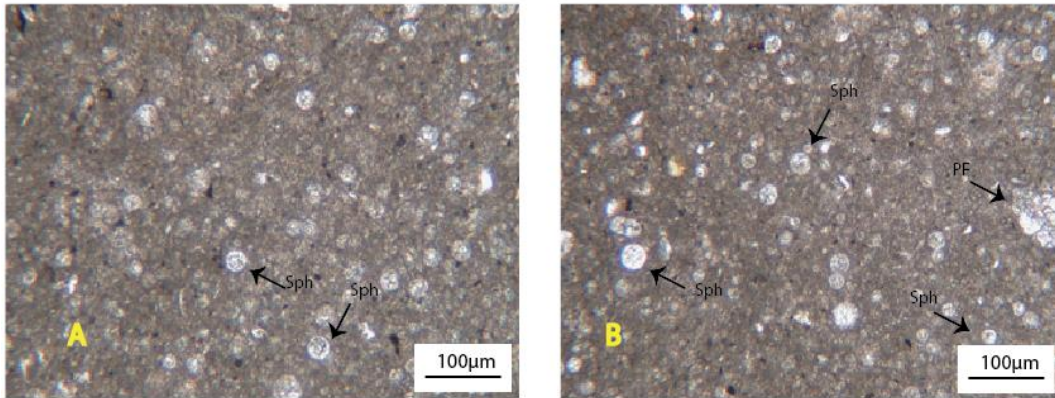


**Figure 3.6:** Microspherule blooms in thin sections A) sample Gk-10, just above the boundary, P0 zone B) sample Gk-26, P1b zone, rich in biserial and triserial planktonic foraminifera Sph: Microspherules, PF: planktonic foraminifera

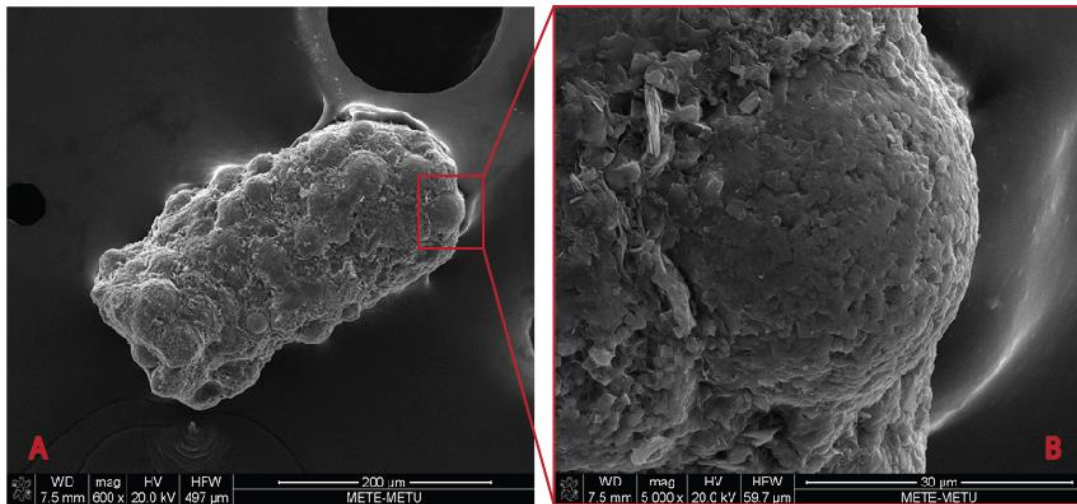


**Figure 3.7:** A) Scanning Electrom Microscope (SEM) Image of microspherule individuals embedded in a clast. Sample from Gk-10, P0 zone, B) Close-up view of microspherule specimen in A

In addition to the *Thoracosphaera* bloom, microtektites are also determined. Since the discovery of the Chicxulub crater in the Yucatan Peninsula (Hildebrand et al., 1991) many microtektite-rich deposits have been documented at the K/Pg boundary in the Gulf of Mexico (e.g. Alvarez et al., 1992; Keller et al, 1994, 2009; Smit, 1992; Schulte et al., 2003, Mateo et al., 2018). Microtektites are rounded silicate glass bodies usually less than 2-5 mm in diameter (Glass, 1990). The chemistry of microtektites are similar to felsic volcanic glasses, with >65% of the SiO<sub>2</sub> content, but with MgO and K<sub>2</sub>O/Na<sub>2</sub>O ratios.

Although they are silicate in origin, the interstitial space filled with calcite and/or biogenic material due to reworking. According to Keller (2012), the iridium analysis was recorded from the microtektites, which is deposited at the K/Pg boundary. However, due to tectonically active environments during K/Pg boundary interval, microtektites can be observed as reworked, coming from slumps or debris flows. On the other hand, Mateo et al. (2018), mentioned that because of the erosional contacts and turbiditic events, the microtektites and microspherules were redeposited in the early Danian sediments and they are mostly altered to calcite and smectite.

In the studied Göynük section, microtektite like structures are observed in both Cretaceous and Paleogene samples. Açıklın et al. (2015) mentioned that the Göynük basin was active during this time interval, and there was clastic influx into the basin (Discuss in Chapter 2). So, the reworking process of the microtektites was possible. In addition, the inside of the microtektites are full of spary calcite. This is the another indicator for reworking, affected from background (Figure 3.8).

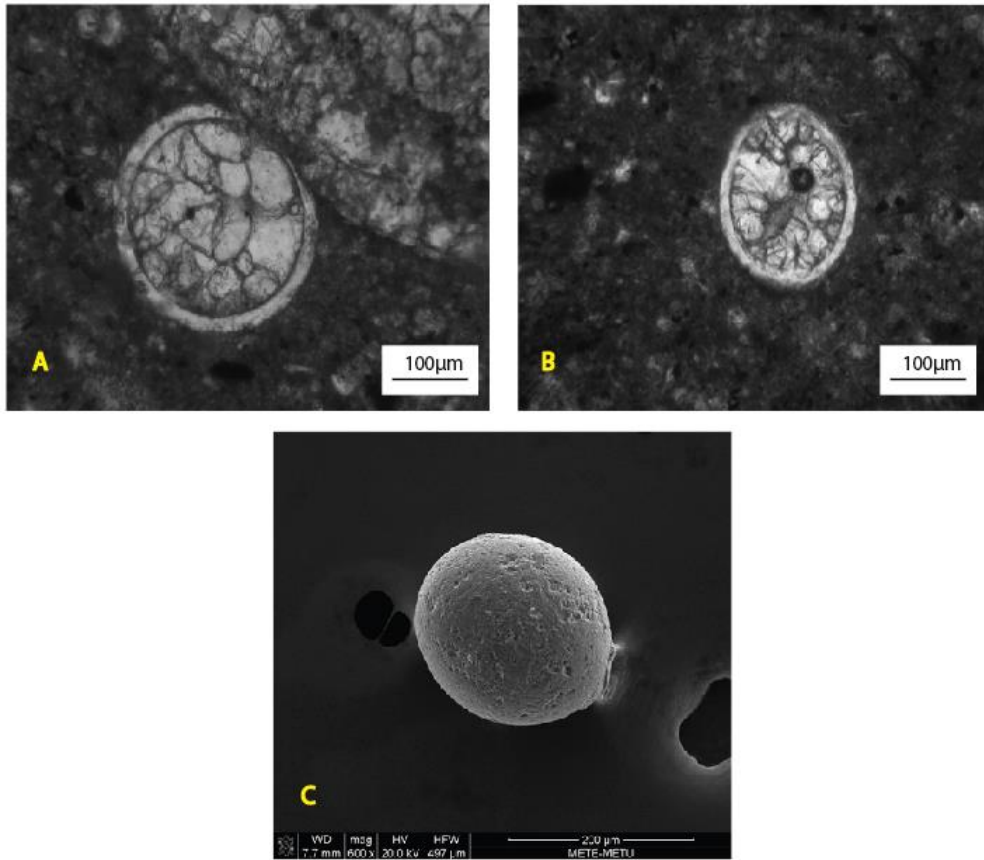


**Figure 3.8:** Microtektites replaced with calcite in both thin-section views and Scanning Electron Microscopy (SEM) view A) sample from Gk-01, inside of the late Maastrichtian, B) sample from Gk-9, 8 cm below the K/Pg boundary, C) sample from Gk-21, in P1a zone

## CHAPTER 4

### MINERALOGICAL AND GEOCHEMICAL FEATURES

Mineralogical content and magnetic susceptibility provide significant evidences on geological processes. Variations in sediment sources caused by weathering, erosion, climate and sea-level changes can be indicated by analyzing mineralogical content (Taylor and McLennan, 1985; Hayashi et al., 1997). For this purpose, different localities from worldwide around the K/Pg boundary have been analyzed by mineralogical, mineral chemistry, and magnetic susceptibility content of the samples (e.g. Punekar et al., 2014; Font et al., 2016, 2017; Sial et al., 2016; Rostami et al., 2018; Grasby et al., 2019).

The changes in the relative abundances of planktonic foraminifera, inferring the K/Pg boundary and evolutionary recovery after the boundary, have been demonstrated in the previous chapter. The objective of mineralogical and mineral chemistry analysis is found out traces of environmental changes that have led to these relative abundance changes and to determine whether these relative abundance changes were related to the three phases of Deccan volcanism or any volcanism in the vicinity of the depositional environment.

Mineralogical and mineral chemistry features, and possible changes through the measured Göynük section, three technical methods were applied as X-ray Diffractometer Analyses (XRD), Electron Probe Micro Analyses (EPMA) and Magnetic Susceptibility (MS). In this chapter, the results from these techniques are given.

## **4.1. Mineralogy and Mineral Chemistry Analysis**

### **4.1.1. X-Ray Diffractometry Analyses**

X-ray diffractometry (XRD) analyses helps to define and compare clay and non-clay minerals, and their origins. XRD analyses were carried out for all of the marl and clayey limestone samples to define both clay and non-clay minerals and to compare clay percentage along the K/Pg boundary. The main content of all samples is calcite because of lithology, discussed in chapter 2. Due to detect the type of clay and non-clay minerals rather than calcite, the analyses were performed on both random and oriented samples (air dry, ethylene glycol, dry up with 350°C and 500°C).

In the Göynük section, the sediments that are mainly composed of calcite, clay minerals (Ca-montmorillonite, kaolinite, and illite) as the essential phases, and quartz, orthoclase, sphene and hematite are also present in minor amounts (Figure 4.1). The calcite content in the section average 70% in volume. Clay minerals appearing even in the random patterns are made up of 14 and 30% of the rocks in volume. Volume of quartz, orthoclase, sphene and hematite are about 10%. However, the other minerals, observed in thin section, are less than 5% in volume that's why the peaks of these phases cannot be observed in the measured random XRD patterns.

The XRD patterns of the random samples were compared from bottom to top of the section to able to distinguish any possible change. After comparison, 12 representative samples from groups of the samples with the same XRD patterns were chosen to signify levels of the mineralogical changes in the section (Figure 4.2). According to XRD patterns, the main changes occur in Ca-montmorillonite, illite, and kaolinite. In other words, the essential changes in random patterns are indicated in clay content of the samples. The described changes are supported by the patterns of the oriented slides (air dried, ethylene glycolated, heated at 350°C and 500°C).

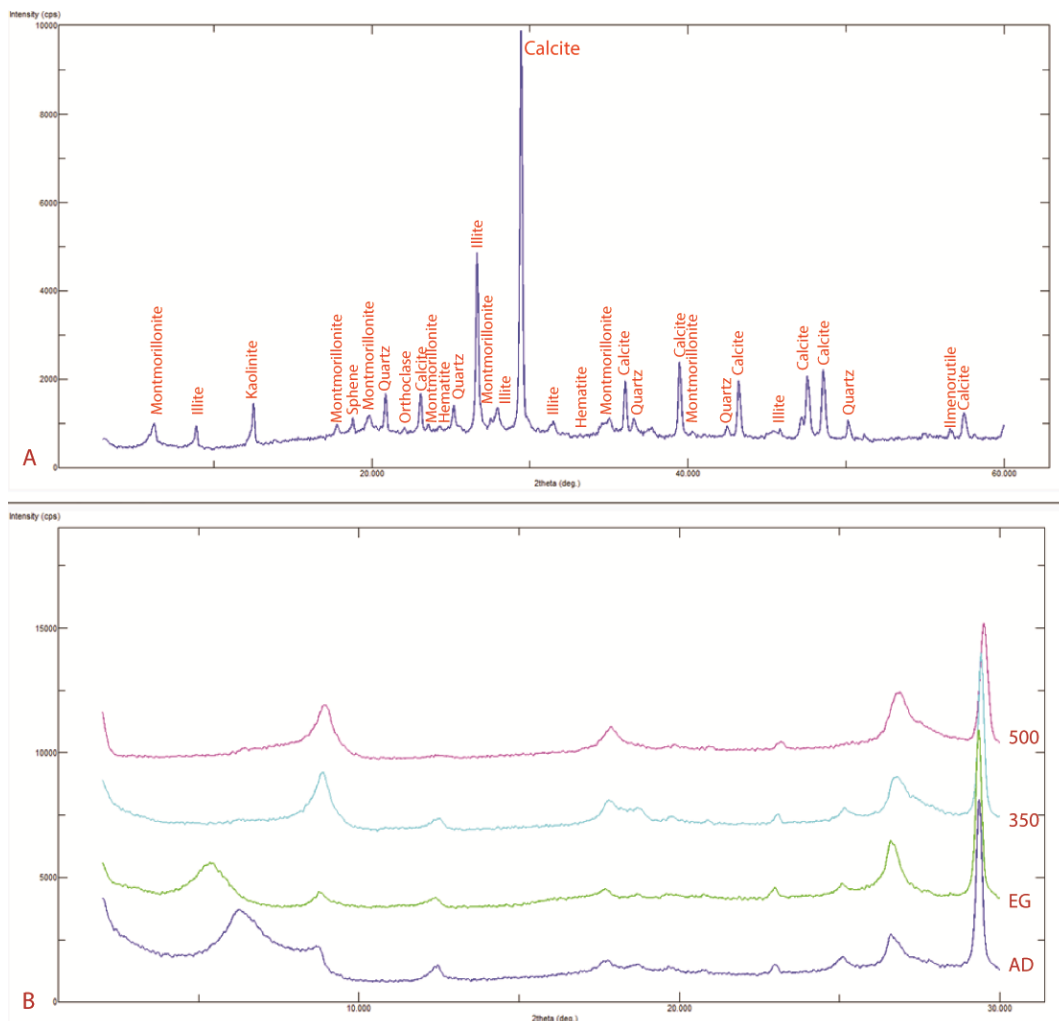


**Figure 4.1:** X-ray diffractograms of the sample Gk-1 A) Random sample pattern, B) Oriented samples (Air-dried (AD), Ethylene Glycol (EG), heated at 350°C (350), and 500°C (500)).

The essential component of the samples is carbonate, detected as calcite, which ranges between 45% to 80% in volume. In some marl deposits, calcite content decreases up to 45%, where the K/Pg boundary is located. According to Keller, 1998, the carbonate content of the boundary bed drops less than 10%. The studies carried in the Stratotype section El Kef, Tunisia, the calcite content drops to 0% at the boundary (Abdelkader

et al., 1997). Moreover, the studies that have been carried out in different localities are clearly resulted that the K/Pg boundary sections revealed a significant decrease in the calcite content at the boundary, which indicates the crisis in the boundary productivity reflecting environmental conditions (Luterbacher and Premoli-Silva, 1964; Adatte et al., 2002a; Molina et al., 1996; Arenillas et al., 2006; Preisinger et al., 2002; Zaid, 2015; Font et al., 2018; Rostami et al., 2018).

Quartz is another non-clay component of the Göynük basin samples. It is recorded as relatively low to moderate in abundance, and its percentage increases from 10% to 40% in the samples. However, the main point about quartz is that the relative abundance increases at the K/Pg boundary which coincides with the drop-in carbonate content (Figure 4.3). The inverse proportion of the carbonates and quartz abundances are clear. The similar behavior is also observed in Haymana basin (Esmeray, 2008), and Dakhla basin (Zaid, 2015).

The other observed non-clay minerals are feldspars as plagioclase and orthoclase. The abundance of feldspars compared to quartz is very limited. It varies 0% to 10% in the samples. Its low values may indicate intensive recycling, dissolution, and kaolinization. Furthermore, ilmenorutile, sphene and hematite, which are volcanic origin minerals, are identified in the XRD patterns (Figure 4.4).

In the Göynük section samples, the total amount of clay mineral percentages in between 15-20% (Table-1). In the section, smectite mineral montmorillonite, kaolinite and illite were the described clay minerals (Figure 4.5). Average amounts of kaolinite, illite and montmorillonite are 10-20%, 20-60% and 10%, respectively.

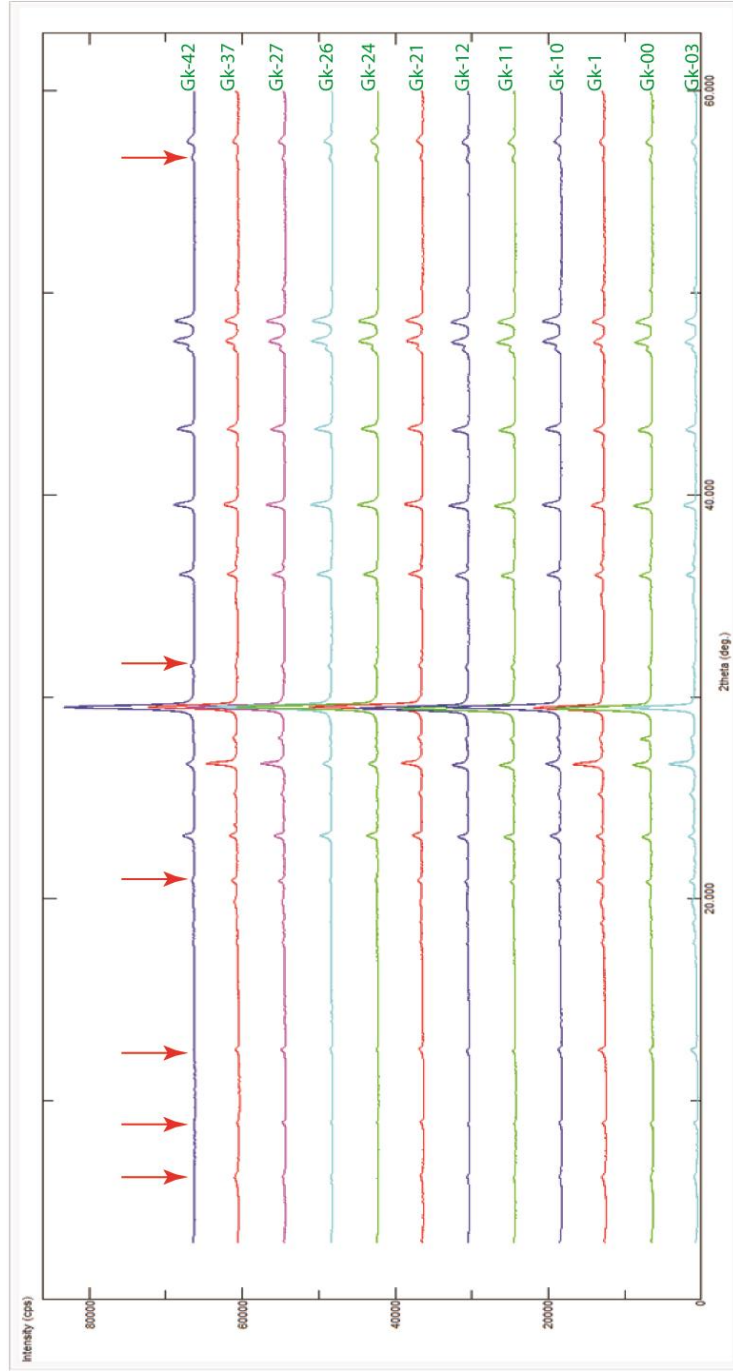


**Figure 4.2:** Representative random XRD patterns of the samples (Red arrows shows the variations from each sample)

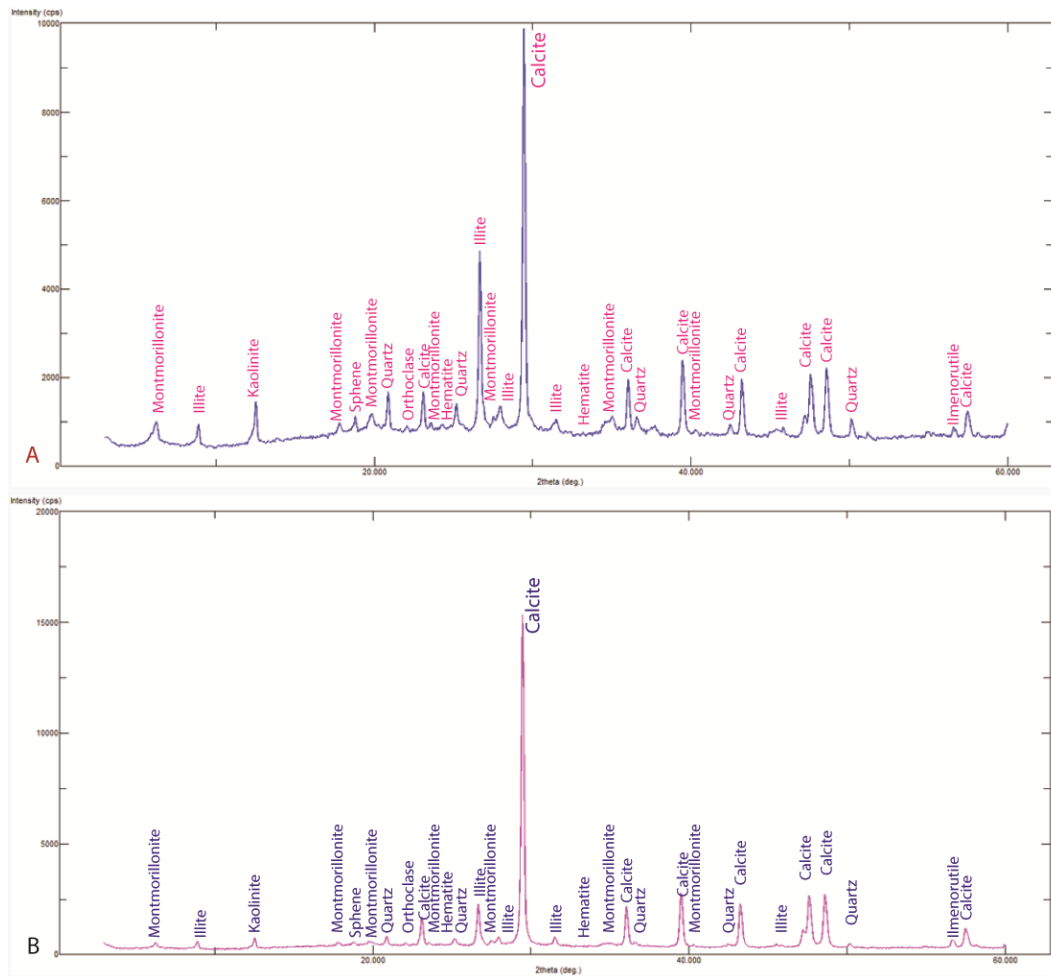


**Figure 4.3:** Random XRD patterns from the Göynük section for the samples A) Gk-1 B) Gk-10 (included K/Pg boundary and P0 zone) showing the decline of both clay and quartz contents at the boundary

Illite, which also includes glauconite, is the common clay minerals in the Göynük samples. It is formed by the decomposition of some micas and feldspars. Kaolinite is the another clay mineral of Göynük samples. Kaolinite is mainly formed under tropical to subtropical humid climatic conditions which has been interpreted as being a product of chemical weathering and leaching of rocks which occur especially the decomposition of orthoclase (Chamley, 1989; Hallam et al., 1997). In addition to a

detrital origin, this clay mineral may also develop by diagenetic processes due to acid rains from volcanism (Ghandour et al., 2003; Font et al., 2014).

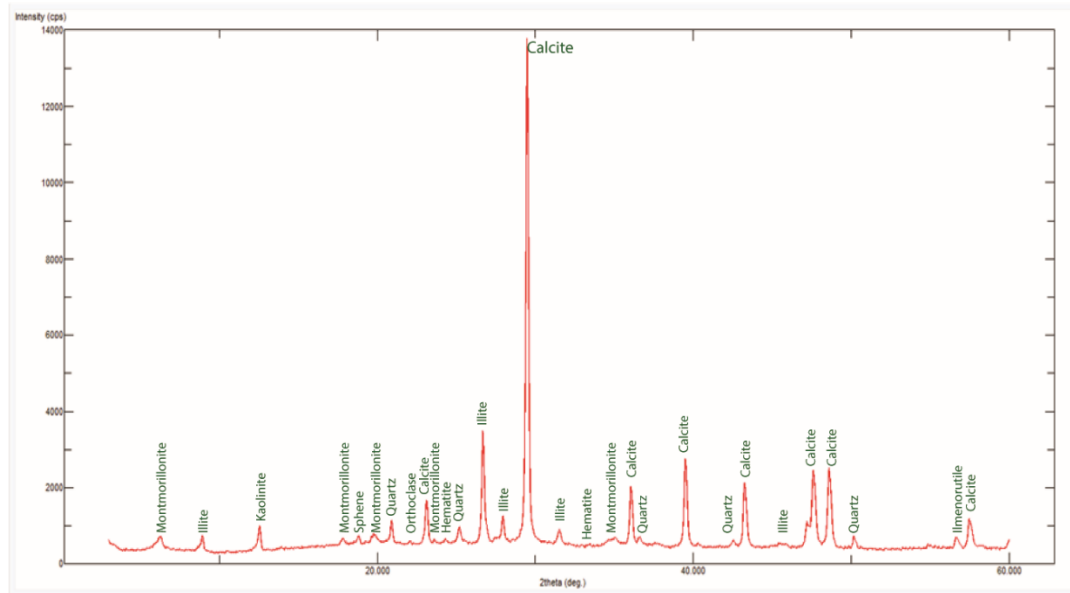


**Figure 4.4:** XRD pattern of the random sample Gk-16 from the Göynük section that show ilmenorutile

Montmorillonite is the most important clay mineral in the Göynük samples. The abundance of this clay mineral in Göynük is in agreement with the obtained results from Açıkalın et al. (2015). There are four main genetic hypotheses for the origin of montmorillonite; reworking of soils and enrichment by differential settling, alteration of volcanic origin materials, transformation of detritals, and authigenesis (Chamley, 1989; Thiry and Jaquin, 1993). Although the presence of detrital origin minerals were identified in thin-sections, the presence of volcanic origin non-clay minerals, sphene, hematite, and ilmenorutile, indicates that montmorillonite is mainly of a volcanic origin.

Amounts of kaolinite and illite are similar to and even higher than montmorillonite content. It is important emphasize that there are fluctuations in total clay amount and their lowest amount coincides with P1b zone (Figure 4.6). Especially, the significant change occurs where the lithology alternates marl to limestone. However, there is an unusual change is noticed in limestone sample Gk-34. In this limestone sample, the total clay percentage is 10. This sample coincides with end of the P1b zone.

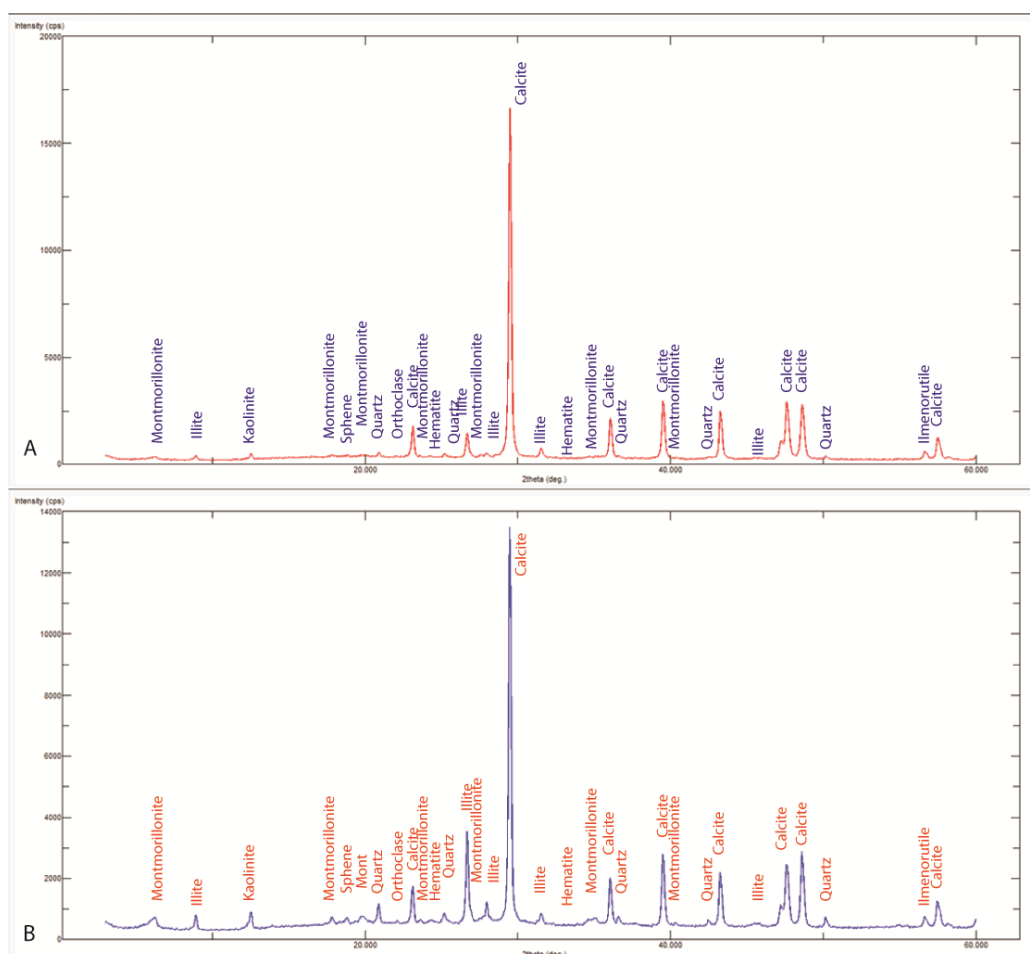


**Figure 4.5:** XRD patterns of random samples from the Göynük section A)Gk-26 B) Gk-27 (The samples started P1b zone and fluctuations can be easily observed).

**Table 4.1:** The percentage data of clay minerals

Sample ID	Sample (gr)	Nonclay (gr)	Clay (gr)	Clay Percentage (%)
Gk-42	10,01	8,28	1,73	17,28
Gk-41	10,01	6,92	3,08	30,82
Gk-40	10,01	8,23	1,77	17,73
Gk-39	10,01	7,73	2,28	22,77
Gk-38	10,00	8,26	1,74	17,44
Gk-37	10,01	7,24	2,76	27,61
Gk-36	10,01	8,20	1,81	18,09
Gk-35	10,00	7,93	2,07	20,71
Gk-34	10,01	9,00	1,01	10,05
Gk-33	10,01	7,96	2,04	20,43
Gk-32	10,00	8,42	1,59	15,86
Gk-31	10,01	7,79	2,22	22,18
Gk-30	10,00	8,44	1,56	15,58
Gk-29	10,00	8,20	1,81	18,05
Gk-28	10,00	7,67	2,33	23,34
Gk-27	10,00	7,87	2,13	21,34
Gk-26	10,00	8,34	1,67	16,67
Gk-25	10,00	8,55	1,45	14,51
Gk-24	10,00	8,50	1,51	15,05
Gk-23	10,00	8,36	1,65	16,47
Gk-22	10,01	7,74	2,26	22,63
Gk-21	10,01	7,93	2,08	20,81
Gk-20	10,01	8,06	1,95	19,50
Gk-19	10,00	7,92	2,08	20,82
Gk-18	10,01	8,00	2,01	20,07
Gk-17	10,00	7,96	2,05	20,45
Gk-16	10,00	7,86	2,14	21,38
Gk-15	10,01	7,79	2,22	22,15
Gk-14	10,00	7,46	2,54	25,44
Gk-13	10,01	7,58	2,43	24,26
Gk-12	10,00	7,63	2,38	23,76
Gk-11	10,01	7,75	2,26	22,57
Gk-10	10,01	8,10	1,91	19,09
Gk-9	10,01	8,05	1,96	19,57
Gk-8	10,00	7,58	2,43	24,24
Gk-7	10,01	7,63	2,38	23,78
Gk-6	10,00	7,82	2,18	21,81
Gk-5	10,06	8,21	1,85	18,37
Gk-4	10,01	8,09	1,92	19,17
Gk-3	10,03	8,23	1,80	17,96
Gk-2	10,04	8,15	1,89	18,79
Gk-1	10,04	7,86	2,18	21,68
Gk-00	10,05	7,93	2,12	21,09
Gk-01	10,01	7,87	2,14	21,40
Gk-02	10,03	7,66	2,37	23,66
Gk-03	10,05	7,73	2,32	23,09
Gk-04	10,01	7,77	2,24	22,37

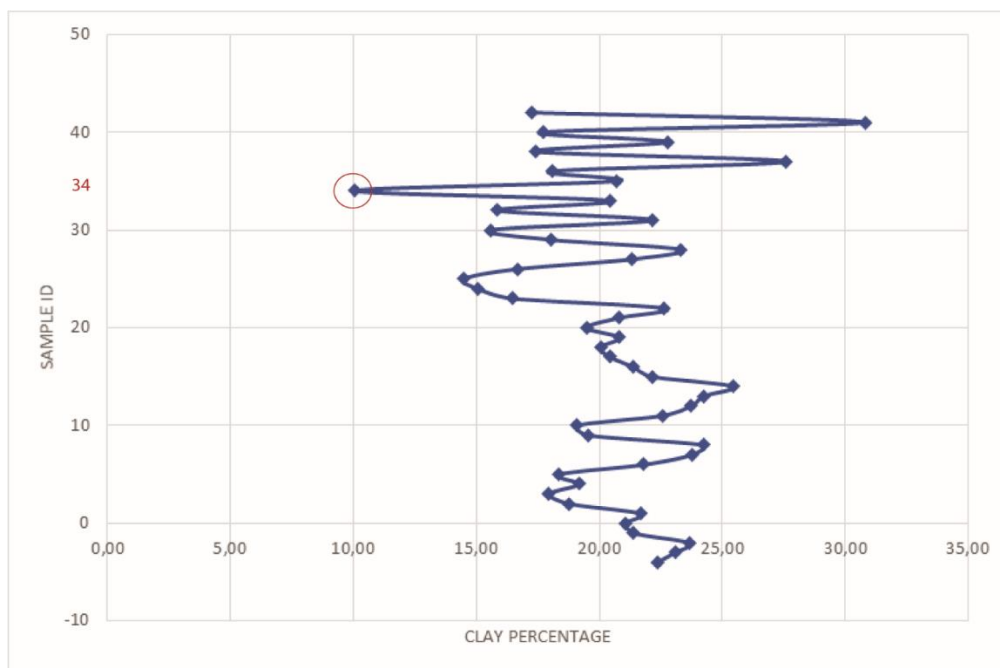


**Figure 4.6:** The graph showing the total clay percentages of the Göynük samples. The lowest value is from end of the P1b zone.

In brief, the XRD analysis gave mineral contents, and the average percentages of clay and non-clay minerals. However, iron-oxides concentrated in the washed samples and some silicates petrographically observed could not be detected by XRD method. This could be due to their abundance less than 5%. To able to characterize the oxide minerals and some possible accessories, EPMA analyses were also performed on some samples (see Section 4.1.2.).

#### 4.1.2. Electron Microprobe Analysis

In order to define possible minerals of less than 5% abundances in the Göynük section samples, further analyses by Electron Probe Micro Analysis (EPMA) were carried out. Moreover, enrichments in questionable elements that infer clues of extinction and delayed recovery can be analyzed by EPMA because EPMA is a widely used modern analytical technique for quantifying and mapping chemical compositions of solid materials.

Only four samples were analyzed by EPMA; two samples are just above the K/Pg boundary, and two of them are 4 m above the boundary, P1b zone, where the planktonic foraminiferal assemblages show variations with similar pattern. The sampling interval 5 cm to 10 cm, and the analyzed samples are Gk-11, Gk-12, Gk-26 and Gk-27.

Polished thin sections of the analyzed samples were prepared at the Department of Geological Engineering, METU and analyses were performed on gold palladium coated samples at the Central Laboratory, METU (see in Chapter 1). In the analyzed samples, which are mainly composed of calcite, quartz and feldspars, additional accessory phases as muscovite, biotite, hornblende, clinopyroxene, sphene, zircon, apatite, ilmenite, rutile, hematite with hematite spherules were identified (Table 4.2).

As silicate minerals in the Göynük section, the most abundant mineral is quartz. EPMA studies on quartz grains show that both rounded and angular types exist in the samples (Figure 4.7, 4.8) and their compositions are pure SiO<sub>2</sub>. Two EDS patterns from euhedral grains show trace amount of Sn (Figure 4.8b, c). Presence of both rounded and angular quartz grains with size in between 50 µm-100 µm may infer origin not only from turbiditic currents but also volcanic ashes.

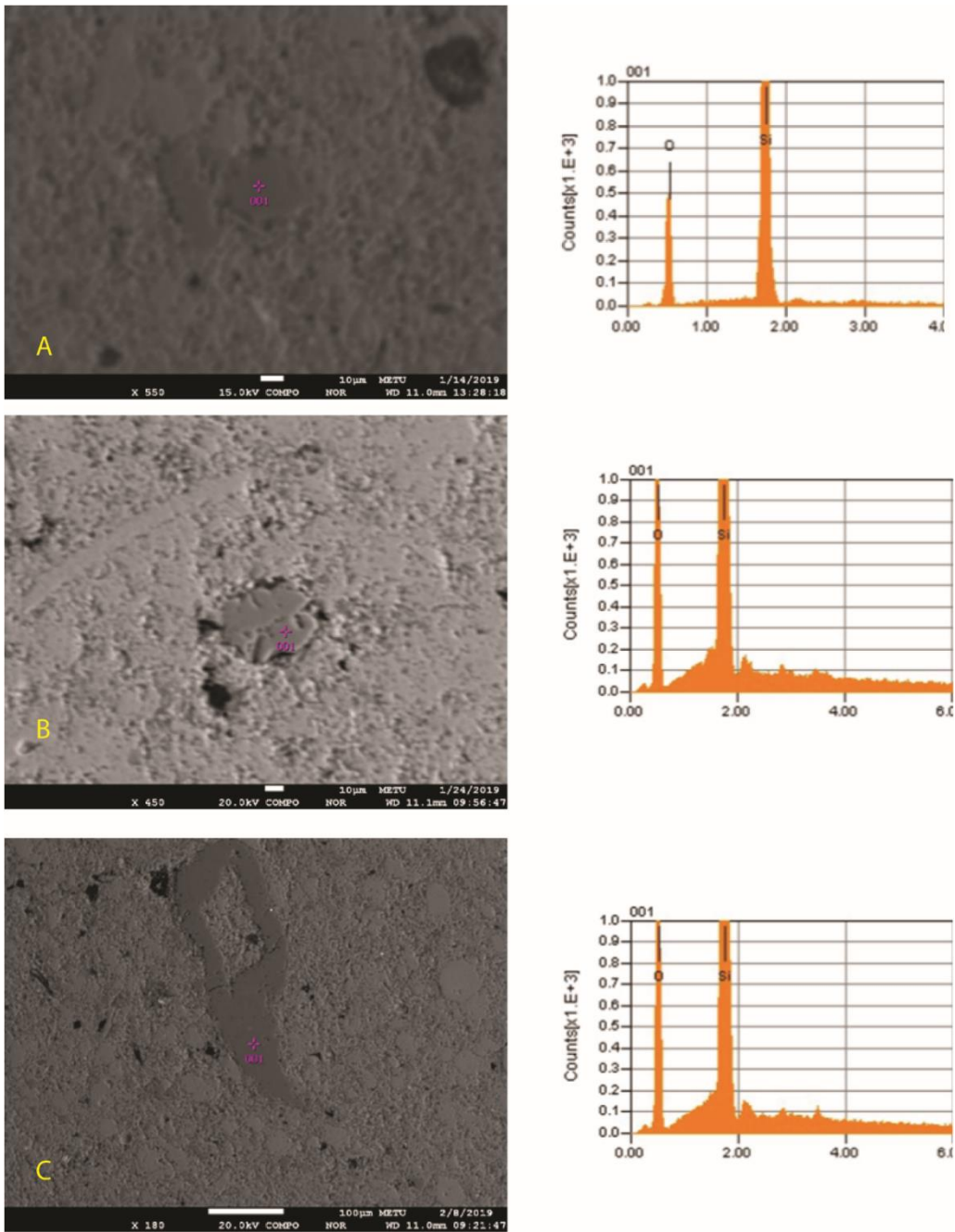


**Figure 4.7:** EPMA BSE images and EDS patterns for rounded to subrounded quartz grains except C, C) the angular quartz grain

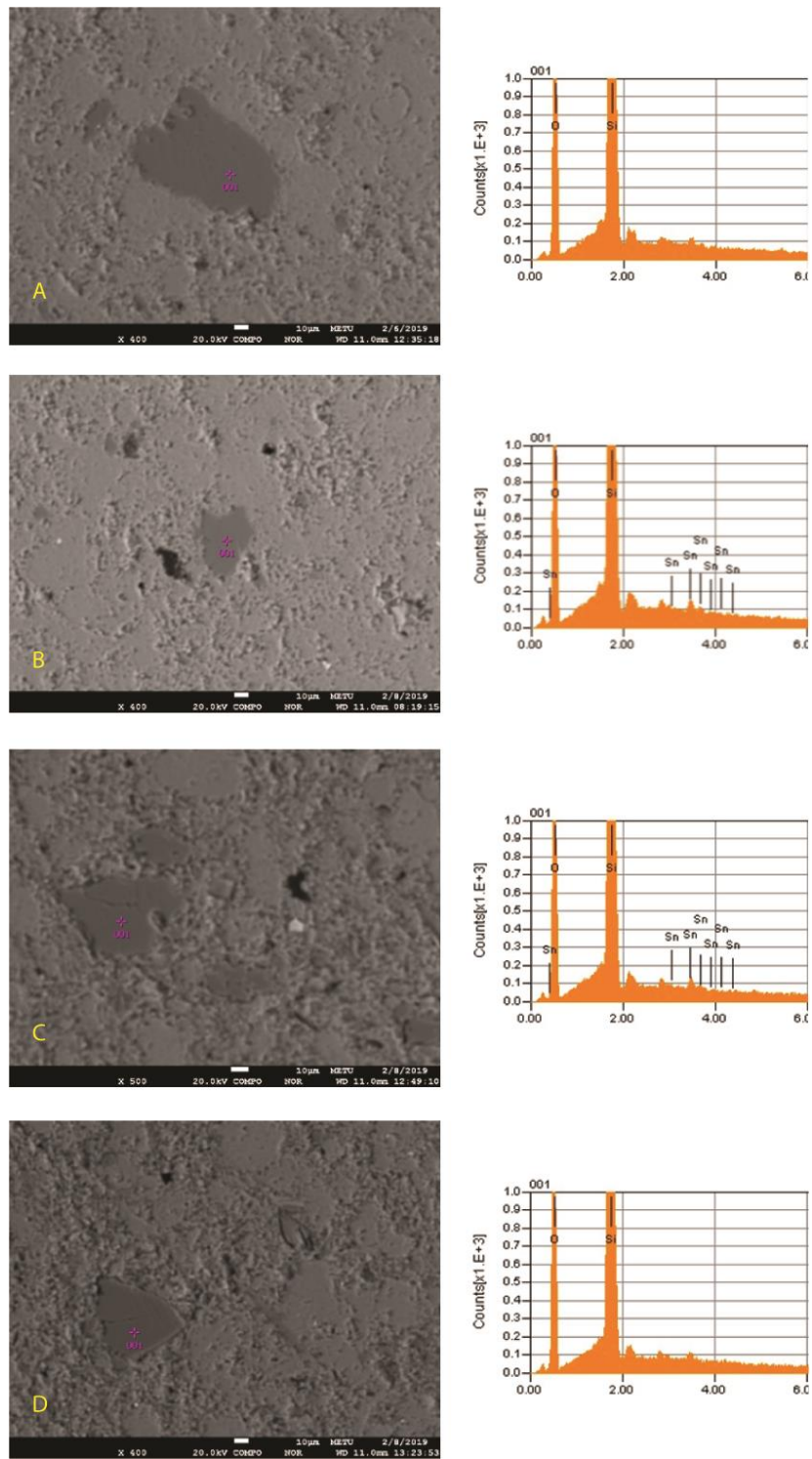


**Figure 4.8:** EPMA BSE images and EDS patterns for angular quartz grains

Feldspars were identified by XRD method in the previous section. They were also imaged and analyzed by EMPA (Figures 4.9, 4.10, 4.11). The feldspar grains are angular, and both Na-rich plagioclase and orthoclase (as alkali feldspar) types are present. Plagioclase grains have variable Na and Ca contents (Figure 4.10). Although most of the feldspar grains were in anhedral in shape, some euhedral grains were also identified, which indicates the similarity with quartz grains.

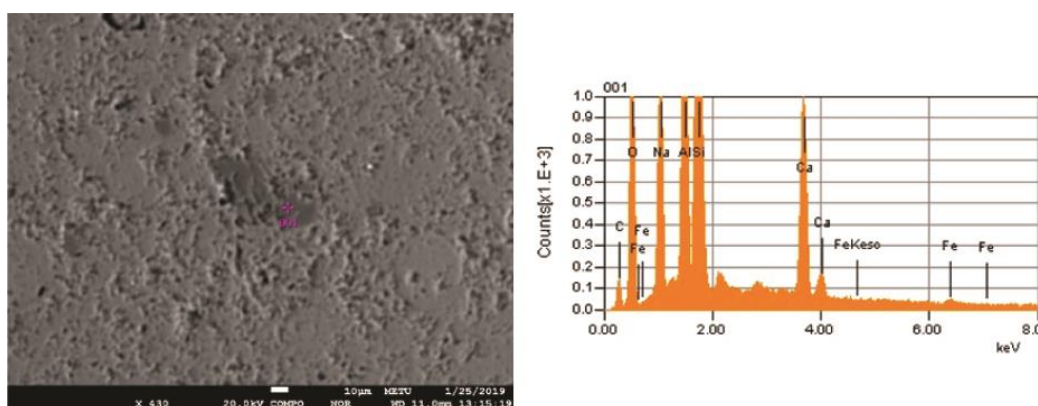


**Figure 4.9:** EPMA BSE images and EDS patterns for plagioclase

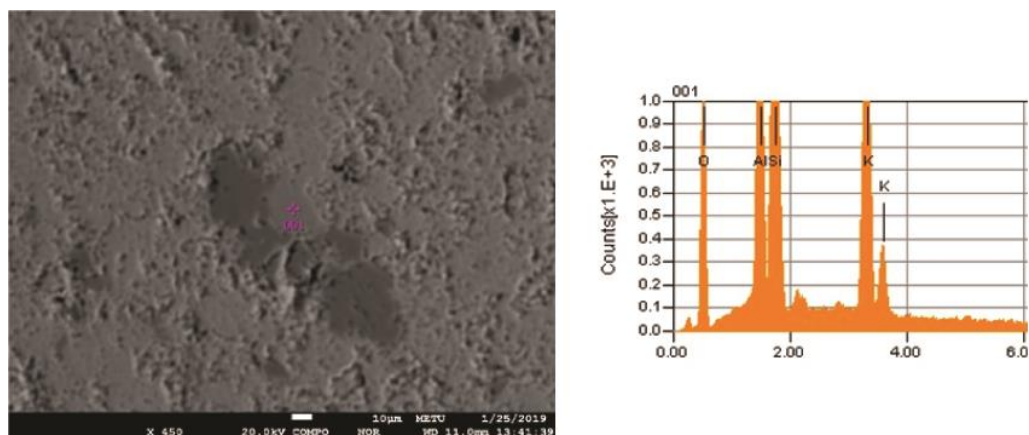


**Figure 4.10:** EPMA BSE images and EDS patterns of orthoclase

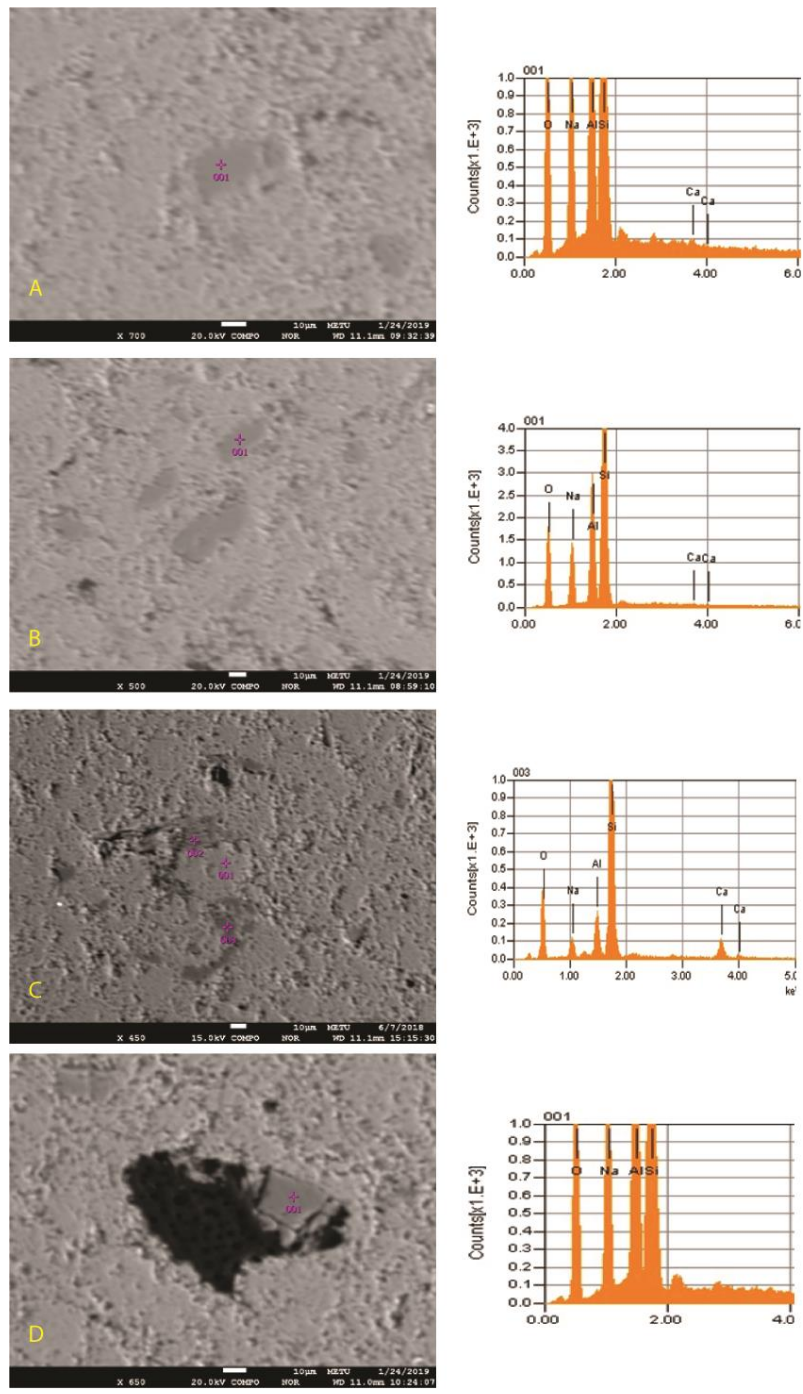


**Figure 4.11:** EPMA BSE images and EDS patterns for plagioclase

In addition, the magmatic phases due to their abundance less than 5% were identified by EPMA as amphibole, biotite, muscovite, whose compositions are given in Table 4.2. They are euhedral in shape and generally oxidized. The most important oxidized mineral that have been identified in the studied samples were biotite. The oxidized biotite indicated the weathering of the environment and it explains the abundance of illite in the XRD analysis (Figure 4.12). Moreover, the map from oxidized biotite revealed that the weathering process was started because of iron content. The foundation of Hg, Pt and even if S with low amounts identified from map results, which were indicated the volcanic origin (Figure 4.13).

Moreover, the quantitative data from an oxidized biotite grain include Fe, Si, Al, Mg, K, Na, Ti, and Ca. The presence of these elements infers a Ti-bearing, oxidized biotite which. These grains are observed in both Gk-12, Gk-26, and Gk-27, including just above the P0 zone and P1b zone. The SEM observations with EDS results show the occurrence of Ti-bearing iron hydroxides and phyllosilicates with a specular, plate-like morphology and grain-sizes <50  $\mu\text{m}$ . The Ca is associated with the sediment matrix, and Si is associated with high-clastic sediment influx.

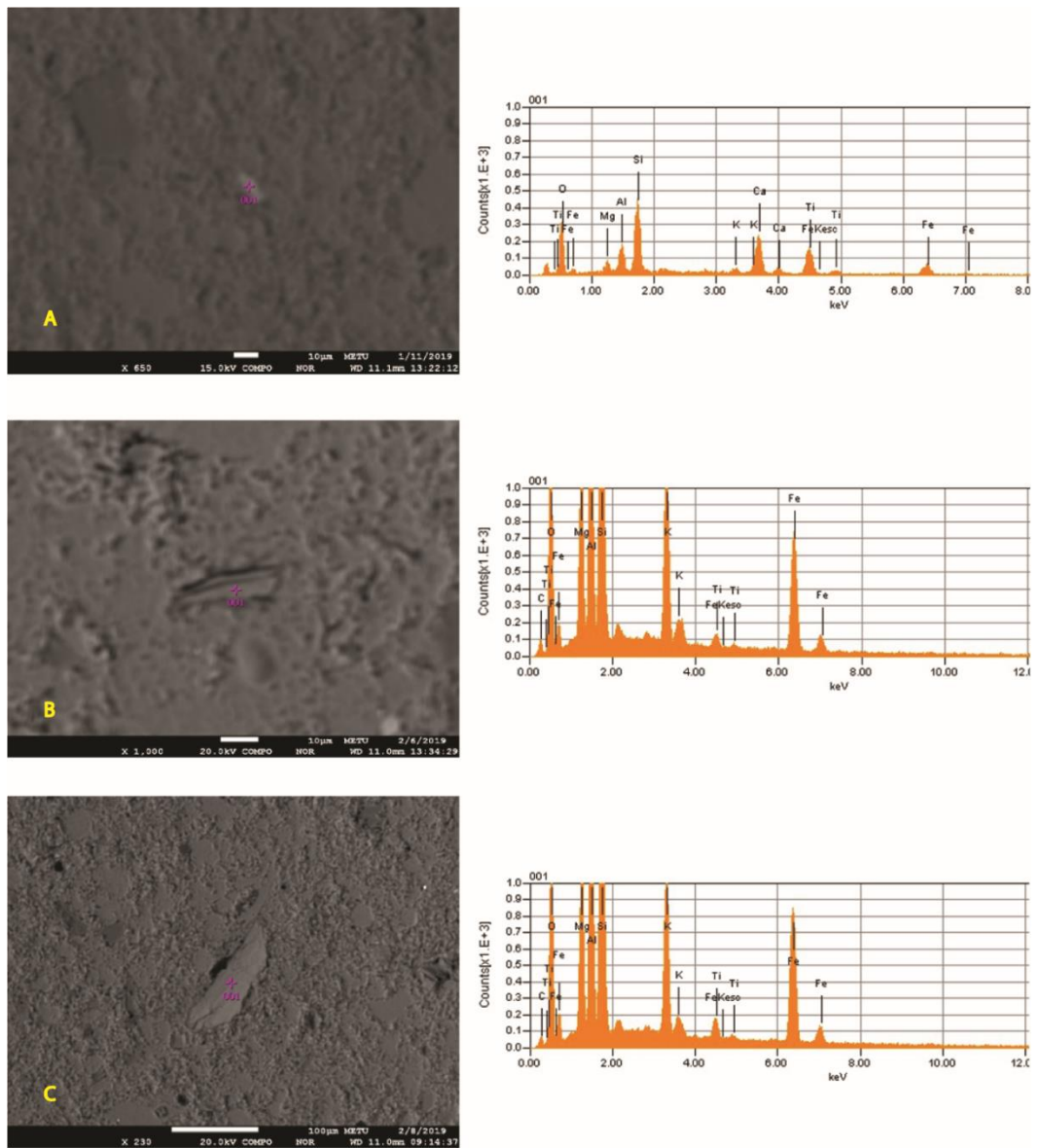


**Figure 4.12:** EPMA BSE images and EDS patterns of oxidized biotite

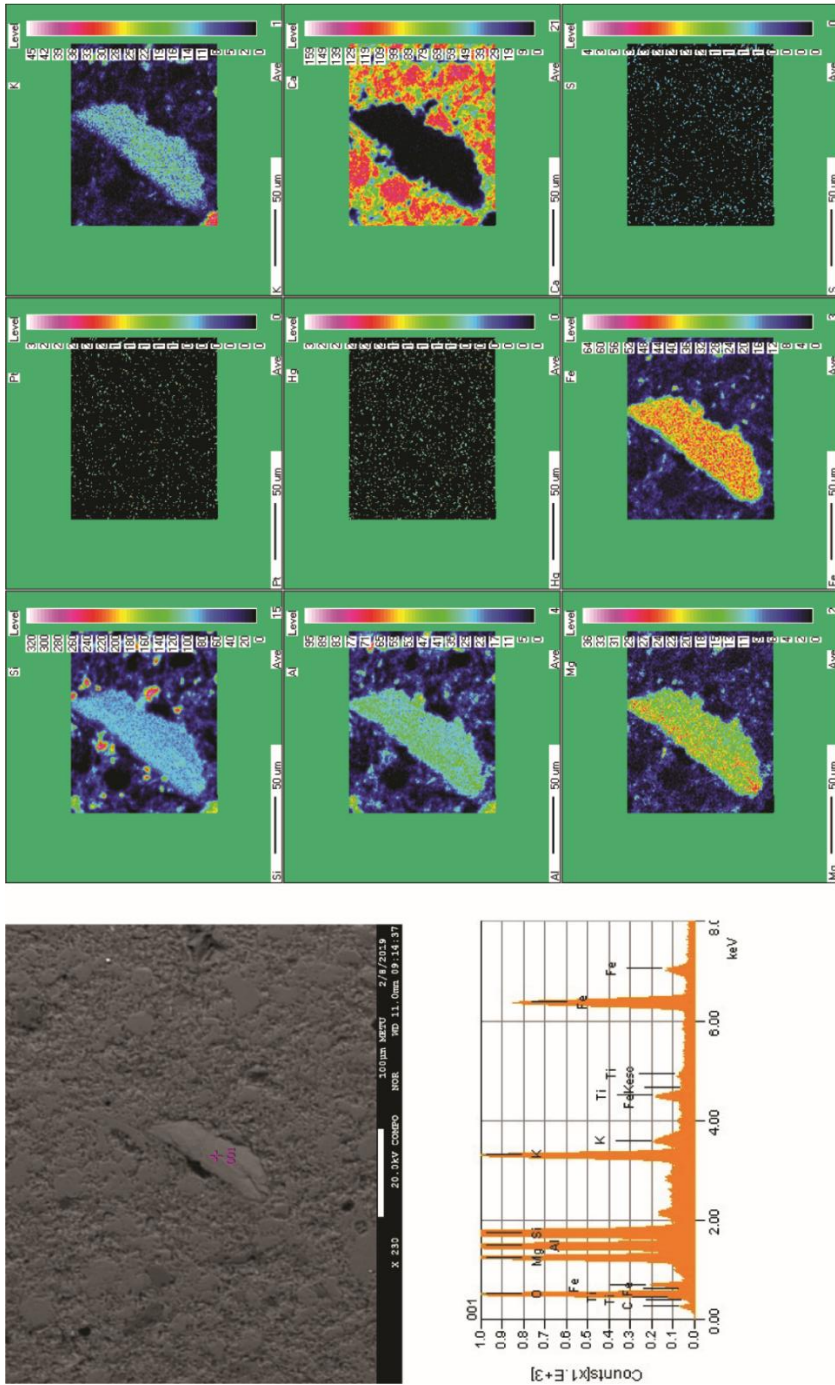


**Figure 4.13:** Back scattered electron (BSE) image with element maps of the oxidized biotite by EPMA

In addition, euhedral to subhedral magmatic phases zircon (Figure 4.14) and sphene (Figure 4.15), were identified in the Göynük samples. Sphene mainly consisting of Ti, Ca, Al, and Si has impurities of Fe, Mg (Figure 4.15).

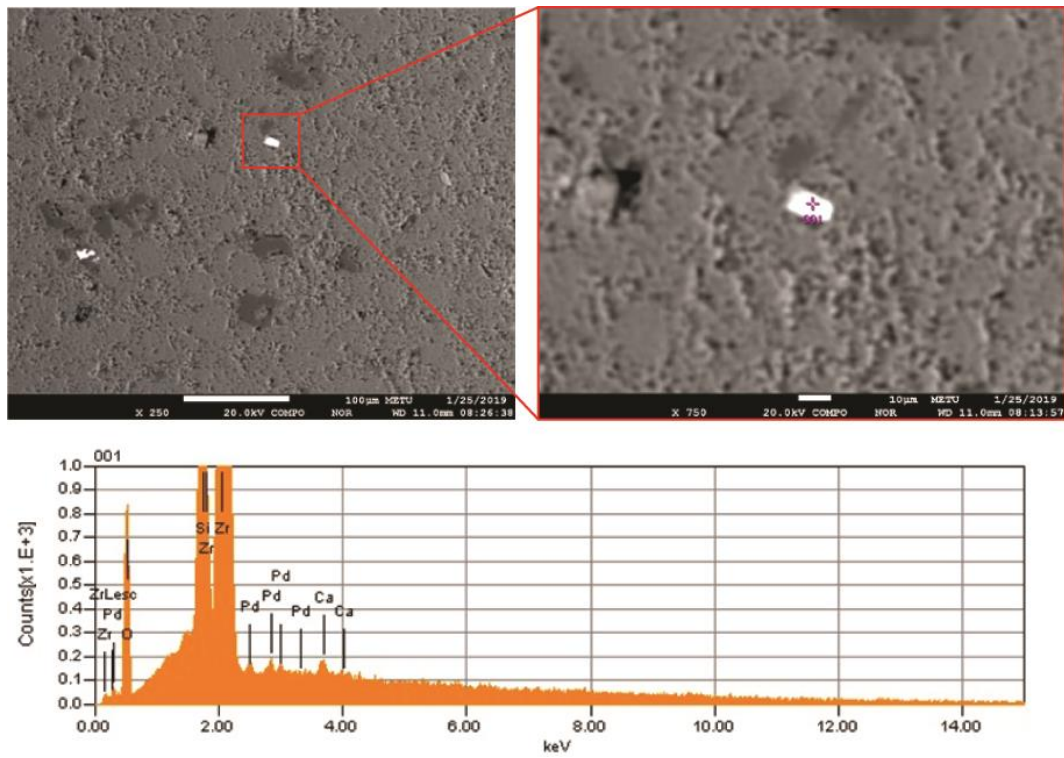


**Figure 4.14:** EPMA BSE images and EDS pattern of zircon

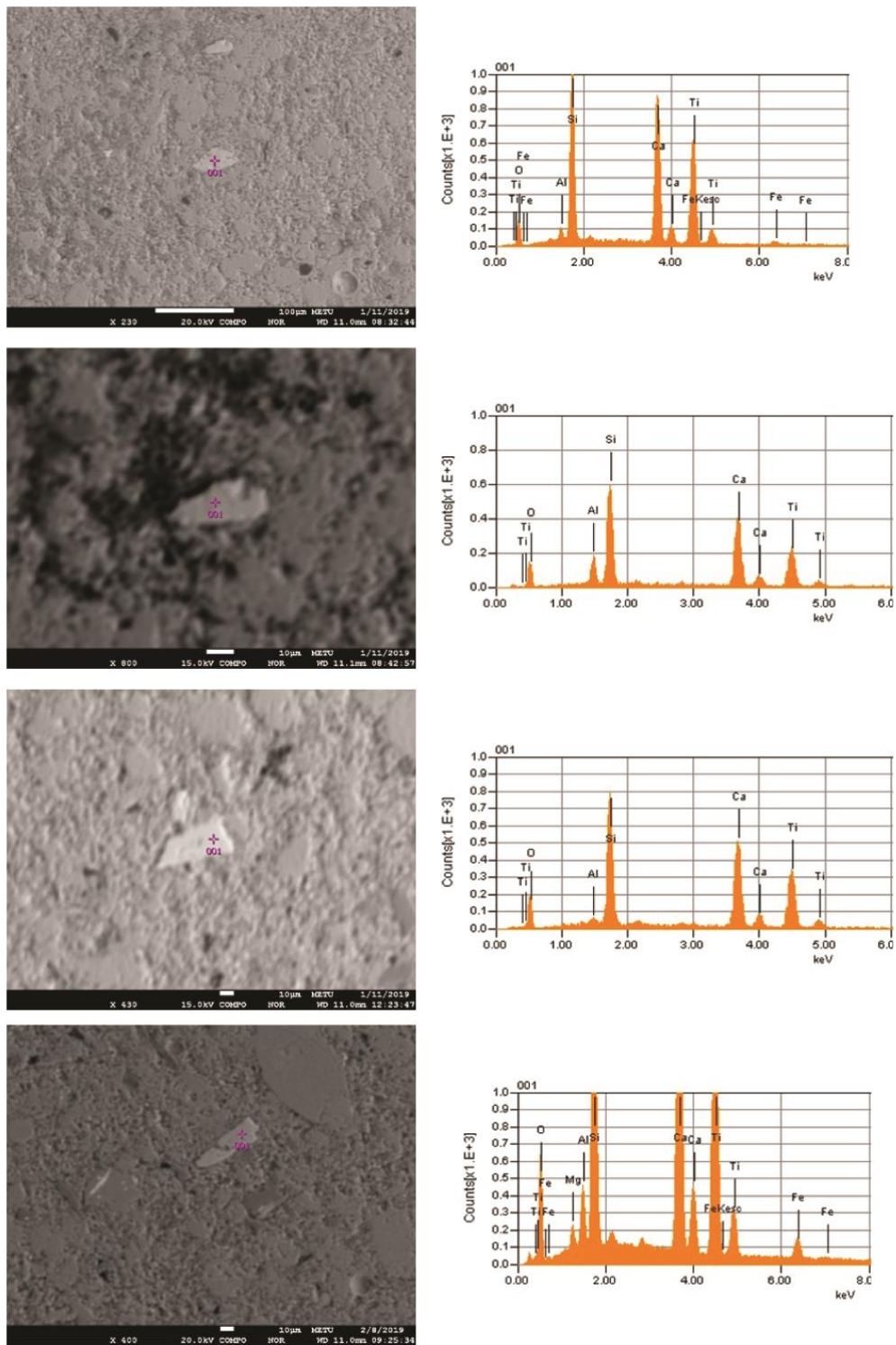


**Figure 4.15:** EPMA BSE images and EDS patterns of sphene

In addition to silicate minerals phosphatic mineral were also identified. Apatite crystals are in higher amount relative to other accessories, which was included Cl and S with minor amounts. Because of Cl is less stable ion, it can be dissolved very easily. However, in the Göynük samples it was detected as minor amounts inside of the apatite crystal (Figure 4.16).

The oxide minerals, on the other hand, were identified as rutile and ilmenite in the Göynük samples. Rutile crystals had formed as full of  $\text{TiO}_2$  without any additional ions (Figure 4.17). Ilmenite crystals were called as Ti-bearing iron oxides in literature, however, Mn, and Ca (from background) with minor amounts was observed in the Göynük samples (Figure 4.18).

The other oxide mineral is hematite which is the most important mineral for the Göynük section. Hematite consists of Mg, Al, Ca impurities. In addition to Ti-rich oxide minerals mentioned above, quantitative data from an oxide grain include Fe, Ca, Al, Si and K which shows the alteration product of akageneite (Figure 4.19).

Moreover, in the analyzed samples, hematite spherules prevalently detected by polarizing light microscope were analyzed by EPMA (Figures 4.20, 4.21, 4.22). Hematite spherules are present as both isolated and aggregated (Figure 4.21). Elemental maps of an aggregate display that Fe is the essential component, but too low Si and Al are also present (Figure 4.21). Maps of Ca, Hg, Pt and Ti, also taken from the same aggregate, display a significant evidence that trace amount of Hg is unusually present. The existence of Hg in the spherules are not reflected in EDS graphs due to trace amount less than 10 ppm (Batanova et al., 2018). The spherules, however, consist of trace amounts of Si, Al, Mg, Mn and Ca that appear on EDS patterns (Figure 4.22), and semi-quantitative EDS measurements (Table 4.3).

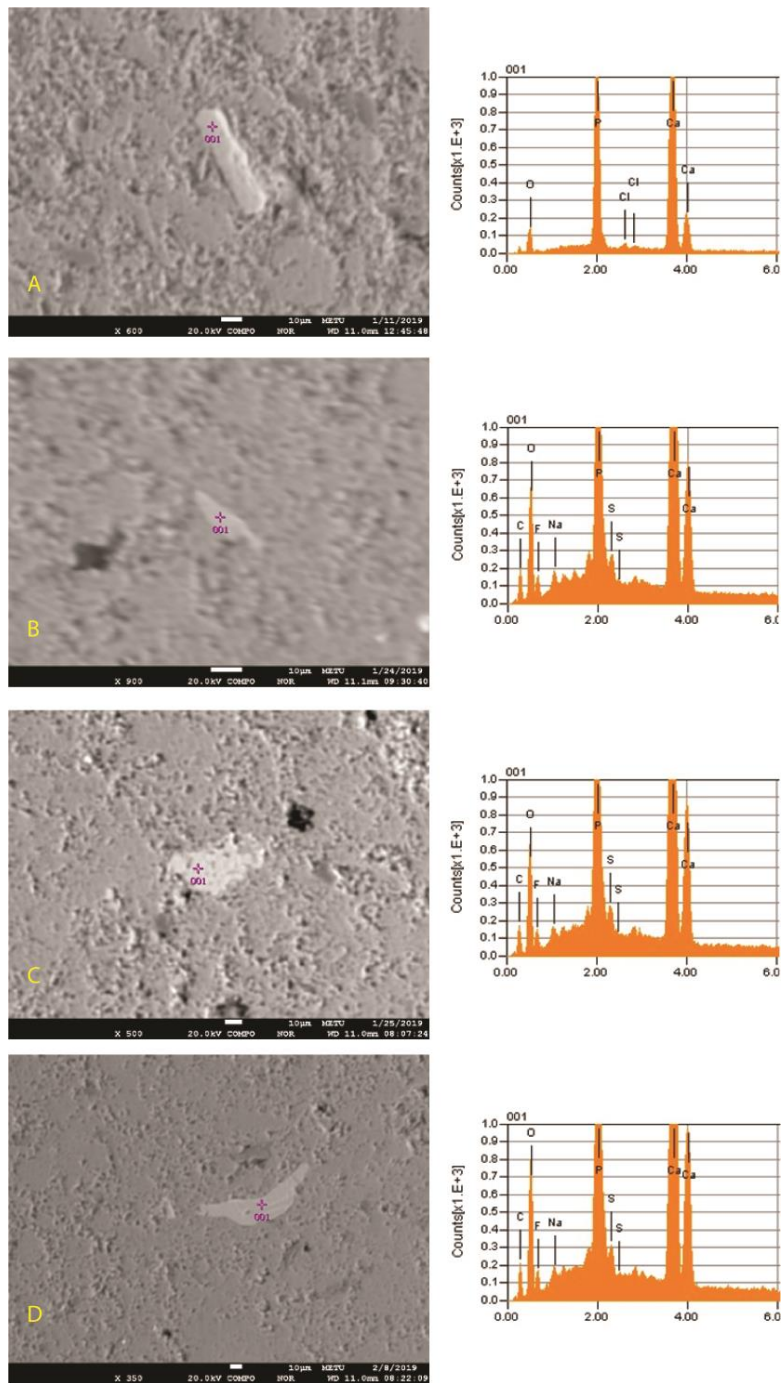


**Figure 4.16:** EPMA BSE images and EDS patterns of apatite

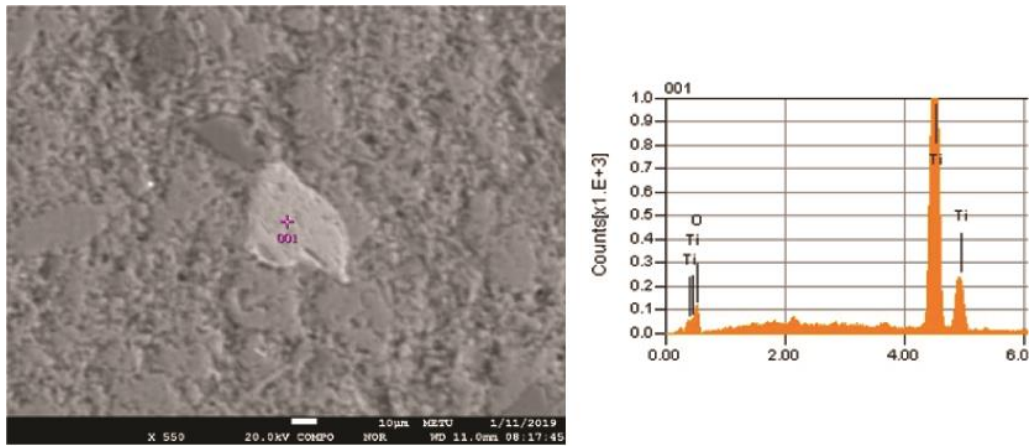


**Figure 4.17:** EPMA BSE images and EDS patterns of rutile

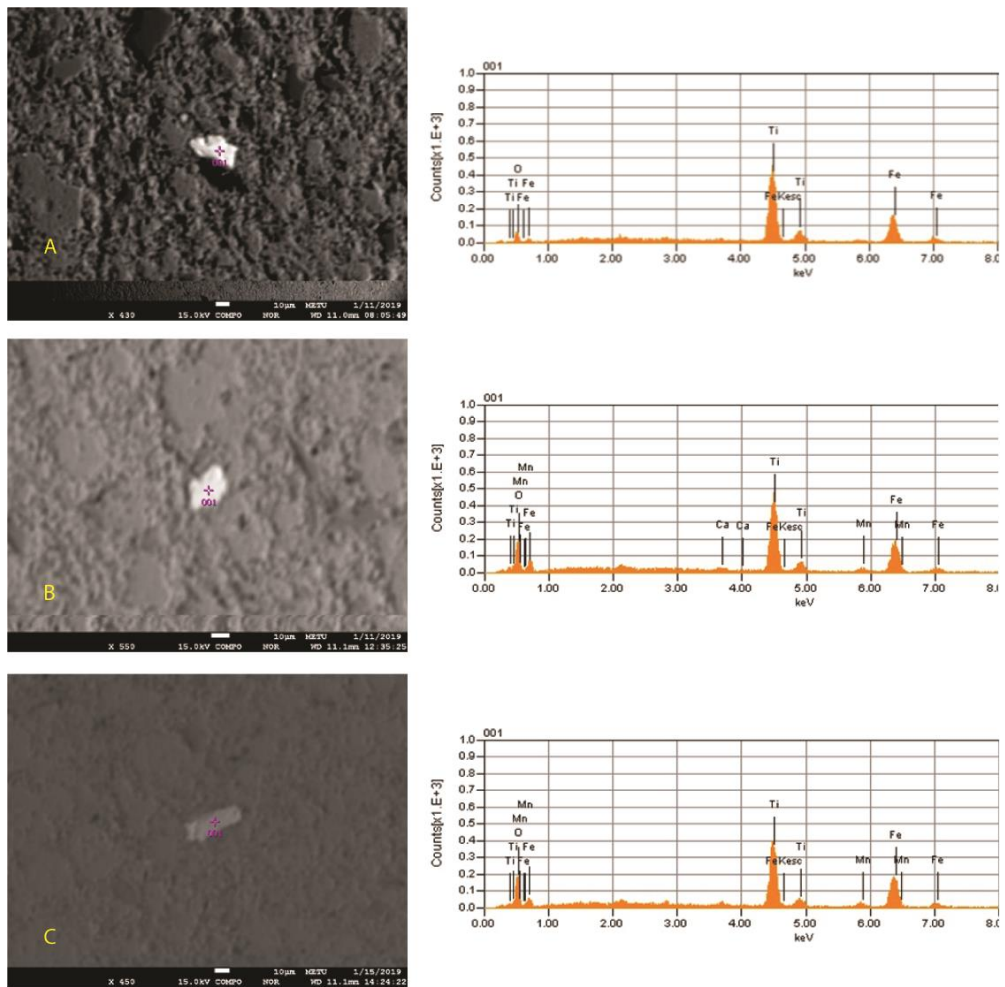


**Figure 4.18:** EPMA BSE images and EDS patterns of ilmenite

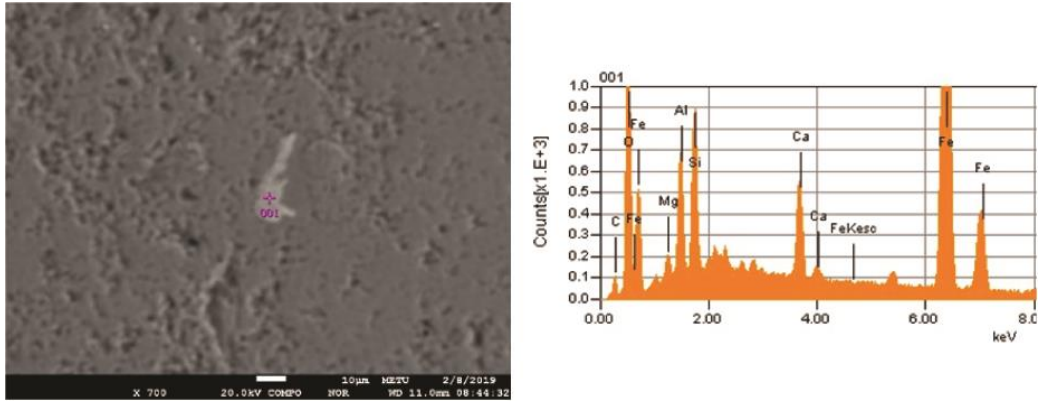


**Figure 4.19:** EPMA BSE images and EDS patterns of Hematite

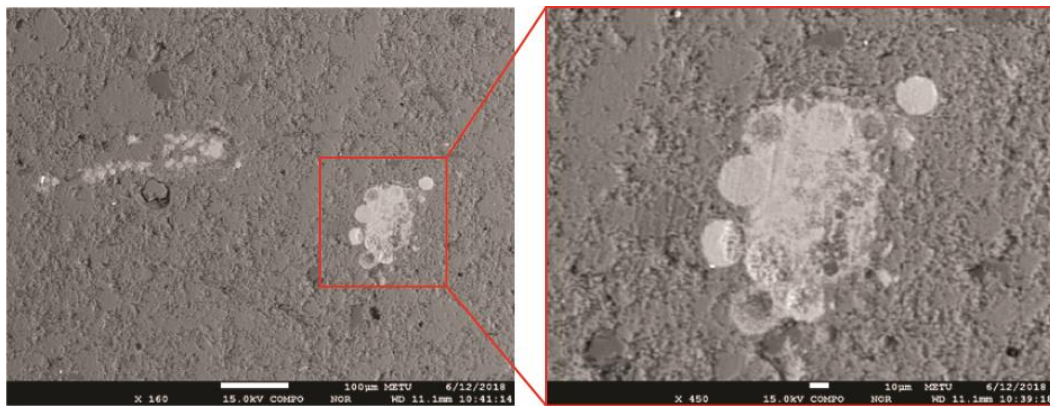


**Figure 4.20:** EPMA back scattered electron (BSE) image showing isolated and aggregated hematite spherules

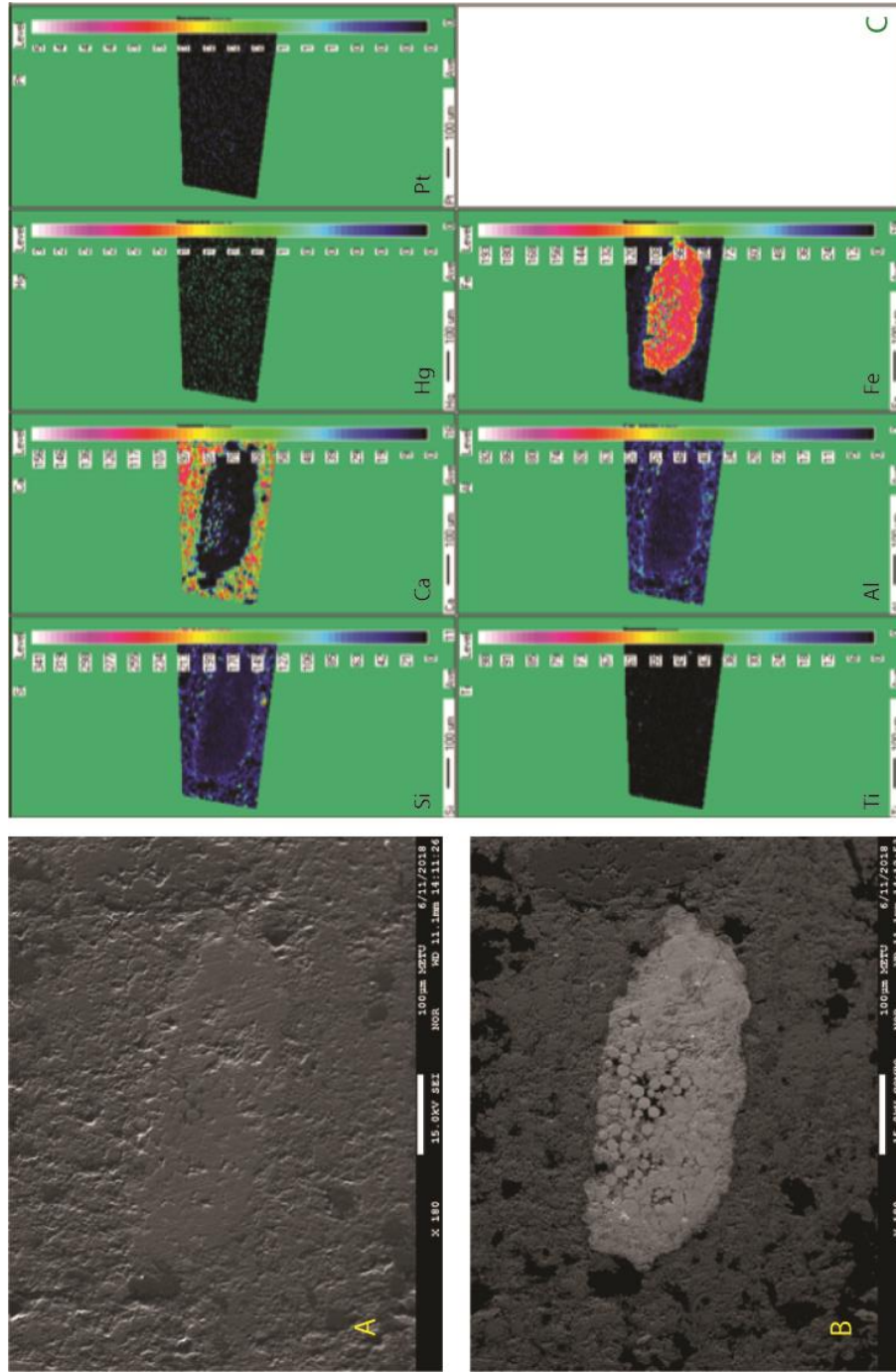


**Figure 4.21:** A) secondary electron (SE) image B) back scattered electron (BSE) image C) element maps of the hematite spherules by EPMA

**Table 4.2:** The quantitative data from Electron Microprobe Analysis (EPMA) of each recorded mineral

Amphibole													
Lithology	Sample	Subsample	Element										Total
			Si	Al	Ti	Fe	Mg	Mn	Ca	Na	K	O	
Marl	Gk-27	F	26,03	16,78	0,04	8,63	20,64	0,15	9,97	0,03	0,35	1,52	84,14
Feldspar													
Lithology	Sample	Subsample	Element										Total
			Si	Al	Ti	Fe	Mg	Mn	Ca	Na	K	O	
Marl	Gk-12	E	65,28	17,94		0,00			0,13	7,58	0,06		90,99
		G1	66,23	18,33		0,07			0,14	9,35	0,05		94,17
		G2	68,60	19,19		0,06			0,29	10,22	0,02		98,38
		G3	65,64	18,35		0,06			0,19	9,22	0,03		93,49
Gk-26		A1	67,31	18,51		0,00			0,24	10,18	0,07		96,31
		A2	67,61	19,01		0,01			0,30	10,04	0,17		97,14
		B	67,57	18,84		0,01			0,19	9,96	0,05		96,62
Gk-27	F	68,20	18,94		0,00			0,18	11,11	0,08		98,51	
Hematite													
Lithology	Sample	Subsample	Element										Total
			Si	Al	Ti	Fe	Mg	Mn	Ca	Na	K	O	
Marl	Gk-26	D	5,78	3,83	0,01	63,29	0,88	0,11	1,90				75,80

**Table 4.2. (cont'd)**

Ilmenite		Sample	Subsample	Element										Total
Lithology				Si	Al	Ti	Fe	Mg	Mn	Ca	Na	K	O	
Marl	Gk-12	D	0,14	0,08	49,41	41,66	0,02	3,32	0,82					95,46
		F	1,11	0,39	44,10	34,70	0,19	2,55	2,24					85,28
	Gk-26	B	1,20	1,40	64,98	20,62	0,30	0,21	1,58					90,29

Iron Bubble		Sample	Subsample	Element										Total
Lithology				Si	Al	Ti	Fe	Mg	Mn	Ca	Na	K	O	
Marl	Gk-12	B	8,03	3,29	0,00	62,28	0,91	0,03	1,75	0,11	0,02			76,42
		I1	6,73	2,09	0,00	67,26	0,58	0,01	0,72					77,39
		I2	5,09	1,04	0,01	69,68	0,60	0,02	0,62					77,06
		I3	7,28	1,94	0,02	63,84	0,77	0,01	0,69					74,55
		I4	6,27	1,37	0,03	68,20	0,69	0,02	0,61					77,19
	Gk-26	A	7,01	2,70	0,00	61,25	0,85	0,03	0,96					72,79
		B	4,28	1,22	0,00	70,55	0,74	0,00	0,47					77,26

**Table 4.2. (cont'd)**

Orthoclase												
Lithology	Sample	Subsample	Element									Total
			Si	Al	Ti	Fe	Mg	Mn	Ca	Na	K	
Marl	Gk-26	C	63,87	17,50		0,01			0,13	0,07	16,29	97,87

**Phyllosilicate and iron-oxides**

Lithology	Sample	Subsample	Element									Total
			Si	Al	Ti	Fe	Mg	Mn	Ca	Na	K	
Marl	Gk-12	E1	48,53	5,65	0,04	20,29	3,70	0,03	0,30	0,06	8,19	90,07
		E2	50,26	4,26	0,08	10,39	13,47	0,15	8,89	1,42	0,09	92,60
Marl	Gk-26	C	48,86	6,80	0,11	22,57	4,19	0,00	0,69	0,09	7,99	94,72
		D1	46,34	29,79	0,14	2,71	2,50	0,03	1,49	0,15	9,86	96,88
		D2	37,92	16,09	1,30	14,98	9,94	0,24	0,82	0,07	7,51	92,25

**Rutile**

Lithology	Sample	Subsample	Element									Total
			Si	Al	Ti	Fe	Mg	Mn	Ca	Na	K	
Marl	Gk-12	C1	0,08	0,05	95,15	0,15	0,00	0,03	0,78	0,03	0,02	97,11
		C2	0,03	0,03	95,77	0,19	0,00	0,01	0,67			96,70
	Gk-26	B	26,57	0,93	69,00	0,26	0,06	0,02	0,62	0,00	0,00	97,46

**Table 4.2. (cont'd)**

Sphene

Lithology	Sample	Subsample	Element										Total
			Si	Al	Ti	Fe	Mg	Mn	Ca	Na	K	O	
Marl	Gk-12	B1	29,13	1,06	37,05	0,14	0,01	0,02	26,76	0,03	0,00	0,82	95,02
		B2	29,46	5,91	29,74	0,68	0,04	0,00	30,44	0,04	0,18	0,84	97,33
		D	29,71	1,01	37,23	0,10	0,02	0,04	27,47	0,00	0,03	0,83	96,44
		G	27,91	3,09	29,03	1,61	0,27	0,05	23,93	0,03	0,15	3,21	89,28
	Gk-26	F	30,26	1,35	38,15	0,11	0,01	0,02	28,05	0,02	0,02	0,85	98,84
	Gk-27	E	28,48	1,84	33,40	1,32	0,25	0,02	29,20	0,00	0,05	0,81	95,37

Quartz

Lithology	Sample	Subsample	Element										Total
			Si	Al	Ti	Fe	Mg	Mn	Ca	Na	K	O	
Marl	Gk-12	E	93,74	0,67	0,01	0,11	0,09	0,01	0,17	0,07	0,10	94,97	
		H1	96,99	0,03	0,03	0,02	0,00	0,00	0,07	0,02	0,01	97,17	
		H2	96,77	0,44	0,00	0,06	0,01	0,00	0,10	0,10	0,03	97,51	
		H3	96,10	0,04	0,00	0,01	0,01	0,00	0,19	0,00	0,01	96,36	
	Gk-26	A	99,28	0,05	0,00	0,03	0,00	0,01	0,18	0,01	0,02	99,58	
		B	97,92	0,05	0,00	0,00	0,01	0,00	0,17	0,06	0,00	98,21	
		C	96,29	0,35	0,03	0,09	0,15	0,01	1,26	0,16	0,04	98,38	

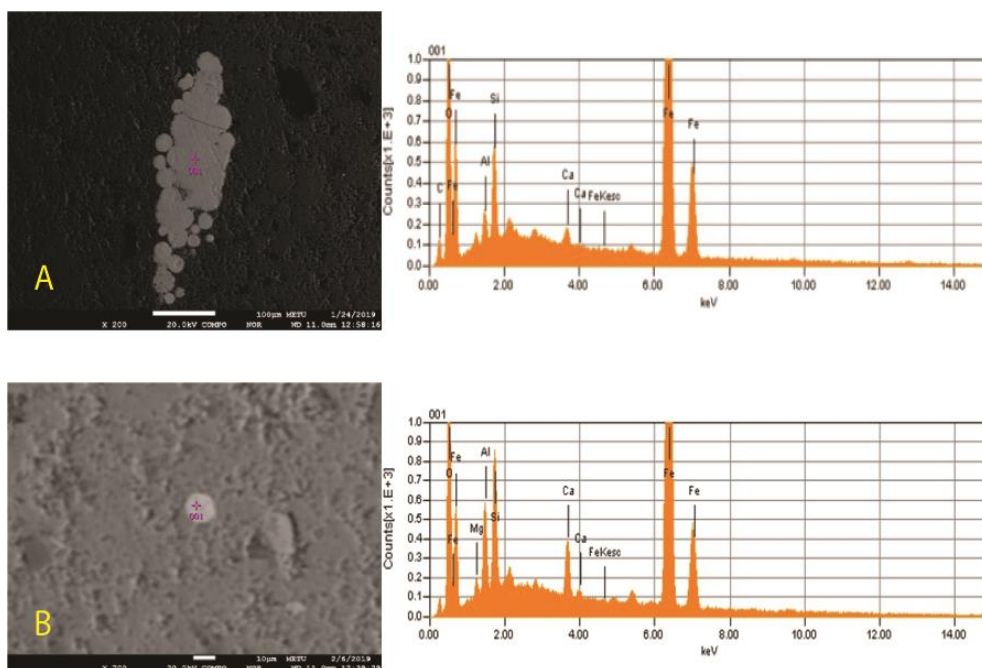


**Figure 4.22:** EPMA back scattered electron images and EDS patterns for A) hematite spherules aggregates B) isolated hematite spherules

**Table 4.3:** Semi-quantitative EDS values for the hematite spherules

Sample	Subsample	C	MgO	Al <sub>2</sub> O <sub>3</sub>	SiO <sub>2</sub>	CaO	FeO	Total
Gk-12	A1	13,81			5,95	68,37	11,87	100,00
	A2				4,66	2,22	93,12	100,00
	A3			3,65	8,88	2,86	84,61	100,00
	B		3,37	5,16	14,06	2,25	75,16	100,00
Gk-26	A	5,01	0,96	1,78	7,83	3,00	81,42	100,00
	B	3,53		1,61	4,72	0,70	89,45	100,00

Element maps by EPMA show that the trace element Ir is present in the groundmass of the sample Gk-12 with microtektites, above the K/Pg boundary (Figure 4.23). Mapping of Hg and Ir displayed that both microtektite and its host groundmass have similar amounts of Ir and Hg despite trace amount of concentrations (Figure 4.23). The Ir peaks was observed in the place where microtektites are present, which indicates the effect of Chicxulub impact in the Göynük basin.

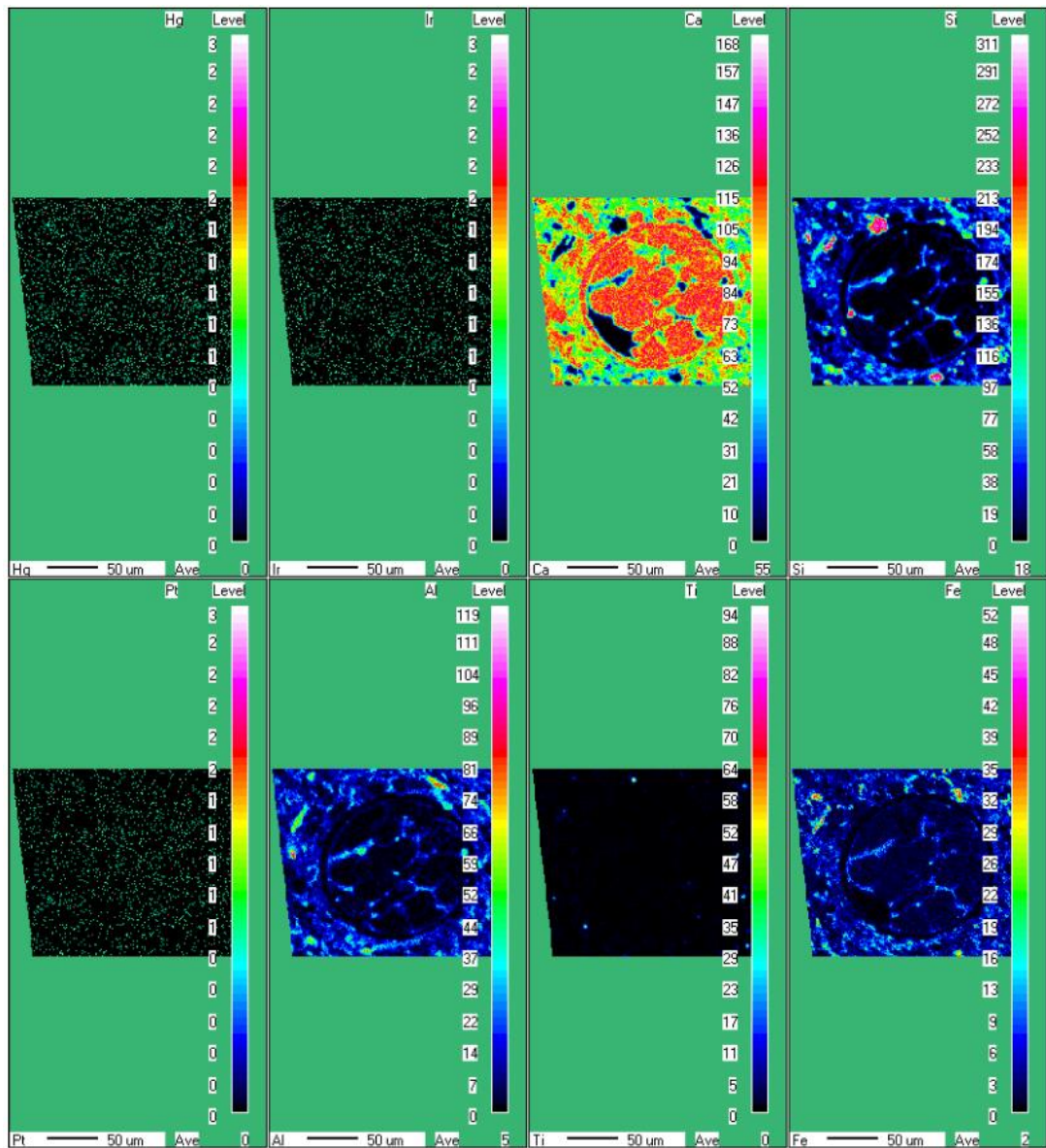


**Figure 4.23:** The map of the microtektite from the sample Gk-12

In summary, EPMA analyses provided to detect the presence of oxide minerals (hematite as alteration product of akageneite ilmenite, rutile), sphene, zircon, apatite, amphibole, biotite, muscovite with less than 5% abundance that leads not to appear in random XRD patterns. Moreover, Hg and Ir were detected in the samples by EPMA.

These minerals together with plagioclase and orthoclase detected by XRD, are almost absent in the samples except for K/Pg boundary and P1b zone.

## 4.2. Magnetic Susceptibility

Magnetic susceptibility method was applied for testing the correlating beds and recognizing the marker horizons that Deccan phases observed. In early studies, magnetic susceptibility analysis tested below and just above the boundary (Ellwood et al., 2003; Font et al., 2016, 2019). However, in this study, magnetic susceptibility method is used for determination of evolutionary recovery stages after the mass extinction. The recovery stage after the mass extinction was discussed, including P1b and P1c zones (Discussed in detail in Chapter 3). The magnetic susceptibility analysis carried out whole section by using both thin sections and rock samples (Table 4.4). In previous studies, the rock samples were only used for magnetic susceptibility analysis (Ellwood et al., 2003; Abrajevitch et al., 2015; Font et al., 2016, 2017, 2019; Rostami et al., 2018). However, the results getting from Göynük section revealed that the both thin section and rock samples can be used, showing the same trend (Figure 4.21, 4.22). These results revealed that not only rock samples, but also thin sections can be used for magnetic susceptibility analysis, which gives the similar patterns. The only difference between them is the amount of results, the thin section results shows the negative results.

In the Göynük Section, at the top of the P1a zone low magnetic susceptibility values were measured and sudden increases were identified at the bottom of P1b zone (Table 4.3). The similar pattern was observed in between below the K/Pg boundary and P0 zone. It is important to note that where microspherules domination is observed, high magnetic susceptibility is present. After these decreasing stages in the top of P1a zone and below the K/Pg boundary, magnetic susceptibility values rapidly increase, where *Guembelitra cretacea* dominated as microfossils.

At the sample Gk-00, where the minor fault plane interpreted in the field, there is an abrupt shift. It is known that the main usage of magnetic susceptibility analysis is the determination of tectonism by using magnetic shifting of beds. Moreover, graphs show weaving changes in the samples from Gk-26 to Gk-42, where marl and limestone alternates. In limestone beds, magnetic susceptibility has higher value than marl deposits.

In brief, the results by magnetic susceptibility in this study well compare with the magnetic susceptibility values in global studies (Ellwood et al., 2003; Abrajevitch et al., 2015; Font et al., 2016, 2017, 2019; Rostami et al., 2018). In addition, this analysis carried out P1b zone, related with phase-3 of the Deccan volcanism, which shows the similar pattern with K/Pg boundary.

**Table 4.4:** The all values from Magnetic Susceptibility Analysis

SampleNo:	Rock Sample				Thin Section			
	Tried 1(e-6)	Tried 2	Tried 3	Average	Tried 1	Tried 2	Tried 3	Average
Gk-42	54.89	55.50	53.55	54.65	-5,99	-7,31	-9,89	-7,73
Gk-41	140.19	139.55	138.22	139.32	-2,68	-4,64	-5,96	-4,43
Gk-40	49.64	48.28	49.55	49.16	-7,27	-7,93	-6,60	-7,26
Gk-39	113.75	122.33	120.96	119.01	-5,97	-5,32	-6,65	-5,98
Gk-38	39.68	37.64	37.70	38.34	-7,94	-9,27	-7,94	-8,38
Gk-37	108.42	111.71	110.41	110.18	-6,63	-7,95	-6,66	-7,08
Gk-36	41.63	40.31	40.99	40.98	-5,30	-5,27	-7,25	-5,94
Gk-35	91.26	88.60	95.89	91.92	-6,60	-6,61	-7,91	-7,04
Gk-34	39.03	35.70	33.72	36.15	-6,62	-5,99	-6,61	-6,41
Gk-33	99.17	98.56	101.14	99.62	-7,29	-7,26	-5,98	-6,84
Gk-32	48.28	47.63	45.64	47.18	-7,31	-7,95	-7,32	-7,53
Gk-31	93.90	95.92	95.19	95.00	-8,59	-7,28	-7,31	-7,72
Gk-30	48.89	50.28	48.26	49.14	-7,94	-8,60	-6,61	-7,72
Gk-29	50.89	50.27	64.83	55.33	-5,95	-7,26	-6,62	-6,61
Gk-28	133.61	132.94	135.62	134.06	-6,57	-7,97	-7,31	-7,28
Gk-27	126.31	127.00	126.96	126.76	-7,90	-7,95	-6,61	-7,49
Gk-26	39.67	35.66	38.36	37.90	-3,98	-6,66	-5,91	-5,51
Gk-25	37.66	37.15	39.68	38.16	-7,32	-7,93	-8,60	-7,95
Gk-24	49.59	52.21	39.68	47.16	-6,66	-7,93	-5,96	-6,85
Gk-23	36.99	37.65	38.34	37.66	-7,29	-7,92	-7,26	-7,49
Gk-22	106.50	104.46	106.45	105.80	-7,24	-8,60	-6,61	-7,48
Gk-21	86.61	83.98	86.67	85.75	-7,29	-7,93	-7,27	-7,49
Gk-20	72.09	72.07	66.82	70.33	-5,91	-5,34	-5,97	-5,74
Gk-19	106.47	104.48	103.78	104.91	-3,34	-3,33	-3,98	-3,55
Gk-18	80.70	81.97	79.99	80.89	-5,94	-5,99	-5,97	-5,97
Gk-17	121.02	117.71	119.73	119.49	-3,98	-4,62	-4,58	-4,39
Gk-16	99.23	101.83	84.61	95.22	-5,29	-4,65	-3,94	-4,62
Gk-15	96.56	95.84	94.57	95.66	-4,64	-4,62	-4,66	-4,64
Gk-14	103.13	119.06	115.07	112.42	-3,35	-2,68	-2,59	-2,88
Gk-13	82.70	83.30	82.65	82.88	-6,66	-5,96	-4,62	-5,75
Gk-12	87.31	91.27	89.92	89.5	-2,66	-3,33	-3,98	-3,32
Gk-11	84.66	84.64	76.06	81.79	-6,59	-4,67	-4,62	-5,29
Gk-10	71.42	68.16	68.82	69.47	-4,03	-5,27	-4,62	-4,64
Gk-9	127.67	124.99	116.42	123.03	-2,04	-2,61	-3,33	-2,66
Gk-8	132.30	132.89	134.23	113.14	1,30	-1,32	-1,94	-0,65
Gk-7	128.31	128.33	128.35	128.33	-3,32	-1,99	-3,28	-2,86
Gk-6	156.06	156.05	146.75	152.95	-4,62	-5,32	-2,63	-4,19
Gk-5	162.69	159.39	144.21	155.43	-1,99	-1,96	-1,99	-1,98
Gk-4	158.66	165.99	165.97	163.54	1,33	-0,03	0,70	0,67
Gk-3	156.03	154.78	154.11	154.97	0,62	2,66	1,34	1,54
Gk-2	365.71	351.15	316.12	344.33	11,23	15,90	14,51	13,88
Gk-1	394.77	375.67	368.38	379.61	4,62	4,62	4,67	4,64
Gk-00	113.75	115.75	115.08	114.86	-5,30	-5,94	-3,92	-5,05
Gk-01	383.55	392.15	388.17	387.96	9,27	11,85	9,24	10,12
Gk-02	417.96	416.00	369.02	400.99	0,63	0,04	-1,29	-0,21
Gk-03	426.56	437.18	433.83	432.52	0,66	2,63	1,99	1,76
Gk-04	557.45	565.41	560.18	561.01	4,64	4,65	6,60	5,30

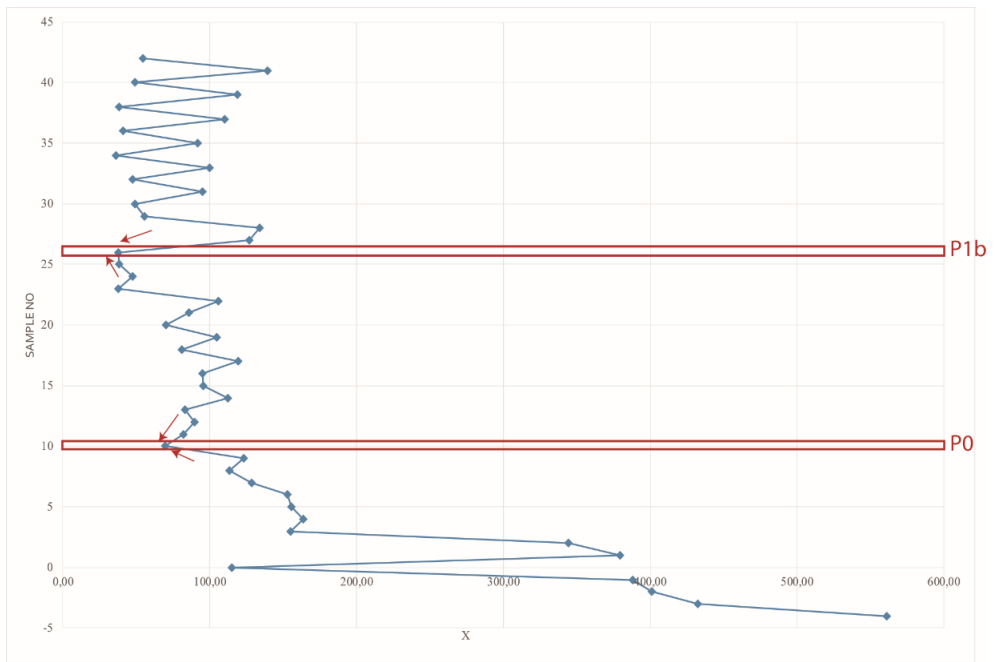


**Figure 4.24:** Magnetic Susceptibility Graph of Rock Samples

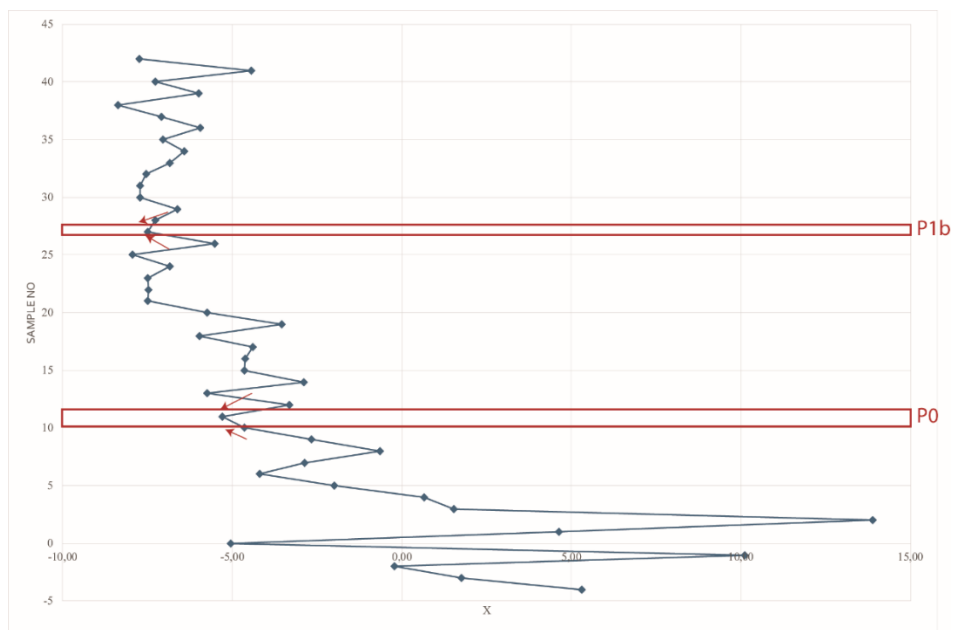


**Figure 4.25:** Magnetic Susceptibility Graph of Thin Sections



## CHAPTER 5

### SYSTEMATIC TAXONOMY

This chapter comprises the description of the both early Danian and late Maastrichtian planktonic foraminiferal taxa with updated synonym list. All characteristic morphologic features of the recorded seen in species. They have been identified from both washed samples and thin sections of the studied samples.

Identifications of Planktonic foraminifera are mainly based on the fundamental studies: Loeblich and Tappan (1988), Postuma (1971), Robaszynski et al. (1984), Nederbragt (1998), Olsson et al. (1999), Premoli-Silva and Verga (2004), Boudagher-Fadel (2012), and Microtax website (<http://www.mikrotax.org/pforams>). Moreover, researches based on the planktonic foraminiferal assemblages are used for classification, such as Keller et al. (2002), Esmeray (2008), Gallala et al. (2009), Karabeyoğlu (2017).

In order to identify the species of planktonic foraminifera taxa, the morphological features have been recognized in detail. These are:

- The test outline; lobate, subtriangular, biconvex, plano-convex etc.
- Test sutures; depressed, raised or beaded.
- Chamber arrangement; serial; biserial or multiserial, spiral; planispiral or trochospiral.
- Shape of chambers; globular, subglobular, triangular, rectangular, etc.
- Number of chambers in the final whorl.
- Umbilicus and umbilicus depth; deep, narrow etc.
- Periphery and peripheral margin; unkeeled, single-keeled, or double-keeled.
- Aperture; umbilical, extraumbilical, equatorial, interiomarginal etc.
- Wall texture; costae, perforate, cancellata etc.

The size of both early Danian and late Maastrichtian planktonic foraminifera assemblages ranges between  $> 63 \mu\text{m}$  in sieve analysis.

### 5.1. Early Danian Planktonic Foraminifera

Taxonomy of Cenozoic planktonic foraminifera are highly debated in order to understand the recovery stages of them after the great mass extinction. The most important part of the Cenozoic taxonomy is the earliest Danian planktonic foraminifera because there are several hypotheses about the origin and the evolution of these forms. Only three species can survive from the mass extinction. These are ; *Guembeltria cretacea*, *Hedbergella holmdelensis*, and *Hedbergella monmouthensis*. These species are the main ancestor of the Paleogene assemblages.

According the previous researches, *Chiloguembelina*, *Woodringina*, *Globoconusa* genera was evolved from the *Guembeltria* genus. Nevertheless, genera *Praemurica*, *Globanomalina*, *Parvularugoglobigerina*, *Eoglobigerina*, *Subbotina* and *Parasubbotina* was evolved genus *Caucasina* (Khalilov, 1951). However, genus *Caucasina* is the benthic origin form. According to Arenillas et. al. (2015), this genus is the ancestor of the first *Parvularugoglobigerinds* on the basis of the similarities on test structure, apertural morphologies, and wall texture. They added the molecular phylogenetic studies that have suggested several episodes of benthic-planktonic transitions in the evolutionary history of the planktonic foraminifera (Figure 5.1).

The early Paleogene (Danian) planktonic foraminiferal assemblages from the studied samples are composed of mainly simple and small-in-size forms. Especially, biserial forms *Chiloguembelina*, *Woodringina* are simple test forms that are Guembeltriid originated forms. However, genera *Praemurica*, *Globanomalina*, *Parvularugoglobigerina*, *Eoglobigerina*, *Subbotina* and *Parasubbotina* are complex, trochospiral but not high-ornamented forms.

In this chapter, the taxonomy of early Danian planktonic foraminifera forms is presented by giving special features, differentiated characteristic features and stratigraphic distributions.

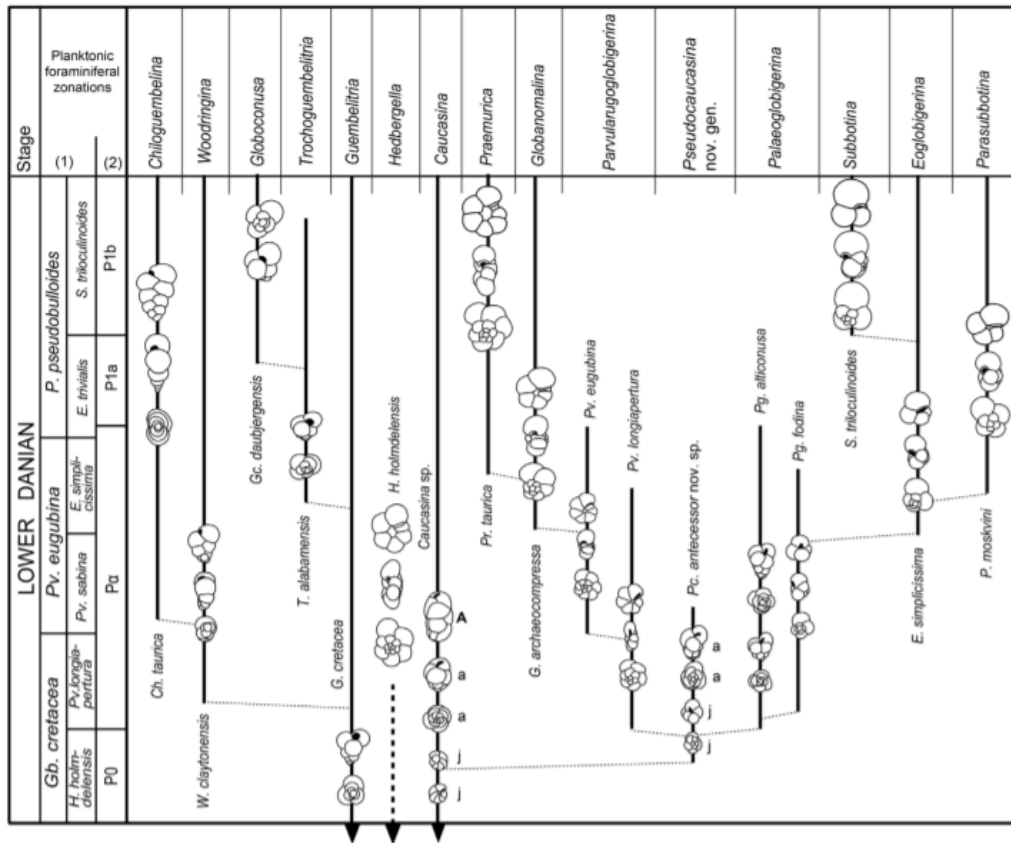


**Figure 5.1:** Proposed phylogenetic relationships of the main earliest Danian planktonic foraminiferal genera based on evidence reported here and previous phylogenetic studies (Modified from Arenillas et al., 2015)

**Family CHILOGUEMBELINIDAE Reiss, 1963**

**Genus *Chiloguembelina* LOEBLICH and TAPPAN, 1956**

Type species: *Chiloguembelina midwayensis* CUSHMAN

***Chiloguembelina midwayensis* CUSHMAN, 1940**

Pl. 1, fig. 1

1940 *Guembelina* (*Chiloguembelina*) *midwayensis* CUSHMAN; p. 65, pl. 11, fig. 15.

1999 *Chiloguembelina midwayensis* CUSHMAN; Olsson et al., p. pl.13, fig. 9, 10, 12, 13; pl. 69, fig. 16-22.

2005 *Chiloguembelina midwayensis* CUSHMAN; Obaidalla, p. 219, pl. 3, fig. 4.

2008 *Chiloguembelina midwayensis* CUSHMAN; Esmeray, p. 173, pl. 19, fig. 21-24.

**Description & Remarks:**

*Chiloguembelina midwayensis* is one of the Early Danian biserial forms. Its test is small, laterally compressed, and increasing chamber size. The wall texture is moderately pustulose and the sutures are moderately depressed. The aperture cannot be identified under the microscope.

The main difference about of the *C. midwayensis* from the other biserial forms is the chamber shape and arrangement. Its chamber size rapidly increases and slightly overlap the previous chamber. The difference from *Chiloguembelina morsei* is the subtriangular chamber shape.

**Stratigraphic Distribution:**

The stratigraphic distribution of *C. midwayensis* is from the Pa zone (Danian) to the P5 zone (Thanetian) (Olsson et al., 1999).

***Chiloguembelina morsei* KLINE, 1943**

Pl. 1, fig. 2-5

1943 *Guembelina (Chiloguembelina) morsei* KLINE; p. 44, pl. 7, fig. 12.

1999 *Chiloguembelina morsei* KLINE; Olsson et al., p. pl. 13, fig. 14, 15; pl. 69, fig. 9-15.

2008 *Chiloguembelina morsei* KLINE; Esmeray, p. 174, pl. 19, fig. 17-20.

**Description & Remarks:**

*Chiloguembelina morsei* is the other biserial forms with smaller test. The chambers overlap like all *Chiloguembelina* species, but the difference is the sutures are deeply depressed and initial chambers are sub-spherical but lateral chambers becomes broader. The chamber size slightly increases.

The *Chiloguembelina morsei* differs from *Chiloguembelina midwayensis* because of narrower test, more globular chambers, and more deeply constricted sutures.

**Stratigraphic Distribution:**

The stratigraphic distribution of *C. morsei* is from the Pa zone (Danian) to the P1c zone (Danian) (Olsson et al., 1999).

***Chiloguembelina subtriangularis* BECKMANN, 1957**

Pl. 2, fig. 1-3

1957 *Chiloguembelina subtriangularis* BECKMANN; p. 91, pl. 21, fig. 5a, b.

1999 *Chiloguembelina subtriangularis* BECKMANN; Olsson et al., p. pl. 13, fig. 17, 18; pl. 70, fig. 1-7.

#### **Description & Remarks:**

The *Chiloguembelina subtriangularis* is small, biserial test with subtriangular in side view. Chambers are slightly inflated, and sutures are nearly horizontal, slightly depressed. The chambers overlapping and increasing nearly twice of breadth in height is the same with other forms. The wall texture is smooth.

The difference from other *Chiloguembelina* species is the globular chamber shapes and weakly depressed sutures.

#### **Stratigraphic Distribution:**

The stratigraphic distribution of *C. subtriangularis* is from the P1c zone (Danian) to the P3b zone (Selandian) (Olsson et al., 1999).

### **Family GLOBIGERINIDAE CARPENTER, PARKER, AND JONES, 1862**

#### **Genus *Eoglobigerina* MOROZOVA, 1959**

Type species: *Globigerina (Eoglobigerina) eobulloides* MOROZOVA, 1959

#### ***Eoglobigerina edita* SUBBOTINA, 1953**

Pl. 2, fig. 4,5

1953 *Globigerina (Eoglobigerina) edita* SUBBOTINA; p. 62, pl. 2, fig. 1a-c.

1999 *Eoglobigerina edita* SUBBOTINA; Olsson et al., p. , pl. 8, fig. 13-18; pl. 9, fig. 1-6; pl. 18, fig. 1-16.

2005 *Eoglobigerina edita* SUBBOTINA; Obaidalla, p. 219, pl. 3, fig. 17.

2008 *Eoglobigerina edita* SUBBOTINA; Esmeray, p. 164, pl. 9, fig. 10-13.

### **Description & Remarks:**

*Eoglobigerina edita* is the high trochospiral form like most of the *Eoglobigerina* sp. forms. It has 4 to 5 globular chambers with increasing gradually in size. Cancellata wall weakly developed and spinose with numerous spine holes along cancellata ridges. The sutures, on the other hand, are moderately depressed. The another characteristic feature about the chambers is the early whorls compactly arranged and closely packed together and strongly lobulate peripheral margin.

*Eoglobigerina edita* is an intermediate form of the *Eoglobigerina eobulloides* and *Eoglobigerina spiralis*. The difference from *Eoglobigerina eobulloides* is a high trochospiral test, and strongly developed cancellata wall structure

### **Stratigraphic Distribution:**

The stratigraphic distribution of *E. edita* is from the Pa zone (Danian) to the P1c zone (Danian) (Olsson et al., 1999).

### ***Eoglobigerina eobulloides* MOROZOVA, 1959**

Pl. 2, fig. 6-8

1959 *Globigerina (Eoglobigerina) eobulloides* MOROZOVA; p. 1115, text fig. 1a-c.

1999 *Eoglobigerina eobulloides* MOROZOVA; Olsson et al., p. pl.8, fig. 10-12; pl.19, fig. 1-15.

2005 *Eoglobigerina eobulloides* MOROZOVA; Obaidalla, p. 223, pl. 5, fig. 4.

2008 *Eoglobigerina eobulloides* MOROZOVA; Esmeray, p. 164, pl. 9, fig. 5-9.

### **Description & Remarks:**

*Eoglobigerina eobulloides* is the moderate to high trochospiral, 4-5 globular chambers. The globular chambers are increasing moderately in size, and the sutures are strongly depressed. In the wall texture, cancellate wall are very weakly developed and not identified under the microscope. , The aperture is from umbilical to extra-umbilical like another genus *Eoglobigerina*.

*Eoglobigerina eobulloides* identification may conflict with the *Globigerina fringe* SUBBOTINA, 1950. However, they are slightly different with each other because *G. fringe* in terms of wall composition, having deeper pores in the wall structure. On the other hand, *Eoglobigerina eobulloides* differs from *Eoglobigerina edita* in terms of wall structure and differs from *Eoglobigerina spiralis* in terms of last chamber size, because *Eoglobigerina eobulloides* have great in size, globular last chamber but *Eoglobigerina spiralis* cambers closely appressed with an umbilical directed aperture.

### **Stratigraphic Distribution:**

The stratigraphic distribution of *E. eobulloides* is from the P0 zone (Danian) to the P1b zone (Danian) (Olsson et al., 1999).

### ***Eoglobigerina spiralis* BOLLI, 1957**

Pl. 2, fig. 9

1957 *Globigerina (Eoglobigerina) spiralis* BOLLI; p. 70, pl. 16, figs. 16-18.

1999 *Eoglobigerina spiralis* BOLLI; Olsson et al., p. 22 pl. 16, fig. 10-12; pl.20, fig. 1-11.

**Description & Remarks:**

*Eoglobigerina spiralis* is high trochospiral, with 4-5 globular chambers. The globular chambers are increasing moderately in size, except last chamber, and the sutures are moderately depressed. In the wall texture, it is more developed than *Eoglobigerina edita*, however, the cancellate ridges not as much as *Eoglobigerina edita*. The aperture is from umbilical to extra-umbilical like another genus *Eoglobigerina*.

**Stratigraphic Distribution:**

The stratigraphic distribution of *E. spiralis* is from the P1c zone (Danian) to the P2 zone (Danian) (Olsson et al., 1999).

**Genus *Globigerina* D'ORBIGNY, 1826**

Type species: *Globigerina bulloides* D'ORBIGNY, 1826

***Globigerina fringa* SUBBOTINA, 1950**

Pl. 3, fig. 1,2

1950 *Globigerina fringa* SUBBOTINA; p.104, pl. 5, fig. 19-21.

1950 *Globigerina fringa* SUBBOTINA; Olsson et al., p. 124, pl. 9, fig. 7-9.

2005 *Eoglobigerina (Globigerina) fringa* SUBBOTINA; Obaidalla, p. 223, pl. 5, fig. 6.

2007 *Eoglobigerina (Globigerina) fringa* SUBBOTINA; Darvishzad et al., p. 142, pl. 2, fig. 15.

2008 *Eoglobigerina (Globigerina) fringa* SUBBOTINA; Esmeray, p. 165, pl. 9, fig. 3,4.

### **Description & Remarks:**

*Globigerina fringa* is small test with increasing chamber size and rounded and lobate periphery. In the final whorl, the chambers are closely adhering to another. The wall structure is cancellate and the sutures are weak to moderately deep.

There is always conflict with *Globigerina fringa* with *E. eobulloides* and *S. cancellata*. The difference from *E. eobulloides* is the wall texture and sutures. The coarsely cancellate wall texture is the same with *S. cancellata*. However, the *S. cancellata* cannot be observed in the P0 zone. In other words, the stratigraphic levels are not the same.

### **Stratigraphic Distribution:**

The stratigraphic distribution of *G. fringa* has been defined in the recent studies from the P0 zone (Danian) to the P1b-c (Danian) (Arenillas et al., 2000; Luciani, 2002; Karoui-Yaakoub et al., 2002).

### ***Globigerina pentagona* MOROZOVA, 1961**

Pl. 3, fig. 3, 4

1961 *Globigerina pentagona* MOROZOVA; p.3510, pl. 6, fig. 3a-c.

1999 *Globigerina pentagona* MOROZOVA; Olsson et al., p. 124, pl. 9, fig. 4-6.

#### **Description & Remarks:**

*Globigerina pentagona* is the moderate to high trochospiral form. It consists of two whorls in general, and each one has 5 globular chambers with gradually increasing in size. Wall composition is smooth and finely perforate. The sutures are moderately deep. However, the aperture cannot be defined.

It may conflict with *Globigerina tetragona* in terms of the number of chambers in the last whorl. However, the identification for *Globigerina pentagona* is the last chamber slightly concave through the umbilical side.

#### **Stratigraphic Distribution:**

The stratigraphic distribution of *G. pentagona* has been defined in the recent studies from the P0 zone (Danian) to the P1c (Danian) (Keller et. al., 2002).

#### ***Globigerina tetragona* MOROZOVA, 1961**

Pl. 3, fig. 5-7

1961 *Globigerina tetragona* MOROZOVA; p.3510, pl. 5, fig. 2a-c.

1999 *Globigerina tetragona* MOROZOVA; Olsson et al., p. 124, pl. 9, fig. 1-3.

**Description & Remarks:**

*Globigerina tetragona* is high trochospiral, two or two and half whorls with four inflated chambers. The chamber size slowly increasing, so, the spiral side is conical and umbilical side is concave in the center. Sutures between the chambers are deeply in the umbilical side. On the other hand, the wall composition is smooth and finely perforate like *G. pentagona*.

The *Globigerina tetragona* differs from other species in terms of the number of chambers and concave chamber arrangement in the umbilical side. The difference from *Globanomalina imitata* is the wall composition, *Globigerina tetragona* has smooth wall composition.

**Stratigraphic Distribution:**

The stratigraphic distribution of *G. tetragona* has been defined in the recent studies from the P0 zone (Danian) to the P1c (Danian) (Keller et al., 2002).

***Globigerina trifolia* MOROZOVA, 1961**

Pl. 3, fig. 8

1961 *Globigerina trifolia* MOROZOVA; p.3510, pl. 4, fig. 1a-c.

1999 *Globigerina trifolia* MOROZOVA; Olsson et al., p. 122, pl. 8, fig. 4-6.

### **Description & Remarks:**

*Globigerina trifolia* is high trochospiral form with gradually increase in chamber size and narrow deep umbilicus. The number of chambers 3-3.5 in a whorl. Sutures are also deep, and wall composition is smooth and finely perforate.

*Globigerina trifolia* differs from *G. daubjergensis* in terms of wall composition because *G. daubjergensis* has rough wall structure.

### **Stratigraphic Distribution:**

The stratigraphic distribution of *G. trifolia* has been defined in the recent studies from the P0 zone (Danian) to the P1b (Danian) (Keller et al., 2002).

### **Genus *Parasubbotina* OLSSON, HEMLEBEN, BERGGREN, and LIU 1992**

Type species: *Globigerina (Parasubbotina) pseudobulloides* PLUMMER, 1926

#### ***Parasubbotina pseudobulloides* PLUMMER, 1926**

Pl. 4, fig. 1-5

1926 *Globigerina (Parasubbotina) pseudo-bulloides* PLUMMER; p. 133, pl. 8, fig. 9a-c.

1999 *Parasubbotina pseudobulloides* PLUMMER; Olsson et al., p. 148, pl. 21, fig. 1-15.

2005 *Parasubbotina pseudobulloides* PLUMMER; Obaidalla, p. 219, pl. 3, fig. 1, 2.

2007 *Parasubbotina pseudobulloides* PLUMMER; Darvishzad et al., p. 142, pl. 2, fig. 17.

2008 *Parasubbotina pseudobulloides* PLUMMER; Esmeray, p. 166, pl. 11, fig. 1, 2;  
pl. 18, fig. 17-20.

#### **Description & Remarks:**

*Parasubbotina pseudobulloides* is one of the easily identification species with low trochospiral test, 5 chambers with increasing in size, spinose wall texture. It has strongly depressed sutures with lobate and rounded periphery.

Its form similar to *Praemurica pseudoinconstants* BLOW, 1979, however, the fundamental difference is the wall texture between them. *Parasubbotina pseudobulloides* has a cancellate, spinose wall texture.

#### **Stratigraphic Distribution:**

The stratigraphic distribution of *P. pseudobulloides* is from the latest part of Pa zone (Danian) to the P3a zone (Selandian) (Olsson et al., 1999).

#### ***Parasubbotina varianta* SUBBOTINA, 1953**

Pl. 5, fig. 1-5

1953 *Parasubbotina varianta* SUBBOTINA; p. 63, pl. 3, fig. 5a-c; pl. 3, figs. 6a-7c,  
10a

1999 *Parasubbotina varianta* SUBBOTINA; Olsson et al., p. 124, pl. 9, fig. 16-18;  
pl. 22, fig. 6-16.

**Description & Remarks:**

*Parasubbotina varianta* is the other forms of genus *Parasubbotina*. It is identified with its very low trochospiral and small test, and the number of chambers with ultimate whorl than the *Parasubbotina pseudobulloides*. It has cancellate wall texture, with moderately to strong depressed sutures. Aperture is umbilical to extraumbilical, with rounded chambers.

**Stratigraphic Distribution:**

The stratigraphic distribution of *P. varianta* is from the P1c zone (Danian) to the O1 zone (Rupelian) (Olsson et al., 1999).

**Genus *Subbotina* BROTZEN and POZARYSKA, 1961**

Type species: *Globigerina (Subbotina) triloculinoidea* PLUMMER, 1926

***Subbotina cancellata* BLOW, 1979**

Pl. 5, fig. 6

1979 *Subbotina cancellata* BLOW; p. 1284, pl. 80, fig. 7.

1999 *Subbotina cancellata* BLOW; Olsson et al., p. 124, pl. 9, fig. 7-9; pl. 24, fig. 1-14; pl. 25, fig. 1-15.

**Description & Remarks:**

The test of *Subbotina cancellata* is coiled, rounded, and trochospiral form. The 3-4 chambers are found in ultimate whorl with gradually increase in size. Coarsely

cancellate wall texture and moderately depressed sutures are other features of this form. Aperture is the umbilical with broad.

The difference of *Subbotina cancellata* from other species is compact and rounded test with slightly lobulate in form. Moreover, the main difference between *Subbotina cancellata* and *Subbotina triangularis* is *Subbotina triangularis* has a distinctly different wall texture.

### **Stratigraphic Distribution:**

The stratigraphic distribution of *S. cancellata* is from the P1c zone (Danian) to the P4 zone (Thanetian) (Olsson et al., 1999).

### ***Subbotina triloculinoides* PLUMMER, 1926**

Pl. 6, fig. 1-3

1926 *Globigerina (Subbotina) triloculinoides* PLUMMER; p. 134, pl. 8, fig. 10a-b.

1999 *Subbotina triloculinoides* PLUMMER; Olsson et al., p. pl. 9, fig. 13-15; pl. 14, fig. 15, 16; pl. 27, fig. 1-13.

2005 *Subbotina triloculinoides* PLUMMER; Obaidalla, p. 221, pl. 4, fig. 6.

2008 *Subbotina triloculinoides* PLUMMER; Esmeray, p. 167, pl. 11, fig. 4-9; pl. 18, fig. 21-28.

### **Description & Remarks:**

The main characteristic of *Subbotina triloculinoides* is its trilobate test with 3-3,5 chambers in the ultimate whorl which increase rapidly in size. The size of the last

chamber is equal to the total of the previous chambers. The cancellate wall texture and strongly depressed sutures are another characteristic feature of this form. The aperture is umbilical.

The main difference between *S. triloculinooides* from *S. trivialis* is the higher increase in chamber size and smaller size of the chambers of the early whorl.

### **Stratigraphic Distribution:**

The stratigraphic distribution of *S. triloculinooides* is from the P1b zone (Danian) to the P4 zone (Thanetian) (Olsson et al., 1999).

### ***Subbotina trivialis* SUBBOTINA, 1953**

Pl. 6, fig. 4-6

1953 *Globigerina (Subbotina) trivialis* SUBBOTINA; p. 64, pl. 4, fig. 4a-c.

1999 *Subbotina trivialis* SUBBOTINA; Olsson et al., p. pl. 9, fig. 10-12; pl. 28, fig. 1-13.

2005 *Subbotina trivialis* SUBBOTINA; Obaidalla, p. 221, pl. 4, fig. 11.

2008 *Subbotina trivialis* SUBBOTINA; Esmeray, p. 167, pl. 11, fig. 10,11.

### **Description & Remarks:**

The main characteristic of *Subbotina trivialis* is throchospiral form with its 4-4,5 almost regular, spherical chambers in the last whorl which differ very slightly in size. The ultimate chamber is equal to, or slightly smaller than the penultimate one. The

chambers are closely packed together and partially overlap each other. The form has cancellate wall texture and strongly depressed sutures with umbilical aperture.

Because of these unique properties, such as high trochospiral form and chamber arrangements in the last whorl, is the easy to identify this form from the other Subbotina species.

### **Stratigraphic Distribution:**

The stratigraphic distribution of *S. trivialis* is from the Pa zone (Danian) to the P2 zone (Selandian). (Olsson et. al., 1999).

## **Family GLOBANOMALIDAE LOEBLICH AND TAPPAN, 1961**

### **Genus *Globanomalina* HAQUE, 1956**

Type species: *Globoconusa (Globanomalina) ovalis* HAQUE, 1956

### ***Globanomalina archeocompressa* BLOW, 1979**

Pl. 7, fig. 1

1979 *Globanomalina archeocompressa* BLOW; p. 1049, pl. 58, text fig. 8, 9.

1999 *Globanomalina archeocompressa* BLOW; Olsson et al., p. pl. 32, fig. 1-10.

### **Description & Remarks:**

*Globanomalina archeocompressa* is the trochospiral Danian forms. The final whorl with 5-6 chambers with increasing in gradually in size. The wall texture is smooth. On

the contrary, the importance about their morphology is the oval shaped chambers. Because of its form it is easily recognized.

**Stratigraphic Distribution:**

The stratigraphic distribution of *G. archeocompressa* is from the P0 zone (Danian) to the P1b zone (Danian) (Olsson et al., 1999).

***Globanomalina compressa* PLUMMER, 1927**

Pl. 7, fig. 2

1927 *Globanomalina compressa* PLUMMER; p. 135, pl. 8, text fig. 1.

1999 *Globanomalina compressa* PLUMMER; Olsson et al., p. pl. 14, fig. 1-3; pl. 32, fig. 11-16; pl. 35, fig. 1-13, 17.

**Description & Remarks:**

*Globanomalina compressa* is the Danian forms, a small, 4 or 5-chambered test with very low trochospiral form. The perforate wall texture, and moderately depressed sutures are found in this form. It has moderate to strong developed peripheral margin, and umbilical-extraumbilical arc.

The difference of this form with the other specie is the flattened last chamber. *Globigerina tetragona* differs from this form in terms of perforate wall composition of this form.

**Stratigraphic Distribution:**

The stratigraphic distribution of *G. compressa* is from the P1c zone (Danian) to the P3a zone (Selandian) (Olsson et al., 1999).

***Globanomalina imitata* SUBBOTINA, 1953**

Pl. 7, fig. 3-5

1953 *Globanomalina imitata* SUBBOTINA; p. 206, pl. 16, text fig. 14.

1999 *Globanomalina imitata* SUBBOTINA; Olsson et al., p. pl. 10, fig. 12-14; pl. 12, fig. 10-12; pl. 36, fig. 7-12, 16.

**Description & Remarks:**

*Globanomalina imitata* is the typical 4- chambered, throchospiral form. The chambers are rapidly increase in size and inflated in shape. The wall texture is smooth, sutures are moderately depressed, and the aperture is umbilical to extraumbilical.

*Globanomalina imitata* differs from *Globanomalina planocompressa* and *Globanomalina compressa* in terms of chamber number, and rapidly increase in chamber size.

**Stratigraphic Distribution:**

The stratigraphic distribution of *G. imitata* is from the P1c zone (Danian) to the P4 zone (Thanetian) (Olsson et al., 1999).

***Globanomalina planocompressa* SHUTSKAYA, 1965**

Pl. 7, fig. 6; Pl. 8, fig. 1

1965 *Globanomalina planocompressa* SHUTSKAYA; p. 179, pl. 1, text fig. 6.

1999 *Globanomalina planocompressa* SHUTSKAYA; Olsson et al., p. pl. 36, fig. 1-6.

**Description & Remarks:**

*Globanomalina planocompressa* is the Danian forms with a small, planispiral, 5-chambered test, and the ultimate whorl gradually increases in size. Similar with the other *Globanomalina* species, chambers are globular to ovoid in shape, and perforate wall texture. The suture is strongly depressed, and the aperture is umbilical to extraumbilical.

The identified difference of *Globanomalina planocompressa* from other species, is having planispiral coiling with deep umbilicus depth.

**Stratigraphic Distribution:**

The stratigraphic distribution of *G. planocompressa* is from the Pa zone (Danian) to the P1c zone (Danian) (Olsson et al., 1999).

**Family GUEMBELITRIIDAE MONTANARO GALLITELLI, 1957**

**Genus *Globoconusa* KHALILOV, 1956**

Type species: *Globoconusa conusa* KHALILOV, 1956 (= *Globigerina daubjergensis* BRONNIMANN, 1953)

***Globoconusa daubjergensis* BRONNIMANN, 1953**

Pl. 8, fig. 2

1953 *Globigerina (Globoconusa) daubjergensis* BRONNIMANN; p. 340, text fig. 1.

1999 *Globoconusa daubjergensis* BRONNIMANN; Olsson et al., p. pl. 8, figs. 4-6;  
pl. 15, figs. 13, 14; pl.64, figs. 1-12.

2007 *Globoconusa daubjergensis* BRONNIMANN; Darvishzad et al., p. 142, pl. 2,  
fig. 16.

2008 *Globoconusa daubjergensis* BRONNIMANN; Esmeray, p. 171, pl. 10, fig. 2, 3;  
pl. 18, fig. 10-16.

**Description & Remarks:**

*Globoconusa daubjergensis* is also one of the smallest Danian forms. It has a high trochospiral test which is noticeably lobulate. Most important feature of the form is its 3-4 gradually increasing globular chambers in the final whorl and distinctly pointed initial spire. The sutures are strongly depressed, and the wall texture has pore mounds.

*Globoconusa daubjergensis* is differentiated by using the wall texture, high throchospiral test, and small in form. In other words, it is easily identified under the microscope.

**Stratigraphic Distribution:**

The stratigraphic distribution of *G. daubjergensis* is from the Pa zone (Danian) to the P1c zone (Danian) (Olsson et al., 1999).

**Genus *Guembelitra* CUSHMAN, 1933**

Type species: *Guembelitra cretacea* CUSHMAN, 1933.

***Guembelitra cretacea* CUSHMAN, 1933**

Pl. 8, fig. 3-5

1933 *Guembelitra cretacea* CUSHMAN; p. 37, pl. 4, fig. 12 a, b.

1999 *Guembelitra cretacea* CUSHMAN; Olsson et al., p. pl. 8, figs. 1-3; pl.13, fig. 3; pl. 63, figs. 1-12.

2008 *Guembelitra cretacea* CUSHMAN; Esmeray, p. 170, pl. 12, fig. 1; pl. 20, fig. 1-15.

2017 *Guembelitra cretacea* CUSHMAN; Karabeyoğlu, p.94, pl. 1, fig. 1-9; pl. 34, fig. 10-13.

**Description & Remarks:**

*Guembelitra cretacea* is one of the most distinguishable species in the Late Maastrichtian and Early Danian with its triserial test. It has globular chambers, depressed sutures and large, semicircular or semi-elliptical aperture at the inner margin of the last-formed chamber. Although Olsson et al. (1999) consider all triserial species as variants of wide-ranging population of *G. cretacea*, there are other triserial *Guembelitra* forms defined in the literature. These are *G. trifolia*, *G. irregularis* and *G. danica*. *G. trifolia* is identified with its very short spire; *G. irregularis* with its irregularly stacked chambers and *G. danica* with its highly regularly arranged chambers and elongate spires (Karoui-Yaakoub et al., 2002). In our study *Guembelitra* forms in the washed samples are very rare. However, in the thin sections these triserial forms were very abundant (especially above the boundary) and easy to

distinguish. Since we had very rare specimens in the washed samples and thin section views were inadequate to differentiate them in species level, all triserial forms identified in this study were classified as *G. cretacea* following the suggestion of Olsson et al. (1999).

### **Stratigraphic Distribution:**

*G. cretacea* is one of the survived species and its stratigraphic distribution is from the *Dicarinella concavata* zone (Coniacian) to the P1b zone (Danian) (Olsson et al., 1999; Premoli-Silva and Verga, 2004).

### **Genus *Parvularugoglobigerina* HOFKER, 1978**

Type species: *Globigerina (Parvularugoglobigerina) eugubina* Luterbacher and Premoli-Silva, 1964

### ***Parvularugoglobigerina alabamensis* LIU AND OLSSON, 1992**

Pl. 8, fig. 6

1992 *Parvularugoglobigerina alabamensis* LIU and OLSSON; p. 341, pl. 2, fig. 1-7.

1999 *Parvularugoglobigerina alabamensis* LIU and OLSSON; Olsson et al., p. pl. 65, figs. 1-6.

### **Description & Remarks:**

*Parvularugoglobigerina alabamensis* looks like *Guembelitra cretacea*, because of high throchospiral and lobate test forms. The globular chambers are gradually increasing in size, the sutures are deeply incised. The wall texture is microperforated.

*Parvularugoglobigerina alabamensis* differs from *Guembelitra cretacea* by 4 chambers, not 3 chambers, in the last whorl. It is also different from *Parvularugoglobigerina extensa* by having a less elongate aperture which is not extent extraumbilically.

**Stratigraphic Distribution:**

The stratigraphic range of the form is generally given confined in the P0 zone to P3b zone (Selandian) (Olsson et al., 1999).

***Parvularugoglobigerina eugubina* LUTERBACHER and PREMOLI-SILVA,  
1964**

Pl. 9, fig. 1-4

1964 *Globigerina (Parvularugoglobigerina) eugubina* LUTERBACHER and PREMOLI-SILVA; p. 105, pl. 2, fig. 8a-c. 1.

1999 *Parvularugoglobigerina eugubina* LUTERBACHER and PREMOLISILVA; Olsson et al., p. pl. 66, figs. 1-12; pl. 67, figs. 1-14.

2005 *Parvularugoglobigerina eugubina* LUTERBACHER and PREMOLISILVA; Obaidalla, p. 219, pl. 3, fig. 9-11.

2008 *Parvularugoglobigerina eugubina* LUTERBACHER and PREMOLISILVA; Esmeray, p. 173, pl. 10, fig. 1.

**Description & Remarks:**

*Parvularugoglobigerina eugubina* exhibits extremely variable morphology (Olsson et al., 1999). In the holotype description it is stated that the form is very small, low to moderately trochospiral and has 6 chambers in the final whorl that increase gradually in size. In our samples the most distinguishable characteristics of *P. eugubina* are its distinct radial sutures on the umbilical side and its prominent final chamber that is distinctly protruding and occupying 1/4 to 1/5 of the test surface.

**Stratigraphic Distribution:**

The stratigraphic range of the form is generally given confined in the Pa zone (Danian) (Olsson et al., 1999).

***Parvularugoglobigerina extensa* BLOW, 1979**

Pl. 9, fig. 5

1979 *Eoglobigerina* (*Parvularugoglobigerina*) *extensa* BLOW; p. 1220, pl. 69, fig. 7; pl. 74, fig. 1, 2

**Description & Remarks:**

*Parvularugoglobigerina extensa* is a moderate to high trochospiral, strongly depressed umbilical and test sutures are strongly depressed. Each of them composed 3 to 4 inflated subglobular chambers, increasing in size. The test wall is perforated but not observed easily under the microscope.

*Parvularugoglobigerina extensa* is different from *Parvularugoglobigerina eugubina* because of high-spired form, and different from *Guembelitria cretacea* because of 4 chambers in the last whorl.

**Stratigraphic Distribution:**

The stratigraphic range of the form is generally given confined in the P0 zone to Pa zone (Danian) (Olsson et al., 1999).

**Family HETEROHELICIDAE CUSHMAN, 1927**

**Genus *Zeauvigerina* FINLAY, 1939**

Type Species: *Zeauvigerina zelandica* FINLAY, 1939, p. 541-542, pl. 69, fig. 4a.

***Zeauvigerina virgata* KHALILOV, 1967**

Pl. 9, fig. 6-7

1967 *Heterohelix* (*Zeauvigerina*) *virgata* KHALILOV; p. 174, fig. 9a, b.

1999 *Zeauvigerina virgata* KHALILOV; Olsson et al., p. pl. 71, figs. 21-23.

**Description & Remarks:**

*Zeauvigerina virgata* is the Early Danian biserial forms with elongate and subrectangular chamber arrangements with uniform chamber addition. The sutures are moderately depressed, and the wall texture is aligned muricae.

The difference with the other *Zeauvigerina* species, it is not finalized with single chamber.

### **Stratigraphic Distribution:**

The stratigraphic distribution of this form is from the P1b zone (Danian) to the P3a zone (Selandian) (Olsson et al., 1999).

### ***Zeauvigerina waiparaensis* JENKINS, 1966**

Pl. 10, fig. 1

1966 *Chiloguembelina (Zeauvigerina) waiparaensis* JENKINS; p. 1095, pl. 1, fig. 1-6.

1999 *Zeauvigerina waiparaensis* JENKINS; Olsson et al., p. pl. 71, figs. 1-18.

2008 *Zeauvigerina waiparaensis* JENKINS; Esmeray, p. 174, pl. 12, fig. 6, 7; pl. 19, fig. 25.

### **Description & Remarks:**

*Zeauvigerina waiparaensis* is the biserial forms and distinguished by its irregular outline of the test and uneven biserial chamber addition. The sutures are moderately depressed, and the wall texture is smooth. Besides the terminal oval-shaped aperture is seen only in this species among the all Danian biserial forms.

The distinguished feature of *Zeauvigerina waiparaensis* is the last chamber, which is overlapping the previous chamber.

### **Stratigraphic Distribution:**

The stratigraphic distribution of *Z. waiparaensis* from is from the Late Maastrichtian to the top of Danian (Olsson et al., 1999).

### **Family TRUNCOROTALOIDIDAE Loeblich and Tappan, 1961**

### **Genus *Praemurica* OLSSON, HEMLEBEN, BERGGREN and LIU, 1992**

Type species: *Globigerina (Praemurica) taurica* MOROZOVA, 1961

### ***Praemurica inconstans* SUBBOTINA, 1953**

Pl. 10, fig. 2

1953 *Globigerina (Praemurica) inconstans* BLOW; p. 58, pl. 3, fig. 1,2

1999 *Praemurica inconstans* SUBBOTINA; Olsson et al., p. pl. 10, figs. 4-8; pl. 14, figs. 13, 14; pl. 59, figs. 1-16.

### **Description & Remarks:**

*Praemurica inconstans* is identified with its low trochospiral test and 5-7 chambers in the last whorl which increase gradually in size. The rate of growth in the chamber size is slightly faster towards to the final chambers.

The main difference with the *Praemurica pseudoinconstans* is the advanced umbilical to conical chamber morphologies and development of incised umbilical sutures.

**Stratigraphic Distribution:**

The stratigraphic distribution of *P. inconstans* is from the P1c zone (Danian) to the P3a zone (Selandian) (Olsson et al., 1999).

***Praemurica pseudoinconstans* BLOW, 1979**

Pl. 10, fig. 3

1979 *Globorotalia (Praemurica) pseudoinconstans* BLOW; p. 1105, pl. 67, fig. 4

1999 *Praemurica pseudoinconstans* BLOW; Olsson et al., p. pl. 60, figs. 1-13.

2008 *Praemurica pseudoinconstans* BLOW; Esmeray, p. 169, pl. 11, fig. 3.

**Description & Remarks:**

*Praemurica pseudoinconstans* is identified with its low trochospiral test and 5-6 chambers in the last whorl which increase gradually in size. The rate of growth in the chamber size is slightly faster towards to the final chambers. Its apertural profile is almost biconvex with rounded peripheral margins. The sutures are strongly depressed.

It resembles *P. pseudobulloides* however its equatorial profile is moderately lobulate and rate of increase in the chamber size is slower.

**Stratigraphic Distribution:**

The stratigraphic distribution of *P. pseudoinconstans* is from the Pa zone (Danian) to the P2 zone (Danian) (Olsson et al., 1999).

***Praemurica taurica* MOROZOVA, 1961**

Pl. 10, fig. 4

1961 *Globigerina (Praemurica) taurica* MOROZOVA; p. 10, fig. 5a-c.

1999 *Praemurica taurica* MOROZOVA; Olsson et al., p. pl. 10, figs. 1-3; pl. 61, figs. 1-15.

2005 *Praemurica taurica* MOROZOVA; Obaidalla, p. 219, pl. 3, fig. 16.

2008 *Praemurica taurica* MOROZOVA; Esmeray, p. 169, pl. 10, fig. 7,8.

**Description & Remarks:**

*Praemurica taurica* is differentiated with its greater number of subspherical chambers in the last whorl (5-6), which increase rapidly and uniformly in size. In equatorial view it has a subpolygonal outline and in axial view equally biconvex appearance. One of the most important characteristics of the form is the nature of its last chamber, which is asymmetrical, flattened at the apertural face and slightly shifted toward the umbilical surface. It is differentiated from the *P. pseudoinconstans* in having often greater number of chambers and less lobate and subpolygonal periphery.

**Stratigraphic Distribution:**

The stratigraphic distribution of *P. taurica* is from the P0 zone (Danian) to the P1b zone (Danian) (Olsson et al., 1999).

**Genus *Woodringina* LOEBLICH and TAPPAN, 1957**

Type species: *Woodringina claytonensis* LOEBLICH and TAPPAN, 1957

***Woodringina claytonensis* LOEBLICH and TAPPAN, 1957**

Pl. 11, fig. 1-2

1957 *Woodringina claytonensis* LOEBLICH and TAPPAN; B, p. 39, fig. 1a-d.

1999 *Woodringina claytonensis* LOEBLICH and TAPPAN; Olsson et al., p. pl. 13, figs. 6-8; pl. 68, figs. 1-6.

2005 *Woodringina claytonensis* LOEBLICH and TAPPAN; Obaidalla, p. 219, pl. 3, fig. 5.

2008 *Woodringina claytonensis* LOEBLICH and TAPPAN; Esmeray, p. 173, pl. 19, fig. 7-16.

**Description & Remarks:**

*Woodringina claytonensis* has tiny test, flaring rapidly and composed of 3-5 pairs of biserial chambers. The most distinguishable morphology of *W. claytonensis* is the slightly twisted plane of biseriality. Furthermore, in some of the species triseriality in the first portion of the test may be observed. However, in the Göynük samples, it is not observed.

It is differentiated from *Woodringina hornerstownensis* in having less number of biserial pairs and more distinctly twisted biserial portion of the test.

**Stratigraphic Distribution:**

The stratigraphic distribution of *W. claytonensis* is from the P0 zone (Danian) to the P1b zone (Danian) (Olsson et al., 1999).

***Woodringina hornerstownensis* OLSSON, 1960**

Pl. 11, fig. 3-4

1960 *Woodringina hornerstownensis* OLSSON; p. 29, pl. 4, fig. 18, 19.

1999 *Woodringina hornerstownensis* OLSSON; Olsson et al., p. pl. 13, figs. 4, 5; pl. 68, figs. 7-14.

2005 *Woodringina hornerstownensis* OLSSON; Obaidalla, p. 219, pl. 3, fig. 3.

2008 *Woodringina hornerstownensis* OLSSON; Esmeray, p.174, pl. 19, fig. 1-6; pl. 12, fig. 2-4.

**Description & Remarks:**

*Woodringina hornerstownensis* is distinguished with its small, elongate, biserial, slightly twisted and rather rapidly tapering test. Like in the *W. claytonensis* the initial part of the test may consist of a whorl of three chambers. It has a slender test; in other words, the test is about twice if broad. *W. hornerstownensis* is differentiated from *W. claytonensis* in having less twisted biserial portion and a greater number of pairs. *Woodringina hornerstownensis* often has six or more pairs of biserial chambers, while *W. claytonensis* is usually limited to five or fewer.

**Stratigraphic Distribution:**

The stratigraphic distribution of *W. hornerstownensis* is given as from the Pa zone (Danian) to the P3b zone (Selandian) in Olsson et al. (1999).

## 5.2. Late Maastrichtian Planktonic Foraminifera

Taxonomy of Mesozoic (late Cretaceous) planktonic foraminifera are easily identified because of successful preservation and larger in size. As mentioned in the previous section, only three species can survive from the mass extinction. In other words, 96% of the Cretaceous planktonic foraminifera assemblages were extinct.

According the previous researches, the species include *Globotruncana*, *Globotruncanita*, *Globotruncanella*, *Rugoglobigerina*, *Plummerita*, *Globigerinelloides*, *Hedbergella*, *Heterohelix*, *Laeviheterohelix*, *Planoglobulina*, *Pseudotextularia*, *Pseudoguembelina*, and *Racemiguembelina* in the late Maastrichtian planktonic foraminiferal assemblages.

The late Cretaceous (Maastrichtian) planktonic foraminiferal assemblages from the studied samples are composed of mainly complex and large-in-size forms. Many forms are high-ornamented, complex wall structural forms.

In this chapter, the taxonomy of late Maastrichtian planktonic foraminifera forms is presented by giving special features, differentiated characteristic features and stratigraphic distributions.

**Order FORAMINIFERIDA EICHWALD, 1830**

**Suborder GLOBIGERININA DELAGE and HÉROURARD, 1896**

**Superfamily GLOBOTRUNCANACEA BROTZEN, 1942**

**Family GLOBOTRUNCANIDAE BROTZEN, 1942**

**Subfamily GLOBOTRUNCANINAE BROTZEN, 1942**

**Genus *Globotruncana* CUSHMAN, 1927**

Type species: *Pulvinulina (Globotruncana) arca* CUSHMAN, 1926

***Globotruncana aegyptiaca* NAKKADY, 1950**

Pl. 12, fig. 1

1950 *Globotruncana aegyptiaca* NAKKADY; p. 690, pl. 80, fig. 20.

1984 *Globotruncana aegyptiaca* NAKKADY; Robaszynski et al., p. 179, pl. 2, fig. 1-6; p. 181, pl. 3, fig. 1-4.

1998 *Globotruncana aegyptiaca* NAKKADY; Nederbragt, p. 399, pl. 1, fig. 6, 7; p. 401, pl. 2, fig. 1.

2002 *Globotruncana aegyptiaca* NAKKADY; Keller et al., p. 280, pl. 3, fig. 14.

2008 *Globotruncana aegyptiaca* NAKKADY; Esmeray, p. 114, pl. 2, fig. 7, 8.

2011 *Globotruncana aegyptiaca* NAKKADY; Korchagin, pl. 5, figs. 3a-c.

2017 *Globotruncana aegyptiaca* NAKKADY; Karabeyoğlu, p. 149, pl. 26, fig. 1-5.

### **Description-Remarks:**

*Globotruncana aegyptiaca* is identified by planoconvex and lobate test with umbilical aperture. It has petaloid chamber shape, and double keeled, subangular structures. Throcospiral structure has wide umbilicus, moderately depressed sutures, and particularly 3 to 5 chambers identified in the last whorl. In addition to these definitions, the wall texture is finely pustulose (Table).

The difference of *Globotruncana aegyptiaca* from other *Globotruncana* species is mainly lesser number of chambers in the last whorl. The double-keeled structure is the same with *Globotruncana arca*. The only difference between them is *Globotruncana aegyptiaca* has raised, beaded sutures, depressed ventrally, and strong curved dorsally.

### **Stratigraphic Distribution:**

The stratigraphic distribution of *Globotruncana aegyptiaca* ranges from the *Globotruncana aegyptiaca* Zone (Campanian) to the end of the *Abathomphalus mayaroensis* Zone (K/P boundary).

### ***Globotruncana arca* CUSHMAN, 1926**

Pl. 12, fig. 2-4

1926 *Pulvinulina (Globotruncana) arca* CUSHMAN; p. 23, pl.3, fig.1.

1984 *Globotruncana arca* CUSHMAN; Robaszynski et al., p. 183, pl. 4, fig. 1-3.

1998 *Globotruncana arca* CUSHMAN; Nederbragt, p. 401, pl. 2, fig. 2.

2002 *Globotruncana arca* CUSHMAN; Keller et al., p. 280, pl. 3, fig. 13.

2004 *Globotruncana arca* CUSHMAN; Premoli-Silva and Verga, p. 104, pl. 34, fig. 3,4; p.105, pl. 35, fig. 1; p. 240, pl. 10, fig. 11-15; p. 241, pl. 11, fig. 1-4.

2008 *Globotruncana arca* CUSHMAN; Esmeray, p. 116, pl. 1, fig. 1, 2; pl. 13, fig. 1-4.

2017 *Globotruncana arca* CUSHMAN; Karabeyoğlu, p. 150, pl. 26, fig. 6-9; pl. 36, fig. 10-11.

### **Description-Remarks:**

*Globotruncana arca* is identified by biconvex, subcircular test outline with trochospiral chamber arrangement. It has petaloid chamber shape, moderate muricate wall texture, and distinctly beaded ornamentation with deep and wide umbilicus. The number of chambers in the final whorl is around 7 to 9. *Globotruncana arca* is double keeled structure with subangular shape. The aperture is umbilical to extraumbilical.

*Globotruncana arca* is confused with other *Globotruncana* species in terms of chamber arrangements, test outline chamber shape etc. However, the main difference about this species is curved and beaded sutures. Moreover, it has well-developed keel as seen in both umbilical and lateral views. *Globotruncana arca* is similar to *Globotruncana mariei* and *Globotruncana orientalis*. The main difference from *Globotruncana mariei* is double-keeled structure and increasing chamber size and greater number of chambers in the last whorl. It is also differentiated from *Globotruncana orientalis* in terms of wider spaced keels.

### **Stratigraphic Distribution:**

The stratigraphic distribution of *Globotruncana arca* ranges from the *Dicarinella asymetrica* zone (Coniacian) to the end of the *Abathomphalus mayaroensis* zone (K/P boundary).

***Globotruncana esnehensis* NAKKADY, 1950**

Pl. 13, fig. 1

1950 *Globotruncana arca* CUSHMAN var. *esnehensis* NAKKADY; p. 690, pl. 90, fig. 23-26.

1984 *Globotruncana esnehensis* NAKKADY; Robaszynski et al., p. 193, pl. 9, fig. 1-4.

2004 *Globotruncana esnehensis* NAKKADY; Premoli-Silva and Verga, p. 106, pl. 36, fig. 3, 4.

2008 *Globotruncana esnehensis* NAKKADY; Esmeray, p.119, pl. 2, fig. 9.

2017 *Globotruncana esnehensis* NAKKADY; Karabeyoğlu, p. 153, pl. 27, fig. 4-7; pl. 36, fig 4-5.

**Description & Remarks:**

*Globotruncana esnehensis* is planoconvex, single-keeled, subangular species with moderate trochospiral test, and raised, beaded sutures. The test outline is circular and inflated chamber in shape. The number of chambers in the final whorl is 5 or 6.

*Globotruncana esnehensis* is rarely confused because its circular test outline and inflated shape is different from other *Globotruncana* species. However, *Globotruncana esnehensis* sometimes may conflict with *Globotruncana dupeblei* in terms of rapidly increases in chamber size, subangular single-keeled structure and convex spiral side. On the contrary, the main difference between them is the number of chambers in the last whorl. *Globotruncana esnehensis* has smaller number rather than *Globotruncana dupeblei*.

**Stratigraphic Distribution:**

The stratigraphic distribution of *Globotruncana esnehensis* ranges from the *Globotruncana falsostuarti* zone to the end of the *Abathomphalus mayaroensis* zone (K/P boundary).

***Globotruncana mariei* BANNER and BLOW, 1960**

Pl. 13, fig. 2

1960 *Globotruncana mariei* BANNER and BLOW; pl. 11, figs.6.

1984 *Globotruncana mariei* BANNER and BLOW; Robaszynski et al., p. 205, pl. 15, figs. 1-6.

2004 *Globotruncana mariei* BANNER and BLOW; Premoli-Silva and Verga, p. 110, pl. 40, fig.1-3; p. 244, pl. 14, fig. 1.

2008 *Globotruncana mariei* BANNER and BLOW; Esmeray, p. 121-122, pl. 12, fig. 3-5; pl. 13, fig 5,6.

2017 *Globotruncana mariei* BANNER and BLOW; Karabeyoğlu, p. 157, pl. 28, fig. 4-8; pl. 36, fig. 7-8.

**Description & Remarks:**

*Globotruncana mariei* is distinguished with its subangular, double-keeled biconvex profile and lobate test outline. The trochospiral chamber arrangement and wide, deep umbilicus is observed as the same with other *Globotruncana* species. The chamber shape is petaloid and sutures are beaded in shape. The number of chambers in the last whorl is 4 or 5.

*Globotruncana mariei* is the same in terms of biconvex, double-keeled, petaloid structure with *Globotruncana orientalis*, *Globotruncana arca*. However, *Globotruncana mariei* differs from them in high rate of increase in chamber size, and the number of chambers.

### **Stratigraphic Distribution:**

The stratigraphic distribution of *Globotruncana mariei* ranges from the beginning of the *Globotruncana elevata* zone (Santonian) to the *Globotruncana gansseri* zone (Late Maastrichtian).

### ***Globotruncana orientalis* EL NAGGAR, 1966**

Pl. 13, fig. 3, 4

1966 *Globotruncana orientalis* EL NAGGAR; p. 125, pl. 12, fig. 4.

1984 *Globotruncana orientalis* EL NAGGAR; Robaszynski et al., p. 207, pl. 16, fig. 1-3; p. 209, pl 17, figs 1-4.

2004 *Globotruncana orientalis* EL NAGGAR; Premoli-Silva and Verga, p. 110, pl. 40, fig. 4; p. 111, pl. 41, fig. 1, 2; p. 244, pl. 14, fig. 2-9.

2008 *Globotruncana orientalis* EL NAGGAR; Esmeray, p. 122, pl. 1, fig., 3-5; pl. 2, fig. 1,2.

2017 *Globotruncana orientalis* EL NAGGAR; Karabeyoğlu, p. 158, pl. 29, fig. 1-3; pl. 36, fig. 6.

### **Description & Remarks:**

*Globotruncana orientalis* is identified with subangular, single keeled, biconvex form. The test outline is subcircular. The chamber arrangements, sutures, chamber shape, and umbilicus depth is the same with many other *Globotruncana* species. The number of in the final whorl changes between 5 to 7.

As mentioned earlier definitions, *Globotruncana orientalis* is similar to many *Globotruncana* species such as *Globotruncana arca*, however, the single keeled structure, and low coiling axis is the main different feature for *Globotruncana orientalis*.

### **Stratigraphic Distribution:**

The stratigraphic distribution of *Globotruncana orientalis* ranges from the middle part of the *Globotruncanita elevata* zone (Santonian) to the *Globotruncana gansseri* zone (Late Maastrichtian).

### **Genus *Globotruncanita* REISS, 1957**

Type species: *Rosalina (Globotruncanita)* DE LAPPARENT, 1918

### ***Globotruncanita conica* WHITE, 1928**

Pl. 13, fig. 5

1928 *Globotruncana (Globotruncanita) conica* WHITE; p. 285, pl. 38, fig. 7.

1984 *Globotruncanita conica* WHITE; Robaszynski et al., p. 227, pl. 26, fig. 1-3.

2004 *Globotruncanita conica* WHITE; Premoli-Silva and Verga, p. 116, pl. 46, fig. 2-4; p. 247, pl. 17, fig. 7-13.

2008 *Globotruncanita conica* WHITE; Esmeray, p. 125, pl. 13, fig. 16, 17.

2017 *Globotruncanita conica* WHITE; Karabeyoğlu, p. 162, pl. 30, fig. 4-6; pl. 36, fig. 23.

### **Description & Remarks:**

*Globotruncanita conica* identified easily by convex view in the spiral side, weakly depressed test sutures, and circular test outline. Moreover, the subrectangular chamber shape is the another identification for *Globotruncanita conica*. Subangular, single-keeled, beaded sutures, moderate to high trochospiral chamber arrangement is the other features for it. The interesting thing about this species is trapezoidal chamber shape.

*Globotruncanita conica* is different from other *Globotruncanita* and *Globotruncana* genera. However, this species was not easily founded in the samples because it is uncommon.

### **Stratigraphic Distribution:**

The stratigraphic distribution of *Globotruncanita conica* ranges from the *Gansserina gansseri* zone (Late Campanian-Early Maastrichtian) to the end of the *Abathomphalus mayaroensis* zone (K/P boundary).

### ***Globotruncanita stuartiformis* DALBIEZ, 1955**

Pl. 13, fig. 6

1955 *Globotruncana (Globotruncanita) elevata* BROTZEN subsp. *Stuartiformis* DALBIEZ; p. 169, text fig 10.

1984 *Globotruncanita stuartiformis* DALBIEZ; Robaszynski et al., p. 239, pl. 32, fig. 1-4.

2004 *Globotruncanita stuartiformis* DALBIEZ; Premoli-Silva and Verga, p. 119, pl. 49, fig. 2-4; p. 249, pl. 19, fig. 8-15.

2008 *Globotruncanita stuartiformis* DALBIEZ; Esmeray, p. 128, pl. 3, fig. 6; pl. 13, fig. 21-27.

2017 *Globotruncanita stuartiformis* DALBIEZ; Karabeyoğlu, p. 165, pl. 31, fig. 7-9; pl. 36, fig. 14-16.

#### **Description & Remarks:**

*Globotruncanita stuartiformis* is identified with medium to large test, moderately to slightly lobate periphery, subangular single-keeled. Its spiral side slightly convex in form. It has raised, beaded sutures, trapezoidal chamber shape. The number of chambers in the last whorl is not as much as *Globotruncanita stuarti*, but it has 5 to 7 chambers. Similar to other *Globotruncanita* forms, its chambers are triangular to rectangular in shape.

The difference of the *Globotruncanita stuartiformis* from *Globotruncanita stuarti* is test outline, more subcircular rather than circular one., and the chambers number in the last whorl.

#### **Stratigraphic Distribution:**

The stratigraphic distribution of *Globotruncanita stuartiformis* ranges from the *Dicarinella asymerica* zone (Conacian) to the end of the *Abathomphalus mayaroensis* zone (K/P boundary).

**Subfamily GLOBOTRUNCANELLINAE MASLAKOVA, 1964**

**Genus *Globotruncanella* REISS, 1957**

Type species: *Globotruncana citae* BOLLI, 1951 (= *Globotruncana havanensis* VOORWIJK, 1937 = *Globorotalia pschadae* KELLER, 1946)

***Globotruncanella minuta* CARON and GONZALEZ DONOSO, 1984**

Pl. 14, fig. 1

1984 *Globotruncanella minuta* CARON and GONZALEZ DONOSO; p. 263, pl. 43, fig. 5.

1984 *Globotruncanella minuta* CARON and GONZALEZ DONOSO; Robaszynski et al., p. 263, pl. 43, fig. 5-8.

2004 *Globotruncanella minuta* CARON and GONZALEZ DONOSO; Premoli-Silva and Verga, p.113, pl. 43, fig. 3, 4; p. 246, pl. 16, fig. 10, 11.

2008 *Globotruncanella minuta* CARON and GONZALEZ DONOSO; Esmeray, p. 133, pl. 4, fig. 9; pl. 14, fig. 9.

2017 *Globotruncanella minuta* CARON and GONZALEZ DONOSO; Karabeyoğlu, p. 146, pl. 24, fig. 6-7.

**Description & Remarks:**

*Globotruncanella minuta* is differentiated from the other *Globotruncanella* species by its lobate chamber shape. It is biconvex trochospiral form with moderately depressed sutures, and globular chamber shape. It is also unkeeled form like many other *Globotruncanella* species.

It differs from *G. havanensis* and *G. petaloidea* with petaloid chambers, where *Globotruncanella minuta* has globular ones.

**Stratigraphic Distribution:**

The stratigraphic distribution of *Globotruncanella minuta* ranges from the *Gansserina gansseri* zone (Late Campanian) to the end of the *Abathomphalus mayaroensis* zone (K/P boundary).

***Globotruncanella petaloidea* GANDOLFI, 1955**

Pl. 14, fig. 2

1955 *Globotruncana (Globotruncanella) petaloidea* GANDOLFI subsp. *petaloidea* GANDOLFI; p. 52, pl. 3, fig. 13.

1984 *Globotruncanella petaloidea* GANDOLFI; Robaszynski et al., p. 267, pl. 44, fig. 1-2.

2002 *Globotruncanella petaloidea* GANDOLFI; Keller et al., p. 277, pl. 1, fig. 8.

2004 *Globotruncanella petaloidea* GANDOLFI; Premoli-Silva and Verga, p. 114, pl. 44, fig. 1, 2; p. 246, pl. 16, fig. 12.

2008 *Globotruncanella petaloidea* GANDOLFI; Esmeray, p. 134, pl. 4, fig. 10-12; pl. 14, fig. 12.

2017 *Globotruncanella petaloidea* GANDOLFI; Karabeyoğlu, p. 143, pl. 23, fig. 1-3.

### **Description & Remarks:**

*Globotruncanella petaloidea* is defined as lobate, petaloid, moderate to high trochospiral form with sprioconvex test. The umbilicus of *Globotruncanella petaloidea* is deep but narrow. It has 4 chambers in the last whorl with increasing rapidly in size.

This form is very similar to *Globotruncanella havanensis*, the only difference between them is 4 petaloid chambers in the last whorl. In general, *Globotruncanella petaloidea* is different with 4 chamber feature from other forms.

### **Stratigraphic Distribution:**

The stratigraphic distribution of *Globotruncanella petaloidea* ranges from the *Gansserina gansseri* zone (Late Campanian) to the end of the *Abathomphalus mayaroensis* zone (K/P boundary).

## **Family RUGOGLOBIGERINIDAE SUBBOTINA, 1959**

### **Genus *Rugoglobigerina* BRONNIMANN, 1952**

Type species: *Globigerina (Rugoglobigerina) rugosa* PLUMMER, 1927

### ***Rugoglobigerina hexacamerata* BRONNIMANN, 1952**

Pl. 14, fig. 3

1952 *Rugoglobigerina (Rugoglobigerina) reicheli hexacamerata* BRONNIMANN; p. 23, pl. 2, fig. 10-12.

1984 *Rugoglobigerina hexacamerata* BRONNIMANN; Robaszynski et al., p. 283, pl. 49, fig. 8.

1998 *Rugoglobigerina hexacamerata* BRONNIMANN; Nederbragt, p. 405, pl. 4, fig. 1-4.

2002 *Rugoglobigerina hexacamerata* BRONNIMANN; Keller et al., p. 279, pl. 2, fig. 5-7.

2004 *Rugoglobigerina hexacamerata* BRONNIMANN; Premoli-Silva and Verga, p.199, pl. 129, fig. 1, 2; p. 269, pl. 39, fig. 1, 2.

2008 *Rugoglobigerina hexacamerata* BRONNIMANN; Esmeray, p. 136, pl. 4, fig. 1; pl. 14, fig. 1,2.

2017 *Rugoglobigerina hexacamerata* BRONNIMANN; Karabeyoğlu, p. 135, pl. 20, fig. 4-5.

#### **Description & Remarks:**

*Rugoglobigerina hexacamerata* is the most easily recognized *Rugoglobigerina* species, in terms of, low trochospire form, and 6 chambers in the last whorl. The chamber shape is globular and lobate test outline. In the umbilical side, very large, deep, and almost circular umbilicus is characterized this form. The last chamber shows the meridional pattern.

*Rugoglobigerina hexacamerata* differs from *Rugoglobigerina rugosa*, and *Rugoglobigerina pennyi* with slowly increasing chambers, and 6 chambers in the last whorl, respectively.

#### **Stratigraphic Distribution:**

The stratigraphic distribution of *Rugoglobigerina hexacamerata* ranges from the Campanian to the end of the *Abathomphalus mayaroensis* zone (K/P boundary).

***Rugoglobigerina pennyi* BRONNIMANN, 1952**

Pl. 14, fig. 4

1952 *Rugoglobigerina (Rugoglobigerina) rugosa pennyi* BRONNIMANN; p. 34, pl. 4, fig. 1-3.

1984 *Rugoglobigerina pennyi* BRONNIMANN; Robaszynski et al., p. 287, pl. 50, fig. 1.

2004 *Rugoglobigerina pennyi* BRONNIMANN; Premoli-Silva and Verga, p. 201, pl. 131, fig. 2-4; p. 269, pl. 39, fig. 7.

2008 *Rugoglobigerina pennyi* BRONNIMANN; Esmeray, p. 139, pl. 4 fig. 2; pl. 14, fig. 6,7.

2017 *Rugoglobigerina pennyi* BRONNIMANN; Karabeyoğlu, p. 138, pl. 20, fig. 9.

**Description & Remarks:**

*Rugoglobigerina pennyi* is the one of the intermediate size *Rugoglobigerina* species, which has low trochospiral, slightly depressed spiral side, inflated chamber shape. The last whorl has 6-7 chambers without any keel structure. The umbilicus is wide and deep.

The importance of *Rugoglobigerina pennyi* is the intermediate form between *Rugoglobigerina rugosa* and *Rugoglobigerina milamensis*. *Rugoglobigerina rugosa* has few chambers in the last whorl and *Rugoglobigerina milamensis* has relatively moderate to high trochospire.

**Stratigraphic Distribution:**

The stratigraphic distribution of *Rugoglobigerina pennyi* ranges from the *Gansserina gansseri* zone (Late Campanian) to the end of the *Abathomphalus mayaroensis* zone (K/P boundary).

***Rugoglobigerina rugosa* PLUMMER, 1926**

Pl. 14, fig. 5

1926 *Globigerina (Rugoglobigerina) rugosa* PLUMMER; p. 38, pl. 2, fig. 10 a.

1984 *Rugoglobigerina rugosa* PLUMMER; Robaszynski et al., p. 283, pl. 49, fig. 4, 6.

2002 *Rugoglobigerina rugosa* PLUMMER; Keller et al., p. 279, pl. 2, fig. 1, 2.

2004 *Rugoglobigerina rugosa* PLUMMER; Premoli-Silva and Verga, p. 202, pl. 132, fig. 1-3; p. 269, pl. 39, fig. 8-11.

2008 *Rugoglobigerina rugosa* PLUMMER; Esmeray,

2017 *Rugoglobigerina rugosa* PLUMMER; Karabeyoğlu, p.134, pl. 20, fig. 2-3; pl. 35, fig. 3-5.

**Description & Remarks:**

*Rugoglobigerina rugosa* is the one of the type species from *Rugoglobigerina* species due to its globular chambers and high ornamented irregularly developed rugosities. This form has closely coiled, 5 rapidly increasing size chambers. The umbilicus is wide and deep, and sutures are depressed in form.

This form is different from other *Rugoglobigerina* species in terms of rapidly increasing chamber size with low trochospire. So, this form can be easily recognized from other ones.

### **Stratigraphic Distribution:**

The stratigraphic distribution of *Rugoglobigerina rugosa* ranges from the *Globotruncanita ventricosa* zone (Campanian) to the end of the *Abathomphalus mayaroensis* zone (K/P boundary).

### **Superfamily PLANOMALINACEA BOLLI, LOEBLICH and TAPPAN, 1957**

#### **Family GLOBIGERINELLOIDIDAE LONGORIA, 1974**

#### **Subfamily GLOBIGERINELLOIDINAE LONGORIA, 1974**

#### **Genus *Globigerinelloides* CUSHMAN & ten DAM, 1948**

Type species: *Globigerinelloides algeriana* CUSHMAN and ten DAM, 1948

#### ***Globigerinelloides asperum* EHRENBERG, 184**

Pl.14, fig. 6

1854. *Phanerostomum (Globigerinelloides) asperum* EHRENBERG; p. 55, pl. 30, fig. 26a, 26b; pl. 32, fig. 24, 42.

2017 *Globigerinelloides asperum* EHRENBERG; Karabeyoğlu, p. 163, pl. 15, fig. 5, 6; pl. 34, fig. 14-19.

**Description & Remarks:**

*Globigerinelloides asperum* is defined as an involute planispiral test with 5-6 globular chambers with rapidly increase in size. The identificatory feature is the dome-like pustules on the test surface. The aperture possessed in the final chamber.

**Stratigraphic Distribution:**

The stratigraphic distribution of *Globigerinelloides asperum* ranges from the base of Santonian to the P0 zone.

***Globigerinelloides messinae* BRONNIMANN, 1952**

Pl. 14, fig. 7

1952. *Globigerinella (Globigerinelloides) messinae messinae* BRONNIMANN; p. 42, pl. 1, fig. 6, 7; text fig. 20a-q.

2004. *Macroglobigerinelloides (Globigerinelloides) messinae* BRONNIMANN; Premoli-Silva and Verga, p. 155, pl. 85, fig. 4-6; p. 256, pl. 26, fig. 1, 2.

2008 *Globigerinelloides messinae* BRONNIMANN; Esmeray, p. 143, pl. 5, fig. 3; pl. 15, fig. 6-8.

**Description & Remarks:**

*Globigerinelloides messinae* is defined as small, compressed test with lobate outline. It has globular chamber shape with planispiral chamber arrangement like other *Globigerinelloides* species. It has 5 chambers and the sutures between the chambers are strongly depressed. The peripheral is rounded and laterally compressed with

rapidly increasing in size. In the innermost chambers the shape and arrangements cannot be recognized. In addition, the wall composition is thin and finely perforated.

### **Stratigraphic Distribution:**

The stratigraphic distribution of *Globigerinelloides messinae* ranges from the base to top Maastrichtian stage.

### ***Globigerinelloides multispinus* LALICKER, 1948**

Pl. 14, fig. 8, 9

1943 *Globigerinelloides multispina* LALICKER; p. 624, pl. 92, figs 1.

2004 *Macroglobigerinelloides (Globigerinelloides) multispinus* LALICKER;  
Premoli-Silva and Verga, p. 156, pl. 86, fig. 1-3; p. 256, pl. 26, fig 3.

2008 *Globigerinelloides multispinus* LALICKER; Esmeray, p. 143, pl. 5, fig. 4.

2017 *Globigerinelloides multispinus* LALICKER; Karabeyoğlu, p. 122, pl. 15, fig. 7-9.

### **Description & Remarks:**

*Globigerinelloides multispinus* is one of the planispiral, involute, and trochoid in the earliest chambers in the all of the other *Globigerinelloides* species. It can be easily recognized because of the chambers in adult stage, which are flattened and the last one is divided into two globular chambers, one of them found in the plane of coiling. The sutures are distinct, depressed. The wall composition is perforated.

### **Stratigraphic Distribution:**

The stratigraphic distribution of *Globigerinelloides multispinus* ranges from the base of the Campanian stage to the top of the Maastrichtian stage.

### ***Globigerinelloides prairiehillensis* PESSAGNO, 1967**

Pl. 15, fig. 1

1967 *Globigerinelloides prairiehillensis* PESSAGNO; p. 277, pl. 60, fig. 2, 3; pl. 80, fig. 1; pl. 90, fig. 1, 2-4; pl. 97, fig. 3, 4.

2004 *Macroglobigerinelloides (Globigerinelloides) prairiehillensis* PESSAGNO; Premoli-Silva and Verga, p. 156, pl. 86, fig. 4-6; p. 256, pl. 26, fig. 4-9.

2008 *Globigerinelloides prairiehillensis* PESSAGNO; Esmeray, p. 145, pl. 5, fig. 2; pl. 15, fig. 9-16.

2017 *Globigerinelloides prairiehillensis* PESSAGNO; Karabeyoğlu, p. 124, pl. 16, fig. 4-6.

### **Description & Remarks:**

*Globigerinelloides prairiehillensis* is defined as lobulate, biumbilicate test with planispirally coiling and 6-7 chambers. The chambers are inflated, and rapidly increasing in size like the other *Globigerinelloides* species. Umbilicus is deep and wide. The wall texture is hyaline and perforated. The important and the different feature of *Globigerinelloides prairiehillensis* is covering the test by fine to medium, papillae.

### **Stratigraphic Distribution:**

The stratigraphic distribution of *Globigerinelloides prairiehillensis* ranges from the *Radotruncana calcarata* zone (Campanian) to middle part of the *Abathomphalus mayaroensis* zone (Late Maastrichtian).

### ***Globigerinelloides subcarinatus* BRONNIMANN, 1952**

Pl. 15, fig. 2

1952 *Globigerinella (Globigerinelloides) messinae subcarinata* BRONNIMANN; p. 44, pl. 1, fig. 10, 11; text fig. 21a-m.

2002 *Globotruncanella (Globigerinelloides) subcarinatus* BRONNIMANN; Keller et al., p. 277, pl. 1, fig. 7.

2004 *Macroglobigerinelloides (Globigerinelloides) subcarinatus* BRONNIMANN; Premoli-Silva and Verga, p. 157, pl. 87, fig. 1-3; p. 256, pl. 26, fig. 10-13.

2008 *Globigerinelloides subcarinatus* BRONNIMANN; Esmeray, p. 146, pl. 5, fig. 5,6; pl. 15, fig. 17, 18.

2017 *Globigerinelloides subcarinatus* BRONNIMANN; Karabeyoğlu, p. 125, pl. 17, fig. 1-3; pl. 34, fig. 20, 21.

### **Description & Remarks:**

*Globigerinelloides subcarinatus* is the one of the easiest forms to identify in the *Globigerinelloides* species because of the outline of the individual chambers are elongate, on the contrary, early chambers are rounded peripherally. The test is small, compressed, and planispiral with lobate outline.

### **Stratigraphic Distribution:**

The stratigraphic distribution of *Globigerinelloides subcarinatus* ranges from the base of the Campanian stage to the end of the *Abathomphalus mayaroensis* zone (K/P boundary).

### **Superfamily ROTALIPORACEA SIGAL, 1958**

#### **Family HEDBERGELLIDAE LOEBLICH and TAPPAN, 1961**

#### **Subfamily HEDBERGELLINAE LOEBLICH and TAPPAN, 1961**

#### **Genus *HEDBERGELLA* BRONNIMANN and BROWN, 1958**

Type species: *Anomalina lorneiana* d'ORBIGNY var. *trochoidea* GANDOLFI, 1942

#### ***Hedbergella holmdelensis* OLSSON, 1964**

Pl. 15, fig. 3

1964 *Hedbergella holmdelensis* OLSSON; p. 160, pl. 1, fig. 2a-c.

2004 *Muricohedbergella (Hedbergella) holmdelensis* OLSSON; Premoli-Silva and Verga, p. 166, pl. 96, fig. 3-5; p. 260, pl. 30, fig. 6-8.

2008 *Hedbergella holmdelensis* OLSSON; Esmeray, p. 147, pl. 5, fig. 10,11; pl. 14, fig. 21-28.

2017 *Hedbergella holmdelensis* OLSSON; Karabeyoğlu, p. 127, pl. 18, fig. 1-3.

### **Description & Remarks:**

*Hedbergella holmdelensis* is important because of the survive species from K/Pg mass extinction. The test is small, very low trochospiral (nearly planispiral), much

compressed form. Rapidly increased chamber size, which are moderately inflated, ovate in shape. Sutures are moderately depressed, and wall is smooth.

### **Stratigraphic Distribution:**

The stratigraphic distribution of *Hedbergella holmdelensis* is from Early Maastrichtian to lower P0 zone (Early Danian).

### ***Hedbergella monmouthensis* OLSSON, 1960**

Pl. 15, fig. 4

1960 *Globorotalia (Hedbergella) monmouthensis* OLSSON; p. 47, pl. 9, fig. 22-24.

2002 *Hedbergella monmouthensis* OLSSON; Keller et al., p. 277, pl. 1, fig. 5, 6.

2004 *Muricohedbergella (Hedbergella) monmouthensis* OLSSON; Premoli-Silva and Verga, p. 167, pl. 97, fig. 1-4; p. 260, pl. 30, fig. 9, 10.

2008 *Hedbergella monmouthensis* OLSSON; Esmeray, p. 148, pl. 5, fig. 8,9; pl. 14, fig. 14-20.

2017 *Hedbergella monmouthensis* OLSSON; Karabeyoğlu, p. 128, pl. 18, fig. 4-7; pl. 35, fig. 1,2.

### **Description & Remarks:**

*Hedbergella monmouthensis* is very low trochospiral, nearly planispiral in form, like *Hedbergella holmdelensis*. Wall structure is calcareous, finely perforate. The number of chambers 4-5, which are lobate, globular in shape, and the final whorl increase rapidly. The main difference between *Hedbergella holmdelensis* and *Hedbergella*

*monmouthensis* is the shape of the chambers, which are differentiated by looking at the profile view.

**Stratigraphic Distribution:**

The stratigraphic distribution of *Hedbergella holmdelensis* is from Early Maastrichtian to lower P0 zone (Early Danian).

**Superfamily HETEROHELICACEA CUSHMAN, 1927**

**Family HETEROHELICIDAE CUSHMAN, 1927**

**Subfamily HETEROHELICINAE CUSHMAN, 1927**

**Genus *Heterohelix* EHRENBERG, 1843**

Type species: *Textularia americana* EHRENBERG, 1843

***Heterohelix globulosa* EHRENBERG, 1840**

Pl. 16, fig. 1, 2

1840 *Textularia (Heterohelix) globulosa* EHRENBERG; p. 135, pl. 4, fig. 2b, 4b, 5b, 7b, 8b.

1991 *Heterohelix globulosa* EHRENBERG; Nederbragt, p. 347, pl. 2, fig. 1, 2.

2002 *Heterohelix globulosa* EHRENBERG; Keller et al., p. 277, pl. 1, fig. 10-13.

2004 *Heterohelix globulosa* EHRENBERG; Premoli-Silva and Verga, p. 140, pl. 70, fig. 5-7; p. 252, pl. 22, fig. 13, 14.

2005 *Heterohelix globulosa* EHRENBERG; Obaidalla, p. 214, pl. 1, fig. 10.

2007 *Heterohelix globulosa* EHRENBERG; Darvishzad et al., p. 142, pl. 2, fig. 14.

2008 *Heterohelix globulosa* EHRENBERG; Esmeray, p. 150, pl. 6, fig. 1-6; pl. 16, fig. 1-7.

2017 *Heterohelix globulosa* EHRENBERG; Karabeyoğlu, p. 96, pl. 3, fig. 1-5; pl. 34, fig. 1-4.

### **Description & Remarks:**

*Heterohelix globulosa* is the one of the important biserial form with globular chambers, smooth surface, strongly depressed sutures. The chambers are gradually increasing in size. The wall texture is calcareous, hyaline and microperforate.

In the Göynük samples, this form is observed in different sizes, and number. However, the main identification is globular chambers with depressed sutures. To compare other *Heterohelix* species, *Heterohelix globulosa* can easily identified.

### **Stratigraphic Distribution:**

The stratigraphic distribution of *Heterohelix globulosa* is from *R. cushmani* zone (Cenomanian) to *Plummerita hariensis* (Maastrichtian) zone.

### ***Heterohelix labellosa* NEDERBRAGT, 1991**

Pl. 16, fig. 3

1991 *Heterohelix labellosa* NEDERBRAGT; p. 347, pl. 2, fig. 3-5.

2004 *Heterohelix labellosa* NEDERBRAGT; Premoli-Silva and Verga, p. 141, pl. 71, fig. 1-3.

2008 *Heterohelix labellosa* NEDERBRAGT; Esmeray, p. 152, pl. 6, fig. 8; pl. 16, fig. 14,15.

2017 *Heterohelix labellosa* NEDERBRAGT; Karabeyoğlu, p. 97, pl. 3, fig. 6.

**Description & Remarks:**

*Heterohelix labellosa* is another biserial form with subglobular chambers. Sutures between chambers are moderately depressed, not as much as *Heterohelix globulosa*. The important feature of *Heterohelix labellosa* is foundation of continuous costae, which covers the test. The juvenile chambers are globular, on the contrary, adult chambers are subglobular to reniform.

**Stratigraphic Distribution:**

The stratigraphic distribution of *Heterohelix labellosa* is from *G. aegyptiaca* zone (Campanian) to *Abathomphalus mayaroensis* zone (K/P boundary).

***Heterohelix planata* CUSHMAN, 1938**

Pl. 16, fig. 4

1938 *Guembelina (Heterohelix) planata* CUSHMAN; p.12, 13, pl. 2, fig. 13, 14.

1991 *Heterohelix planata* CUSHMAN; Nederbragt, p. 349, pl. 3, fig. 3-4.

2004 *Heterohelix planata* CUSHMAN; Premoli-Silva and Verga, p. 142, pl. 72, fig. 7-9.

2017 *Heterohelix planata* CUSHMAN; Karabeyoğlu, p. 99, pl. 4, fig. 1-3; pl. 34, fig. 6.

**Description & Remarks:**

*Heterohelix planata* is defined by compressed, inflated chamber shape. The test covers with thin and discontinuous costae. The main difference from other *Heterohelix* species is observable costae and subglobular chambers.

**Stratigraphic Distribution:**

The stratigraphic distribution of *Heterohelix planata* is from *D. asymetrica* zone (Coniacian) to *Abathomphalus mayaroensis* zone (K/P boundary).

***Heterohelix punctulata* CUSHMAN, 1938**

Pl. 16, fig. 5

1938 *Guembelina (Heterohelix) punctulata* CUSHMAN; p. 13, pl. 2, fig. 15, 16.

1991 *Heterohelix punctulata* CUSHMAN; Nederbragt, p. 349, pl. 3, fig. 5-7.

2017 *Heterohelix planata* CUSHMAN; Karabeyoğlu, p. 99, pl. 4, fig. 4-6.

**Description & Remarks:**

*Heterohelix punctulata* is defined by globular chamber shape with broad and rounded test. In the early portion is keeled, cannot be seen under the microscope. The costae are slightly observed only early portions. The main difference from other species is the founding fine vertical lines in the early portion and smooth wall texture in the last chambers.

### **Stratigraphic Distribution:**

The stratigraphic distribution of *Heterohelix planata* is from *D. asymetrica* zone (Coniacian) to *Abathomphalus mayaroensis* zone (K/P boundary).

### **Genus *Laeviheterohelix* NEDERBRAGT, 1991**

Type species: *Guembelina pulchra* BROTZEN, 1936

### ***Laeviheterohelix glabrans* CUSHMAN, 1938**

Pl. 16, fig. 6

1938 *Guembelina (Laeviheterohelix) glabrans* CUSHMAN; p. 15, pl. 3, fig. 1, 2.

1991 *Laeviheterohelix glabrans* CUSHMAN; Nederbragt, p. 353, pl. 5, fig. 6.

2004 *Laeviheterohelix glabrans* CUSHMAN; Premoli-Silva and Verga, p. 147, pl. 77, fig. 9, 10; p. 254, pl. 24, fig. 1, 2.

2008 *Laeviheterohelix glabrans* CUSHMAN; Esmeray, p. 157, pl. 16, fig. 12-14.

2017 *Laeviheterohelix glabrans* CUSHMAN; Karabeyoğlu, p. 102, pl. 5, fig. 6-8.

### **Description & Remarks:**

*Laeviheterohelix glabrans* is identified by biserial form with weakly depressed sutures, smooth wall structure. *Laeviheterohelix glabrans* has periphery in the early portion and slightly keeled. Nearly flat chambers in shape (arched shape) is identificatory feature for this form.

### **Stratigraphic Distribution:**

The stratigraphic distribution of *Laeviheterohelix glabrans* is from *G. havanensis* zone (Campanian) to *Abathomphalus mayaroensis* zone (K/P boundary).

### **Genus *Planoglobulina* CUSHMAN, 1927**

Type species: *Guembelina (Planoglobulina) acervulinoides* EGGER, 1899

### ***Planoglobulina carseyae* PLUMMER, 1931**

Pl. 17, fig. 1

1931 *Ventilabrella (Planoglobulina) carseyae* PLUMMER; p. 178, 179, pl. 9, fig. 7-10.

1991 *Planoglobulina carseyae* PLUMMER; Nederbragt, p. 357, pl. 7, fig. 2, 3.

2004 *Planoglobulina carseyae* PLUMMER; Premoli-Silva and Verga, p. 172, pl. 102, fig. 5; p. 173, pl. 103, fig. 1-5; p. 261, pl. 31, fig. 12, 13.

2008 *Planoglobulina carseyae* PLUMMER; Esmeray, p.159, pl. 8, fig. 6; pl. 17, fig. 9-11

2017 *Planoglobulina carseyae* PLUMMER; Karabeyoğlu, p. 106, pl. 8, fig. 78; pl. 9, fig. 1-2; pl. 33, fig. 1-3.

### **Description & Remarks:**

*Planoglobulina carseyae* is v-shaped structure started with biserial in the early stages and continue with multiserial form. The chambers shape is inflated, and the sutures

are strongly depressed. The wall texture is finely costae. The difference between *Planoglobulina carseyae* to other *Planoglobulina* species is the well-developed costae, and the last chambers position.

### **Stratigraphic Distribution:**

The stratigraphic distribution of *Planoglobulina carseyae* is from *G. havanensis* (Campanian) to *Plummerita hariensis* (Maastrichtian) zone.

### **Genus *Pseudotextularia* RZEHAK, 1891**

Type species: *Cuneolina (Pseudotextularia) elegans* RZEHAK, 1891

### ***Pseudotextularia elegans* RZEHAK, 1891**

Pl. 17, fig. 2, 3

1891 *Cuneolina (Pseudotextularia) elegans* RZEHAK; p. 4.

1988 *Pseudotextularia elegans* RZEHAK; Keller, p. 250, pl. 1, fig. 17.

1991 *Pseudotextularia elegans* RZEHAK; Nederbragt, p. 363, pl. 10, fig. 1, 2.

2002 *Pseudotextularia elegans* RZEHAK; Keller et al., p. 280, pl. 3, fig. 5.

2004 *Pseudotextularia elegans* RZEHAK; Premoli-Silva and Verga, p. 185, pl. 115, fig. 1-3; p. 264, pl. 34, fig. 6-13.

2007 *Pseudotextularia elegans* RZEHAK; Darvishzad et al., p. 141, pl. 1, fig. 14.

2008 *Pseudotextularia elegans* RZEHAK; Esmeray, p. 160, pl. 7, fig. 1-4; pl. 17, fig. 1-4.

2017 *Pseudotextularia elegans* RZEHAK; Karabeyoğlu, p. 108, pl. 10, fig. 1-2; pl. 33, fig. 13-14.

**Description & Remarks:**

*Pseudotextularia elegans* is identified by biserial, reniform chamber shape with moderately depressed sutures. The well-developed costae are observed under the microscope. In addition to these definitions the interiomarginal aperture can identify easily. It differs from the *P. nuttalli* in being much more coarsely costate and in having more compressed chambers.

**Stratigraphic Distribution:**

The stratigraphic distribution of *Pseudotextularia elegans* is from *G. havanensis* (Campanian) to *Plummerita hariensis* (Maastrichtian) zone.

***Pseudotextularia nuttalli* VOORWIJK, 1937**

Pl. 18, fig. 1

1937 *Guembelina (Pseudotextularia) nuttalli* VOORWIJK; p. 192, pl. 2, fig. 1-9.

1991 *Pseudotextularia nuttalli* VOORWIJK; Nederbragt, p. 363, pl. 10, fig. 4, 6.

2004 *Pseudotextularia nuttalli* VOORWIJK; Premoli-Silva and Verga, p. 186, pl. 116, fig. 3-5; p. 264, pl. 34, fig. 14.

2008 *Pseudotextularia nuttalli* VOORWIJK; Esmeray, p. 160, pl. 7, fig. 5-7; pl. 17, fig. 4, 5.

2017 *Pseudotextularia nuttalli* VOORWIJK; Karabeyoğlu, p. 108, pl. 10, fig. 3-4; pl. 33, fig. 15-16.

### **Description & Remarks:**

*Pseudotextularia nuttalli* is biserial forms with reniform shape of the chambers and moderately depressed sutures. In the wall texture, costae is finely founded, however, under the microscope these costae structure is hard to see. The one of the difference in between *Pseudotextularia nuttalli* and *Pseudotextularia elegans* is the these costae structure. The shape of the chambers is subglobular. The aperture cannot easily observe under the microscope.

### **Stratigraphic Distribution:**

The stratigraphic distribution of *Pseudotextularia nuttalli* is from *D. concavata* (Turonian) to *Plummerita hariensis* (Maastrichtian) zone.

### **Subfamily PSEUDOGUEMBELININAE ALIYULLA, 1977**

#### **Genus *Pseudoguembelina* BRONNIMANN and BROWN, 1953**

Type species: *Guembelina (Pseudoguembelina) excolata* CUSHMAN, 1926

#### ***Pseudoguembelina costulata* CUSHMAN, 1938**

Pl. 18, fig. 2

1938 *Guembelina (Pseudoguembelina) costulata* CUSHMAN; p. 16, 17, pl. 3, fig. 7-9.

1991 *Pseudoguembelina costulata* CUSHMAN; Nederbragt, p. 359, pl. 8, fig. 3, 4.

2004 *Pseudoguembelina costulata* CUSHMAN; Premoli-Silva and Verga, p. 179, pl. 109, fig. 3-6; p. 263, pl. 33, fig. 9-12.

2005 *Pseudoguembelina costulata* CUSHMAN; Obaidalla, p. 214, pl. 1, fig. 2.

2008 *Pseudoguembelina costulata* CUSHMAN; Esmeray, p. 161, pl. 7, fig. 7-9.

2017 *Pseudoguembelina costulata* CUSHMAN; Karabeyoğlu, p. 113, pl. 12, fig. 1-2.

### **Description & Remarks:**

Test of *Pseudoguembelina costulata* is biserial and compressed. The chambers are subrectangular in shape. The coarsely costae is observed in the wall. *Pseudoguembelina costulata* is different from other forms in terms of chambers arrangement and shape. Each chamber was slightly inflated and cover the previous one.

### **Stratigraphic Distribution:**

The stratigraphic distribution of *Pseudoguembelina costulata* is from *G. elevata* (Santonian) to *Abathomphalus mayaroensis* zone (K/P boundary).

### ***Pseudoguembelina hariaensis* NEDERBRAGT, 1991**

Pl. 18, fig. 3, 4

1991 *Pseudoguembelina hariaensis* NEDERBRAGT; p. 359, pl. 8, fig. 6, 7; p. 361, pl. 9, fig. 1, 2.

2002 *Pseudoguembelina hariaensis* NEDERBRAGT; Keller et al., p. 279, pl. 2, fig. 12.

2004 *Pseudoguembelina hariaensis* NEDERBRAGT; Premoli-Silva and Verga, p. 180, pl. 110, fig. 1-4.

2005 *Pseudoguembelina hariaensis* NEDERBRAGT; Obaidalla, p. 214, pl. 1, fig. 3.

2007 *Pseudoguembelina hariaensis* NEDERBRAGT; Darvishzad et al., p. 142, pl. 2, fig. 2.

2008 *Pseudoguembelina hariaensis* NEDERBRAGT; Esmeray, p.162, pl. 7, fig. 10-12; pl. 17, fig.7.

2017 *Pseudoguembelina hariaensis* NEDERBRAGT; Karabeyoğlu, p. 114, pl. 12, fig. 3-8.

#### **Description & Remarks:**

*Pseudoguembelina hariaensis* is defined as biserial test followed by two or rarely more sets of multiserial chamberlets. In the biserial part, chambers are subglobular, nearly flat, deep sutured, and subparallel to each other. The test of *Pseudoguembelina hariaensis* is also covered with costae like the other species of this genus, however, costae is discontinuous.

#### **Stratigraphic Distribution:**

The stratigraphic distribution of *Pseudoguembelina hariaensis* is found in *Plummerita hariaensis* (Maastrichtian) zone.

#### **Genus: *Racemiguembelina* MONTANARO GALLITELLI, 1957**

Type species: *Guembelina (Racemiguembelina) fructicosa* EGGER, 1899

#### ***Racemiguembelina fructicosa* EGGER, 1899**

Pl. 18, fig. 5

1899 *Guembelina (Racemiguembelina) fructicosa* EGGER; p. 35, pl. 14, fig. 8, 9, 24.

- 1991 *Racemiguembelina fructicosa* EGGER; Nederbragt, p. 363, pl. 10, fig. 5.
- 2002 *Racemiguembelina fructicosa* EGGER; Keller et al., p. 280, pl. 3, fig. 2.
- 2004 *Racemiguembelina fructicosa* EGGER; Premoli-Silva and Verga, p. 187, pl. 117, fig. 1-6; p. 265, pl. 35, fig. 1-3.
2005. *Racemiguembelina fructicosa* EGGER; Obaidalla, p. 214, pl. 1, fig. 4.
2007. *Racemiguembelina fructicosa* EGGER; Darvishzad et al., p. 142, pl. 2, fig. 4.
- 2008 *Racemiguembelina fructicosa* EGGER; Esmeray, p. 162, pl. 8, fig. 7, 8; pl. 17, fig. 13.
- 2017 *Racemiguembelina fructicosa* EGGER; Karabeyoğlu, p. 111, pl. 11, fig. 1-2.

#### **Description & Remarks:**

*Racemiguembelina fructicosa* is different from the other multiserial forms with its conical shape and multiserial chamberlets developing in 3-dimension after the initial biserial stage. It has multiple aperture, however, in the Göynük section, cannot be observed because of preservation failure. The chambers are inflated and the sutures are moderately depressed. Main differences between *Racemiguembelina fructicosa* from the other species in this genus is the multispiral view.

#### **Stratigraphic Distribution:**

The stratigraphic distribution of *Racemiguembelina fructicosa* is from *Racemiguembelina fructicosa* (Maastrichtian) to *Plummerita hariensis* (Maastrichtian) zone.

***Racemiguembelina powelli* SMITH and PESSAGNO, 1973**

Pl. 18, fig. 6

1973 *Racemiguembelina powelli* SMITH and PESSAGNO; p. 35-37, pl. 11, fig. 4-12.

1991 *Racemiguembelina powelli* SMITH and PESSAGNO; Nederbragt, p. 365, pl. 11, fig. 1.

2002 *Racemiguembelina powelli* SMITH and PESSAGNO; Keller et al., p. 280, pl. 3, fig. 3.

2004 *Racemiguembelina powelli* SMITH and PESSAGNO; Premoli-Silva and Verga, p. 188, pl. 118, fig. 1-4.

2008 *Racemiguembelina powelli* SMITH and PESSAGNO; Esmeray, p.163, pl. 8, fig. 9; pl. 17, fig. 14.

2017 *Racemiguembelina powelli* SMITH and PESSAGNO; Karabeyoğlu, p. 112, pl. 11, fig. 3-5; pl. 33, fig. 6.

**Description & Remarks:**

*Racemiguembelina powelli* is another multiseriate form without initial biserial form. It is also equally biconvex in view with inflated chambers and strongly depressed sutures. The coarse costae can easily be observed in the wall.

**Stratigraphic Distribution:**

The stratigraphic distribution of *Racemiguembelina powelli* is from *G. havanensis* (Campanian) to *Plummerita hariensis* (Maastrichtian) zone.



## CHAPTER 6

### DISCUSSION & CONCLUSION

#### 6.1. Discussion

The main aim of this study is to reveal the evolutionary recovery of the planktonic foraminifera after the K/Pg boundary. For this purpose, a multidisciplinary study including biostratigraphy and mineralogy was carried out. In the Göynük Basin, the stratigraphic section in 8,55 m thick was measured from the Seben Formation composed of marls and clayey limestones, and a total of 47 samples were collected. The planktonic foraminiferal assemblages of the samples were determined by using the detailed taxonomical analysis. Based on the marker bioevents such as LOD and FOD of some species, the biostratigraphic framework was established. In this framework, there are five biozones in ascending order; *Pseudoguembelina hariaensis* Zone, P0 Zone, P1a Zone, P1b Zone, and P1c Zone. The K/Pg boundary was delineated between the *P. hariaensis* and P0 zones. In order to reveal the evolutionary recovery of the planktonic foraminifera after the K/Pg mass extinction, the quantitative analysis was carried out and the relative diversity and abundances of the species were determined. The life-history strategists were used for determining the evolutionary recovery patterns by using K-, r/K-, r-strategists. Furthermore, the microfacies, mineralogical, geochemical and magnetic susceptibility analyzes were performed to determine the environmental changes during this time period. Finally, in the light of these findings, an assumption has been made about the possible causes of the delayed recovery of the planktonic foraminifera with mass-extinction occurred aftermaths of the K/Pg boundary.

### **6.1.1. Planktonic Foraminiferal Turnover and Mass extinction and Recovery Pattern at Göynük Section**

The planktonic foraminifera are the most valuable fossil group for determination of the K/Pg boundary. Smit (1982) described firstly the pattern of planktonic foraminiferal extinction. Liu and Olsson (1994) and Olsson et al. (1999) considered *Hedbergella holmdelensis*, *H. monmouthensis*, and *Guembelitra cretacea* to be the only survivors of the end-Cretaceous mass extinction. Similar with these studies, the other previous studies revealed that the *Hedbergella holmdelensis*, *H. monmouthensis*, and *Guembelitra cretacea* are the only survivors after the mass extinction (Keller 1988, 1989a, 1989b, 1993; Pardo et al., 1996; Luciani, 2002; Keller et al., 2012; Punekar et al., 2014a, 2014b, 2016, Rostami et al., 2018). The Göynük section represents a complete section for studying the planktonic foraminiferal turnover and the pattern of evolutionary recovery across the K/Pg boundary by using its well-preserved planktonic foraminiferal assemblages. However, *Guembelitra cretacea* is one of the survival species across the K/Pg boundary in the studied section.

The environmental conditions of *Guembelitra* thrived are questionable. In previous studies, the bloom of this species occurred in shallow and deep-water environments, near shores and in the open ocean, at high and low latitudes (Keller, 2002). As understanding from previous description, the bloom of *Guembelitra* does not indicate a specific to temperature, water depths, and/or salinity ranges. However, the results reveal that the blooms were occurred during times of low productivity, eutrophic waters, and disruption of normal water conditions. According to Keller (2008), these unexpected environmental conditions with low productivity may reflect the high environmental stress, and reduced habitat competition because of disappearing the ecological specialists. Similarly, in this study, the *Guembelitra* blooms are observed in the P0 zone, just after the K/Pg boundary. They were observed as increasing number of individuals, but not called as a bloom (Punekar et al., 2014). The first appearance

of newly evolved Danian species are recorded in the P1a zone which is characterized by abrupt increases in more complex species in the genera *Parvularugoglobigerina*, *Globigerina*, *Eoglobigerina*, *Parasubbotina*. In addition, less complex, generalist, species are also recognized in the genera *Chiloguembelina*, and *Woodringina*. This pattern supports the catastrophic mass extinction of planktonic foraminifera across the K/Pg boundary and their relatively rapid recovery in the early Danian (D'Hont, 1991; Kaiho and Lamolda, 1999; Arenillas et al., 2000; Gallala et al., 2009; Hull et al., 2011; Gallala, 2013; Punekar et al., 2014; Mateo et al., 2016; Rostami et al., 2018). In P1b zone, the rate of evolution in the planktonic foraminifera decline and the abundance of generalists, biserial species and *Guembelitra cretacea*, opportunistic species, suddenly increase. However, complex species, *Eoglobigerina*, *Globigerina*, *Parasubbotina*, *Subbotina*, *Globanomalina*, *Parvularugoglobigerina*, and *Praemurica* are also recognized with smaller-in-size. This pattern indicates that the ecological stress is increased, and the mesotrophic environmental conditions prevail during the P1b region. According to Punekar et al. (2014), this high stressed-environment and low diversity mark the delayed marine recovery through the P1b zone. The decreasing abundance of survivor species with increasing evolution rate and diversity are noted in the P1c zone. The larger and phylogenetically more evolved, complex species dominate this biozone. This part is called as the onset of marine recovery.

MacArthur and Wilson (1967) expressed the responses of organisms to any environmental conditions as life-historical strategies. Biotic responses and strategies of the species to any changes on the environmental conditions have been widely studied in every ecosystem (Keller, 2002, 2008; Punekar et al., 2014) and this response is universal and can be expressed by a simple naming; life history strategies. They defined three types of strategies; K-strategists, high diversity, well-ornamented complex species, r-strategists, simple morphological, opportunistic species, and intermediate (K/r-strategists) strategists, morphologically simple but diversified species. As mentioned above, *Guembelitra cretacea* is the only opportunistic species

that can survive the mass extinction. In other words, it is the r-strategists. The generalist species, intermediate-strategists, are dominated in the P1b zone, at the time of increasing high-stress conditions. On the contrary, the Cretaceous planktonic foraminiferal assemblages, before the mass extinction, are called as the K-strategists because of their complex, well-ornamented, high variability in their morphology. Similar to the Cretaceous forms, the P1c zone shows the same pattern at the time of onset recovery.

### **6.1.2. Mineralogical and Mineral Chemistry Results**

In previous studies carried on Gubbio section in Italy (Luterbacher and Premoli-Silva, 1964), El Mellah in Tunisia (Adatte et al., 2002a), Erto section in Italy (Luciani, 2002), Caravaca and Agost in Spain (Molina et al., 1996; Arenillas et al., 2006), Bjala in Bulgaria (Preisinger et al., 2002), and Dakhla in Egypt (Zaid, 2015) revealed a significant decrease in calcite content at the K/Pg boundary, which indicates the crisis in the boundary productivity reflecting environmental conditions. The researches claimed that the carbonate production rapidly declines after the mass extinction of the calcareous microfossils such as planktonic foraminifera. Although they passed out from the K/Pg boundary, the benthic foraminifera continue to evolve at the boundary and also some dinoflagellate cysts and phytoplankton production continue which can be related to the resumption of carbonate production.

According to Keller (1998) carbonate content of the boundary bed drops less than 10%. The studies carried in the Stratotype section El Kef, Tunisia, showed that calcite content drops to 0% at the boundary (Ben Abdelkader et al., 1997). Moreover, the studies in different localities clearly displayed a significant decrease in calcite content at the K/Pg boundary sections, which indicates crisis in boundary productivity reflecting environmental conditions (Luterbacher and Premoli-Silva, 1964; Adatte et al., 2002a; Molina et al., 1996; Arenillas et al., 2006; Preisinger et al., 2002; Bond et

al., 2014; Zaid, 2015; Font et al., 2018; Rostami et al., 2018). In the Haymana basin, the percentage of CaCO<sub>3</sub> is around 40% at the boundary but just dropped at the base of P0 zone (Esmeray, 2008). Due to tectonically active region, carbonate content may vary with sea-level fluctuations and terrestrial sediment influx with tectonic pulses in the Haymana basin. During P1a biozone, the carbonate content gradually increases due to start of recovery stage and reestablish calcareous plankton in the system. Similarly, Açıkalın et al. (2016) mentioned that the Göynük Basin is abundant in calcareous microfossils, confirming biogenic origin of the carbonates. In the studied Göynük section, the carbonate content fluctuations are observed in both P0 and P1b zones. The decline of the carbonate content across the K/Pg boundary coincides with the global result. However, there was not any previous researches about the clay content in the early Danian sediments (P1a, P1b, and P1c). In the measured Göynük section, the negative shifting on the clay content was identified in P1b zone.

The changes in the relative abundances of planktonic foraminifera, inferring the K/Pg boundary and evolutionary recovery after the boundary was identified in the measured Göynük section. With the decrease of planktonic foraminifera, calcite content also decreases while non-carbonate minerals reversely increase. Clay minerals (Ca-montmorillonite, kaolinite and illite), quartz, feldspar, ilmenorutile and accessory amounts of Fe-Ti oxides and silicates are present in the samples. There is a decrease in clay content (montmorillonite, kaolinite and illite) in both P0 and P1b biozones. The accessory phases as biotite, muscovite, hornblende, clinopyroxene, zircon, apatite, sphene, hematite, hematite spherules, rutile, ilmenorutile and ilmenite are detected across the K/Pg boundary and the P1b zone by the help of XRD and EPMA analyses.

The presence of hematite with spherule in-shape and Ti-bearing iron oxides is important because they indicate possibly secondary origin resulting from oxidation of primary magnetite and akaganeite during diagenesis (Font et al., 2014, 2018; Rostami et al., 2018). Akaganeite, rarely identified in the samples, provides significant evidence to think about volcanic affect in the depositional area, because it is a rare

mineral occurring natural condition, especially in lavas of high temperature (Font et al., 2014). In the volcanic plume, like Deccan lava flows, the compound  $\text{FeCl}_2$  transport into the stratosphere by penetrative convection together with huge amounts of aerosols containing dissolved acid species ( $\text{Fe}^{2+}$ ,  $\text{Cl}^-$ ). These penetrative convections produce heating in stratosphere. On the contrary, the troposphere has cooling, so, the ions can drop the earth surface by acid rains (Robock, 2000; Kaminski et al., 2011; Font et al., 2014) (Figure 6.1). This pattern valid not only Deccan trap but also any other volcanism like Siberian Trap. According to studies carried on Siberian trap, the possible cause of the Permian/Triassic mass extinction, akageneite was indicated in the boundary samples (Grasby et al., 2015; Courtillot and Fluteau, 2014; Chen et al., 2019). At Bidart (France) and Gubbio (Italy), this mineral is identified in the samples at the K/Pg boundary (Font et al., 2016, 2018).

Moreover, all the identified accessories (sphene, rutile, and ilmenite) and silicate minerals (especially Ca-amphibole, biotite, muscovite) are also possibly magmatic origin in the Göynük section because Ti-rich phases infer Ti-rich environment and volcanism (Font et al., 2018). Moreover, euhedral crystals of amphibole and biotite are highly oxidized possibly resulted during volcanic eruption, the results gave in chapter 4 in detail. In addition, presence of both anhedral and euhedral quartz grains, and both Na-plagioclase and orthoclase type feldspars may lead to think their magmatic origin.

In literature, Hg concentrations, being the another indicator for volcanism, were measured in ppb values, and found very low in Danian limestones (Zaid, 2015; Font et al., 2016, 2017; Sial et al., 2016; Rostami et al., 2018; Grasby et al., 2019). Distinctively from early studies, no analysis can be carried on Maastrichtian sediments. In the Göynük section, Hg was identified in the dough of both across the K/Pg boundary and P1b zone. However, its concentration could not be quantitatively measured because of too low amounts in the samples. Despite its trace amount in the groundmass of the samples in the Göynük section, the presence of Hg supports Deccan volcanism as possible cause of extinction.

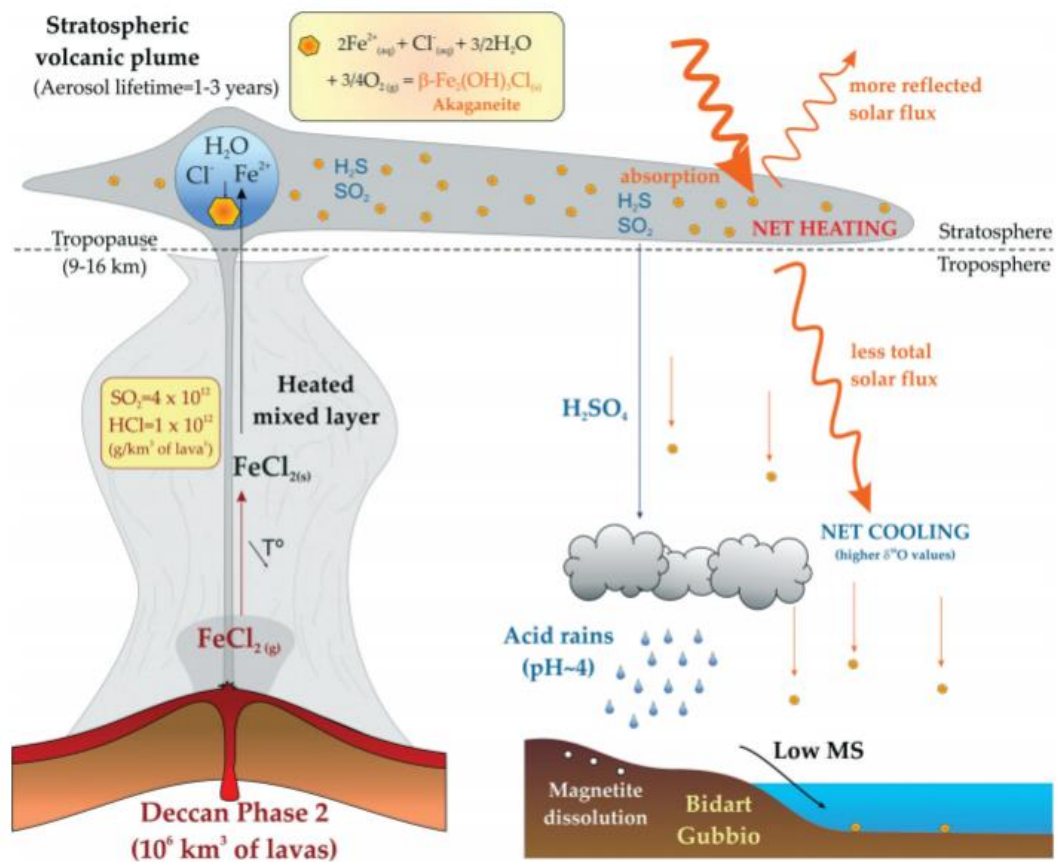


**Figure 6.1:** Conceptual model of the sedimentary marine record of continental magnetite dissolution caused by volcanic acid rains (Font et al., 2014).

Magnetic susceptibility analyses were also done, and results were compared with the global results. The decline on the peak just below the K/Pg boundary and sudden increase after the boundary gives clue for environmental anomaly. The same pattern observed around the P1b zone, the decline just below the zone and sudden increase in P1b zone. However, the shifting on the Hisarözü member was caused by the lithological changes of limestone-marl deposits.

In literature, low magnetic susceptibility values were identified just below the K/Pg boundary (Font et al., 2014, 2016, 2018). This level coincides with the presence of

akaganéite phase and Hg anomalies, which hypothesized as volcanic in origin. However, the researches were mainly based on K/Pg boundary (Figure 6.2). The results from Göynük samples gave similar pattern with K/Pg boundary and P1b zone.

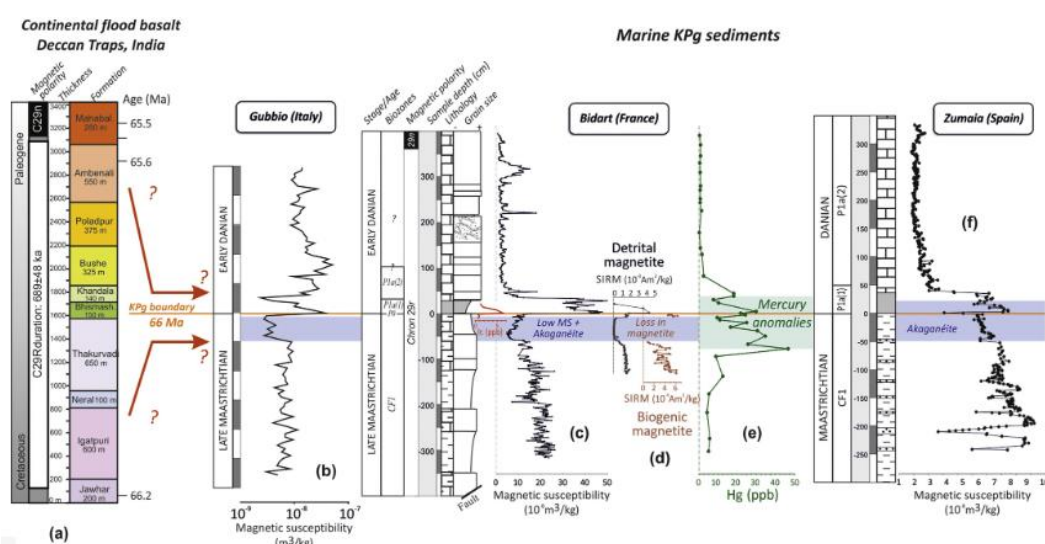


**Figure 6.2:** Correlation of a) the age (U–Pb dating on zircon; Schoene et al., 2015) of the Deccan lavas flow in India with the KPg marine sedimentary records marked by b) the low MS interval at Gubbio (Italy) (Ellwood et al., 2003); c) the low MS interval containing akaganéite (Font et al., 2011), d) the depletion in detrital and biogenic magnetite (Font et al., 2014), and e) mercury anomalies at Bidart (France) (Font et al., 2016); and f) the magnetite-depleted interval containing akaganéite at Zumaia (Font et al., 2018)

### 6.1.3. The Reasons Behind the Delayed Recovery: Chicxulub or Deccan

All these results discussed above, revealed that the cause of the K/Pg mass extinction and the density/diversity differences between biozones, especially P1b. The cause and timing of the K/Pg mass extinction has been subjected to multiple analyses since 1980, and there still remain unsolved issues. According to previous studies, two competitive

hypotheses are considered as the cause of K/Pg mass extinction; Chicxulub impact and Deccan volcanism.

The first suggested hypothesis is the bolide impact hypothesis as the cause of K/Pg mass extinction based on the discovery of shocked quartz, Ni-rich spinels, microtektites, microspherules, and Ir anomaly in the boundary beds (Alvarez et al., 1980; Hildebrand et al., 1991; Claeys et al., 2002; Huber et al., 2002; Macload et al., 2007; Schulte et al., 2010). However, the most critical part of this hypothesis is the age of impact. The paleomagnetic data revealed that the impact was occurred inside of the CF1 zone in other words below the boundary (Schulte et al., 2010; Keller et al., 2013). Keller et al. (2013) claimed that the single spherule layer is not proof of the Chicxulub impact causes the K/Pg mass extinction. They mentioned that the every studied section is located in active regions in terms of slumps, debris flows etc. Moreover, the reworked species, especially late Maastrichtian, are observed inside of the Danian sediments. This indicates the long-term deposition associated with erosion, transportation and redeposition. The Ir anomaly on the other hand, were observed the places where the founding of microtektites. It means that the main evidence for the Chicxulub impact is the microtektites. Moreover, microspherules can be also evidence for impact theory. In Turkey, Karabeyoğlu (2017) defined the bloom of microspherules at the boundary in the Haymana basin.

Similarly, in the studied Göynük section, the bloom of microspherules were also recorded in the P0 zone. In addition to microspherules, the microtektites were also observed within both the Uppermost Maastrichtian and Lowest Danian deposits with full of spary calcite. The observations revealed that the microtektites were reworking in the Göynük basin. Interestingly, the EPMA map shows the Ir in the dough of the microtektite from P1b samples (Figure 6.3).

The second hypothesis is the Deccan volcanism, which is the one of the largest igneous province events that cause the global mass extinction all around the world (Keller et al., 2002). The evidences show that Deccan trap has major basalt flows, providing the

immediate effects of volcanic eruptions on the marine life. After the establishment of the biozonation, the K/Pg mass extinction and the density/diversity differences between biozones, particularly in the P1b zone have been revealed. According to Punekar et al. (2014), the abrupt change of the evolutionary pattern of the planktonic foraminifera coincides with the Deccan phase-3. In the Göynük samples, this sudden change of the life history strategies in the P1b zone, increase in abundance of intermediate and r-strategies, coincide with the global results in India (Punekar et al., 2014) (Figure 6.3). Moreover, the presence of magmatic origin minerals such as apatite, hematite, hematite spherules, ilmenite, etc. coincides with the Deccan phase-2 and phase-3, respectively.

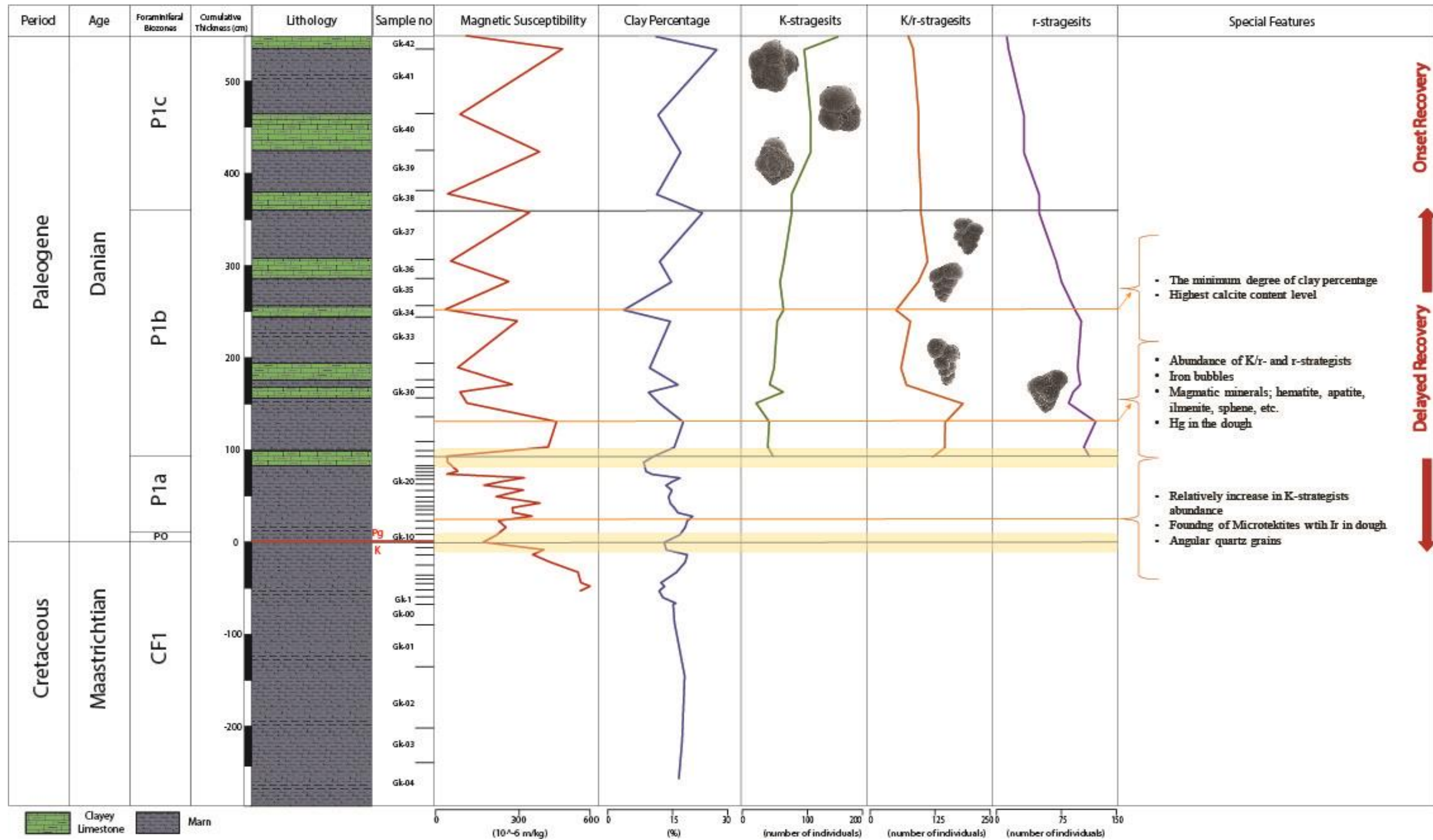


**Figure 6.3:** Summary of major results in the Göynük section. Note also the good correlation between the biozones and the results



In brief, in the Göynük section, the micropaleontological and mineralogical changes recorded in this study might be related to the Deccan volcanism. It can be deduced that the Deccan phase-2 caused to the K/Pg mass extinction, the phase-3 to the delayed recovery after the K/Pg mass extinction. It cannot be ignored the possibility of which these changes might be related to volcanic activities during this time interval in Turkey.

The effect of the both volcanism and impact were observed in the studied Göynük section. The microspherules, and microtektites with Ir in the dough, shows the effects of Chicxulub bolide impact. On the contrary, the pattern of the evolutionary recovery, delayed recovery, in the P1b zone can be reach in the Göynük and foundation of volcanic origin minerals, which show the possible effect of Deccan volcanism. In the studied Göynük section, both of two hypotheses can be corrected (Figure 6.4).

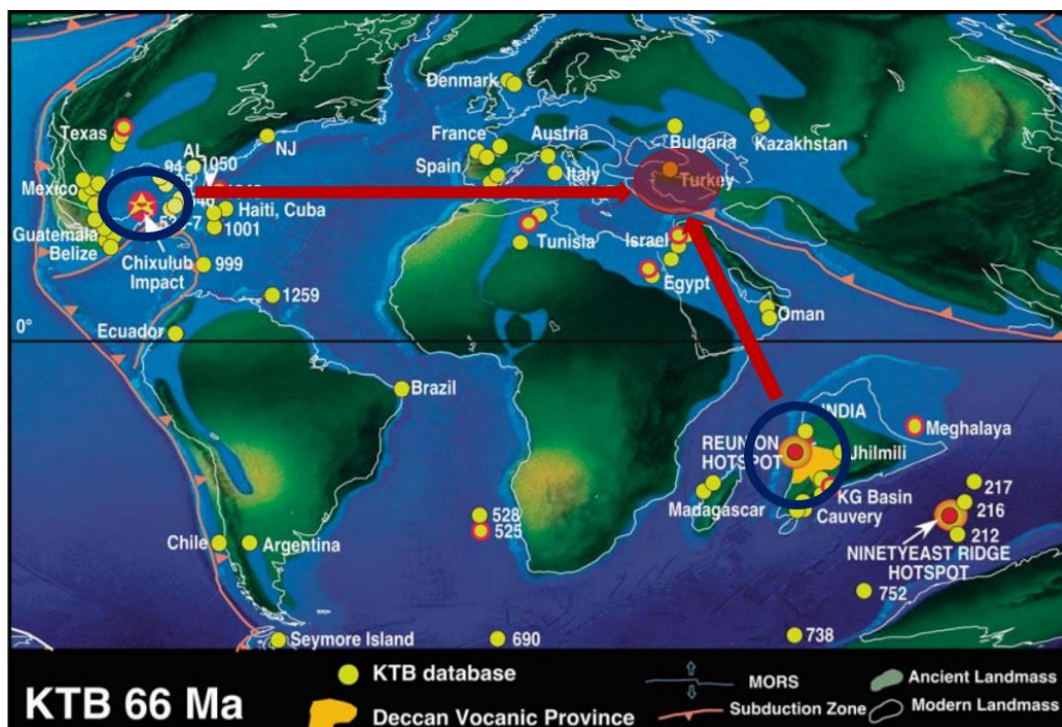


**Figure 6.4:** Paleogeographic Distribution map with Deccan Trap and Chicxulub impact (Modified from Punekar et al., 2014)

## 6.2. Conclusion

The Göynük section presents a detailed, expanded record of paleontological and mineralogical changes across the K/Pg boundary interval in the Central Sakarya Region, Turkey. The pattern of planktonic foraminiferal extinction at the Göynük section records extinction event that claimed nearly all of the latest Maastrichtian species. The bloom of *Guembelitra cretacea*, at the P0 zone are defined with the evolution of the planktonic foraminiferal assemblages in early Danian sediments. The unexpected pattern of the planktonic foraminifera, in other words, changing on the life-history strategies, indicates the sudden changes on the paleoenvironments at P1b zone. Likewise, the mineralogical and magnetic susceptibility analyses revealed the same patterns with biostratigraphy.

- In the Göynük Basin, the stratigraphic section in 8, 55 m thick was measured from the Seben Formation composed of marls and its Hisarözü member alternation of marls and clayey limestones.
- A total of 47 samples were collected.
- The planktonic foraminiferal assemblages of the samples were determined by using the detailed taxonomical analysis such as the number of chambers, test size, presence/absence of keel and/or any ornamentation, and sutural properties. A total of 62 species belonging to 24 genera were identified.
- Based on the marker bioevents such as LOD and HOD of some species, the biostratigraphic framework was established. In this framework, there are five biozones in ascending order; *Pseudoguembelina hariaensis* Zone, P0 Zone, P1a Zone, P1b Zone, and P1c Zone.
- The K/Pg boundary was delineated between the *P. hariaensis* and P0 zones by using the extinction of Cretaceous planktonic foraminifera species with the survival species, *Guembelitra cretacea*, and the evolution of the Paleogene planktonic foraminifera assemblages.

- For understanding the evolutionary recovery pattern after the K/Pg mass extinction, the quantitative analysis was carried out in the P1b and P1c biozones. The relative diversity and abundances of the species were determined with the help of life-history strategists. The abundances of biserial forms *Chiloguembelina* and *Woodringina* genera, r-/K-strategists, depleted on the diversity of complex planktonic foraminifera species, and the high-density of *Guembelitra cretacea*, r-strategist, was observed in the P1b zone. On the contrary, the depletion of *Guembelitra cretacea*, and the other opportunistic species, the increase in the diversity of complex forms, K-strategists, were indicated in the P1c zone. The numerical values revealed these changes and delayed recovery in the P1b zone in detail.
- The bloom of microspherules, was recorded in the P0 zone. On the other hand, the microtektites were observed within both the uppermost Maastrichtian and lowest Danian deposits.
- Furthermore, the microfacies, mineralogic, geochemical and magnetic susceptibility analyzes were performed to determine the environmental changes during this time period. The XRD analysis was applied to all samples and decreases of the clay content in both the K/Pg boundary and the P1b zone have been determined. The EPMA analysis, however, was applied to the samples at the K/Pg boundary and the P1b zone. As a result of this analysis, the magmatic origin minerals such as mica minerals; biotite, muscovite, and oxide minerals; apatite, hematite ilmenite, sphene etc. have been recorded.
- The magnetic susceptibility analysis has been performed on both rock samples and thin sections of the samples and similar pattern has been obtained. The results coincided with the global results carried on both the Gubbio, Italy and the Bidart, France sections. This is the first study in the world that the magnetic susceptibility analyses were carried out in the P1b and P1c zones.
- Finally, the presence of the microtektites and microspherules probably indicate the effects of the Chicxulub impact. In the light of mineralogical, and

geochemical findings, the possible cause of the delayed recovery of the planktonic foraminifera aftermaths of the K/Pg mass-extinction might be Deccan volcanism.

## REFERENCES

- Abdüsselamoğlu, S., 1956. Göynük, Mudurnu ve Beydili bölgesinin jeolojisi. MTA Rapor No: 2391.
- Abrajevitch, A., Font, E., Florindo, F., & Roberts, A. P., 2015, Asteroid impact vs. Deccan eruptions: The origin of low magnetic susceptibility beds below the Cretaceous–Paleogene boundary revisited, *Earth and Planetary Science Letters*, 430, 209-223. doi:10.1016/j.epsl.2015.08.022.
- Abramovich, S., and Keller, G., 2002, High stress late Maastrichtian paleoenvironment: Inference from planktonic foraminifera in Tunisia: *Paleogeography, Paleoclimatology, Paleoecology*, v. 178, p. 145-164, doi: 10.1016/S0031-0182(01)00394-7.
- Abramovich, S., and Keller, G., 2003, Planktonic foraminiferal response to the latest Maastrichtian abrupt warm event: A case study from South Atlantic DSDP Site 525A: *Marine Micropaleontology*, v. 48, no. 3-4, p. 225-249, doi: 10.1016/S0377-8398(03)00021-5.
- Abramovich, S., Keller, G., Adatte, T., Stinnesbeck, W., and Hottinger, L., 2002, Age and paleoenvironment of the Maastrichtian to Paleocene of the Mahajanga Basin, Madagascar: A multidisciplinary approach: *Marine Micropaleontology*, v. 47, p. 17-70, doi: 10.1016/S0377-8398(02)00094-4.
- Açikalın, S., Vellekoop, J., Ocakoglu, F., Yılmaz, I. Ö., Smit, J., Altiner, S. O., Goderis, S., Vonhof, H., Speiker, R. P., Woelders, L., Fornaciari, E., and Brinkhuis, H., 2015, Geochemical and paleontological characterization of a new K–Pg Boundary locality from the Northern branch of the Neo-Tethys: Mudurnu-Göynük Basin, NW Turkey, *Cretaceous Research*, 52, p. 251-267.
- Açikalın, S., Ocakoğlu, F., Yılmaz, I., Vonhof, H., Hakyemez, A., & Smit, J., 2016. Stable isotopes and geochemistry of a Campanian–Maastrichtian pelagic

- succession, Mudurnu–Göynük Basin, NW Turkey: Implications for palaeoceanography, palaeoclimate and sea-level fluctuations. *Palaeogeography, Palaeoclimatology, Palaeoecology*, 441, 453–466. doi: 10.1016/j.palaeo.2015.10.005
- Adatte, T., Keller, G., Stinnesbeck, W., 2002a, Late Cretaceous to early Paleocene climate and sea-level fluctuations: the Tunisian record, *Palaeogeography, Palaeoclimatology, Palaeoecology*, 178, 165–196.
- Adatte, T., Keller, G., Burns, S., Stoykova, K. H., Ivanov, M. I., Vangelov, D., Kramar, U., Stüben, D., 2002b, Paleoenvironment across the Cretaceous-Tertiary transition in eastern Bulgaria, *Geol. Soc. Am. Spec. Pap.*, 356, 231–251.
- Adatte, T., Keller, G., Stüben, D., Harting, M., Kramar, U., Stinnesbeck, W., Benjamini, C., 2005. Late Maastrichtian and K/T paleoenvironment of the eastern Tethys (Israel): mineralogy, trace and platinum group elements, biostratigraphy and faunal turnovers. *Bulletin De La Societe Geologique De France*, 176(1), 37–55. doi: 10.2113/176.1.37
- Adatte, T., Keller, G., and Baum, G., 2011, Age and origin of the Chicxulub impact and sandstone complex, Brazos River, Texas: Evidence from lithostratigraphy and sedimentology, in Keller, G., and Adatte, T., eds., *The End-Cretaceous Mass Extinction and the Chicxulub Impact in Texas: Society for Sedimentary Geology (SEPM) Special Publication 100*, p. 43-80.
- Alegret, L., Molina, E., Thomas, E., 2003, Benthic foraminiferal turnover across the Cretaceous/Paleogene boundary at Agost (southeastern Spain): paleoenvironmental inferences, *Marine Micropaleontology*, 48(3-4), 251–279, doi: 10.1016/s0377-8398(03)00022-7.
- Alegret, L., & Thomas, E., 2004, Benthic foraminifera and environmental turnover across the Cretaceous/Paleogene boundary at Blake Nose (ODP Hole 1049C,

- Northwestern Atlantic), *Palaeogeography, Palaeoclimatology, Palaeoecology*, 208(1-2), 59–83, doi: 10.1016/j.palaeo.2004.02.028.
- Alegret, L., & Thomas, E., 2013, Benthic foraminifera across the Cretaceous/Paleogene boundary in the Southern Ocean (ODP Site 690): Diversity, food and carbonate saturation, *Marine Micropaleontology*, 105, 40–51. doi: 10.1016/j.marmicro.2013.10.003.
- Altner, D., Koçyiğit, A., Farinacci, A., Nicosia, U., Conti, M.A., 1991. Jurassic–Lower Cretaceous stratigraphy and paleogeographic evolution of the southern part of north-western Anatolia (Turkey). *Geol. Romana* 27, 13–80.
- Altınlı, E., 1973a, Orta Sakarya Jeolojisi. Cumhuriyetin 50. Yılı Yerbilimleri Kongresi, Tebliğler, 159-191.
- Altınlı, E., 1973b, Bilecik Jurasığı, 50. Yıl Yer Bil. Kong. Bildiriler, Ankara, p. 159-192.
- Altınlı, E., 1976. Geology of the northern portion of the middle Sakarya river. *İst. Üniv. Fen Fak. Mecm. Seri B, C. 41 (1-4)*, s. 35-56.
- Altınlı, E., 1977, Geology of the eastern territory of Nallıhan (Ankara province). *İ.Ü. Fen Fak. Mecm., Ser. B*, 42, 29-44.
- Alvarez, L. W., Alvarez, W., Asaro, F., & Michel, H. V., 1980, Extraterrestrial Cause for the Cretaceous-Tertiary Extinction. *Science*, 208(4448), 1095–1108. doi: 10.1126/science.208.4448.1095
- Arenillas, I., Arz, J.A., Molina, E., and Dupuis, C., 2000, The Cretaceous/Tertiary boundary at Ain Settara, Tunisia: Sudden catastrophic mass extinction in planktonic foraminifera: *Journal of Foraminiferal Research*, v. 30, p. 202-218, doi: 10.2113/0300202.
- Arenillas, I., Alegret, L., Arz, J. A., Liesa, C., Meléndez, A., Molina, E., Rosales-Domínguez, C., 2002. Cretaceous-Tertiary boundary planktic foraminiferal

mass extinction and biochronology at La Ceiba and Bochil, Mexico, and El Kef, Tunisia. Special Paper 356: Catastrophic Events and Mass Extinctions: Impacts and Beyond, 253–264. doi: 10.1130/0-8137-2356-6.253

Arenillas, I., Arz, J. A., Molina, E., 2004. A new high-resolution planktic foraminiferal zonation and subzonation for the lower Danian. *Lethaia*, 37, 79–95.

Arenillas, I., Arz, J.A., Grajales-Nishimura, J.M., Murillo-Muneton, G., Alvarez, W., Camargo-Zanguera, A., Molina, E., and Rosales-Dominguez, C., 2006, Chicxulub impact event is Cretaceous/Paleogene boundary in age: New micropaleontological evidence: *Earth and Planetary Science Letters*, v. 249, p. 241–257, doi:10.1016/j.epsl.2006.07.020.

Arenillas, I., & Arz, J. A., 2016, Benthic origin and earliest evolution of the first planktonic foraminifera after the Cretaceous/Palaeogene boundary mass extinction. *Historical Biology*, 29(1), 25–42. doi: 10.1080/08912963.2015.1119133

Bayhan, E., 2007. Clay mineralogy of the Upper Cretaceous-Lower Tertiary sedimentary sequences of the Kalecik Region (Central Anatolia, Turkey). *Yerbilimleri, Hacettepe Üniversitesi Yerbilimleri Uygulama ve Araştırma Merkezi Dergisi*, 28/2, 127-136.

Ben Abdelkader, O., Ben Salem, H., Donze, P., Maamouri, A. L., Meon, H., Robin, E., Rocchia, R., Froget, L., 1997. The K/T stratotype section of El Kef (Tunisia): events and biotic turnovers. *Geobios*, 21, 235-245.

Berggren, W., A., Kent, D., V., Swisher, C., C., Aubry, M., P., 1995. A revised Cenozoic geochronology and chronostratigraphy. *SEPM, Special Publication*, 54, 129-212.

Beseme, P., 1968. Sürümdere senklinali bitümlü kayacının jeolojik incelemesi (Gölpazarı-Bilecik). *MTA Enstitüsü Raporu, Derleme No: 4847*, 22 s.

Blow, W., H., 1979. *The Cainozoic Globigerinida*. 3 Vols., Brill, Leiden. 1413 p.

- Bond, D.P.G., and Wignall, P.B., 2014, this volume, Large igneous provinces and mass extinctions: An update, in Keller, G., and Kerr, A.C., eds., *Volcanism, Impacts, and Mass Extinctions: Causes and Effects*: Geological Society of America Special Paper 505, doi:10.1130/2014.2505(02).
- Bonté, P., Delacotte, O., Renard, M., Laj, C., Boclet, D., Jehanno, C., & Rocchia, R. (1984). An iridium rich layer at the Cretaceous/Tertiary boundary in the Bidart Section (southern France). *Geophysical Research Letters*, 11(5), 473-476. doi:10.1029/gl011i005p00473
- Brönnimann, P., 1952. Globigerinidae from the Upper Cretaceous (Cenomanian-Maestrichtian) of Trinidad, B.W.I. *Bull. Am. Paleontol.*, 34, 1-70.
- Canudo, J.I., Keller, G., and Molina, E., 1991, Cretaceous/Tertiary boundary extinction pattern and faunal turnover at Agost and Caravaca, SE Spain: *Marine Micropaleontology*, v. 17, p. 319–341, doi:10.1016/0377-8398(91)90019-3.
- Chamley, H., 1989. *Clay Sedimentology*. Springer-Verlag, Berlin, 623 p.
- Chen, J., & Xu, Y. (2019). Establishing the link between Permian volcanism and biodiversity changes: Insights from geochemical proxies. *Gondwana Research*, 75, 68-96. doi:10.1016/j.gr.2019.04.008
- Chenet, A.-L., Quidelleur, X., Fluteau, F., Courtillot, V., and Bajpai, S., 2007, 40K/40Ar dating of the main Deccan large igneous province: Further evidence of Cretaceous-Tertiary boundary age and short duration: *Earth and Planetary Science Letters*, v. 263, p. 1–15, doi:10.1016/j.epsl.2007.07.011.
- Chenet, A.-L., Fluteau, F., Courtillot, V., Gerard, M., and Subbarao, K.V., 2008, Determination of rapid Deccan eruptions across the Cretaceous- Tertiary boundary using paleomagnetic secular variation: Results from a 1200-m-thick section in the Mahabaleshwar: *Journal of Geophysical Research*, v. 113, B04101, doi:10.1029/2006JB004635.

- Chenet, A.-L., Courtillot, V., Fluteau, F., Gerard, M., Quidelleur, X., Khadri, S.F.R., Subbarao, K.V., and Thordarson, T., 2009, Determination of rapid Deccan eruptions across the Cretaceous-Tertiary boundary using paleomagnetic secular variation: 2. Constraints from analysis of eight new sections and synthesis for a 3500-m-thick composite section: *Journal of Geophysical Research*, v. 114, B06103, doi:10.1029/2008JB005644.
- Coccioni, R., Marsili, A., 2007. The response of benthic foraminifera to the K–Pg boundary biotic crisis at Elles (northwestern Tunisia). *Palaeogeography, Palaeoclimatology, Palaeoecology*, doi:10.1016/j.palaeo.2007.02.046.
- Coccioni, R., Luciani, V., Marsili, A., 2006. Cretaceous oceanic anoxic events and radially elongated chambered planktonic foraminifera: Paleocological and paleoceanographic implications. *Palaeogeography, Palaeoclimatology, Palaeoecology*, 235, 66–92.
- Courtillot, V., and Fluteau, F., 2014, this volume, A review of the embedded time scales of flood basalt volcanism with special emphasis on dramatically short magmatic pulses, in Keller, G., and Kerr, A.C., eds., *Volcanism, Impacts, and Mass Extinctions: Causes and Effects: Geological Society of America Special Paper 505*, doi:10.1130/2014.2505(15).
- Cowie, J. W., Zieger, W., Remane, J., 1989. Stratigraphic Commission accelerates progress, 1984–1989. *Episodes*, 112, 79–83.
- Culver, S. J., 2003, Benthic foraminifera across the Cretaceous–Tertiary (K–T) boundary: a review, *Marine Micropaleontology*, 47(3-4), 177–226. doi: 10.1016/s0377-8398(02)00117-2.
- D'Orbigny, A. D., 1839, Foraminiferes. In de la Sagra, R., (ed.), *Histoire Physique, Politique et Naturelle de l'He de Cuba*, Bertrand (Paris).

- Dunham, R., J., 1962. Classification of carbonate rocks according to the depositional texture in: Ham, W. E. (ed.): Classification of carbonate rocks. A symposium. AAPG Memoir 1, 108-171.
- Dupuis, C., Steurbaut, E., Molina, E., Rauscher, R., Tribovillard, N., Arenillas, I., Lefevre, I., 2001. The Cretaceous-Palaeogene (K/P) boundary in the Aïn Settara section (Kalaat Senan, Central Tunisia): lithological, micropalaeontological and geochemical evidence. Bulletin De l'Institut Royal Des Sciences Naturelles De Belgique, Sciences De La Terre, 71, 169–190.
- Eicher, D. L., 1976, Geologic time, 2<sup>nd</sup> edition, Englewood Cliffs, NJ: Prentice-Hall.
- Ellis, B., Messina, A., 1941–2004. Catalogue of Micropaleontology, Catalogue of Foraminifera. American Museum of Natural History, Special Publication.
- Esmeray, S., 2008, Cretaceous/Paleogene Boundary in the Haymana Basin, Central Anatolia, Turkey: Micropaleontological, Mineralogical and Sequence Stratigraphic Approach, M.Sc. Thesis, Middle East Technical University, 271 p.
- Esmeray-Senlet, S., Özkan-Altiner, S., Altiner, D., Miller, K. G., 2015, Planktonic foraminiferal biostratigraphy, microfacies analysis and sequence stratigraphy across the Cretaceous/Paleogene boundary in the Haymana Basin, Central Anatolia, Turkey, J. Sediment. Res., 85, p. 489–508, doi:10.2110/jsr.2015.31.
- Flügel, E., 2004. Microfacies of carbonate rocks: analysis, interpretation and application. Springer, 976 p.
- Foley, E.J., 1938, Göynük civarında yapılan bir istikşaf gezisi. MTA Enstitüsü Raporu, Derleme No: 786, 17 s.
- Font, E., Nédélec, A., Ellwood, B.B., Mirão, J., and Silva, P.F., 2011, A new sedimentary benchmark for the Deccan Traps volcanism?: Geophysical Research Letters, v. 38, L24309, doi:10.1029/2011GL049824.

- Font, E., Fabre, S., Nédélec, A., Adatte, T., Keller, G., Veiga-Pires, C., Ponte, J., Mirão, J., Khozyem, H., and Spangenberg, J., 2014, this volume, Atmospheric halogen and acid rains during the main phase of Deccan eruptions: Magnetic and mineral evidence, in Keller, G., and Kerr, A.C., eds., *Volcanism, Impacts and Mass Extinctions: Causes and Effects: Geological Society of America Special Paper 505*, doi:10.1130/2014.2505(18).
- Font, E., Adatte, T., Sial, A. N., Lacerda, L. D. D., Keller, G., & Punekar, J., 2016, Mercury anomaly, Deccan volcanism, and the end-Cretaceous mass extinction. *Geology*, 44(2), 171–174. doi: 10.1130/g37451.1
- Font, E., Carlut, J., Rémazeilles, C., Mather, T. A., Nédélec, A., Mirão, J., & Casale, S., 2017, End-Cretaceous akaganéite as a mineral marker of Deccan volcanism in the sedimentary record. *Scientific Reports*, 7(1). doi: 10.1038/s41598-017-11954-y
- Font, E., Adatte, T., Andrade, M., Keller, G., Bitchong, A. M., Carvalho, C., Ferreira, J., Diogo, Z. & Mirão, J. 2018. Deccan volcanism induced high stress environment during the Cretaceous–Paleogene transition at Zumaia, Spain: Evidence from magnetic, mineralogical and biostratigraphic records. *Earth and Planetary Science Letters* 484, 53–66.
- Gallala, N., Zaghbib-Turki, D., Arenillas, I., Arz, J. A., & Molina, E., 2009, Catastrophic mass extinction and assemblage evolution in planktic foraminifera across the Cretaceous/Paleogene (K/Pg) boundary at Bidart (SW France). *Marine Micropaleontology*, 72(3-4), 196–209. doi: 10.1016/j.marmicro.2009.05.001
- Gedik, İ., Aksay, A., 2002. 1/100000 ölçekli Türkiye Jeoloji Haritaları No:38, Adapazarı H25 Paftası, MTA — Jeoloji Etütleri Dairesi, Ankara. (in Turkish).

- Geller, J., & Engle, P., 2002, Sample preparation for electron probe microanalysis - Pushing the limits. *Journal of Research of the National Institute of Standards and Technology*, 107(6), 627. doi: 10.6028/jres.107.051
- Gertsch, B., Keller, G., Adatte, T., Garg, R., Prasad, V., Fleitmann, D., and Berner, Z., 2011, Environmental effects of Deccan volcanism across the Cretaceous-Tertiary transition in Meghalaya, India: *Earth and Planetary Science Letters*, v. 310, p. 272–285, doi:10.1016/j.epsl.2011.08.015.
- Göncüoğlu, M.C., Turhan, N., Şentürk, K., Özcan, A., Uysal, Ş., Yaliniz, M.K., 2000. Geotraverse across northwestern Turkey: tectonic units of the Central Sakarya region and their evolution. In: Bozkurt, E., Winchester, J.A., Piper, J.D.A. (Eds.), *Tectonics and Magmatism in Turkey and the Surrounding Area*. Geological Society, London, Special Publication 173, pp. 139–161.
- Görmüş, M., Karaman, E., 1992. Facies changes and new stratigraphical data in the Cretaceous – Tertiary boundary around Söbüdağ (Çünür – Isparta). *Geosound*, 21, 43- 57.
- Grasby, S. E., Beauchamp, B., Bond, D. P. G., Wignall, P. B., Talavera, C., Galloway, J. M., Piepjohn, K., Reinhardt, L. & Blomeier, D., 2015. Progressive environmental deterioration in NW Pangea leading to the Latest Permian Extinction. *Geological Society of America Bulletin* 127, 1331–47.
- Grasby, S. E., Them, T. R., Chen, Z., Yin, R., & Ardakani, O. H., 2019. Mercury as a proxy for volcanic emissions in the geologic record. *Earth-Science Reviews*, 196, 102880. doi:10.1016/j.earscirev.2019.102880
- Hallam, A. and Wignall, P. B., 1997, *Mass extinctions and their aftermath*, Oxford University Press.
- Hart, M. B., Fitzpatrick, M. E., & Smart, C. W. (2016). The Cretaceous/Paleogene boundary: Foraminifera, sea grasses, sea level change and sequence

- stratigraphy. *Palaeogeography, Palaeoclimatology, Palaeoecology*, 441, 420-429. doi:10.1016/j.palaeo.2015.06.046
- Hildebrand, A. R., Penfield, G. T., Kring, D. A., Pilkington, M., Z., A. C., Jacobsen, S. B., & Boynton, W. V. 1991. Chicxulub Crater: A possible Cretaceous/Tertiary boundary impact crater on the Yucatán Peninsula, Mexico. *Geology*, 19(9), 867. doi: 10.1130/0091-7613(1991)019<0867:ccapct>2.3.co;2
- Huston, M. (1979). A General Hypothesis of Species Diversity. *The American Naturalist*, 113(1), 81-101. doi: 10.1086/283366
- İnan, N., Temiz, H., 1992. Niksar (Tokat) yöresinde Kretase/Tersiyer geçişinin litostratigrafik ve biyostratigrafik özellikleri. *Türkiye Jeoloji Bülteni*, 35, 39-47.
- Kalafatçıoğlu, A.ve Uysallı, H., 1964. Beypazarı-Nallıhan-Seben civarının jeolojisi. *MTA Dergisi*, Sayı 62, s. 1-11.
- Karabeyoğlu, A. U., 2017, Planktonic Foraminiferal Diversity and Abundance Changes Across Cretaceous-Paleogene Boundary Beds in The Haymana Basin and New Observations on The Extinction Horizon. Ankara: MSc. Thesis, Middle East Technical University.
- Karoui-Yaakoub, N., Zaghbib-Turki, D., Keller, G., 2002. The Cretaceous- Tertiary (K-T) mass extinction in planktic foraminifera at Elles I and El Melah, Tunisia. *Palaeogeography, Palaeoclimatology, Palaeoecology*, 178, 233 – 255.
- Keller, G., 1988a, Extinction, survivorship and evolution of planktic foraminifers across the Cretaceous/Tertiary boundary at El Kef, Tunisia: *Marine Micropaleontology*, v. 13, p. 239–263, doi:10.1016/0377-8398(88)90005-9.
- Keller, G., 1988b, Biotic turnover in benthic foraminifera across the Cretaceous-Tertiary boundary at El Kef, Tunisia: *Paleogeography, Paleoclimatology, Paleoecology*, v. 66, p. 153–171, doi:10.1016/0031-0182(88)90198-8.

- Keller, G., 1989a, Extended period of extinctions across the K/T boundary in planktic foraminifera of continental shelf sections: Implications for impact and volcanism theories: *Geological Society of America Bulletin*, v. 101, p. 1408–1419, doi:10.1130/0016-7606(1989)101<1408:EPOEAT>2.3.CO;2.
- Keller, G., 1989b, Extended K/T boundary extinctions and delayed population change in planktic foraminiferal faunas from Brazos River, Texas: *Paleoceanography*, v. 4, no. 3, p. 287–332, doi:10.1029/PA004i003p00287.
- Keller, G., 1993, The Cretaceous-Tertiary boundary transition in the Antarctic Ocean and its global implications: *Marine Micropaleontology*, v. 21, p. 1–45, doi:10.1016/0377-8398(93)90010-U.
- Keller, G., 1996. The K-T mass extinction in planktonic foraminifera: Biotic constraints for catastrophe theories. In: McLeod, N., Keller, G. (eds.), *Cretaceous-Tertiary mass extinction: biotic and environmental changes*. W. W. Norton & Company, New York-London, 49–84.
- Keller, G., 2001, The End-Cretaceous mass extinction in the marine realm: Year 2000 assessment: *Planetary and Space Science*, v. 49, no. 8, p. 817–830, doi:10.1016/S0032-0633(01)00032-0.
- Keller, G., 2002, Guembelitria-dominated late Maastrichtian planktic foraminiferal assemblages mimic early Danian in central Egypt: *Marine Micropaleontology*, v. 47, p. 71–99, doi:10.1016/S0377-8398(02)00116-0.
- Keller, G., 2003, Biotic effects of impacts and volcanism: *Earth and Planetary Science Letters*, v. 215, no. 1–2, p. 249–264, doi:10.1016/S0012-821X(03)00390-X.
- Keller, G., 2004, Low-diversity, late Maastrichtian and early Danian planktic foraminiferal assemblages of the eastern Tethys: *Journal of Foraminiferal Research*, v. 34, no. 1, p. 49–73, doi:10.2113/0340049.

- Keller, G., & Pardo, A., 2004, Disaster opportunists Guembelitrinidae: Index for environmental catastrophes. *Marine Micropaleontology*, 53(1-2), 83-116. doi:10.1016/j.marmicro.2004.04.012
- Keller, G., 2005, Biotic effects of late Maastrichtian mantle plume volcanism: Implications for impacts and mass extinctions: *Lithos*, v. 79, no. 3–4, p. 317–341, doi: 10.1016/j.lithos.2004.09.005.
- Keller, G., 2008a, Cretaceous climate, volcanism, impacts and biotic effects: *Cretaceous Research*, v. 29, no. 5–6, p. 754–771, doi: 10.1016/j.cretres.2008.05.030.
- Keller, G., 2008b, Impact stratigraphy: Old principle, new reality, in Evans, K.R., Horton, J.W., and King, D.T., eds., *The Sedimentary Record of Meteorite Impacts: Geological Society of America Special Paper 437*, p. 147–178.
- Keller, G., 2011, Cretaceous-Tertiary mass extinction in marginal and open marine environments: Texas, U.S.A., and Tunisia, in Keller, G., and Adatte, T., eds., *The End-Cretaceous Mass Extinction and the Chicxulub Impact in Texas: Society for Sedimentary Geology (SEPM) Special Publication 100*, p. 197–226.
- Keller, G., 2014, this volume, Deccan volcanism, the Chicxulub impact, and the end-Cretaceous mass extinction: Coincidence? Cause and effect?, in Keller, G., and Kerr, A.C., eds., *Volcanism, Impacts, and Mass Extinctions: Causes and Effects: Geological Society of America Special Paper 505*, doi:10.1130/2014.2505(03).
- Keller, G., and Abramovich, S., 2009, Lilliput effect in late Maastrichtian planktic foraminifera: Response to environmental stress: *Palaeogeography, Palaeoclimatology, Palaeoecology*, v. 284, p. 47–62, doi: 10.1016/j.palaeo.2009.08.029.

- Keller, G., and Benjamini, C., 1991, Paleoenvironment of the eastern Tethys in the early Danian: *Palaios*, v. 6, p. 439–464, doi:10.2307/3514984.
- Keller, G., and Pardo, A., 2004, Disaster opportunists Guembelitrinidae— Index for environmental catastrophes: *Marine Micropaleontology*, v. 53, p. 83–116, doi: 10.1016/j.marmicro.2004.04.012.
- Keller, G., Barrera, E., Schmitz, B., and Matsson, E., 1993, Gradual mass extinction, species survivorship, and long term environmental changes across the Cretaceous-Tertiary boundary in high latitudes: *Geological Society of America Bulletin*, v. 105, no. 8, p. 979–997, doi:10.1130/0016-7606(1993)105<0979:GMESSA>2.3.CO;2.
- Keller, G., Li, L., and MacLeod, N., 1995, The Cretaceous/Tertiary boundary stratotype section at El Kef, Tunisia: How catastrophic was the mass extinction?: *Palaeogeography, Palaeoclimatology, Palaeoecology*, v. 119, p. 221–254, doi:10.1016/0031-0182(95)00009-7.
- Keller, G., Adatte, T., Gardin, S., Bartolini, A., and Bajpai, S., 2008, Main Deccan volcanism phase ends near the K-T boundary: Evidence from the Krishna-Godavari Basin, SE India: *Earth and Planetary Science Letters*, v. 268, p. 293–311, doi:10.1016/j.epsl.2008.01.015.
- Keller, G., Khosla, S.C., Sharma, R., Khosla, A., Bajpai, S., and Adatte, T., 2009, Early Danian planktic foraminifera from Cretaceous-Tertiary intertrappean beds at Jhilmili, Chindwara District, Madhya Pradesh, India: *Journal of Foraminiferal Research*, v. 39, no. 1, p. 40–55, doi:10.2113/gsjfr.39.1.40.
- Keller, G., Bhowmick, P.K., Upadhyay, H., Dave, A., Reddy, A.N., Jaiprakash, B.C., and Adatte, T., 2011a, Deccan volcanism linked to the Cretaceous- Tertiary boundary (KTB) mass extinction: New evidence from ONGC wells in the Krishna-Godavari Basin, India: *Journal of the Geological Society of India*, v. 78, p. 399–428, doi:10.1007/s12594-011-0107-3.

- Keller, G., Adatte, T., Bhowmick, P., Upadhyay, H., Dave, A., Reddy, A., & Jaiprakash, B. 2012. Nature and timing of extinctions in Cretaceous-Tertiary planktic foraminifera preserved in Deccan intertrappean sediments of the Krishna–Godavari Basin, India. *Earth and Planetary Science Letters*, 341-344, 211–221. doi: 10.1016/j.epsl.2012.06.021
- Keller, G., Khozyem, H.M., Adatte, T., Malarkodi, N., Spangenberg, J.E., and Stinnesbeck, W., 2013, Chicxulub impact spherules in the North Atlantic and Caribbean: Age constraints and Cretaceous-Tertiary boundary hiatus: *Geological Magazine*, v. 150, no. 5, p. 885–907, doi:10.1017/S0016756812001069.
- Kennett, J. P., & Watkins, N. D. 1970. Geomagnetic Polarity Change, Volcanic Maxima and Faunal Extinction in the South Pacific. *Nature*, 227(5261), 930–934. doi: 10.1038/227930a0
- Knitter, H., 1979. Eine verbesserte Methode zur Gewinnung von Mikrofosilien aus harten, nicht schlammbaren Kalken. *Geol. Bl. Nor-Bayern*, 29, 182 – 186.
- Koçyiğit, A., 1991. An example of an accretionary forearc basin from Central Anatolia and its implications for the history of subduction of Neo-Tethys in Turkey. *Geological Society of American Bulletin*, 103, 22-36.
- Kominz, M. A., Browning, J. V., Miller, K. G., Sugarman, P. J., Mizintseva, S., & Scotese, C. R. 2008. Late Cretaceous to Miocene sea-level estimates from the New Jersey and Delaware coastal plain coreholes: An error analysis. *Basin Research*, 20(2), 211-226. doi:10.1111/j.1365-2117.2008.00354.x.
- Koutsoukos, E. A., 1996, Phenotypic experiments into new pelagic niches in early Danian planktonic foraminifera: Aftermath of the K/T boundary event. *Geological Society, London, Special Publications*, 102(1), 319-335. doi:10.1144/gsl.sp.1996.001.01.24.

- Koutsoukos, E. A. M., 2006. The Cretaceous-Paleogene Boundary at the Poty Section, NE Brazil: foraminiferal record and sequence of events-a review. *Anuário do Instituto de Geociências, UFRJ*, 29/1, 95-107.
- Li, L., and Keller, G., 1998a, Maastrichtian climate, productivity and faunal turnovers in planktic foraminifera of South Atlantic DSDP Sites 525A and 21: *Marine Micropaleontology*, v. 33, no. 1–2, p. 55–86, doi:10.1016/S0377-8398(97)00027-3.
- Lirer, F., 2000. A new technique for retrieving calcareous microfossils from lithified lime deposits. *Micropaleontology* 46, 365–369.
- Loeblich, A., R., Jr. and Tappan, H., 1988. Foraminiferal genera and their classification. Von Nostrand Reinhold Company, New York, 2v, 970 p.
- Luciani, V., 2002, High resolution planktonic foraminiferal analysis from the Cretaceous/Tertiary boundary at Ain Settara (Tunisia): Evidence of an extended mass extinction: *Palaeogeography, Palaeoclimatology, Palaeoecology*, v. 178, no. 3, p. 299–319, doi:10.1016/S0031-0182(01)00400-X.
- Luterbacher, H. P., Premoli-Silva, I., 1964. Biostratigrafia del limite cretaceo-terziario nell'Appennino centrale. *Rivista Italiana di Paleontologia*, 70, 67–117.
- MacArthur, R. H., & Wilson, E. O. (1967). *The Theory of Island Biogeography*. Princeton: Princeton University Press.
- MacLeod, N., and Keller, G., 1991a, Hiatus distributions and mass extinctions at the Cretaceous/Tertiary boundary: *Geology*, v. 19, p. 497–501, doi:10.1130/0091-7613(1991)019<0497:HDAMEA>2.3.CO;2.
- MacLeod, N., and Keller, G., 1994, Comparative biogeographic analysis of planktic foraminiferal survivorship across the Cretaceous/Tertiary (K/T) boundary: *Paleobiology*, v. 20, no. 2, p. 143–177.

- Malarkodi, N., Keller, G., Fayazudeen, P.J., and Mallikarjuna, U.B., 2010, Foraminifera from the early Danian intertrappean beds in Rajahmundry Quarries, Andhra Pradesh, SE India: *Journal of the Geological Society of India*, v. 75, p. 851–863, doi:10.1007/s12594-010-0066-0.
- Mateo, P., Keller, G., Adatte, T., Bitchong, A. M., Spangenberg, J. E., Vennemann, T., & Hollis, C. J., 2018, Deposition and age of Chicxulub impact spherules on Gorgonilla Island, Colombia. *GSA Bulletin*. doi: 10.1130/b35287.1
- Meriç, E., 1974. Sur la Presence du Genre Loftusia aux envirom de Göynük (Bolu, No de la Turguie). *İst. Üniv. Fen Fak. Seri B*, 39 (3-4), s.227-232.
- Meriç, E., Şengüler, İ., 1986. Göynük (Bolu, KB Anadolu) Çevresindeki Üst Kretase – Paleosen Stratigrafisi Üzerine Yeni Görüşler. *Jeoloji Mühendisliği Dergisi* 29, s.61-64.
- Molina, E., Arenillas, I., Arz, J. A., 1996, The Cretaceous/Tertiary boundary mass extinction in planktic foraminifera at Agost, Spain. *Revue de Micropaleontologie*, 39, p. 225– 243.
- Molina, E., Alegret, L., Arenillas, I., Arz, J., Gallala, N., Hardenbol, J., von Salis, K., Steurbaut, E., Vanhenberghe, N., and Zaghib-Turki, D., 2006, The global boundary stratotype section and point for the base of the Danian Stage (Paleocene, Paleogene, “Tertiary,” Cenozoic) at El Kef, Tunisia—Original definition and revision: *Episodes*, v. 29, no. 4, p. 263–273.
- Mount, J., 1985. Mixed siliciclastic and carbonate sediments: a proposed firstorder textural and compositional classification. *Sedimentology*, 32, 435- 442.
- Nederbragt, A., J., 1991. Late Cretaceous biostratigraphy and development of Heterohelicidae (planktic foraminifera). *Micropaleontology*, 37, 4, 329 –372.
- Nederbragt, A., J., 1998. Quantitative biogeography of late Maastrichtian planktic foraminifera. *Micropaleontology*, 44/4, 385 – 412.

- Nielsen, J. K., Jakobsen, S. L., 2004. Extraction of calcareous macrofossils from the Upper Cretaceous white chalk and other sedimentary carbonates in Denmark and Sweden: the acid-hot water method and the waterblasting technique. *Palaeontologia Electronica* 7/4, 1-11.
- Ocakoglu, F., Yilmaz, I.O., Demircan, H., Altner, O.S., Hakyemez, A., Islamoglu, Y., Tekin, U.K., Önoglu, N., Yıldız, A., Uchman, A., Szulc, A., Açıkalin, S., 2007, Orta Sakarya Bölgesi Geç Kretase-Paleojen Çökellerinin Sekans Stratigrafisi, The Scientific and Technological Research Council of Turkey (TUBITAK, Project no: 104Y153). Final Report, 450pp. (in Turkish).
- Ocakoglu, F., Yilmaz, I.O., Açıkalin, S., 2009. Orta Sakarya Bölgesi, Kretase-Tersiyer istifinin kaynak bölge ve paleoklimsel açılardan incelenmesi, ESOGÜ-Bilimsel Araştırma Projeleri, 200715024 no'lu proje Final Raporu. (in Turkish). Olsson, R.K., Hemleben, C., Berggren, W.A., and Huber, B.T., 1999, Atlas of Paleocene Planktonic Foraminifera: Smithsonian Contributions to Paleobiology 85: Washington, DC, Smithsonian Institution Press, 252 p.
- Ocakoglu, F., Hakyemez, A., Açıkalin, S., Altner, S. Ö., Büyükmeriç, Y., Licht, A., ... Campbell, C., 2018, Chronology of subduction and collision along the İzmir-Ankara suture in Western Anatolia: records from the Central Sakarya Basin. *International Geology Review*, 61(10), 1244–1269. doi: 10.1080/00206814.2018.1507009
- Obaidalla, N.A., 2000. Planktonic foraminiferal biostratigraphy and faunal turnover events during the Late Cretaceous-early Tertiary along the Red Sea coast, Egypt. *Journal of African Earth Sciences*, 31, 571-595.
- Okay, A.I., Tüysüz, O., 1999. Tethyan sutures of northern Turkey. *Geol. Soc. Lond. Spec. Publ.* 156, 475–515.

- Okay, A., Monod, O., Monie, P., 2002. Triassic blueschists and eclogites from northwest Turkey: vestiges of the Paleo-Tethyan subduction. *Lithos* 65, 155–178.
- Olsson, R., K., 1964. Late Cretaceous planktonic foraminifera from New Jersey and Delaware. *Micropaleontology*, 10/2, 157-188.
- Olsson, R. K., 1997. El Kef blind test III results. *Mar. Micropaleontol.*, 29, 80- 84.
- Olsson, R. K., Hemleben, C., Berggren, W. A., and Huber, B. T., 1999. Atlas of Paleocene planktonic foraminifera. *Smithsonian Contributions to Paleobiology*, 85, 252 p.
- Önal, M., Helvacı, C., İnci, U., Yağmurlu, F., Meriç, E., Tansel, İ., 1988. Çayırhan, Kuzeybatı Ankara Kuzeyindeki Soğukçam Kireçtaşı, Nardin Formasyonu, ve Kızılçay Grubunun stratigrafisi, yaşı, fasiyesi ve depolanma ortamları. *TPJD Bülteni*, C. 1/2, s. 152-163.
- Özcan, Z., Okay, A. I., Özcan, E., Hakyemez, A., Özkan-Altın, S., 2012, Late Cretaceous-Eocene Geological Evolution of the Pontides Based on New Stratigraphic and Palaeontologic Data Between the Black Sea Coast and Bursa (NW Turkey), *Turkish J. Earth Sci.*, 21, p. 933-960.
- Pardo, A., Ortiz, N., Keller, G., 1996. Latest Maastrichtian foraminiferal turnover and its environmental implications at Agost, Spain, in MacLeod, N., and Keller, G., eds., *Cretaceous-Tertiary mass extinction: New York*, W.W. Norton and Co., p. 139–172.
- Pardo, A., Adatte, T., Keller, G., Oberhänsli, H., 1999. Paleoenvironmental changes  $\epsilon$  across the Cretaceous-Tertiary boundary at Koshak, Kazakhstan, based on planktic foraminifera and clay mineralogy. *Palaeogeography, Palaeoclimatology, Palaeoecology* 154 (3), 247e273

- Pardo, A., and Keller, G., 2008, Biotic effects of environmental catastrophes at the end of the Cretaceous: *Guembelitria* and *Heterohelix* blooms: *Cretaceous Research*, v. 29, no. 5–6, p. 1058–1073, doi: 10.1016/j.cretres.2008.05.031.
- Parker W.C., Arnold A.J., 1999, Quantitative methods of data analysis in foraminiferal ecology. In: *Modern Foraminifera*. Springer, Dordrecht
- Perch-Nielsen, K., Mckenzie, J., & He, Q., 1982, Biostratigraphy and isotope stratigraphy and the ‘catastrophic’ extinction of calcareous nannoplankton at the Cretaceous/Tertiary boundary. *Geological Society of America Special Papers Geological Implications of Impacts of Large Asteroids and Comets on the Earth*, 353–372. doi: 10.1130/spe190-p353
- Pessagno, E., A., Jr., 1967. Upper Cretaceous planktonic foraminifera from the western Gulf Coastal Plain. *Paleontographica Americana*, 5, 245-445.
- Peypouquet, J., P., Grousset, F., Mourguiart, P., 1986. Paleooceanography of the Mesogean Sea based on ostracods of the northern Tunisian continental shelf between the Late Cretaceous and Early Paleogene. *Geologische Rundschau*, 75, 159-174.
- Postuma, J., A., 1971. *Manual of planktonic foraminifera*. Elsevier Publishing Company, 420 p.
- Preisinger, A., Aslanian, S., Brandstaetter, F., Grass, F., Stradner, H., & Summesberger, H. 2002. Cretaceous-Tertiary profile, rhythmic deposition, and geomagnetic polarity reversals of marine sediments near Bjala, Bulgaria. *Special Paper 356: Catastrophic Events and Mass Extinctions: Impacts and Beyond*, 213–229. doi: 10.1130/0-8137-2356-6.213
- Premoli-Silva, I., Verga, D., 2004. *Practical manual of Cretaceous Planktonic Foraminifera*. International School on Planktonic Foraminifera, 3. Course: Cretaceous. Verga & Rettori eds. Universities of Perugia and Milan, Tipografia Pontefelcino, Perugia (Italy), 283 p.

- Punekar, J., Keller, G., Khozyem, H.M., Hamming, C., Adatte, T., Tantawy, A.A., and Spangenberg, J., 2014, Late Maastrichtian–early Danian high-stress environments and delayed recovery linked to Deccan volcanism: *Cretaceous Research*, v. 49, p. 63–82.
- Punekar, J., Mateo, P., and Keller G., 2014, Effects of Deccan volcanism on paleoenvironment and planktic foraminifera: A global survey, In Keller, G., and Kerr, A.C., (eds.), *Volcanism, Impacts, and Mass Extinctions: Causes and Effects: Geological Society of America Special Paper 505*, p. 1–28, doi:10.1130/2014.2505(01).
- Raup, D. M., and Sepkoski, J. J., Jr., 1982, Mass extinctions in the marine fossil record: *Science*, v. 215, p. 1501–1503, doi: 10. 1126/science .215.4539.1501.
- Rinaldi, R., 2013, Introduction: EBSD at the 10th EMAS Regional Workshop on Electron Probe Microanalysis of Materials Today: Practical Aspects. *Microscopy and Microanalysis*, 19(4), 919–919. doi: 10.1017/s1431927613001967
- Robaszynski, F., 1998. Cretaceous planktonic foraminiferal biozonation in Exxon chart 2000.
- Robaszynski, F., Caron, M., Gonzalez Donoso, J. M., Wonders, A. H. & The European Working Group on Planktonic Foraminifera, 1984. Atlas of Late Cretaceous globotruncanids. *Revue de Micropaléontologie*, 26, 145–305.
- Robaszynski, F., Caron, M., 1995, Foraminifères planctoniques du Crétacé: commentaire de la zonation Europe-Méditerranée, 6, p. 681-692.
- Rondot, J., 1956. 1/100.000'lik 39/2 (güney kısmı) ve 39/4 nolu paftaların jeolojisi Seben-Nallıhan-Beypazarı ilçeleri. MTA Enstitüsü Raporu, Derleme No: 2517, 55 s.
- Rostami, M. A., Leckie, R. M., Font, E., Frontalini, F., Finkelstein, D., & Koeberl, C., 2018, The Cretaceous-Paleogene transition at Galanderud (northern Alborz,

Iran): A multidisciplinary approach. *Palaeogeography, Palaeoclimatology, Palaeoecology*, 493, 82-101. doi:10.1016/j.palaeo.2018.01.001

Sagular, E. K., & Görmüş, M. (2006). New stratigraphical results and significance of reworking based on nannofossil, foraminiferal and sedimentological records in the Lower Tertiary sequence from the northern Isparta Angle, Eastern Mediterranean. *Journal of Asian Earth Sciences*, 27(1), 78-98. doi:10.1016/j.jseaes.2005.02.002

Saner, S., 1977. Geyve-Osmaneli-Gölpazarı-Taraklı alanının jeolojisi: Eski çökeltme ortamı ve çökeltmenin evrimi. MTA Enstitüsü Raporu, Derleme No: 6306, 312 s.

Saner, S., 1980, Mudurnu-Göynük Havzasının Jura ve Sonrası Çökeltim Nitelikleriyle Paleocoğrafya Yorumlaması. *Bulletin of the Geological Society of Turkey*, 23, 39-52.

Schulte, P., Alegret, L., Arenillas, I., Arz, J.A., Barton, P.J., Bown, P.R., Bralower, T.J., Christeson, G.L., Claeys, P., Cockell, C.S., Collins, G.S., Deutsch, A., Goldin, T.J., Goto, K., Grajales-Nishimura, J.M., Grieve, R.A.F., Gulick, S.P.S., Johnson, K.R., Kiessling, W., Koeberl, C., Kring, D.A., MacLeod, K.G., Matsui, T., Melosh, J., Montanari, A., Morgan, J.V., Neal, C.R., Nichols, D.J., Norris, R.D., Pierazzo, E., Ravizza, G., Rebolledo-Vieyra, M., Reimold, W.U., Robin, E., Salge, T., Speijer, R.P., Sweet, A.R., Urrutia-Fucugauchi, J., Vajda, V., Whalen, M.T., and Willumsen, P.S., 2010, The Chicxulub asteroid impact and mass extinction at the Cretaceous-Paleogene boundary: *Science*, v. 327, p. 1214-1218, doi:10.1126/science.1177265.

Schulte, P., Speijer, R., Mai, H., Kontny, A., 2006. The Cretaceous-Paleogene (K/P) boundary at Brazos, Texas: sequence stratigraphy, depositional events and the Chicxulub impact. *Sediment. Geol.*, 184, 77-109.

- Self, S., Jay, A.E., Widdowson, M., Keszthelyi, L.P., 2008. Correlation of the Deccan and Rajahmundry Trap lavas: Are these the longest and largest lava flows on Earth? *Journal of Volcanology and Geothermal Research* 172, 3-19, doi:10.1016/j.jvolgeores.2006.11.012
- Schöbel, S., de Walla, H., Ganerødb, M., Panditc, M.K., Rolf, C., 2014. Magnetostratigraphy and  $^{40}\text{Ar}$ – $^{39}\text{Ar}$  geochronology of the Malwa Plateau region (Northern Deccan Traps), central western India: Significance and correlation with the main Deccan Large Igneous Province sequences. *Journal of Asian Earth Sciences* 89, 28-45.
- Sial, A., Chen, J., Lacerda, L., Frei, R., Tewari, V., Pandit, M., . . . Pereira, N. (2017). Reply to comments by Sanjay K. Mukhopadhyay, Sucharita Pal, J. P. Shrivastava on the paper by Sial et al. (2016) Mercury enrichments and Hg isotopes in Cretaceous–Paleogene boundary successions: Links to volcanism and palaeoenvironmental impacts. *Cretaceous Research* 66, 60–81. *Cretaceous Research*, 76, 84-88. doi:10.1016/j.cretres.2017.03.004
- Sial, A.N., Lacerda, L.D., Ferreira, V.P., Frei, R., Marquillas, R.A., Barbosa, J.A., Gaucher, C., Windmöller, C.C., and Pereira, N.S., 2013, Mercury as a proxy for volcanic activity during extreme environmental turnover: The Cretaceous–Paleogene transition: *Palaeogeography, Palaeoclimatology, Palaeoecology*, v. 387, p. 153–164.
- Silva, I. P., & Sliter, W. V., 1999, Cretaceous paleoceanography: Evidence from planktonic foraminiferal evolution. *Special Paper 332: Evolution of the Cretaceous Ocean-Climate System*, 301-328. doi:10.1130/0-8137-2332-9.301
- Schoene, B., Samperton, K.M., Eddy, M.P., Keller, G., Adatte, T., Bowring, S.A., Khadri, S.F.R., Gertsch, B., 2015. U–Pb geochronology of the Deccan Traps and relation to the end-Cretaceous mass extinction. *Science* 347, 182–184.

- Schulte, P., & Kontny, A. (2005). Chicxulub impact ejecta from the Cretaceous-Paleogene (K-P) boundary in northeastern México. Special Paper 384: Large Meteorite Impacts III, 191-221. doi:10.1130/0-8137-2384-1.191
- Schulte, P., Deutsch, A., Salge, T., Berndt, J., Kontny, A., Macleod, K., . . . Krumm, S. (2009). A dual-layer Chicxulub ejecta sequence with shocked carbonates from the Cretaceous-Paleogene (K-Pg) boundary, Demerara Rise, western Atlantic. *Geochimica Et Cosmochimica Acta*, 73(4), 1180-1204. doi:10.1016/j.gca.2008.11.011
- Sial, A., Chen, J., Lacerda, L., Frei, R., Tewari, V., Pandit, M. Pereira, N. 2016. Mercury enrichment and Hg isotopes in Cretaceous-Paleogene boundary successions: Links to volcanism and palaeoenvironmental impacts. *Cretaceous Research*, 66, 60-81. doi: 10.1016/j.cretres.2016.05.006
- Smit, J., 1982, Extinction and evolution of planktonic foraminifera after a major impact at the Cretaceous/Tertiary boundary, in Silver, L.T., and Schultz, P.H., eds., *Geological Implications of Impacts of Large Asteroids and Comets on the Earth: Geological Society of America Special Paper 190*, p. 329-352.
- Stchepinsky, V., 1940a. Göynük-Mudurlu-Nallıhan mıntıkası cevher zenginlikleri hakkında rapor. MTA Enstitüsü Raporu,Derleme No: 1058, 10 s.
- Stchepinsky, V., 1940b. Göynük-Mudurlu-Nallıhan mıntıkasının umumi jeolojisi hakkında rapor. MTA Enstitüsü Raporu,Derleme No: 975, 16 s.
- Şeker, H. ve Kesgin, Y., 1991. Nallıhan-Mudurnu-Seben-Bey pazarı arasında kalan bölgenin jeolojisi ve petrol olanakları. TPAO Arama Grubu Bşk.Rapor No: 2907, 42 s.
- Şengör, A. M. C., Yılmaz, Y., 1981, Tethyan evolution of Turkey: a plate tectonic approach, *Tectonophysics*, 75, p. 181-241.

- Tantawy, A.A.A., 2003, Calcareous nannofossil biostratigraphy and paleoecology of the Cretaceous–Tertiary transition in the central eastern desert of Egypt: *Marine Micropaleontology*, v. 47, no. 3, p. 323–356.
- Tobin, T.S., Ward, P.D., Steig, E.J., Olivero, E.B., Hilburn, I.A., Mitchell, R.N., Diamond, M.R., Raub, T.D., and Kirschvink, J.L., 2012, Extinction patterns,  $\delta^{18}\text{O}$  trends, and magnetostratigraphy from a southern high-latitude Cretaceous-Paleogene section: Links with Deccan volcanism: *Palaeogeography, Palaeoclimatology, Palaeoecology*, v. 350–352, p. 180–188, doi:10.1016/j.palaeo.2012.06.029.
- Türkünal, S., 1963. Nallıhan-Mudurnu ve Seben arasında kalan bölgenin jeolojisi. *TJK Bülteni*, C. 8, Sayı 1-2, s. 55-69.
- Twitchett, R.J., 2006. The palaeoclimatology, palaeoecology and palaeoenvironmental analysis of mass extinction events. *Palaeogeography, Palaeoclimatology, Palaeoecology*, 232 (2-4) : 190 - 213. doi: 10.1016/j.palaeo.2005.05.019
- Ürgün, S., 1956, Gölpazarı – Geyve – Taraklı – Gölpazarı civarının jeolojisi, MTA Raporu, No. 2711.
- Vardar, E., 2018, Deep Sea Benthic Foraminiferal Diversity and Abundance Changes Across Cretaceous-Paleogene Boundary Beds In The Haymana Basin (Ankara, Turkey): Paleoenvironmental Implications: MSc. Thesis, Middle East Technical University.
- Vellekoop, J., Sluijs A., Smit J., Schouten S., Weijers J. W. H., Sinninghe Damsté J. S., and Brinkhuis H., 2014, Rapid short-term cooling following the Chicxulub impact at the Cretaceous-Paleogene boundary, *Proc. Natl. Acad. Sci. U.S.A.*, 111(21), p. 7537-7541, doi:10.1073/pnas.1319253111.
- Vellekoop, J., Smit J., van de Schootbrugge B., Weijers J. W. H., Galeotti S., Sinninghe Damsté J. S., and Brinkhuis H., 2015, Palynological evidence for prolonged cooling along the Tunisian continental shelf following the K–Pg

- boundary impact, *Paleogeography Paleoclimatology Paleoecology*, 426, p. 216-228.
- Verga, D., Premoli-Silva, I., 2003. Early Cretaceous planktonic foraminifera from the Tethys: the small, few-chambered representatives of the genus *Globigerinelloides*. *Cretaceous Research*, 24, 305–334.
- Vogt, P. R. 1972. Evidence for Global Synchronism in Mantle Plume Convection, and Possible Significance for Geology. *Nature*, 240(5380), 338–342. doi: 10.1038/240338a0
- Ward, W. C., Keller, G., Stinnesbeck, W., & Adatte, T. (1995). Yucatán subsurface stratigraphy: Implications and constraints for the Chicxulub impact. *Geology*, 23(10), 873. doi:10.1130/0091-7613(1995)0232.3.co;2
- Wignall, P. 2001. Large igneous provinces and mass extinctions. *Earth-Science Reviews*, 53(1-2), 1–33. doi: 10.1016/s0012-8252(00)00037-4
- Yıldız, A., & Gürel, A. (2005). Palaeontological, diagenetic and facies characteristics of Cretaceous/Paleogene boundary sediments in the Ordu, Yavuzlu and Uzunisa areas, Eastern Pontides, NE Turkey. *Cretaceous Research*, 26(2), 329-341. doi:10.1016/j.cretres.2005.01.003
- Zaid, S. M. (2015). Integrated petrographic, mineralogical, and geochemical study of the Late Cretaceous–Early Tertiary Dakhla Shales, Quseir–Nile Valley Province, central Egypt: Implications for source area weathering, provenance, and tectonic setting. *Arabian Journal of Geosciences*, 8(11), 9237-9259. doi:10.1007/s12517-015-1875-7
- Zaghib-Turki, D., s Karoui-Yaakoub, N., Rocchia, R., Robin, E., & Belayouni, H. (2000). Enregistrement des événements remarquables de la limite Crétacé–Tertiaire dans la coupe d'Ellès (Tunisie). *Earth and Planetary Science*, 331, 141–149.



## APPENDICES

### A. PLATES

#### PLATE 1

**Figure 1:** *Chiloguembelina midwayensis* (Cushman, 1940), longitudinal view, a) Gk-36, b) Gk-34, c) Gk-20, Early Danian, Seben Formation

**Figure 2:** *Chiloguembelina morsei* (Kline, 1943), longitudinal view, a) Gk-42, b) Gk-38, Early Danian, Seben Formation

**Figure 3:** *Chiloguembelina morsei* (Kline, 1943), longitudinal view, Gk-21, Early Danian, Seben Formation

**Figure 4:** *Chiloguembelina morsei* (Kline, 1943), longitudinal view, a) Gk-28, b) Gk-29, Early Danian, Seben Formation

**Figure 5:** *Chiloguembelina morsei* (Kline, 1943), longitudinal view, Gk-33, Early Danian, Seben Formation

PLATE 1

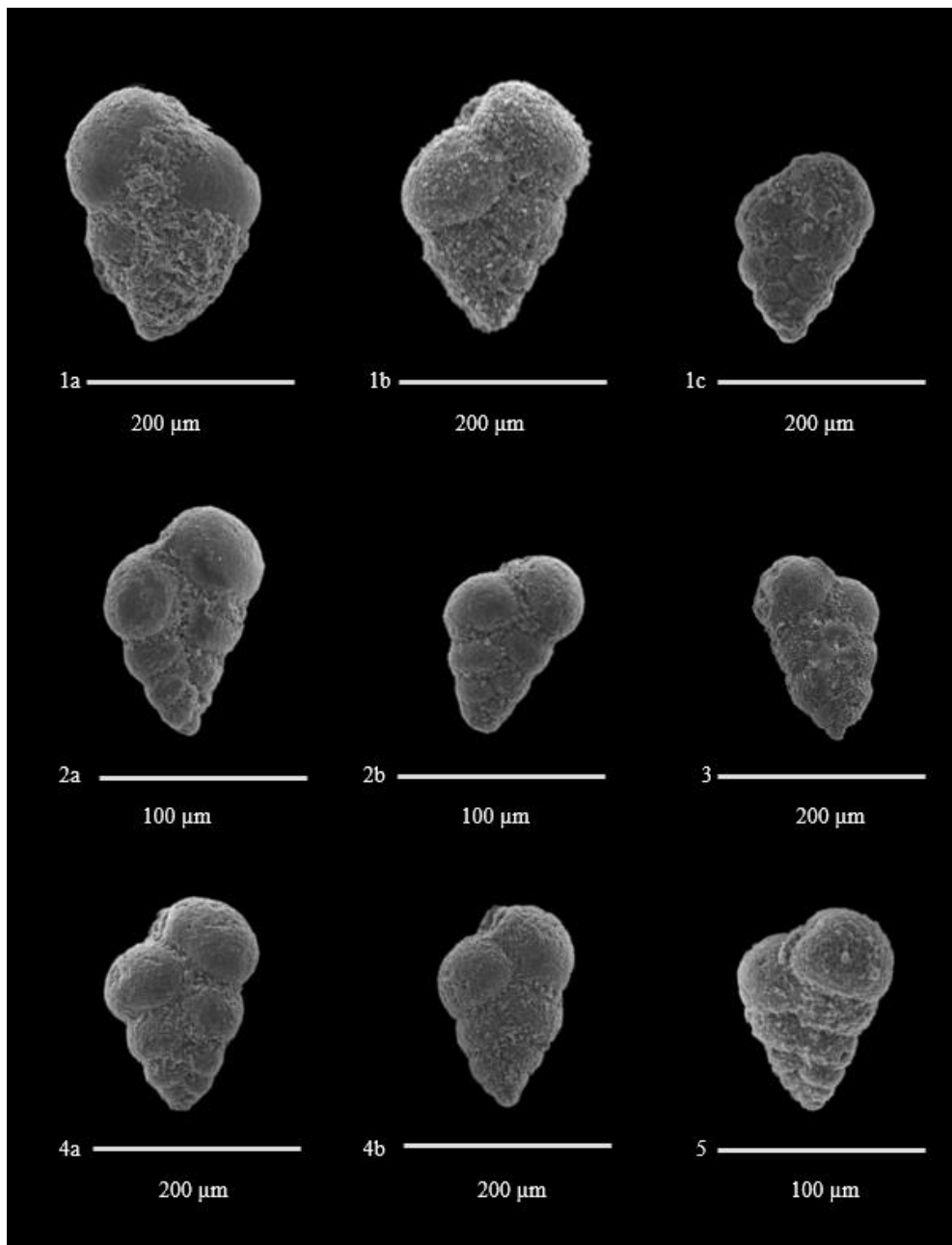


## PLATE 2

**Figure 1:** *Chiloguembelina subtriangularis* (Beckmann, 1957), longitudinal view, Gk-42, Early Danian, Seben Formation

**Figure 2:** *Chiloguembelina subtriangularis* (Beckmann, 1957), longitudinal view, Gk-42, Early Danian, Seben Formation

**Figure 3:** *Chiloguembelina subtriangularis* (Beckmann, 1957), longitudinal view, Gk-40, Early Danian, Seben Formation

**Figure 4:** *Eoglobigerina edita* (Subbotina, 1953), spiral view, Gk-41, Early Danian, Seben Formation

**Figure 5:** *Eoglobigerina edita* (Subbotina, 1953), umbilical view, Gk-34, Early Danian, Seben Formation

**Figure 6:** *Eoglobigerina eobulloides* (Morozova, 1959), spiral view, Gk-27, Early Danian, Seben Formation

**Figure 7:** *Eoglobigerina eobulloides* (Morozova, 1959), umbilical view, Gk-26, Early Danian, Seben Formation

**Figure 8:** *Eoglobigerina eobulloides* (Morozova, 1959), umbilical view, Gk-26, Early Danian, Seben Formation

**Figure 9:** *Eoglobigerina spiralis* (Bolli, 1957), spiral view, Gk-40, Early Danian, Seben Formation

PLATE 2

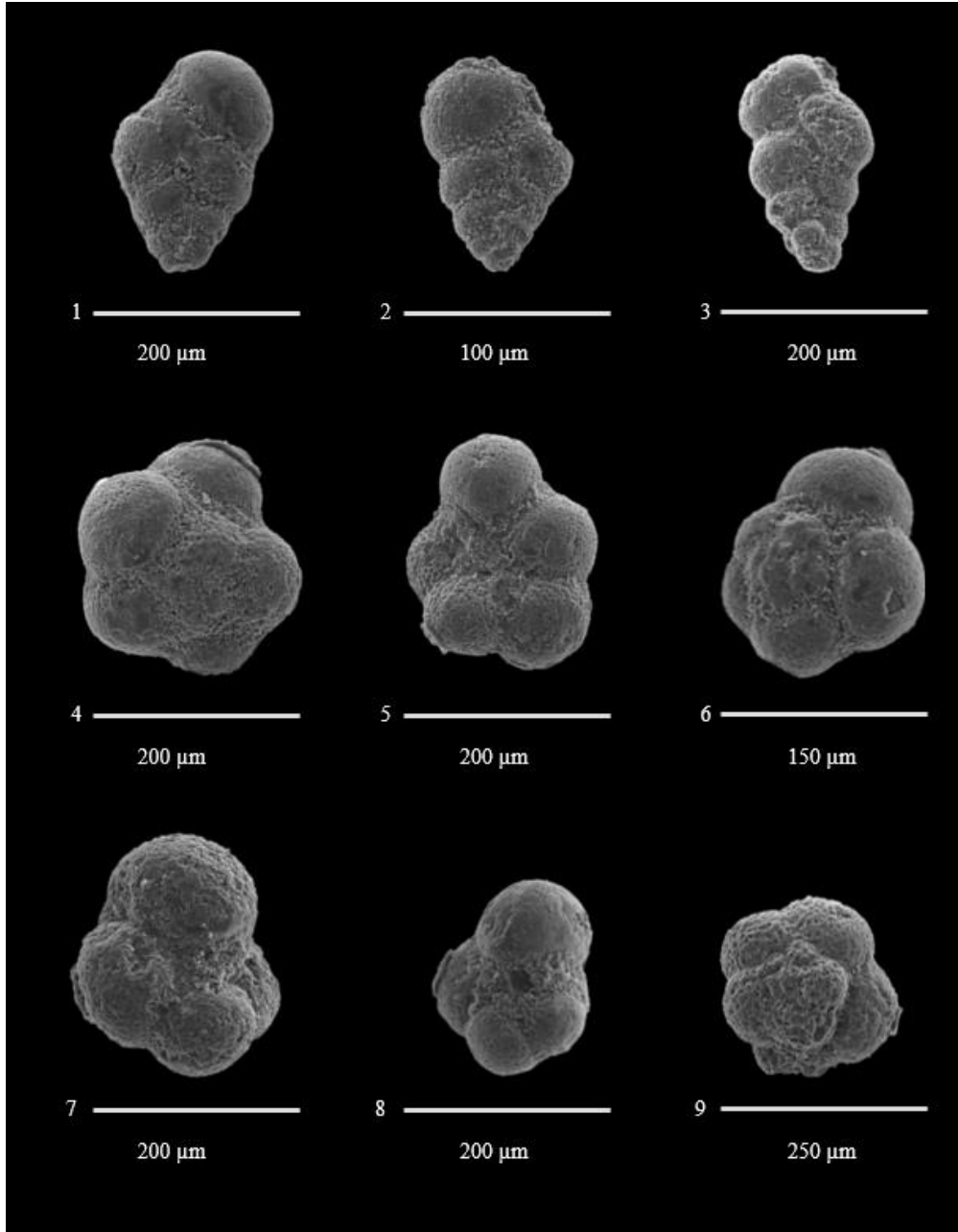


### PLATE 3

**Figure 1:** *Globigerina fringa* (Subbotina, 1950), spiral view, Gk-22, Early Danian, Seben Formation

**Figure 2:** *Globigerina fringa* (Subbotina, 1950), umbilical view, Gk-24, Early Danian, Seben Formation

**Figure 3:** *Globigerina pentagona* (Morozova, 1961), umbilical view, Gk-22, Early Danian, Seben Formation

**Figure 4:** *Globigerina pentagona* (Morozova, 1961), umbilical view, Gk-22, Early Danian, Seben Formation

**Figure 5:** *Globigerina tetragona* (Morozova, 1961), umbilical view, Gk-19, Early Danian, Seben Formation

**Figure 6:** *Globigerina tetragona* (Morozova, 1961), umbilical view, Gk-22, Early Danian, Seben Formation

**Figure 7:** *Globigerina tetragona* (Morozova, 1961), umbilical view, Gk-22, Early Danian, Seben Formation

**Figure 8:** *Globigerina trifolia* (Morozova, 1961), spiral view, Gk-22, Early Danian, Seben Formation

PLATE 3

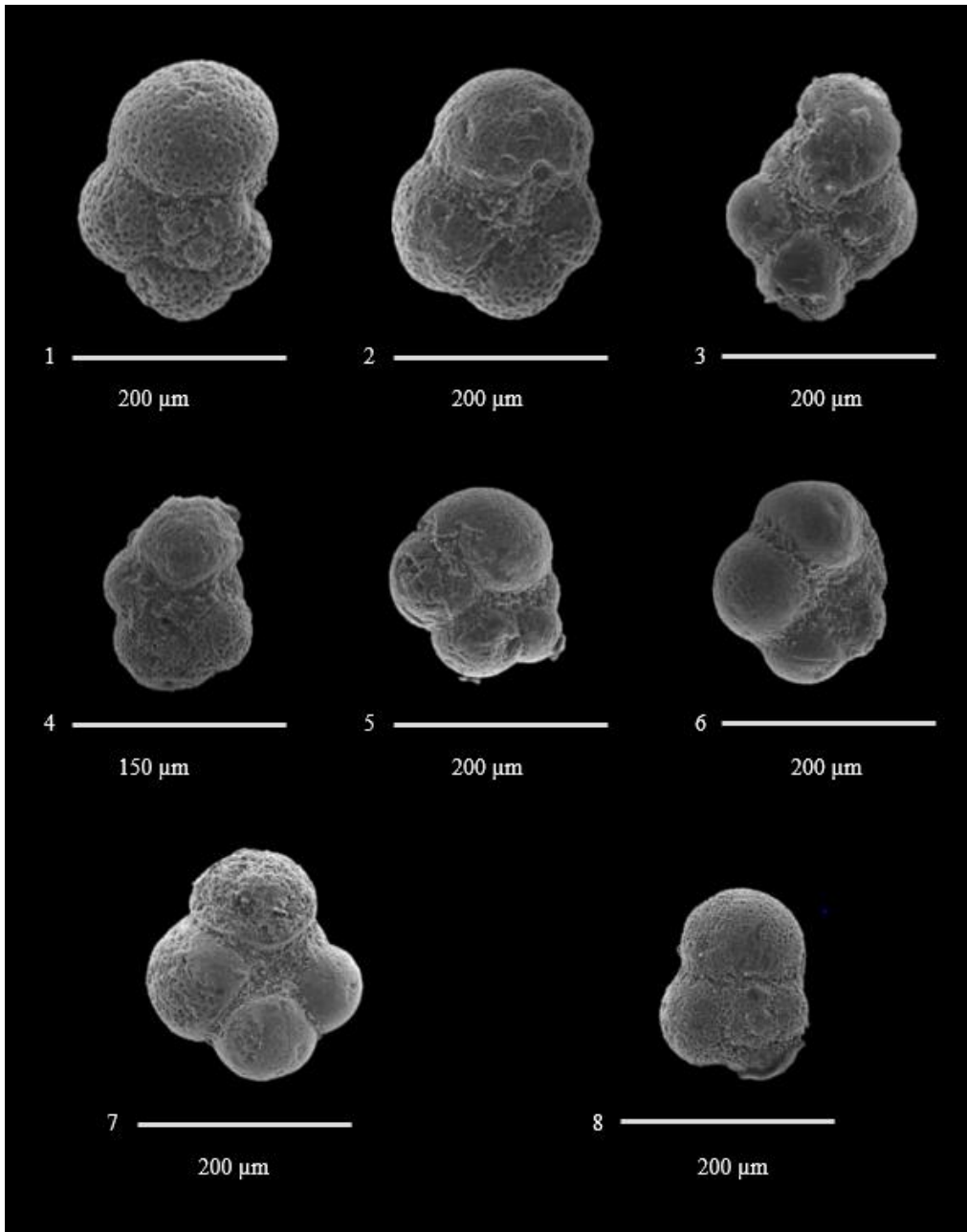


## PLATE 4

**Figure 1:** *Parasubbotina pseudobulloides* (Plummer, 1926), spiral view, Gk-23 , Early Danian, Seben Formation

**Figure 2:** *Parasubbotina pseudobulloides* (Plummer, 1926), umbilical view, a) Gk-42 , b) Gk-42 , c) Gk-40 , Early Danian, Seben Formation

**Figure 3:** *Parasubbotina pseudobulloides* (Plummer, 1926), spiral view, a) Gk- 33, b) Gk-32 , Early Danian, Seben Formation

**Figure 4:** *Parasubbotina pseudobulloides* (Plummer, 1926), umbilical view, Gk- 26, Early Danian, Seben Formation

**Figure 5:** *Parasubbotina pseudobulloides* (Plummer, 1926), umbilical view, Gk- 34, Early Danian, Seben Formation

PLATE 4

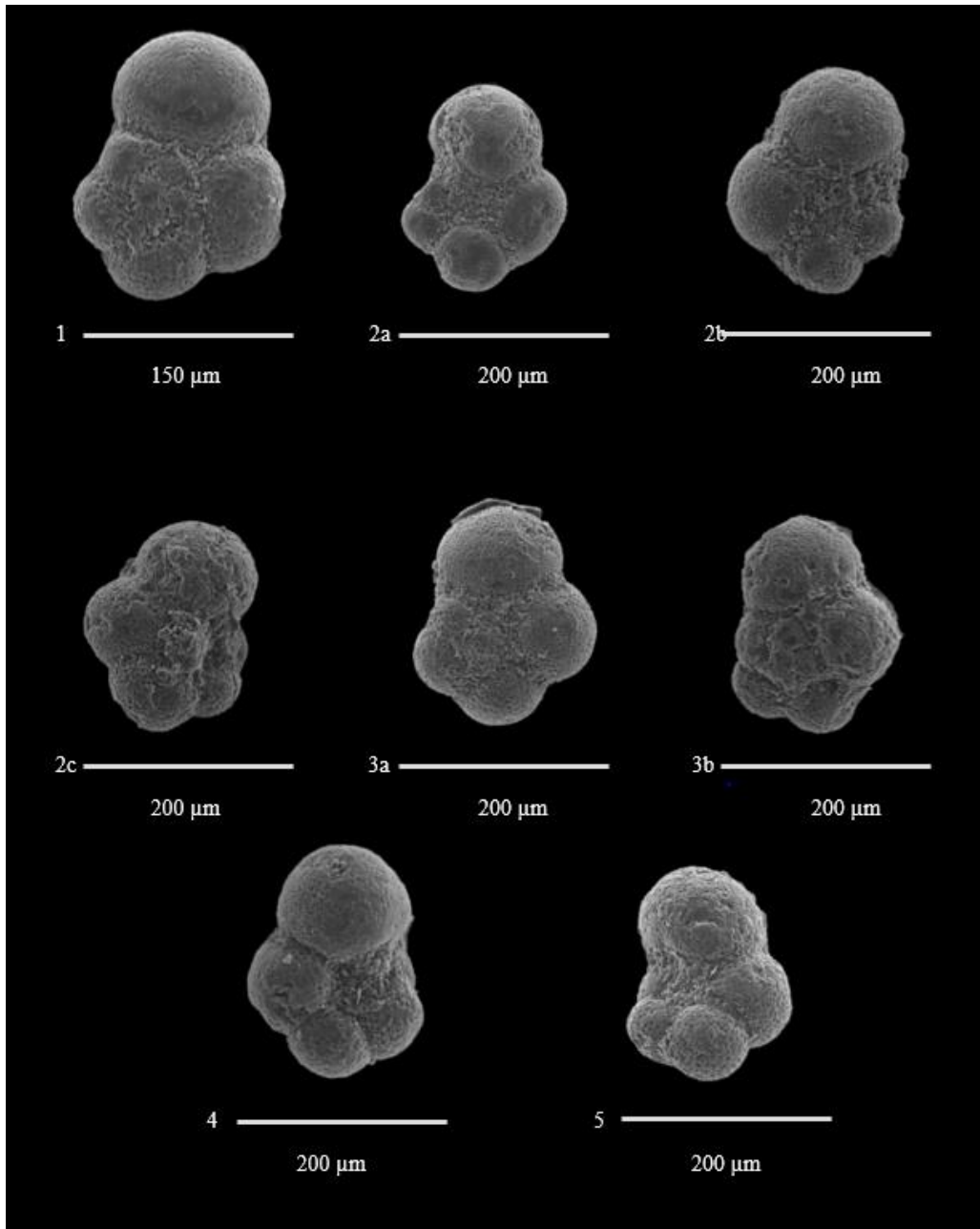


## PLATE 5

**Figure 1:** *Parasubbotina varianta* (Subbotina, 1953), umbilical view, Gk-42 , Early Danian, Seben Formation

**Figure 2:** *Parasubbotina varianta* (Subbotina, 1953), umbilical view, Gk-40, Early Danian, Seben Formation

**Figure 3:** *Parasubbotina varianta* (Subbotina, 1953), spiral view, Gk-40, Early Danian, Seben Formation

**Figure 4:** *Parasubbotina varianta* (Subbotina, 1953), a) spiral view, Gk-41 , b) umbilical view, Gk-41, Early Danian, Seben Formation

**Figure 5:** *Parasubbotina varianta* (Subbotina, 1953), umbilical view, Gk- 42, Early Danian, Seben Formation

**Figure 6:** *Subbotina cancellata* (Blow, 1979), a) spiral view, Gk-42, b) umbilical view, Gk-40 , Early Danian, Seben Formation

PLATE 5

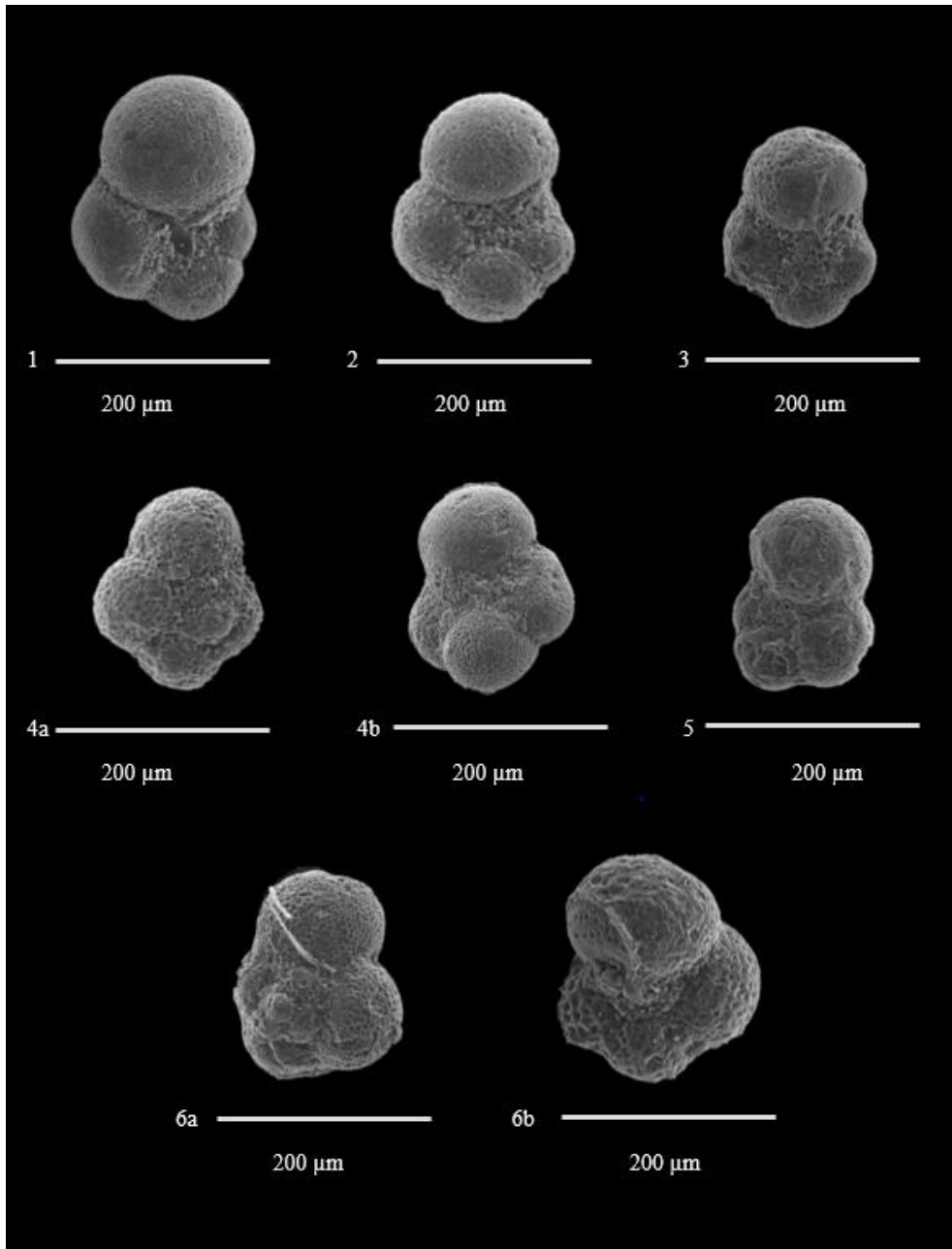


## PLATE 6

**Figure 1:** *Subbotina triloculinoides* (Plummer, 1926), a) spiral view, Gk-42 , b) umbilical view, Gk-36, c) spiral view, Gk-32, Early Danian, Seben Formation

**Figure 2:** *Subbotina triloculinoides* (Plummer, 1926), umbilical view, a) Gk-28, b) Gk-30, Early Danian, Seben Formation

**Figure 3:** *Subbotina triloculinoides* (Plummer, 1926), spiral view, Gk-33, Early Danian, Seben Formation

**Figure 4:** *Subbotina trivialis* (Subbotina, 1953), spiral view, Gk-31 Early Danian, Seben Formation

**Figure 5:** *Subbotina trivialis* (Subbotina, 1953), spiral view, Gk-38 Early Danian, Seben Formation

**Figure 6:** *Subbotina trivialis* (Subbotina, 1953), spiral view, Gk-41 Early Danian, Seben Formation

PLATE 6

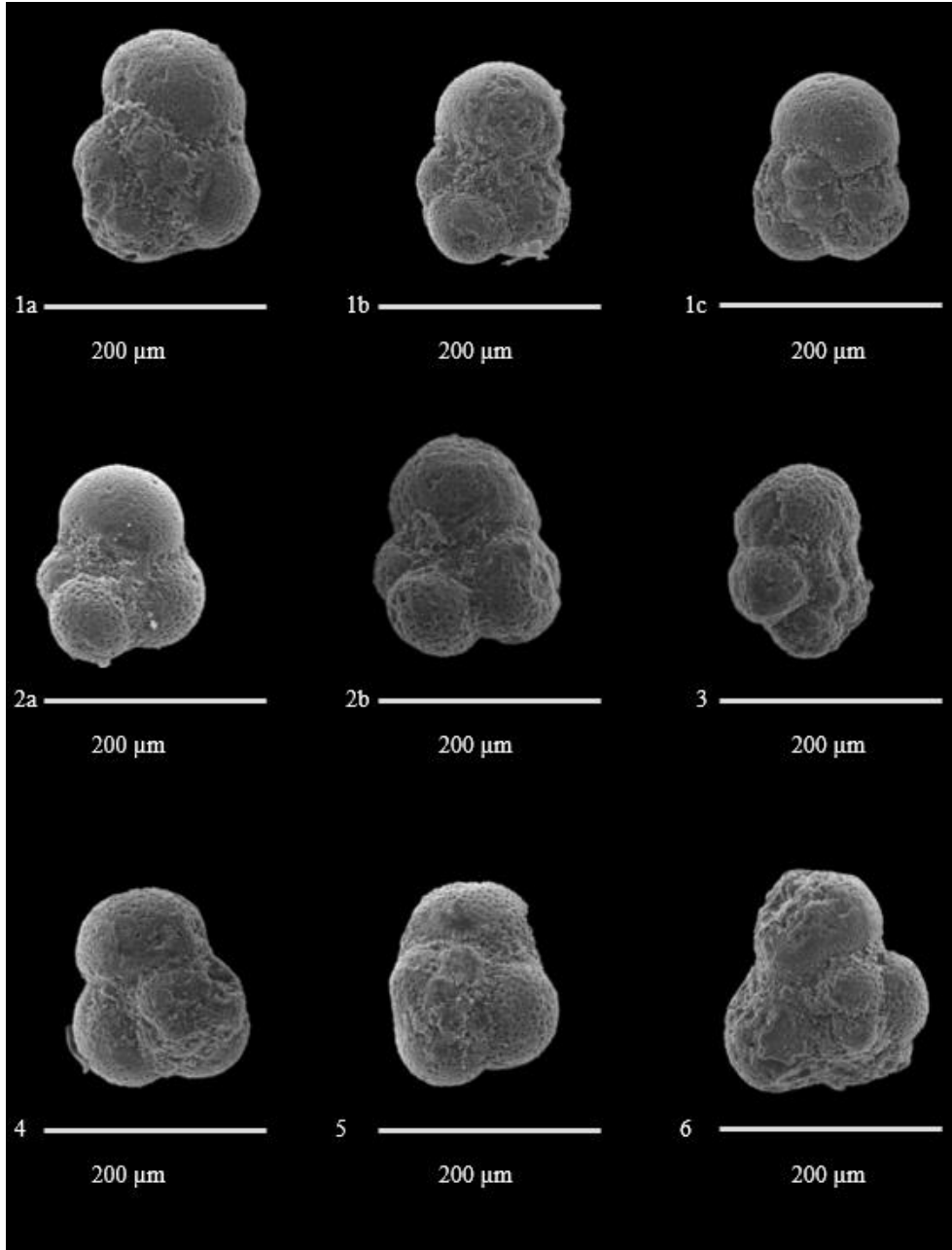


## PLATE 7

**Figure 1:** *Globanomalina archeocompressa* (Blow, 1979), spiral view, Gk-29, Early Danian, Seben Formation

**Figure 2:** *Globanomalina compressa* (Plummer, 1927), spiral view, Gk-41, Early Danian, Seben Formation

**Figure 3:** *Globanomalina imitata* (Subbotina, 1953), umbilical view, Gk-41, Early Danian, Seben Formation

**Figure 4:** *Globanomalina imitata* (Subbotina, 1953), a) umbilical view, Gk-40, b) umbilical view, Gk-40, c) spiral view, Gk-42, Early Danian, Seben Formation

**Figure 5:** *Globanomalina imitata* (Subbotina, 1953), a) umbilical view, Gk-41, b) spiral view, Gk-41, Early Danian, Seben Formation

**Figure 6:** *Globanomalina planocompressa* (Shutskaya, 1965), umbilical view, Gk-38, Early Danian, Seben Formation

PLATE 7

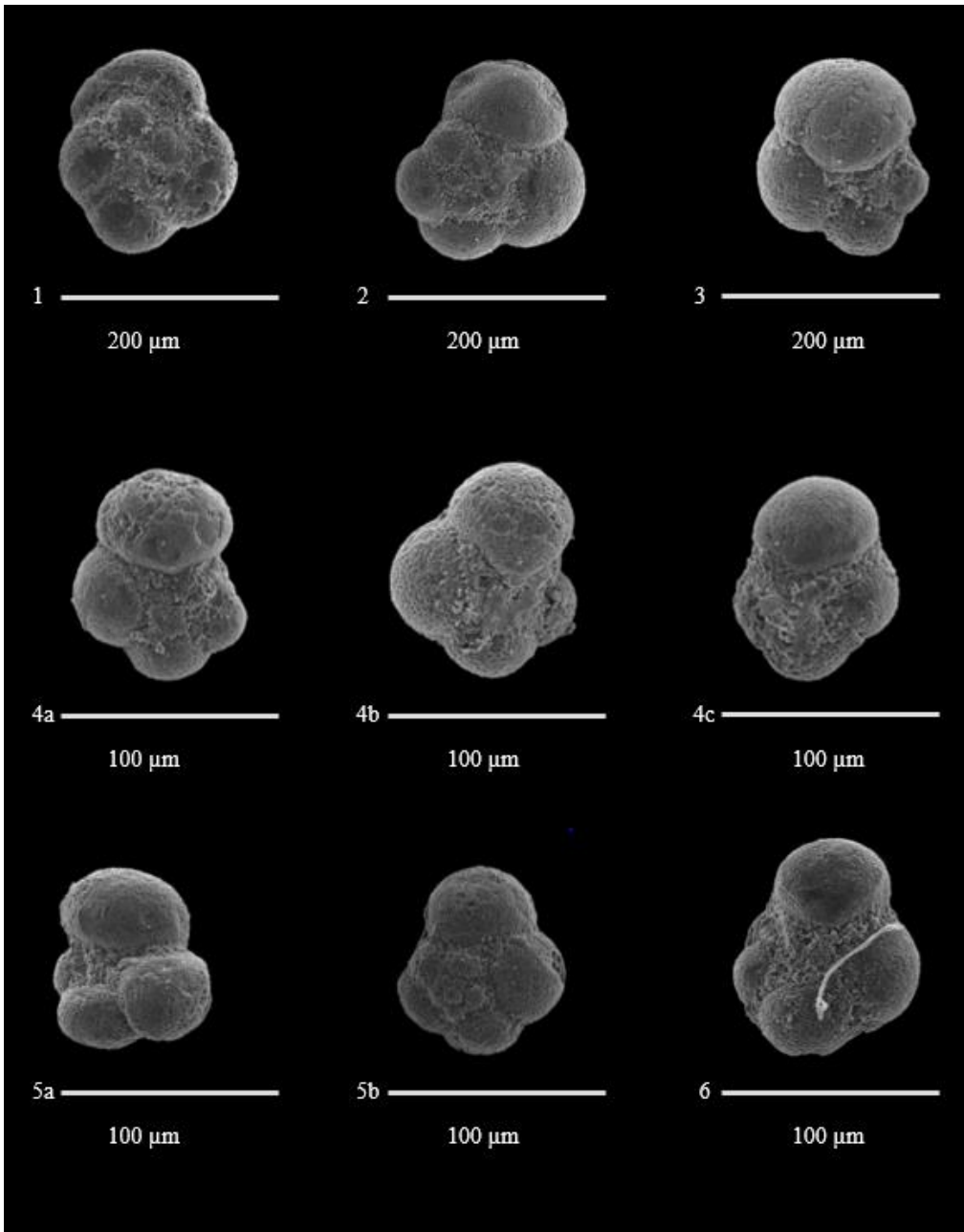


## PLATE 8

**Figure 1:** *Globanomalina planocompressa* (Shutskaya, 1965), umbilical view, Gk-36, Early Danian, Seben Formation

**Figure 2:** *Globoconusa daubjergensis* (Brönnimann, 1953), umbilical view, a) Gk-35, b) Gk-35, Early Danian, Seben Formation

**Figure 3:** *Guembelitria cretacea* (Cushman, 1933), longitudinal view, Gk-9, Early Danian, Seben Formation

**Figure 4:** *Guembelitria cretacea* (Cushman, 1933), longitudinal view, a) Gk-10, b) Gk-10, Early Danian, Seben Formation

**Figure 5:** *Guembelitria cretacea* (Cushman, 1933), longitudinal view, Gk-27, Early Danian, Seben Formation

**Figure 6:** *Parvularugoglobigerina alabamensis* (Liu and Olsson, 1992), spiral view, Gk-31, Early Danian, Seben Formation

PLATE 8

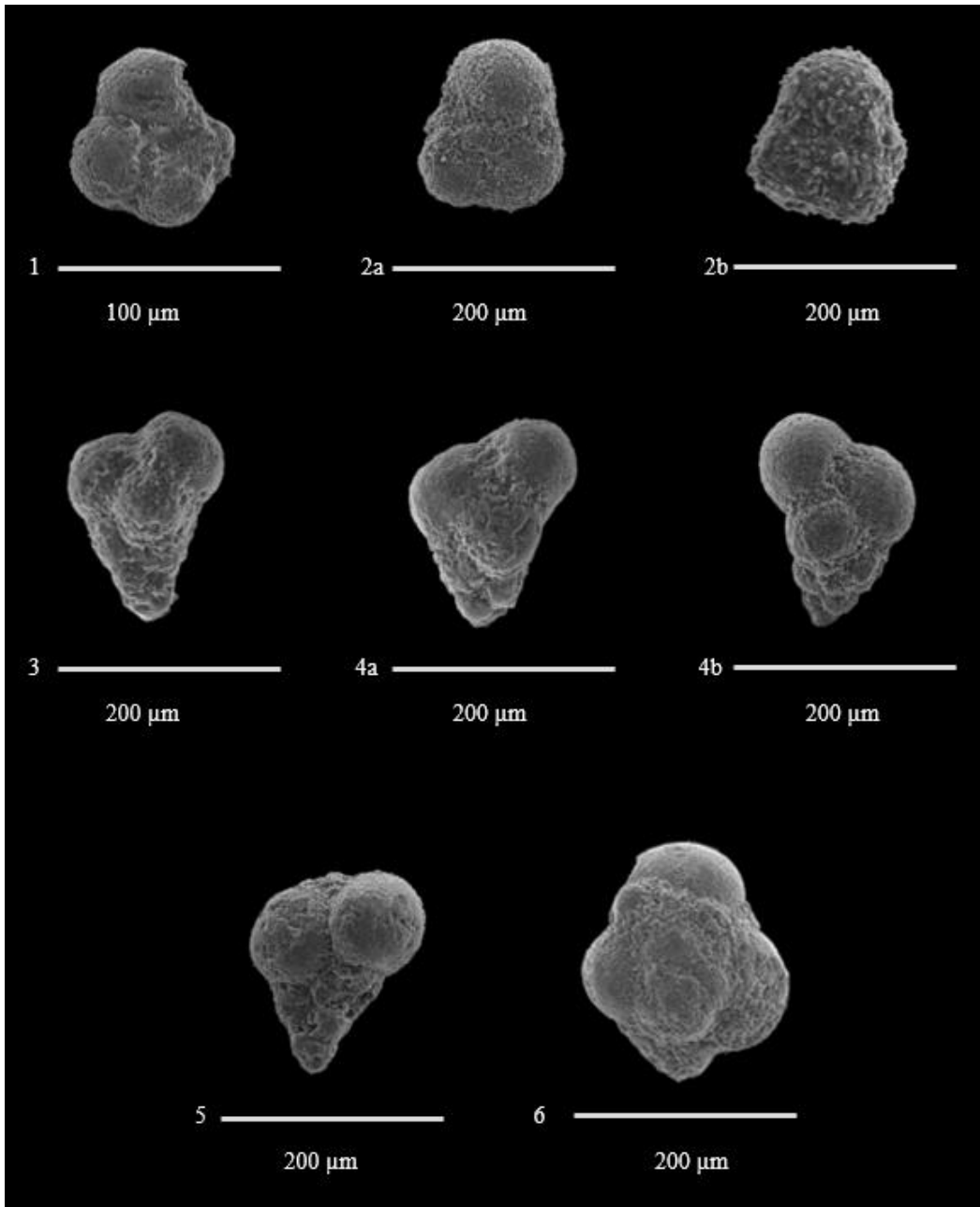


## PLATE 9

**Figure 1:** *Parvularugoglobigerina eugubina* (Luterbacher and Premoli-Silva, 1964), umbilical view, Gk-11, Early Danian, Seben Formation

**Figure 2:** *Parvularugoglobigerina eugubina* (Luterbacher and Premoli-Silva, 1964), umbilical view, Gk-13, Early Danian, Seben Formation

**Figure 3:** *Parvularugoglobigerina eugubina* (Luterbacher and Premoli-Silva, 1964), umbilical view, Gk-15, Early Danian, Seben Formation

**Figure 4:** *Parvularugoglobigerina eugubina* (Luterbacher and Premoli-Silva, 1964), umbilical view, Gk-21, Early Danian, Seben Formation

**Figure 5:** *Parvularugoglobigerina extensa* (Blow, 1979), umbilical view, a) Gk-13, b) Gk-23, Early Danian, Seben Formation

**Figure 6:** *Zeauvigerina virgata* (Khalilov, 1967), longitudinal view, a) Gk-36, b) Gk-33, Early Danian, Seben Formation

**Figure 7:** *Zeauvigerina virgata* (Khalilov, 1967), longitudinal view, a) Gk-30, b) Gk-30, Early Danian, Seben Formation

PLATE 9

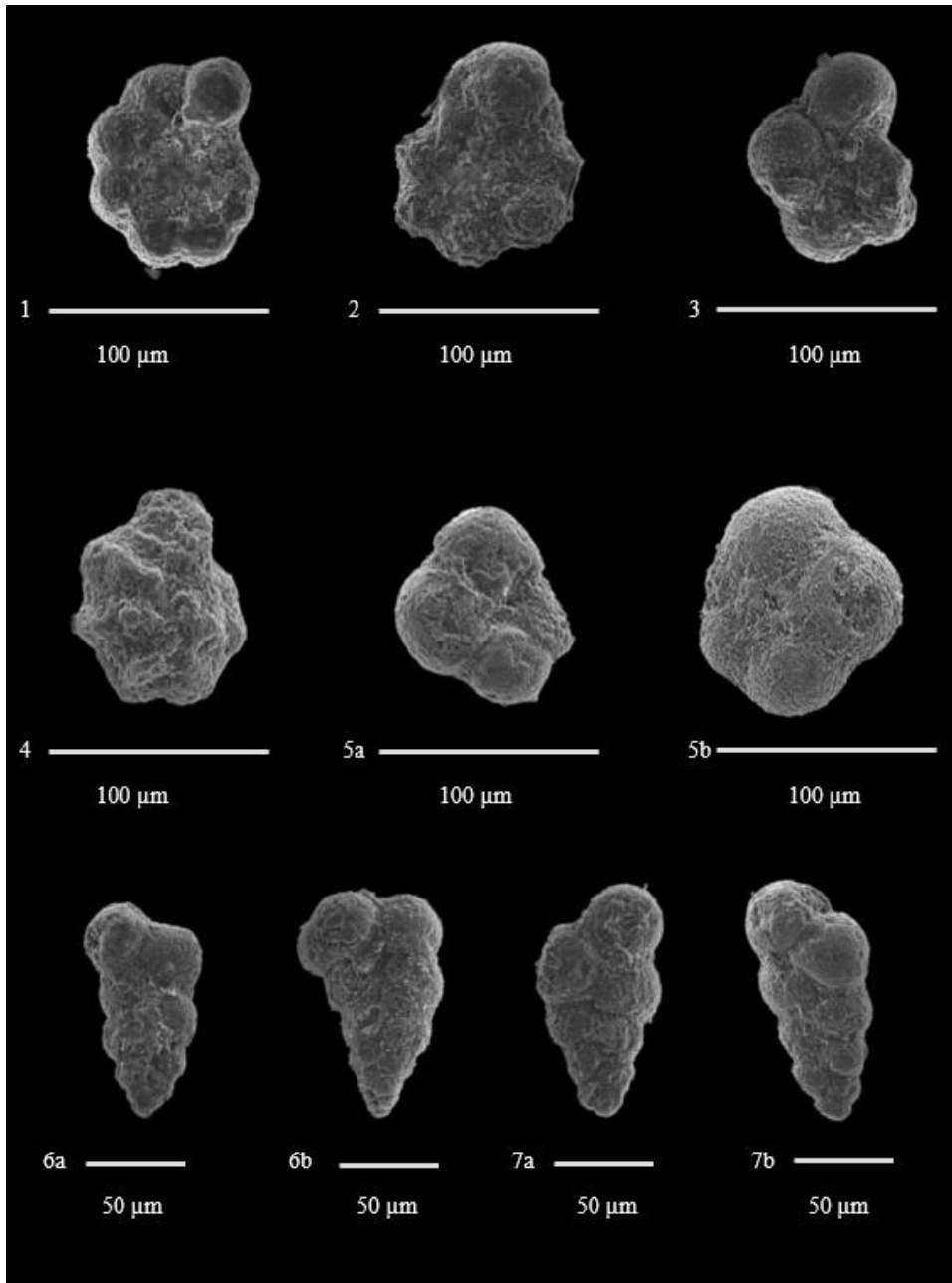


## PLATE 10

**Figure 1:** *Zeauvigerina waiparaensis* (Jenkins, 1966), longitudinal view, a) Gk-42, b) Gk-42, c) Gk-40, Early Danian, Seben Formation

**Figure 2:** *Praemurica inconstans* (Subbotina, 1953), umbilical view, Gk-42, Early Danian, Seben Formation

**Figure 3:** *Praemurica pseudoinconstans* (Blow, 1979), spiral view, Gk-38, Early Danian, Seben Formation

**Figure 4:** *Praemurica taurica* (Morozova, 1961), umbilical view, a) Gk-28, b) Gk-28, Early Danian, Seben Formation

PLATE 10

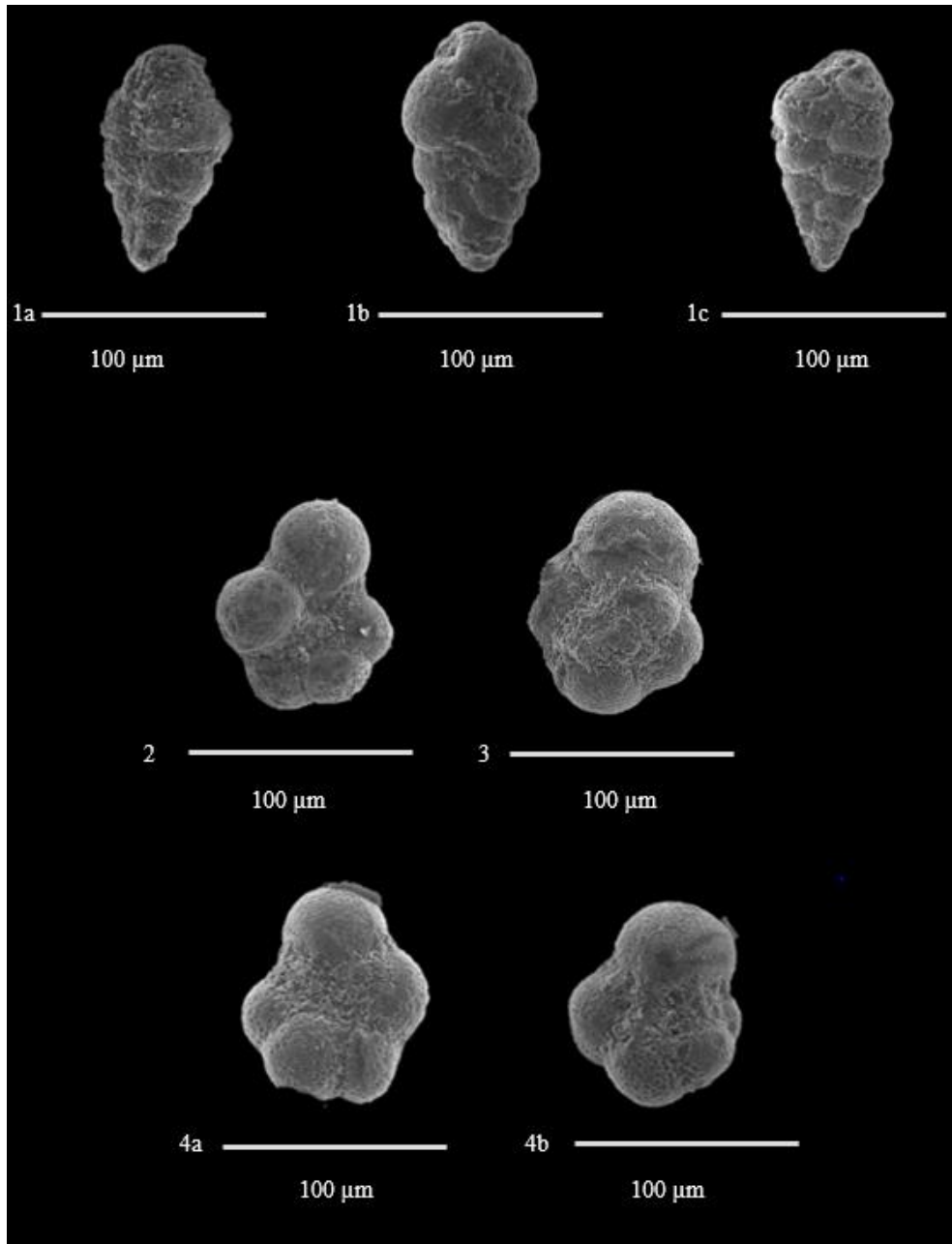


## PLATE 11

**Figure 1:** *Woodringina claytonensis* (Loeblich and Tappan, 1957), longitudinal view, a) Gk-35, b) Gk-35, c) Gk-35, Early Danian, Seben Formation

**Figure 2:** *Woodringina claytonensis* (Loeblich and Tappan, 1957), longitudinal view, a) Gk-31, b) Gk-30, Early Danian, Seben Formation

**Figure 3:** *Woodringina hornerstownensis* (Olsson, 1960), longitudinal view, a) Gk-42, b) Gk-40, c) Gk-40, d) Gk-38, Early Danian, Seben Formation

PLATE 11

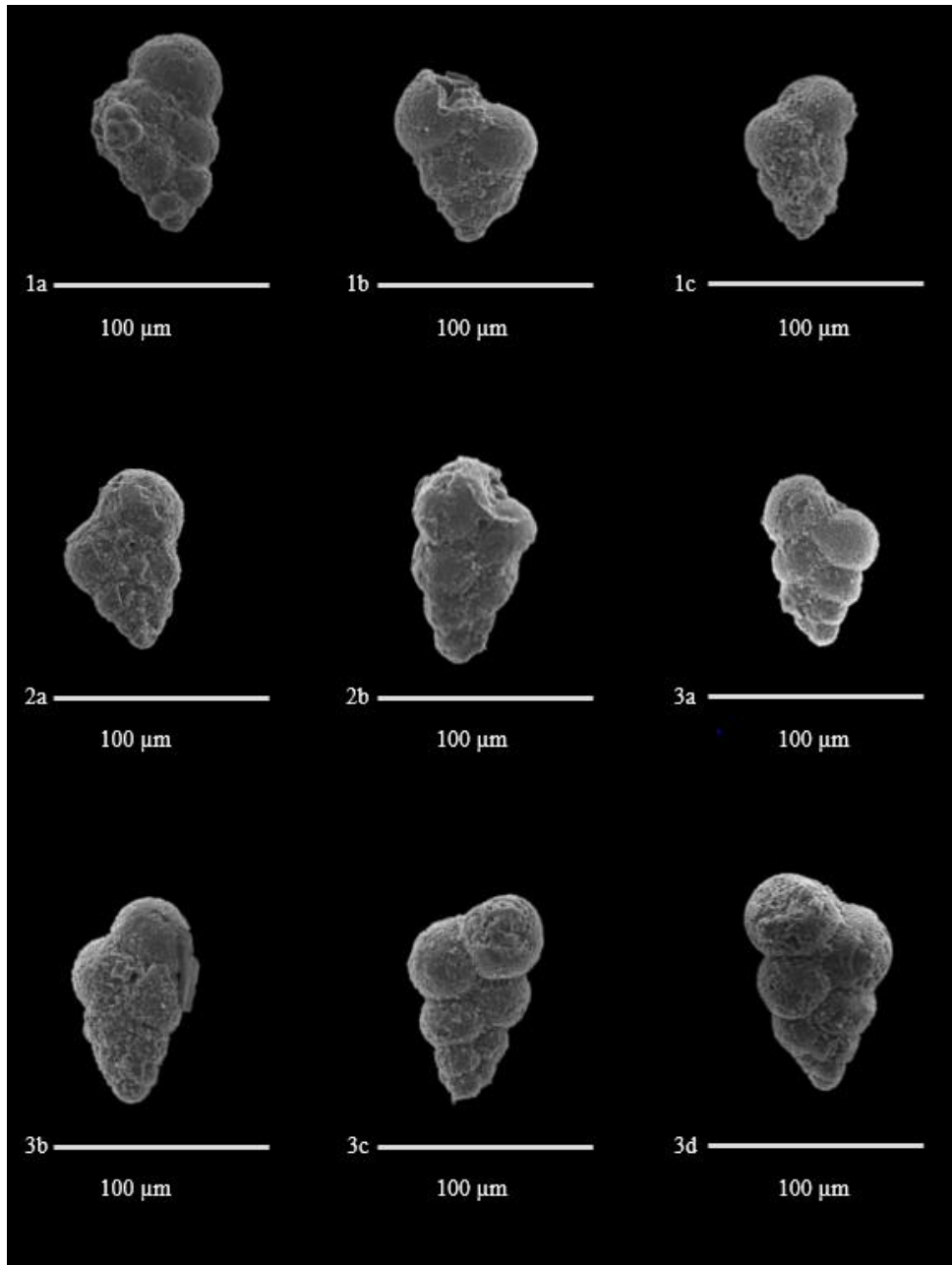


## PLATE 12

**Figure 1:** *Globotruncana aegyptiaca* (Nakkady, 1950), a) spiral view, Gk-04, b) umbilical view, Gk-04, c) umbilical view, Gk-03, Late Maastrichtian, Seben Formation

**Figure 2:** *Globotruncana arca* (Cushman, 1926), umbilical view, a) Gk-04, b) Gk-04, c) Gk-01, Late Maastrichtian, Seben Formation

**Figure 3:** *Globotruncana arca* (Cushman, 1926), umbilical view, Gk-1, Late Maastrichtian, Seben Formation

**Figure 4:** *Globotruncana arca* (Cushman, 1926), umbilical view, Gk-1, Late Maastrichtian, Seben Formation

PLATE 12

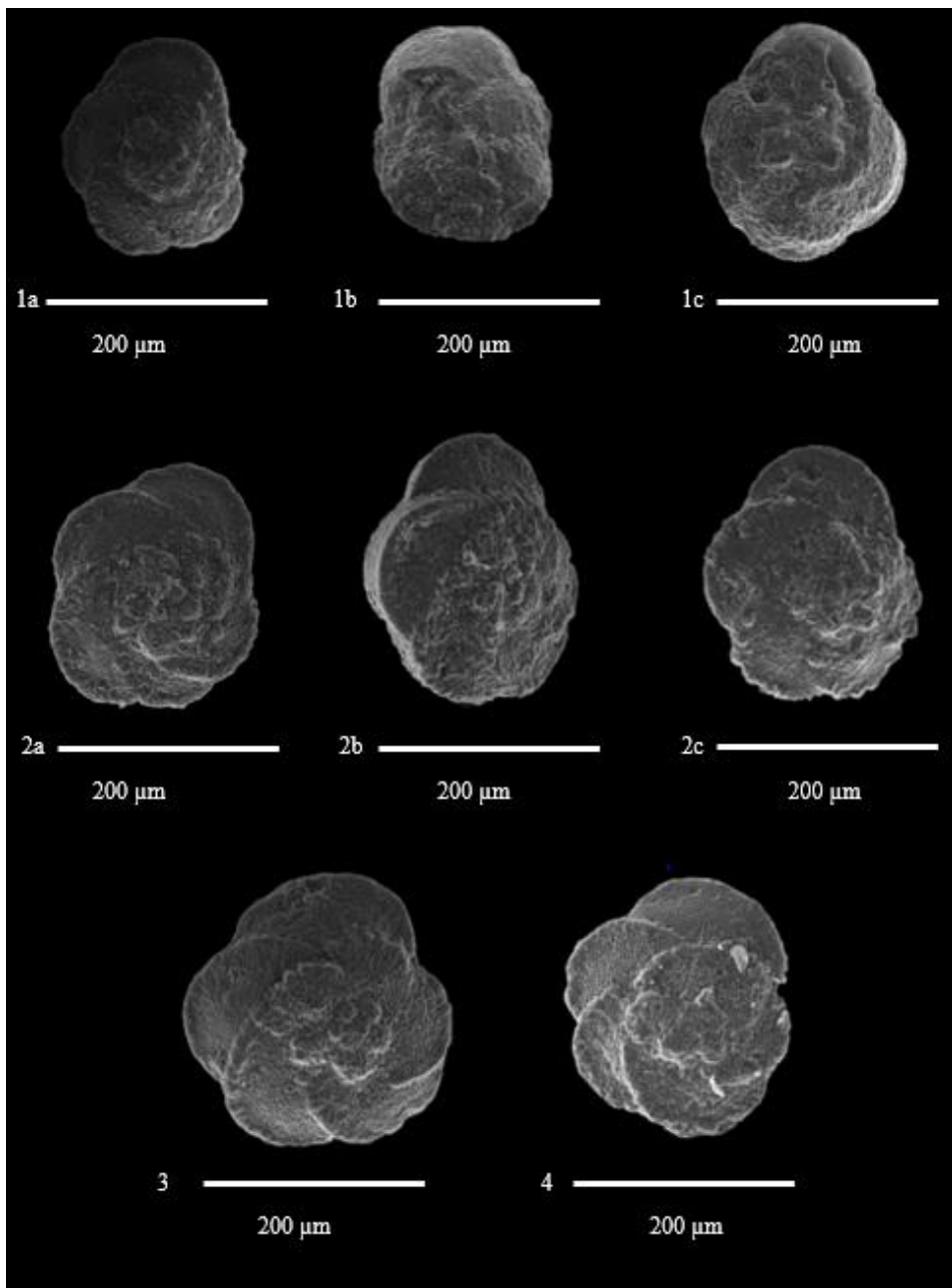


## PLATE 13

**Figure 1:** *Globotruncana esnehensis* (Nakkady, 1950), a) spiral view, Gk-04, b) spiral view, Gk-04, c) umbilical view, Gk-04, Late Maastrichtian, Seben Formation

**Figure 2:** *Globotruncana mariei* (Banner and Blow, 1960), a) spiral view, Gk-04, b) umbilical view, Gk-04, Late Maastrichtian, Seben Formation

**Figure 3:** *Globotruncana orientalis* (El Nagggar, 1966), spiral view, Gk-04, Late Maastrichtian, Seben Formation

**Figure 4:** *Globotruncana orientalis* (El Nagggar, 1966), side view, Gk-04, Late Maastrichtian, Seben Formation

**Figure 5:** *Globotruncanita conica* (White, 1928), spiral view, Gk-03, Late Maastrichtian, Seben Formation

**Figure 6:** *Globotruncanita stuartiformis* (Dalbiez, 1955), spiral view, Gk-04, Late Maastrichtian, Seben Formation

PLATE 13

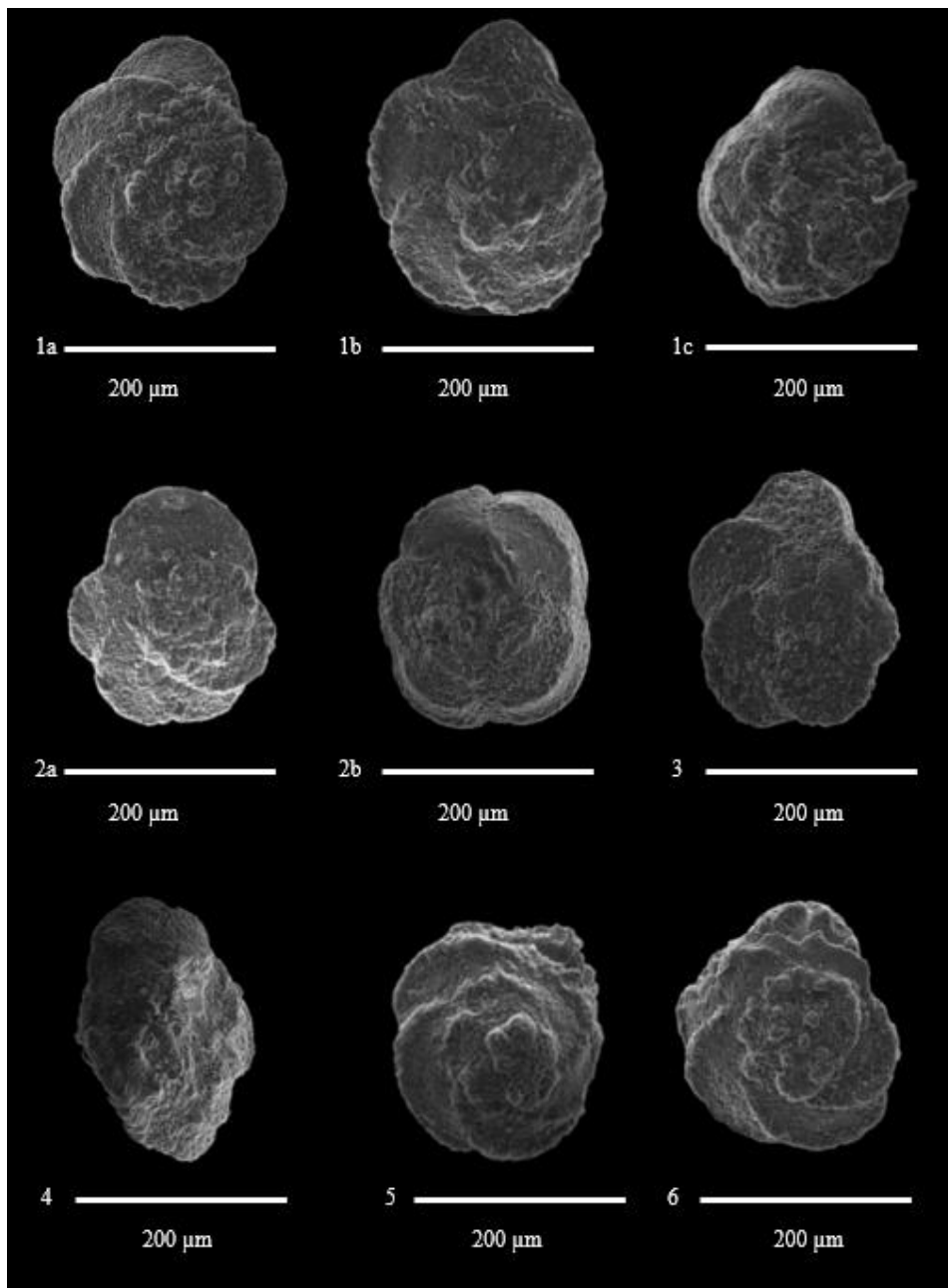


## PLATE 14

**Figure 1:** *Globotruncanella minuta* (Caron and Gonzalez Donoso, 1984), spiral view, Gk-04, Late Maastrichtian, Seben Formation

**Figure 2:** *Globotruncanella petaloidea* (Gandolfi, 1955), umbilical view, Gk-04, Late Maastrichtian, Seben Formation

**Figure 3:** *Rugoglobigerina hexacamerata* (Brönnimann, 1952), umbilical view, Gk-01, Late Maastrichtian, Seben Formation

**Figure 4:** *Rugoglobigerina pennyi* (Brönnimann, 1952), spiral view, Gk-1, Late Maastrichtian, Seben Formation

**Figure 5:** *Rugoglobigerina rugosa* (Plummer, 1926), umbilical view, Gk-03, Late Maastrichtian, Seben Formation

**Figure 6:** *Globigerinelloides asperum* (Ehrenberg, 1840), umbilical view, Gk-04, Late Maastrichtian, Seben Formation

**Figure 7:** *Globigerinelloides messinae* (Brönnimann, 1952), umbilical view, Gk-03, Late Maastrichtian, Seben Formation

**Figure 8:** *Globigerinelloides multispinus* (Lalicker, 1948), umbilical view, Gk-04, Late Maastrichtian, Seben Formation

**Figure 9:** *Globigerinelloides multispinus* (Lalicker, 1948), umbilical view, Gk-01, Late Maastrichtian, Seben Formation

PLATE 14

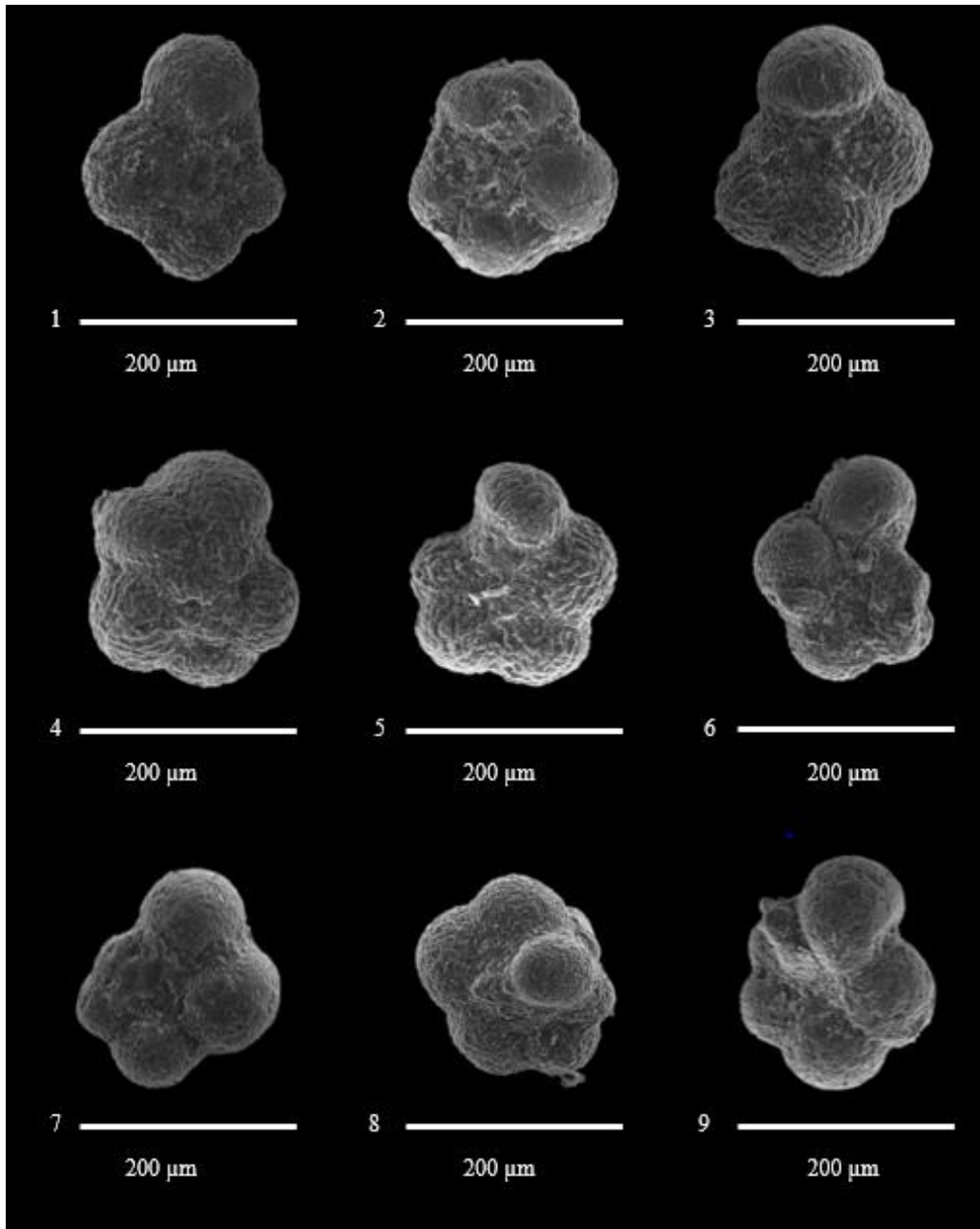


## PLATE 15

**Figure 1:** *Globigerinelloides prairiehillensis* (Pessagno, 1967), umbilical view, Gk-02, Late Maastrichtian, Seben Formation

**Figure 2:** *Globigerinelloides subcarinatus* (Brönnimann, 1952), spiral view, Gk-04, Late Maastrichtian, Seben Formation

**Figure 3:** *Hedbergella holmdelensis* (Olsson, 1964), umbilical view, a) Gk-04, b) Gk-04, Late Maastrichtian, Seben Formation

**Figure 4:** *Hedbergella monmouthensis* (Olsson, 1960), umbilical view, a) Gk-01, b) Gk-5, Late Maastrichtian, Seben Formation

PLATE 15

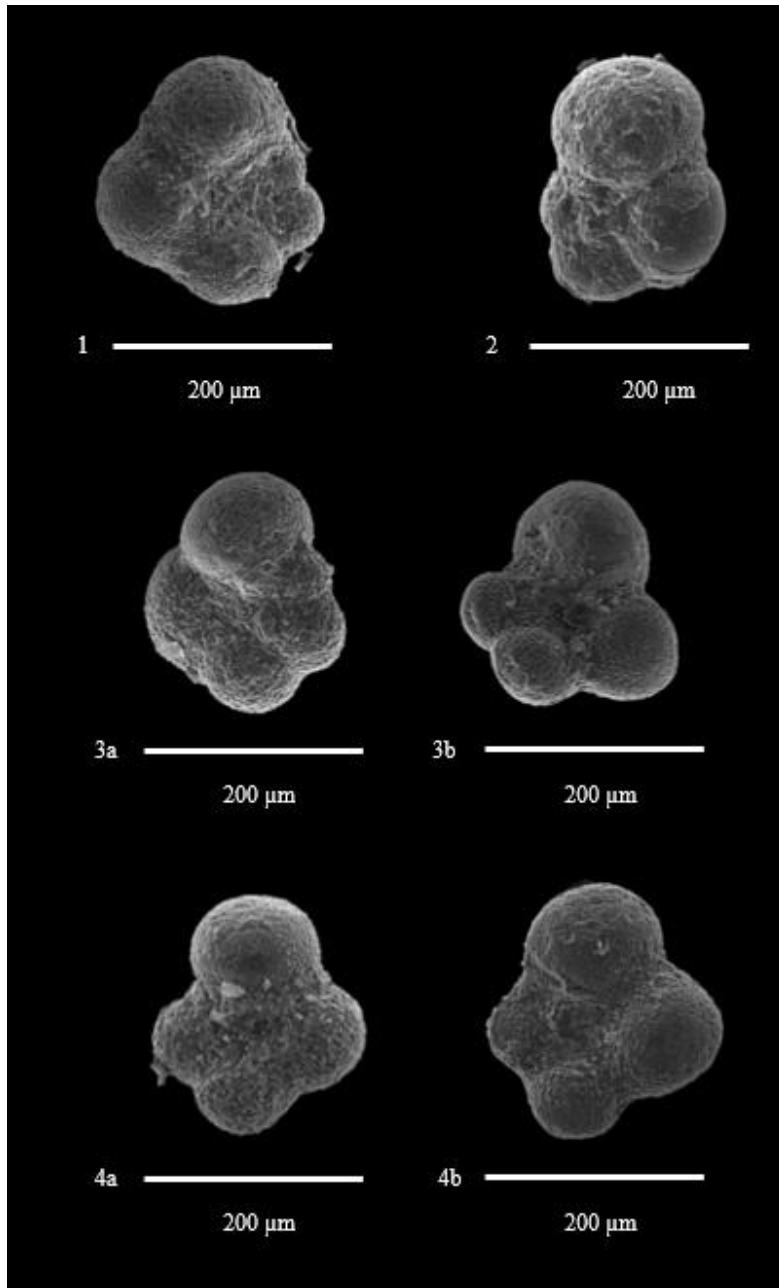


## PLATE 16

**Figure 1:** *Heterohelix globulosa* (Ehrenberg, 1840), longitudinal view, a) Gk-03, b) Gk-03, c) Gk-02, Late Maastrichtian, Seben Formation

**Figure 2:** *Heterohelix globulosa* (Ehrenberg, 1840), longitudinal view, Gk-02, Late Maastrichtian, Seben Formation

**Figure 3:** *Heterohelix labellosa* (Nederbragt, 1991), longitudinal view, Gk-01, Late Maastrichtian, Seben Formation

**Figure 4:** *Heterohelix planata* (Cushman, 1938), longitudinal view, Gk-01, Late Maastrichtian, Seben Formation

**Figure 5:** *Heterohelix punctulata* (Cushman, 1938), longitudinal view, Gk-02, Late Maastrichtian, Seben Formation

**Figure 6:** *Laeviheterohelix glabrans* (Cushman, 1938), longitudinal view, Gk-01, Late Maastrichtian, Seben Formation

PLATE 16

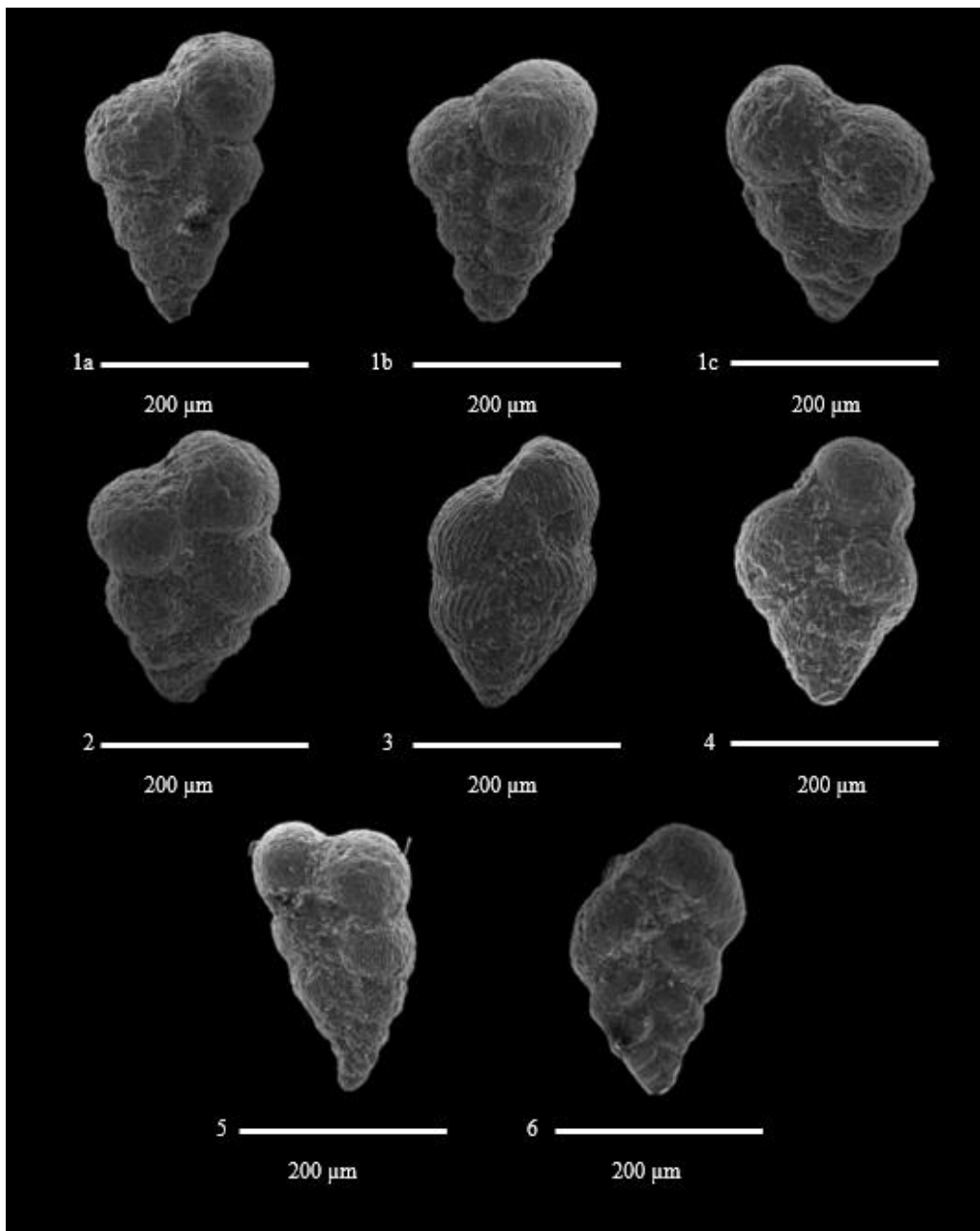


## PLATE 17

**Figure 1:** *Planoglobulina carseyae* (Plummer, 1931), longitudinal view, a) Gk-01, b) Gk-01, Late Maastrichtian, Seben Formation

**Figure 2:** *Pseudotextularia elegans* (Rzehak, 1891), longitudinal view, a) Gk-2, b) Gk-2, c) Gk-2, Late Maastrichtian, Seben Formation

**Figure 3:** *Pseudotextularia elegans* (Rzehak, 1891), longitudinal view, a) Gk-2, b) Gk-2, Late Maastrichtian, Seben Formation

PLATE 17

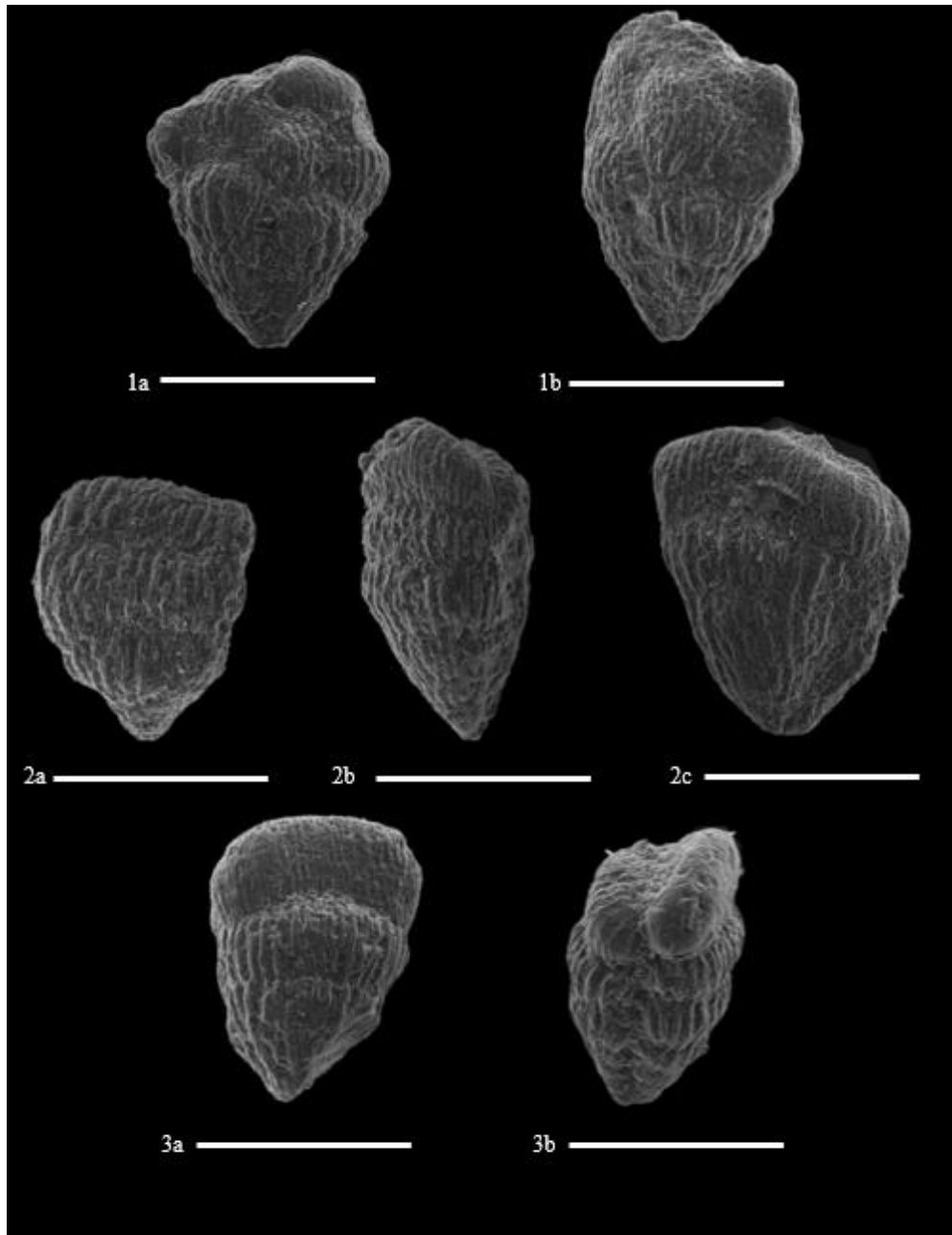


## PLATE 18

**Figure 1:** *Pseudotextularia nuttalli* (Voorwijk, 1937), longitudinal view, Gk-04, Late Maastrichtian, Seben Formation

**Figure 2:** *Pseudoguembelina consulata* (Cushman, 1938), longitudinal view, Gk-04, Late Maastrichtian, Seben Formation

**Figure 3:** *Pseudoguembelina hariaensis* (Nederbragt, 1991), longitudinal view, Gk-04, Late Maastrichtian Seben Formation

**Figure 4:** *Pseudoguembelina hariaensis* (Nederbragt, 1991), longitudinal view, Gk-7, Late Maastrichtian, Seben Formation

**Figure 5:** *Racemiguembelina fructicosa* (Egger, 1899), longitudinal view, Gk-03, Late Maastrichtian, Seben Formation

**Figure 6:** *Racemiguembelina powelli* (Smith and Pessagno, 1973), longitudinal view, Gk-02, Late Maastrichtian, Seben Formation

PLATE 18

